The Role of Insulin Receptor Substrate Signalling Pathways in the Regulation of Energy Homeostasis

Hind Al-Qassab

Supervisor: Professor Dominic Withers
Centre for Diabetes & Endocrinology
Rayne Institute
University College London
London WC1E 6JJ

Thesis submitted to the University of London
for the degree of Doctor of Philosophy

June 2007

ProQuest LLC
789 East Eisenhower Parkway
P.O. Box 1346
Ann Arbor, MI 48106-1346

Acknowledgments

I would like to thank Professor Dominic Withers for giving me the opportunity to work in his laboratory and for his guidance and encouragement throughout. I would also like to express my gratitude to the Medical Research Council for sponsoring this research.

I wish to thank all members of the Withers laboratory, past and present, for their support. The positive and friendly atmosphere created by all has contributed greatly to my experiences over the last three years. I am especially grateful to those individuals who have contributed to this work, and particularly thank Dr. Marc Claret, Dr. Melanie Clements, Helen Heffron, Steve Lingard, Dr. Irina Neganova and Dr. Colin Selman for their help and expertise. I would also like to thank my dear friends Sarah Ahmed and Danielle Aw, for their encouragement, support and friendship.

Finally, I am eternally grateful to my parents, Hisham and Nahida, and my sisters Sura and Nuha. Without the love and support of my family, I would be lost and so I dedicate this work to them.

Abstract

Leptin and insulin act as adiposity signals signalling in the brain to regulate energy homeostasis. However, in contrast to leptin, the precise details of the cell types and signalling pathways involved in the actions of insulin have not been well defined. The dominant view in the field at the commencement of this work was largely extrapolated from studies on leptin action. It was therefore suggested that insulin exerted its effects on energy balance by inhibiting orexigenic NPY/AgRP and activating anorexigenic POMC/CART neurons of the arcuate nucleus region of the hypothalamus. thereby co-ordinately regulating energy homeostasis.

Mouse genetic studies have demonstrated that insulin receptor substrate (IRS) 2, a major downstream effector of insulin signalling, plays a key role in the regulation of glucose and energy homeostasis. Mice lacking *Irs2* in all tissues exhibit insulin resistance, hyperglycaemia and β-cell failure. In addition, *Irs2* null female mice are hyperphagic, obese and infertile. However, the precise contribution of CNS IRS2 signalling in the actions of insulin and leptin, and the identity of the neuronal circuits in which IRS2 acts to regulate energy homeostasis, are unclear. The PI3K signalling pathway has been implicated in mediating the effects of insulin and leptin, in part acting downstream of IRS signalling. However, the precise hypothalamic cell types in which PI3K signalling acts also remain to be defined.

To address these issues, mice with deletion of *Irs2* in all neurons *(NesCreIrs2KO)*, POMC neurons *(POMCCreIrs2KO)* and AgRP neurons *(AgRPCreIrs2KO)* were generated. Animals lacking the PI3K p110β catalytic subunit in POMC *(POMCCrep110βKO)* and AgRP neurons *(AgRPCrep110βKO)* were also generated. *NesCreIrs2KO* animals were obese, hyperphagic and long, suggesting altered melanocortin function. Despite hyperleptinaemia, *NesCreIrs2KO* animals were leptin sensitive suggesting that IRS2 pathways are not required for leptin action. Reproductive function in *NesCreIrs2KO* females was normal. In addition, *NesCreIrs2KO* mice

displayed hyperglycaemia, mild glucose intolerance and hyperinsulinaemia. In contrast, *POMCCreIrs2KO and AgRPCreIrs2KO* mice exhibited normal hypothalamic function and glucose homeostasis. *AgRPCrep110βKO* mice were lean and hypophagic. Conversely, *POMCCrep110βKO* animals demonstrated increased adiposity and are hyperphagia.

Taken together, these studies highlight a key role for CNS IRS2 pathways in the regulation of energy homeostasis but demonstrate that CNS IRS2 pathways act in neuronal populations distinct from POMC and AgRP/NPY neurons to regulate energy homeostasis. In contrast, p110β-mediated signals in POMC and AgRP neurons play a key role in the regulation of energy homeostasis. Overall, these studies have provided new insights into the role insulin receptor substrate signalling mechanisms in the hypothalamic regulation of energy homeostasis.

Contents

List of Figures

Chapter 1: Introduction

Chapter 2: Materials and Methods

Chapter 3: Characterisation of *NesCreIrs2KO* animals

Chapter 4: Characterisation of *POMCCreIrs2KO* animals

Chapter 5: Characterisation of *AgRPCreIrs2KO* animals

Chapter 6: Characterisation of *AgRPCrep110βKO* animals

Chapter 7: Characterisation of *POMCCrep110βKO* animals

List of Tables

Abbreviations

2-AG	2-arachidonoylglycerol
α-MSH	Alpha-melanocyte stimulating hormones
3V	Third ventricle
AgRP	Agouti-related protein
AMP	Adenosine monophosphate
AMPK	AMP-activated protein kinase
ARC	Arcuate nucleus
ATP	Adenosine triphosphate
BAT	Brown adipose tissue
BBB	Blood brain barrier
BMI	Body Mass Index
CAMP	Cyclic adenosine monophosphate
CART	Cocaine-amphetamine-regulated transcript
CCK	Cholecystokinin
CDNA	Complementary DNA
CNF	Ciliary neurotrophic factor
CNS	Central nervous system
CRH	Corticotrophin releasing hormones
CSF	Cerebrospinal fluid
DEXA	Dual-energy x-ray absorptiometry
DMH	Dorsomedial hypothalamus
DMV	Dorso-motor nucleus of the vagus
ELISA	Enzyme-linked immunoabsorbance assay
ERK	Extracellular signal-regulated kinase
FBG	Fasted blood glucose
FFA	Free Fatty Acid
Fox	Forkhead box-containing protein
FSH	Follicle stimulating hormones
G6pc	Glucose 6-phosphatase
Gab1	Grb2-associated binder-1
GABA	Gamma-aminobutyric acid
GDP	Guanine diphosphate

GH	Growth hormone
Ghr	Ghrelin Receptor
GI	Gastrointestinal tract
GLP-1	Glucagon-like peptide 1
GLUT-4	Glucose transporter protein-4
GnRH	Gonadotropin-releasing hormone
GPCR	G-protein coupled receptor
Grb2	Growth factor receptor-bound protein-2
GSK-3	Glycogen synthase kinase-3
GTP	Guanine triphosphate
GTT	Glucose tolerance test
HFD	High fat diet
HGP	Hepatic glucose production
HPA	Hypothalamic-pituitary-adrenal
HPO	Horseradish peroxidase
I.p.	Intraperitoneal
ICC	Immunocytochemistry
ICV	Intracerebroventricular
Igf-1	Insulin growth factor-1
Igf-1R	Insulin growth factor-1 receptor
IgG	Immunoglobulin G
IL2	Interleukin 2
IR	Insulin receptor
IRS	Insulin receptor substrate
JAK2	Janus-kinase 2
JNK	c-Jun-N-terminal kinase
KATP channel	ATP-activated potassium channel
Kcal	Kilocalorie
KO	Knockout
LH	Luteinising hormones
LHA	Lateral hypothalamus
LoxP	Locus of 'cross(x)-over'
MAPK	Mitogen-activated protein kinase
MC-R3	Melanocortin 3 receptor

MC-R4	Melanocortin 4 receptor
MCH	Melanin-concentrating hormone
ME	Median eminence
MEFs	Mouse embryonic fibroblasts
MEK	MAPK- and ERK-related kinase
MRI	Magnetic resonance imaging
mRNA	Messenger RNA
MTII	Melatonin II
MTOR	Mammalian target of rapamycin
NIRKO	Neuron-specific insulin receptor knockout
NPY	Neuropeptide Y
NTS	Nucleus of the solitary tract
ObRb	Leptin long-form receptor
OXM	Oxyntomodulin
p70s6k	P70 ribosomal s6 protein kinase
PBS	Phosphate buffered saline
PC1	Prohormone convertase-1
PC2	Prohormone convertase-2
Pck1	Phosphoenolpyruvate carboxykinase, cytosolic isoform
PCR	Polymerase chain reaction
PDE3B	Phosphodiesterase 3B
PDK-1	Phosphoinositide-dependent kinase-1
PFA	Paraformaldehyde
PH	Pleckstrin homology
PI3K	Phosphatidylinositol-3 kinase
PI-3P	Phosphatidylinositol-3-phosphate
PIP3	Phosphatidylinositol 3,4,5-tris-phosphate
PKA	Protein kinase A
PKB	Protein kinase B
PKC	Protein kinase C
POMC	Proopiomelanocortin
PP	Pancreatic polypetide
PTB	Phosphotyrosine binding
PVN	Paraventricular nucleus

pY	Tyrosine phosphorylated
PYY	Peptide YY
R26R	Gt(Rosa)26Sortm1Sor
RIA	Radioummunoassay
RIP	Rat insulin II promoter
RMR	Resting metabolic rate
RPM	Rotations per minute
RT	Room temperature
RTK	Receptor tyrosine kinase
SDS-PAGE	Sodium dodecyl sulphate polyacrylamide gel electrophoresis
S.E.M.	Standard error of the mean
Ser	Serine
SF1	Steroidogenic factor-1
SH2	Src homology-2
Shc	SH2-containing protein
Shp2	SH2 domain phosphatase-2
SOCS	Suppressor of cytokine signalling
Sos	Son of sevenless
STAT3	Signal transducer and activators of transcription 3
STZ-DM	Streptozotocin induced diabetes
T2DM	Type 2 diabetes
TNF-α	Tumour necrosis factor-alpha
Thr	Threonine
TRH	Thyrotropin-releasing hormone
TSC1	Tuberous sclerosis complex 1, hamartin
TSC2	Tuberous sclerosis complex 2, tuberin
Tyr T	Tyrosine
UCP	Uncoupling protein
VMH	Ventromedial hypothalamus
VTA	Ventral tegmental area
WAT	White adipose tissue
WHO	World Health Organisation

Chapter 1
Introduction

1 Introduction

1.1 Obesity: a worldwide epidemic

Obesity is defined medically as a state of increased body weight, more specifically adipose tissue, of sufficient magnitude to produce adverse health consequences (Kopelman, 2000). Traditionally viewed as an affliction solely of Western society, this is no longer the case- the global incidence of obesity has increased by over 75% since 1980 (Flegal et al., 1998). In 2005, approximately 1.6 billion people in the world were overweight, with at least 400 million of these obese, leading the World Health Organisation (WHO) to proclaim obesity as a global epidemic (Cummings and Schwartz, 2003). The WHO further projects that by 2015, approximately 2.3 billion adults will be overweight and more than 700 million will be obese. In the UK alone, approximately 64% of the population is overweight with 23% of these classified as obese (WHO, 2007).

The prevalence of obesity is commonly assessed by using body mass index (BMI), defined as the weight in kilograms divided by the square of the height in metres (kg/m^2). A BMI over 25 kg/m^2 is defined as overweight, and a BMI of over 30 kg/m^2 as obese (Kopelman, 2000).

1.2 How does excess body fat impact health?

Increased adiposity is a major risk factor for a number of diseases, and is particularly linked with the development of insulin resistance, type 2 diabetes mellitus (T2DM), hypertension, dyslipidaemias, coronary heart disease (CHD), increased incidence of certain forms of cancer, respiratory complications and osteoarthritis (Kopelman, 2000). Although it is difficult to estimate the impact on public health due to its complex interactions with factors such as age and smoking, it has been estimated that in

developed countries 2-7% of total health care costs are attributable to obesity (Seidell et al., 1996). Thus, understanding the mechanisms that regulate energy homeostasis, and the nature of any defects in these systems in obese subjects, has both significant health care and economic implications.

1.3 Regulation of energy balance – a complex homeostatic process

In order for an organism to maintain energy balance it must ensure that energy intake matches energy expenditure. To do so requires the integration of numerous signals such as those indicating the levels of internal energy stores and dietary nutrient content, and adjusting factors such as energy expenditure, hormone levels, and feeding behaviour accordingly.

The finding that body fuel stored in the form of adipose tissue remains relatively constant over time, despite short-term variations in energy intake and expenditure, demonstrates the existence of precise regulatory mechanisms that maintain energy balance (Keesey and Powley, 1986; Stallone et al., 1991). For example, the average individual consumes approximately 900,000 kcal over the course of a year with the estimated age related drift in weight being less than 0.25 kg per year for males between the ages of 20 and 60 years. Such a weight gain implicates an excess energy intake of less than 0.2 % over the whole year. It is highly unlikely that such a precise level of regulation could be maintained without the existence of a complex system that continually matches energy intake and expenditure (Weigle, 1994). Additional evidence for the existence of precise mechanisms aimed at the maintenance of body fuel stores come from various experimental approaches designed to alter body fat content. In all studies, individuals were able to induce compensatory responses that resulted in the restoration of baseline adiposity levels (Drenick and Johnson, 1978; Edholm, 1977; Faust et al., 1977a; Faust et al., 1977b).

1.4 Energy homeostasis and 'The Lipostatic Theory'

The biological system that regulates body adiposity was hypothesised more than 50 years ago by Gordon Kennedy (Kennedy, 1953). He postulated that humoral signals generated in proportion to body fat stores have the ability to provide negative feedback to brain areas involved in the regulation of energy homeostasis. Thus, when the stability of body fat stores is threatened, the brain receives afferent input in proportion to the current level of body fat, and is then able to engage appropriate mechanisms to maintain fat stores.

Several criteria must be met by an afferent humoral signal (McMinn et al., 2000). To be considered as such a signal, a compound must be secreted in proportion to body fat stores and enter the brain in proportion to its circulating level. In addition, a signal transduction system that mediates the effects of the signal should be located in key CNS regions involved in energy homeostasis regulation. Finally, administration of the putative signal into the circulation or directly into the brain should result in a concordant reduction in food intake and body weight. Currently only two hormones, insulin and leptin, satisfy all the criteria required of such a signal.

1.5 Insulin and leptin: roles in the CNS control of energy homeostasis

1.5.1 Insulin and the central regulation of energy homeostasis

Following Kennedy's lipostatic theory (Kennedy, 1953), it was Woods and Porte who first hypothesised that insulin represented an afferent signal to the brain that had the ability to couple changes in adiposity to compensatory changes in food intake (Woods et al., 1979). Many lines of evidence, summarised below, have strongly supported this initial hypothesis.

Firstly, levels of plasma insulin correlate directly with body weight and especially with total body adiposity, with higher basal insulin levels found in obese individuals (Bagdade et al., 1967; Polonsky et al., 1988a). In addition, obese animals and humans secrete more insulin in response to a meal than lean individuals (Bagdade et al., 1967; Woods et al., 1974), with the degree of glucose-stimulated secretion a direct function of body fat (Polonsky et al., 1988b)

Secondly, insulin receptors (IR) and IR messanger RNA (mRNA) are widely distributed in key CNS regions involved in the regulation of food intake and body weight. For example, a high density of insulin receptors are found in the arcuate nucleus (ARC) of the hypothalamus, an important candidate region in energy homeostasis regulation by adiposity signals. Consistent with its role as a putative adiposity signal, insulin has been found to enter the brain via a saturable transport process that allows transport from the plasma to brain interstitial fluid (Hachiya et al., 1988).

Finally with regards to the final criterion of a putative adiposity signal, the administration of exogenous insulin directly into the brain has been shown to reduce food intake and increase energy expenditure (Air et al., 2002; Woods et al., 1996; Woods et al., 1974; Woods et al., 1979). Even peripheral administrations of insulin, in amounts that do not cause hypoglycaemia, have been associated with a decrease in food intake (McGowan et al., 1990; Nicolaidis and Rowland, 1976; Woods et al., 2003). Consistent with these findings, the administration of antibodies against insulin directly into the brain, also result in an increase in food intake (McGowan et al., 1992; Strubbe and Mein, 1977).

1.5.2 Leptin and the central regulation of energy homeostasis

Twenty years after Kennedy first proposed his lipostatic theory of energy homoeostasis, parabiosis experiments by Coleman added considerable weight to his arguments. *Obese*

(*ob/ob*) and *diabetes* (*db/db*) animals animals are two spontaneously occurring murine models of obesity, diabetes and hyperinsulinaemia, When normal mice were surgically coupled to *ob/ob* animals to create a common circulation, this resulted in reductions in the food intake and body weight of the *ob/ob* mouse (Coleman, 1973). In contrast, when normal mice were coupled to *db/db* animals, this resulted in a wasting effect on the parabiotic normal mice (Coleman and Hummel, 1969). Finally, when *ob/ob* and *db/db* mice were coupled to one another, *ob/ob* mice displayed reduced food intake and body weight (Coleman, 1973).

Taken together, these results led to the hypothesis that the o*b* locus is necessary for the production of a humoral satiety factor, whereas the *db* locus encoded a molecule required for the response to this factor. As *ob/ob* and *db/db* mice are hyperinsulinaemic as expected to their degree of obesity, the missing adiposity signal was unlikely to be insulin.

The hormone leptin (Greek: leptos = thin), a 167 amino acid polypeptide, was discovered in 1994 by positional cloning of the *ob* locus by Zhang and colleagues, and was heralded as a previously unknown adiposity signal (Zhang et al., 1994). The identification of leptin led rapidly to the cloning of its cognate receptor, encoded by the *db* locus (Tartaglia et al., 1995).

Leptin, like insulin, meets all the criteria required of a putative adiposity signal. Firstly, it is secreted by adipocytes (and at lower levels in gastric epithelium and the placenta) and circulates in the periphery in direct proportion to total adiposity. The actual stimulus for secretion is related more to the metabolic activity of the fat cell than to actual fat storage (Woods and Seeley, 2000) such that dissociations can occur between stored fat and leptin release (Ahren et al., 1997; Wisse et al., 1999). Nonetheless, over the course of a day, plasma leptin levels are a reliable indicator of body fat.

Secondly, a signal transduction system has also been shown to exist in the brain with leptin being transported into the CNS via a saturable process (Banks et al., 1996; Schwartz et al., 1996b). Leptin receptors (LepRs) have been localised to many brain areas, including within key hypothalamic nuclei implicated in the regulation of energy homeostasis such as the ARC (Banks et al., 1996; Baskin et al., 1999; Schwartz et al., 1996c).

Thirdly, the administration of leptin locally into the brain has been extensively shown to decrease food intake and body weight (Campfield et al., 1995; Pelleymounter et al., 1995; Seeley et al., 1996). This response is dose dependent and not secondary to illness or incapacitation (Thiele et al., 1997).

1.5.3 Other signals involved in the regulation of food intake and body weight

It should be noted that in addition to insulin and leptin, a wide range of other hormones have been shown to affect food intake and body weight (Figure 1.1). These include adipose tissue derived hormones, pancreatic hormones and hormones of the gastrointestinal tract (Stanley et al., 2005). These peripheral signals, involved in the short-term regulation of meal initiation, meal size and satiety, are proposed to interact with the longer-term acting adiposity signals to affect food intake and body weight. Nutrients (for example amino acids, free fatty acids and glucose) cytokines (for example interleukin-6, tumour necrosis factor-alpha) and monoamines (noradrenaline, serotonin, dopamine) have also been implicated as acting in the CNS to regulate food intake and body weight (Havel, 2001).

An in-depth discussion of these hormonal and non-hormonal signals is beyond the scope of this thesis. However the properties of the various signals and their effect on energy homeostasis are summarised in Table 1.1 and Table 1.2 below.

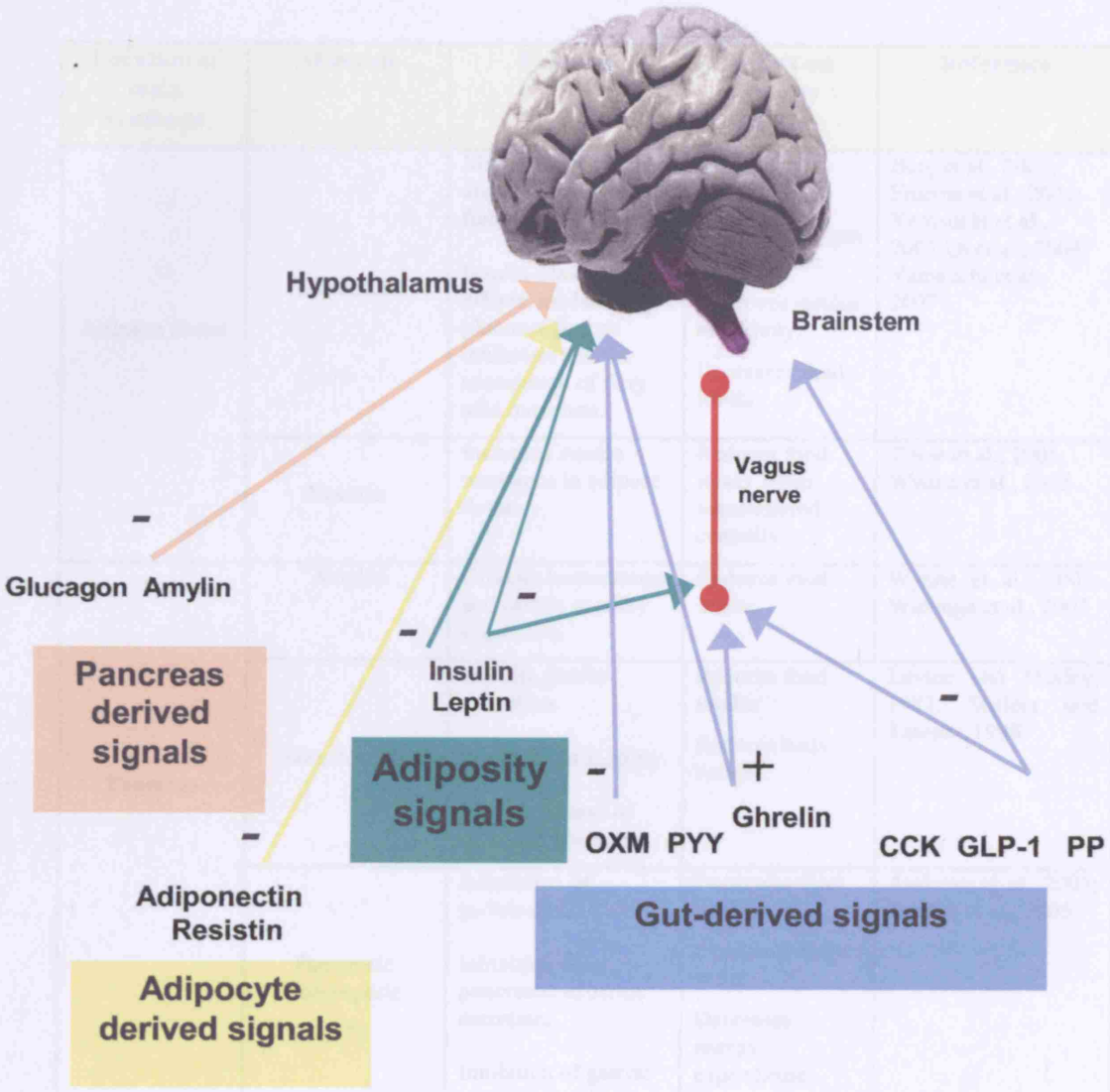

Figure 1.1: Energy homeostasis is controlled by peripheral signals from adipose tissue, pancreas, and the gastrointestinal tract. Peripheral signals from the gut include peptide YY (PYY), oxyntomodulin (OXM), ghrelin, pancreatic polypeptide (PP), glucagon-like peptide 1 (GLP-1), and cholecystokinin (CCK). These gut-derived peptides and adiposity signals influence central circuits in the hypothalamus and brain stem to produce a negative (–) or positive (+) effect on energy balance. Consequently, the drive to eat and energy expenditure can be adjusted to ensure that over a set period of time, the stability of body weight is maintained.

Location of main synthesis	Molecule	Function	Effect on energy balance	Reference
Adipose tissue	Adiponectin	Major antidiabetic and antiatherogenic functions. Insulin-sensitising effects, mediated by gluconeogenesis inhibition and the stimulation of fatty acid oxidation.	Reduces body weight. Increases oxygen consumption. Improves insulin sensitivity. Decreases lipid levels.	Berg et al., 2001; Fruebis et al., 2001; Yamauchi et al., 2001;Qi et al., 2004; Yamauchi et al., 2007
	Resistin	Increases insulin resistance in adipose tissue.	Reduces food intake when administered centrally.	Tovar et al., 2005; Wynne et al., 2005
Pancreas	Amylin	Glucose homeostasis and gastric motility regulation.	Reduces food intake.	Wynne et al., 2005; Wielinga et al., 2007
	Somatostatin	Inhibits gastric secretions. Reduces gut motility. Inhibits release of other gut hormones.	Reduces food intake. Reduces body weight.	Levine and Morley, 1982; Scalera and Tarozzi, 1998
	Pancreatic Polypeptide (PP)	Relaxation of gallbladder. Inhibition of pancreatic exocrine secretion. Inhibition of gastric emptying.	Decreases food intake. Decreases body weight. Decreases energy expenditure. Improves insulin resistance and dyslipidaemias.	Asakawa et al., 2003; Stanley et al., 2005
Gastrointestinal tract	Cholecystokinin (CCK)	Promotes gallbladder contraction. Increases secretion of pancreatic enzymes. Inhibits gastric acid secretion. Delays gastric emptying.	Reduces meal size and duration. No effect on food intake due to increased meal frequency.	Gibbs et al., 1973; Kissileff et al., 1981; Stanley et al., 2005

Gastrointestinal tract	Ghrelin	Promotes release of GH and other pituitary hormones. Promotes gastric motility and PP release.	Increases food intake. Increases body weight. Reduces fat utilisation.	Tschop et al., 2000; Wren et al., 2001a; Wren et al., 2001b
	Bombesin	Stimulates gallbladder contraction. Stimulates bile flow. Increases secretion of digestive enzymes from pancreas.	Reduces food intake.	Gibbs et al., 1979; Smith et al., 1981
	Pancreatic Polypeptide YY3-36 (PYY)	Delays gastric emptying, pancreatic and gastric secretion. Increases ileal absorptions of fluids and electrolytes.	Inhibits food intake. Reduces body weight. Improves glyceamic control.	Adrian et al., 1985; Hoentjen et al., 2001; Batterham et al., 2002; Challis et al., 2003; Pittner et al., 2004
	Oxyntomodulin (OXM)	Inhibits gastric acid production. Reduces gastric motility.	Reduces food intake. Reduces body weight.	Dakin et al., 2001; Dakin et al., 2002; Cohen et al., 2003; Dakin et al., 2004; Wynne et al., 2005
	Glucagon-like peptide 1 (GLP-1)	Incretin effect on insulin secretion. Suppresses glucagon release. Promotes pancreatic β-cell growth. Inhibits gastric emptying and secretion.	Reduces food intake. Reduces blood glucose levels.	Turton et al., 1996; Meeran et al., 1999; Edwards et al., 2001; Tang-Christensen et al., 2001; Verdich et al., 2001; Zander et al., 2002; Yamamoto et al., 2003; Baggio et al., 2004

Table 1.1: Peripheral hormonal signals and the regulation of energy balance. Table summarising the location of synthesis of peripheral hormones, and the effect on energy balance upon peripheral administration.

Signals acting in the CNS to regulate food intake and body weight		Effect on energy balance	Reference
Momamines	Serotonin (5-HT)	Anabolic	Blundell, 1984; Leibowitz et al., 1988; Jackson et al., 1997
	Dopamine	Catabolic (LHA) and anabolic (VMH)	Fetissov et al., 2000
	Noradrenaline	Catabolic	Leibowitz and Miller, 1969; Leibowitz, 1988
Amino acid neurotransmitters	Gamma-aminobutyric acid (GABA)	Anabolic	van den Pol, 2003
	Glutamate	Catabolic	van den Pol, 2003
Endocannaboids	anandamide, 2-arachidonoylglycerol (2-AG), noladin ether, NADA, and virodhamine	Anabolic	Di Marzo and Matias, 2005
Endogenous opiods	β-endorphin, dynorphin, and enkephalins	Anabolic	Cooper et al., 1985; Levine and Billington, 1989; Lambert et al., 1993; Kotz et al., 1997; Levine and Billington, 1997; Kalra et al., 1999
Cytokines	Tumour necrosis factor-alpha (TNF-α), Interleukins-1 (IL1), Interleukin-6 (IL6) and Ciliary neurotrophic factor (CNF)	Anabolic	Plata-Salaman, 1995
Nutrients	Glucose	Anabolic	Smith and Epstein, 1969; Thompson and Campbell, 1977; Woods et al., 1984; Novin et al., 1985
	Protein (amino acids)	Catabolic	Bray, 1997
	Fat (triglycerides, fatty acids and apolipoproteins)	Catabolic	Woods et al., 1984
	Metabolites (lactate, pyruvate and ketones)	Catabolic	Fisler et al., 1995; Nagase et al., 1996

Table 1.2: Table summarising a variety of non-hormonal signals (of both peripheral and CNS origin) and their effect upon energy balance.

1.6 Roles of insulin and leptin as adiposity signals

The physiological roles that insulin and leptin play in the regulation of food intake and body weight, involves their ability to engage and regulate key neurochemical pathways or 'central effector' pathways, located in the brain that influence energy intake and energy expenditure. Central effectors can be divided into two broad categories: anabolic effectors that elicit increased food intake, decreased energy expenditure, and consequently increased stored energy in the form of adipose tissue and catabolic effectors that have the opposite effects (Kaiyala et al., 1995; Schwartz, 1997; Schwartz et al., 2000).

Insulin and leptin are proposed to activate catabolic effector pathways and suppress anabolic effectors pathways (Figure 1.2). For example, in response to fasting and weight loss, adiposity and thus adipose derived factor signalling is decreased. This results in the activation of CNS anabolic effectors and the inhibition of catabolic effectors, resulting in an overall increase in food intake and decrease in energy expenditure (Woods et al., 1998).

Many key details of these catabolic and anabolic effector systems have emerged in the past few years. These systems have been shown to be an interconnected series of discrete neurotransmitter systems and axonal pathways in the brain. The best known of these CNS systems are in the ventral hypothalamus, and there has been extensive investigation into their specific locations over the last century.

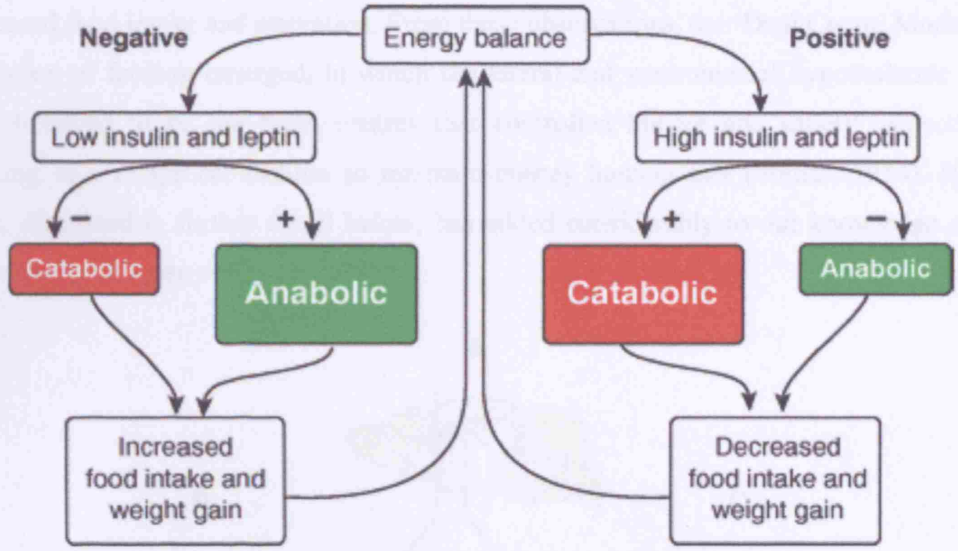

Figure 1.2: Model showing how a change in body adiposity is coupled to compensatory changes of food intake. Leptin and insulin are adiposity signals, secreted in proportion to body fat content, which act in the hypothalamus to stimulate catabolic, while inhibiting anabolic, effector pathways. These pathways have opposing effects on energy balance, and it is the balance between these two pathways that determines the amount of body fuel stored as fat. Adapted from Woods et al., 1998.

1.7 Identification of the hypothalamic nuclei involved in the regulation of energy homeostasis

Brain lesioning and electrical stimulation studies, performed over six decades ago, first implicated the hypothalamus as a major centre controlling food intake and body weight (Hetherington, 1940). The hypothalamus consists of many nuclei involved in the regulation of food intake, including the ventromedial hypothalamus (VMH), the dorsomedial hypothalamus (DMH), the lateral hypothalamic area (LHA), the paraventricular nucleus (PVN) and the arcuate nucleus (ARC) (Figure 1.3).

Hetherington and Ranson observed that medial hypothalamic lesions within the ARC, VMH, PVN and DMN nuclei resulted in uncontrolled hyperphagia and obesity (Hetherington, 1940). In contrast, destruction of the lateral hypothalamus resulted in

decreased food intake and starvation. From these observations, the 'Dual Centre Model' for regulation of feeding emerged, in which the lateral and ventromedial hypothalamic areas were believed to be the brain centres that controlled hunger and satiety respectively, working in a reciprocal fashion to maintain energy homeostasis (Stellar, 1954). Recent work, discussed in further detail below, has added considerably to our knowledge of the distinct roles of these various nuclei.

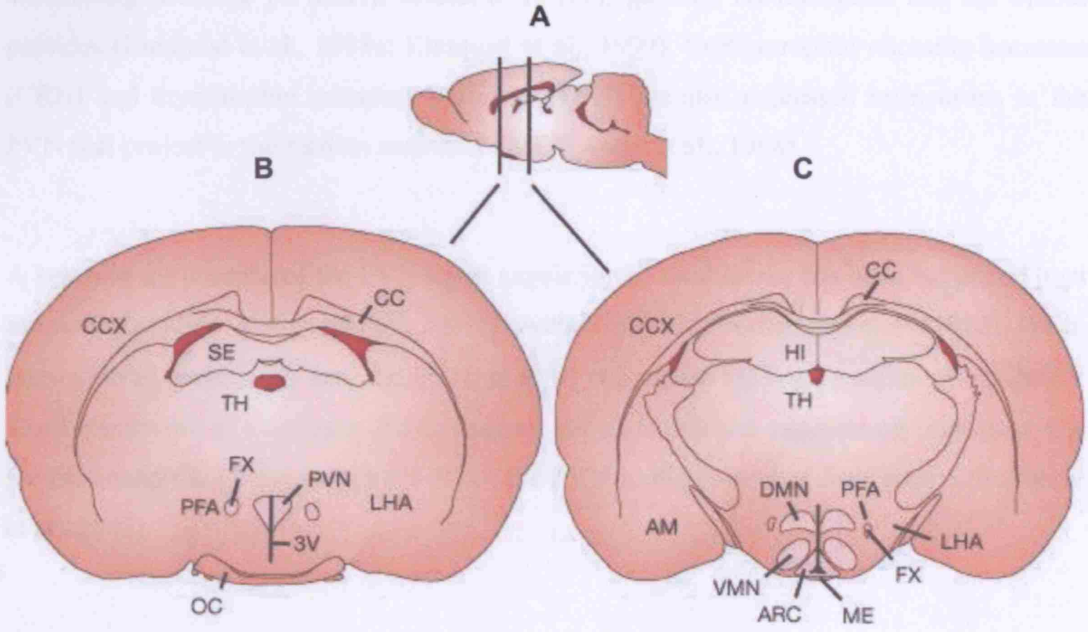

Figure 1.3: Main hypothalamic regions involved in the regulation of food intake. A: Longitudinal view of mouse brain, with olfactory bulb at anterior end on the left and the caudal hindbrain on the right. Cross-sections of the brain at two levels (indicated by the vertical lines) are shown as B and C. First order neurons are found in the arcuate nucleus (ARC) and project anteriorly to the paraventricular nucleus (PVN), the perifornical area (PFA) adjacent to the fornix (Fx) and lateral hypothalamic area (LHA). Other regions implicated in regulating food intake include the ventromedial nucleus (VMN) and the dorsomedial nucleus (DMN). Abbreviations of other brain structures: AM, amygdala; CC, corpus callosum; CCX, cerebral cortex; HI, hippocampus; ME, median eminence; OC, optic chiasm; SE, septum; TH, thalamus; 3V, third ventricle. Adapted from Barsh and Schwartz, 2002.

1.7.1 The paraventricular nucleus

The paraventricular nucleus (PVN) lies beside the top of the third ventricle in the anterior hypothalamus. This nucleus is an integrating centre on which a number of neural pathways that influence energy homeostasis converge. It is rich in terminals containing numerous appetite modifying neurotransmitters including; neuropeptide Y (NPY), alpha-melanocyte stimulating hormone (α-MSH), serotonin (5-HT), galanin, noradrenaline and the opioid peptides (Elmquist et al., 1998a; Elmquist et al., 1999). Corticotrophin releasing hormone (CRH) and thyrotrophin releasing hormone (TRH) are also expressed by neurons in the PVN that project to the median eminence (ME) (Arase et al., 1988).

A key role for neurons of the PVN in the regulation of food intake has been suggested by a number of studies (Michaud et al., 2001; Sawchenko, 1998; Weingarten et al., 1985). When administered specifically into the PVN, α-MSH suppresses feeding (Audinot et al., 2002). The recent work of Balthasar and colleagues supports this and suggests an important role for melanocortin 4 receptors (MC4-R) of the PVN in the control of food intake (Balthasar et al., 2005).

1.7.2 The ventromedial nucleus

The ventromedial hypothalamic nucleus (VMH) is one of the largest hypothalamic nuclei. Recent studies have shown a high abundance of leptin receptors in neurons of the VMH, and evidence indicates that this region may be an important target for circulating leptin (Meister et al., 1989). The VMH has direct connections with the DMH, PVN and the LHA (Williams et al., 2001).

1.7.3 The dorsomedial nucleus

The dorsomedial hypothalamus (DMH) is located immediately dorsal to the VMH. It has extensive direct connections with other medial hypothalamic nuclei such as the PVN, the

lateral hypothalamic area (LHA) and the brainstem. Neurons within the DMH have been shown to contain a high number of both insulin and leptin receptors on their surface (Kalra et al., 1999).

1.7.4 The lateral hypothalamic area

The lateral hypothalamic area (LHA) is vaguely defined and comprises a large diffuse population of neurons including defined subpopulations that express orexins and melanin-concentrating hormone (MCH) (de Lecea et al., 1998; Marsh et al., 2002). NPY, AgRP (agouti- related protein) and α-MSH terminals are abundant in the LHA, and are in contact with the orexin and MCH cells (Broberger et al., 1998a; Elias et al., 1998; Horvath et al., 1999).

1.8 The arcuate nucleus: a primary sensor of peripheral signals

The arcuate nucleus (ARC), which consists of an elongated collection of neuronal cell bodies, is located in the mediobasal hypothalamus above the base of the third ventricle (3V). This nucleus has extensive reciprocal connections with other hypothalamic regions, including the PVN, DMH, VMH and LHA (Figure 1.3).

The ARC is uniquely positioned to act as a site of metabolic sensing and to integrate endocrine information regarding the supply and demand of energy in the body. This is because the ARC-ME area is one of the 'circumventricular' organs in which the blood-brain barrier (BBB) is specially modified. Thus, neurons within this area are accessible to circulating hormones and nutrients (Broadwell and Brightman, 1976). It has been proposed that nutrients and hormones may also gain access to the ARC by diffusion across the ependyma from the cerebrospinal fluid (CSF) in the third ventricle (Elmquist et al., 1998b).

Two primary adjacent populations of neurons within the ARC are hypothesised to integrate signals of nutritional status and influence energy homeostasis (Cone et al., 2001). The first of these neuronal populations co-express the orexigenic NPY and AgRP neuropeptides that affect energy balance by their ability to stimulate food intake and decrease energy expenditure. The second neuronal population co-expresses the anorexigenic POMC and cocaine-amphetamine-regulated-transcript (CART) neuropeptides, which affect energy balance by their ability to inhibit food intake and stimulate energy expenditure.

Projections between ARC POMC/CART and NPY/AgRP neurons are thought to allow cross-talk and hence a co-ordinated response (Cowley et al., 2001). These neuropeptide systems located in the ARC are discussed in further detail below.

1.9 POMC/CART anorexigenic neurons

The POMC gene encodes a 31-36 kDa pre-pro-hormone from which seven mature peptide hormones are derived via post-translational cleavage by various prohormone convertases, such as pro-hormone convertases 1 and 2 (PC1 and PC2) (MacNeil et al., 2002). Of all the POMC derived peptides, α-MSH is considered the most important regulator of feeding (Hillebrand et al., 2002).

CART is an anorexigenic neuropeptide, originally identified by differential display polymerise chain reaction (PCR) as a novel mRNA, stimulated after acute administration of psychomotor stimulants (Douglass et al., 1995). In the rat, the CART precursor is spliced into two products of 116 and 129 amino acids. These two splice products are further processed in a tissue specific manner (Douglass et al., 1995). Currently five forms of CART are known; $CART_{(55\text{-}86)}$, $CART_{(54\text{-}102)}$, $CART_{(55\text{-}102)}$, $CART_{(61\text{-}102)}$ and $CART_{(62\text{-}102)}$ (Thim et al., 1999).

1.9.1 Neuroanatomy of POMC/CART neurons

Within the CNS, the major site of POMC expression originates in neurons of the ARC. In the mouse brain there are approximately 3,000 POMC positive cells. These neurons also co-express CART. POMC/CART cell bodies are found throughout the rostrocaudal extent of the ARC and periarcuate area of the hypothalamus (Jacobowitz and O'Donohue, 1978; Joseph et al., 1983 ; Nilaver et al., 1979 ; Watson et al., 1978). From the ARC, POMC/CART neurons project broadly to other hypothalamic nuclei including the PVN, DMN, LHA and VMH (Bagnol et al., 1999; Elias et al., 1999; Jacobowitz and O'Donohue, 1978). These neurons also send descending sets of projections to the brainstem (Cone, 2005). Approximately half of the α–MSH immunoreactivity in the brainstem is thought to derive from hypothalamic POMC/CART neurons and the other half from a smaller (~300) population of POMC neurons in the brainstem (Joseph and Michael, 1988; Pilcher et al., 1988).

1.9.2 Effect of POMC and CART on energy balance

Both chronic infusions and acute intracerebroventricular (ICV) administration of α-MSH or synthetic analogues such as melatonin II (MTII) have been shown to result in strong reductions in food intake, body weight and adiposity in wild type and genetically obese rodents (Li et al., 2003; Pierroz et al., 2002; Williams et al., 2001; Yaswen et al., 1999). It has been demonstrated that administration of these peptides also increases metabolic rate and sympathetic outflow (Dunbar and Lu, 2000) and partially compensates for the alteration in body temperature regulation in leptin deficient *ob/ob* mice (Forbes et al., 2001). When injected into the third ventricle α-MSH also significantly inhibits food intake of food-deprived rats (Tsukamura et al., 2000).

Both acute and chronic ICV injection of CART peptide dose dependently reduce food intake, body weight and NPY-induced food intake in lean animals (Kristensen et al., 1998; Lambert et al., 1998) and also obese *fa/fa* rats (Larsen et al., 2000). Consistently, injections

of CART antibodies increase food intake in rodents (Kristensen et al., 1998; Lambert et al., 1998). The ICV administration of CART has also been shown to induce activation of the hypothalamic-pituitary-adrenal (HPA) axis (Stanley et al., 2001) and inhibit gastric acid secretion and gastric emptying (Okumura et al., 2000). An important role for CART in energy metabolism is also suggested by the finding that CART injection in the PVN results in increased expression of uncoupling proteins (UCPs) I, II and III in adipose tissue and muscle (Kong et al., 2003; Wang et al., 2000).

1.9.3 Melancortin and CART receptors

The effect of the melanocortins is mediated by the melancortin receptors (MC-Rs) of which five are currently known. These are MC-R1, MC-R2, MC-R3, MC-R4 and MC-R5. They are G-protein-coupled receptors (GPCRs). When activated, GPCRs function through adenylate cyclase to increase intra-cellular cyclic adenosine monophosphate (cAMP) concentrations. These receptors have differing affinity for POMC products and are expressed at varying levels in different tissues (Mountjoy et al., 1994). Both MC-R3 and MC-R4 are expressed in hypothalamic nuclei implicated in energy homeostasis including the VMH, DMH and ARC (Harrold et al., 1999; Roselli-Rehfuss et al., 1993). Interestingly, POMC and AgRP neurons in the ARC selectively express MC-R3 but not MC-R4, suggesting a role for this receptor in feedback regulation of the melanocortinergic circuitry (Bagnol et al., 1999).

Genetic studies in mice suggest that both MC-R3 and MC-R4 mediate pathways regulating energy expenditure and adiposity, but only the MC-R4 mediates the anorectic/feeding effects of the melanocortins axes (Butler et al., 2000; Butler et al., 2001; Chen et al., 2000; Huszar et al., 1997).

The mechanisms that mediate the effects of CART are still poorly understood, and so far no receptor has been identified.

1.9.4 Evidence for the role of POMC and CART from murine models

Further evidence for a key role for α-MSH in the central control of feeding and energy balance comes from genetic studies in rodents and humans. Humans with α-MSH deficiency due to either a mutation in the *Pomc* sequence or processing of the POMC polypeptide demonstrate hypopigmentation, adrenal insufficiency and early onset obesity (Carroll et al., 2005; Krude et al., 2003; Obici et al., 2001).

Targeted deletion of the *Pomc* gene in mice also results in obesity. This has been shown to be due to reductions in metabolic rate, alterations in lipid metabolism and hyperphagia (Challis et al., 2004; Yaswen et al., 1999). The loss of even one copy of the *Pomc* gene in mice has been demonstrated to be sufficient to render these animals highly susceptible to diet induced obesity (DIO) (Challis et al., 2004).

Despite the described anorexigenic effects of CART on energy homeostasis, *Cart* null mice display normal body weight and food intake on a normal chow diet but do appear to be less sensitive to pain (Bannon et al., 2001). On a high fat diet (HFD), these animals exhibit an increase in food intake, body weight and fat mass (Wortley et al., 2004).

1.10 NPY/AgRP orexigenic neurons

NPY, first isolated in 1982, is a 36 amino acid neurotransmitter belonging to the pancreatic polypeptide (PP) family (Tatemoto et al., 1982). Processing of the pro-NPY peptide results in the formation of six NPY fragments, with the effect of NPY on feeding thought to be mediated by the $NPY_{(1-36)}$ intact peptide (Flood and Morley, 1989).

Agouti is normally expressed within the hair follicle where it antagonises α-MSH on the MC-R1, inducing a colour switch from eumalanin (black/brown) to phaeomelanin (red/yellow) (Barsh et al., 1999; Ollmann et al., 1998; Wolff et al., 1999). The yellow coat,

hyperphagia and obesity of the A^y mouse is known to be due to widespread ectopic expression of this protein (Bultman et al., 1992; Morgan et al., 1999). The existence in the brain of an "agouti-like" protein was suggested by the fact that though only normally expressed in hair follicles, the agouti protein is a highly specific MC-R4 antagonist (Lu et al., 1994). This hypothesis was confirmed when the *agouti-related protein (Agrp)* gene was isolated in 1997 and found to encode a 12 amino acid peptide with 25% homology to the agouti protein (Shutter et al., 1997).

1.10.1 Neuroanatomy of NPY/AgRP neurons

The main site of NPY expression in the hypothalamus is within the ARC, where it is co-localised with agouti-related protein (AgRP) in 90% of neurons (Broberger et al., 1998b). ARC NPY/AgRP neurons project to adjacent hypothalamic nuclei including dorsally and anteriorly to the PVN, DMH, VMH, LHA, perifornical area (PFA) and also ventrally to the ME. The ARC-PVN projection is particularly dense (Bai et al., 1985). In some hypothalamic nuclei such as the PVN and DMH, AgRP is thought to be released from NPY endings in the same synaptic complex as α-MSH and acts as a competitive antagonist at both the MC-R3 and MC-R4 (Ollmann et al., 1997).

1.10.2 Effects of NPY and AgRP on energy balance

Several studies have shown $NPY_{(1-36)}$ to be a potent orexigenic peptide with the ability to over-ride both short and long term mechanisms of satiety and body weight regulation (Akabayashi et al., 1994; Stanley et al., 1986). A single bolus ICV injection of $NPY_{(1-36)}$ results in the potent stimulation of food intake in rodents, sheep and monkeys (Clark et al., 1984; Larsen et al., 1999; Miner et al., 1989). NPY administration has also been shown to decrease energy expenditure (Billington et al., 1991), suppress sympathetic nerve activity (Egawa et al., 1991), inhibit the thyroid axis (Fekete et al., 2002) and increase lipogenesis of white adipose tissue (WAT) (Billington et al., 1991; Stanley et al., 1986).

Similarly to NPY, injections of AgRP and synthetic AgRP analogues have been shown to stimulate food intake, increase body weight, decrease oxygen consumption and decrease the capacity of brown adipose tissue (BAT) to expend energy (Fan et al., 1997; Rossi et al., 1998). The stimulatory effect of a single injection is apparent within 4 hours and lasts up to 6 days, which is a longer duration than seen with NPY.

A physiological role for the hypothalamic NPY/AgRP system in energy homeostasis is also suggested by the fact that the production and release of these neuropeptides is affected by changes in energy balance and nutritional state (Kalra et al., 1999). For example, in a state of negative energy when leptin levels are low (e.g. during fasting) or deficient (*ob/ob* mouse), expression levels of NPY are increased (Schwartz et al., 1996c; Wilding et al., 1993). In contrast, in states of positive energy balance, both leptin and insulin decrease NPY expression in the ARC (Krysiak et al., 1999; Schwartz et al., 1992). With regards to AgRP, an 18-fold increase in AgRP mRNA is observed after a 48-h fast in mice (Hahn et al., 1998). In contrast, levels are reduced by DIO in rats (Harrold et al., 1999).

1.10.3 Receptors

Recently six different NPY receptors have been characterised. These are GPCRs and have been designated Y_1–Y_6 (Larhammar, 1996). These not only mediate the effects of NPY but also other members of the pancreatic polypeptide (PP) family such as peptide YY (PYY) and pancreatic polypeptide (PP). Cloning studies have confirmed the existence of NPY-Y1, -Y2, -Y4 and Y5 receptors as distinct entities in the hypothalamus (Williams et al., 2001), where as the NPY-Y3 receptor subtype has been mapped mainly to the nucleus tractus solitarius (NTS) of the brainstem (Grundemar et al., 1991).

The C-terminal region of AgRP, which is sufficient for receptor binding, shares ~40% sequence homology with agouti, although they bind to distinct sets of receptors. Agouti binds to MC-R1 and MC-R4 while AgRP acts as a high affinity antagonist to MC-R3 and

MC-R4 (Ollmann et al., 1997; Yang et al., 1997). By being able to bind to MC-R3 and MC-R4 in the ARC, AgRP acts as an antagonist to α-MSH at these receptors.

1.10.4 Evidence for role of NPY and AgRP from murine models

Although a large body of evidence indicates that NPY is an important orexigenic neuropeptide, mice on a mixed genetic background lacking NPY show no abnormalities in food intake or body weight regulation (Qian et al., 2002; Thorsell and Heilig, 2002), This is possibly due to the presence of compensatory mechanisms or alternative orexigenic pathways, as well as redundancy in orexigenic signalling (Wynne et al., 2005). *Npy* null animals do however demonstrate an increase in fast-induced feeding (Bannon et al., 2000)

Interestingly, on a C57BL/6 background, *Npy* ablation is associated with an increase in body weight and adiposity and a significant defect in refeeding after a fast. This indicates that genetic background must be taken into account when the biological role of NPY (and indeed all genes) is studied (Segal-Lieberman et al., 2003). When *Npy* is genetically knocked out in *ob/ob* mice, this results in reduction of the hyperphagia and obesity associated with these animals, indicating the full response to leptin deficiency requires intact NPY signalling (Erickson et al., 1996).

The importance of AgRP in the regulation of appetite was confirmed with the development of transgenic mice over-expressing AgRP in the hypothalamus (Ollmann et al., 1997). These transgenics, although retaining their wildtype coat colour, were found to phenotypically resemble both the A^y and *MC-R4* null mice. They exhibited hyperphagia, obesity, increased body length, hyperinsulinaemia, late onset hyperglycaemia and pancreatic-islet hyperplasia (Ollmann et al., 1997).

At around 2-3 months of age, *Agrp* null animals exhibit subtle changes in response to feeding, following both a fast and treatment with MTII (Wortley et al., 2005). From 6

months of age onwards, *AgRP* null animals exhibit robust reductions in body weight and adiposity, increased metabolic rate, increased body temperature, and increased locomotor activity. In addition, *Agrp* null animals display increased levels of circulating thyroid hormone and increased expression of UCP-1 in BAT. These results provide further proof of the importance of the AgRP neuronal system in the regulation of energy homeostasis. With regards to the role of the actual neuron, four different approaches have been used to selectively target AgRP neurons for death, with all studies reporting a lean and hypophagic phenotype (Bewick et al., 2005; Gropp et al., 2005; Luquet et al, 2005; Xu et al, 2005a).

1.11 A model for the central control of food intake and body weight by insulin and leptin

Prior to the commencement of this work, the dominant view held in the field was that insulin and leptin regulated energy homeostasis via their actions on the POMC/CART and NPY/AgRP neurons of the ARC. This model is outlined below.

Insulin and leptin in the circulation enter the ARC region of the hypothalamus via the ME where the BBB is not present. They bind to their corresponding receptors present on the first-order NPY/AgRP and POMC/CART neurons. NPY/AgRP neurons are inhibited by leptin and insulin and are consequently activated in conditions where insulin and leptin are low. POMC/CART neurons are stimulated by leptin and insulin and are consequently activated in conditions where insulin and leptin are high (Schwartz et al., 2000). These first order neurons in the ARC integrate information concerning the energy balance of the individual and relay this to second-order neurons located in other hypothalamic regions involved in the control of food intake and body weight (Figure 1.4). For example, ARC NPY/AgRP and POMC/CART neurons project to TRH neurons of the PVN (Fekete et al., 2000). This ensures the transduction of peripheral signals into behavioural and metabolic responses that attempt to maintain body fat stores at a constant level (Barsh and Schwartz, 2002). Table 1.3 below summarises the different second-order neuronal populations of the various 'downstream' hypothalamic nuclei involved in transduction of the insulin/leptin adiposity signal into a response which effects the overall energy homeostasis status of the individual.

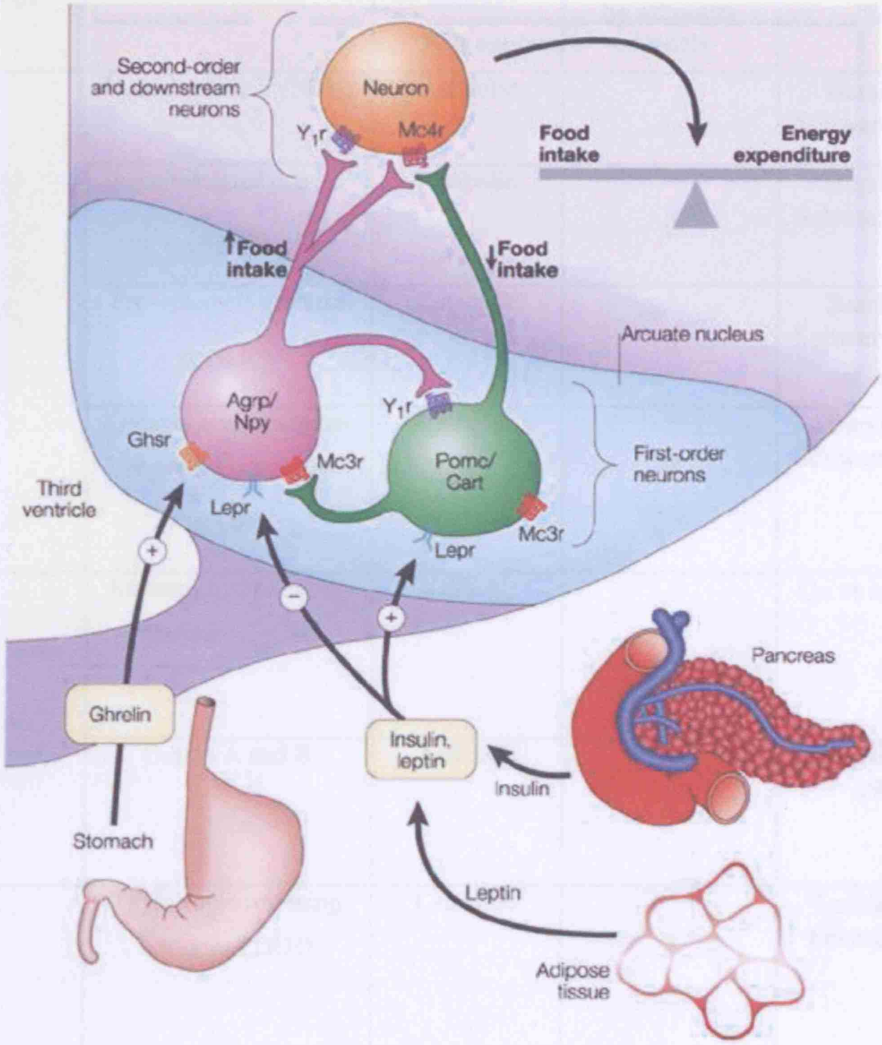

Figure 1.4: Summary of the control of energy homeostasis by arcuate nucleus neurons. The adiposity signals, insulin and leptin, circulate in proportion to body adipose stores and inhibit NPY/AgRP neurons and stimulate the adjacent POMC/CART neurons. Lower insulin and leptin levels are therefore predicted to activate NPY/AgRP neurons, while inhibiting POMC/CART. Ghsr, growth hormone secretagogue receptor; Lepr, leptin receptor; Mc3r/Mc4r, melanocortin 3/4 receptor; Y1r, neuropeptide Y1 receptor. Adapted from Barsh and Schwartz, 2002.

Hypothalamic Nucleus	Neuropeptide	Effect on energy Balance	Regulation by adiposity signals	Reference
ARC	Neuropeptide Y (NPY)	Anabolic	⇓	Barsh and Schwartz, 2002
	Agouti-related protein (AgRP)	Anabolic	⇓	Barsh and Schwartz, 2002
	Pro-opiomelanocortin (POMC)	Catabolic	⇑	Barsh and Schwartz, 2002
	Cocaine-amphetamine-regulated transcript (CART)	Catabolic	⇑	Barsh and Schwartz, 2002
LHA	Melanin concentrating hormone (MCH)	Anabolic	⇓	Qu et al., 1996
	Orexin A and B	Anabolic	⇓	Sakurai et al., 1998
PVN	Thyrotropin releasing hormone (TRH)	Catabolic	⇑	Lechan and Fekete, 2006
	Corticotrophin releasing hormone (CRH)	Catabolic	⇑	Rothwell, 1990; Mercer et al., 1996
	Galanin-like peptide	Anabolic	⇓	Gundlach, 2002

Table 1.3: Summary of the main first-order and second-order neuronal populations found in the various hypothalamic nuclei implicated in energy homeostasis. The effect of the neuropeptides on energy balance and the regulation of their expression by adiposity signals are also summarised.

1.12 Role of the CNS in the regulation of peripheral glucose homeostasis

In addition to its role in energy balance regulation, recent work has also highlighted a role for the brain in the regulation of peripheral glucose homeostasis and compensatory responses to hypoglycaemia (such as pancreatic glucagon release and sympathoadrenal activation). Lesions in the VMH of rats have been shown to suppress counter regulatory responses to hypoglycaemia (Borg et al., 1994) consistent with previous findings implicating a key role for this nucleus in regulating peripheral glucose homeostasis (Oomura et al., 1969). Specific neurons in both the VMH and LHA have also been shown to have the capability of sensing changes in ambient glucose concentrations (Funahashi et al., 1999; Oomura et al., 1969).

Such a role for the CNS is not a novel concept and in fact was proposed more than 150 years ago by the French physiologist Claude Bernard. He showed in rabbits that "piqûre" (pricking) of the floor of the fourth ventricle of the brain resulted in glucosuria (Bernard, 1855), and thus hypothesised that the CNS plays an essential role in the control of peripheral blood glucose levels.

Such evidence implicating hypothalamic pathways as key regulators of glucose homeostasis has renewed interest in the mechanisms linking obesity and diabetes, and suggests a role for hypothalamic dysfunction in the pathophysiology of diabetes.

1.12.1 Central insulin action and peripheral glucose metabolism

In addition to the direct effects of insulin on the liver, its role in regulating hepatic glucose production (HGP) via signalling events in the hypothalamus has drawn increasing attention. Insulin has been shown to modify peripheral glucose homeostasis through hypothalamic insulin receptors. *NIRKO* mice, with targeted disruption of the IR specifically in the brain, do not suppress HGP normally in response to a hyperinsulinaemic clamp (Fisher et al., 2005) In addition, central insulin administration has been shown to result in increased insulin sensitivity of peripheral tissues associated with a reduction in HGP (Obici et al.,

2002b). Interestingly, blockade of central ATP-activated potassium channel (K_{ATP} channels) with the sulfonylurea tolbutamide abolishes this effect (Obici et al., 2002b).

In support for the role of K_{ATP} channels in mediating the effects of central insulin action on peripheral glucose utilisation, a recent study has shown that insulin acts on K_{ATP} channels in hypothalamic neurons to control HGP via a method involving a decrease in hepatic glucose-6-phosphatase and phosphoenolpyruvate kinase expression (Pocai et al., 2005) Transection of the vagal nerve to the liver nullified this effect, pointing to a role for the autonomous nervous system in transmitting insulins central actions to the periphery. Despite significant advances in understanding with regards to the signalling events involved in K_{ATP} channel activation, the exact identity of the hypothalamic neuronal populations involved in the regulation of hepatic glucose output are still unclear. However, two recent studies have implicated the ARC as a key site for regulating peripheral glucose homeostasis.

In STZ-DM rats (with uncontrollable diabetes induced by streptozotocin), the blockade of hypothalamic insulin signalling was achieved via the infusion of a PI3K inhibitor into the ARC, prior to peripheral insulin injection. This was found to attenuate insulin-induced glucose lowering by approximately 35% - 40% (Gelling et al., 2006). Conversely, increased PI3K signalling, induced by hypothalamic overexpression of either IRS2 or AKT, enhanced the glycaemic response to insulin by approximately 2-fold in STZ-DM rats. These results thus indicate a crucial role for intact ARC insulin signalling in the peripheral response to insulin treatment.

In the second study, Morton et al (Morton et al., 2005) also used adenoviral microinjection techniques to express the LepR or a constitutively active mutant of AKT in the mediobasal hypothalamus. In both cases they showed that this resulted in improved peripheral insulin sensitivity and glucose response in rats lacking a functional leptin receptor (Morton et al., 2005).

Although the use of such microinjecting adenoviral technology does not allow the specific targeting of specific cell types, these studies have nonetheless highlighted a key role for the

ARC in the regulation of peripheral glucose homeostasis. Although the exact identity of the hypothalamic neurons that control hepatic glucose output remain unknown, the melanocortin pathway has been implicated (Farooqi et al., 2003; Marks and Cone, 2001; Obici et al., 2001; Schwartz, 2001). Melanocortin signalling acutely affects insulin levels and glucose uptake, and humans with MC-R4 mutations are extremely insulin resistant, more so than would be predicted by their degree of obesity (Fan et al., 1997; Farooqi et al., 2003; Obici et al., 2001).

1.13 Obesity, diabetes and insulin resistance

1.13.1 A triad of metabolic disorders

Obesity, insulin resistance and type 2 diabetes mellitus (T2DM) are a tightly linked common triad of metabolic disorders (Kahn and Flier, 2000). Despite major advances in unravelling the complex networks regulating food intake and energy balance, our understanding of the precise pathophysiological relationships between obesity, insulin resistance and T2DM is still rudimentary.

1.13.2 Diabetes Mellitus

Diabetes mellitus is currently the most common metabolic disease in the world with more than 180 million individuals affected worldwide. Global estimates for the year 2030 predict a further growth of more than 50%, to reach a total of 366 million affected individuals. Most of this increase will occur as a result of a 150% rise in the developing countries of Africa, Asia, and South America (WHO, 2007).

Of all of those with diabetes worldwide, 90% of individuals have T2DM, the non-insulin-dependent form of diabetes (Cummings and Schwartz, 2003).

1.13.3 Diabetes- a life threatening condition

Cardiovascular morbidity in patients with T2DM is two to four times greater than that of non-diabetic people (Zimmet et al., 2001). It is also important to note that the life expectancy of affected individuals is also reduced (Damsgaard et al., 1997; Gu et al., 1998; Sasaki et al., 1997). Indeed, each year 3.2 million deaths are attributable to diabetes worldwide (WHO 2007).

1.13.4 The pathophysiology of T2DM

T2DM is a polygenic disease and may involve polymorphisms in multiple genes encoding proteins involved in insulin signalling, insulin secretion and intermediary metabolism. Identifying the genetic variants that increase risk of T2DM has been a significant challenge. Recent studies have added considerably to our knowledge of the molecular mechanisms involved in the development of this disease.

The latest genome wide association studies of T2DM have revealed diabetes susceptibility loci in and around the genes *IGF2BP2*, *CDKAL1*, *CDKN2A/CDKN2B*, *TCF7L2*, *SLC30A8*, *HHEX*, *FTO*, *PPARG*, and *KCNJ1* (Saxena et al., 2007; Scott et al., 2007; Sladek et al., 2007; Zeggini et al., 2007). These studies confirm the existence of at least ten T2DM loci, and emphasise the contribution of multiple variants of modest effect. The regions identified underscore the importance of pathways influencing pancreatic β-cell development and function in the etiology of T2DM.

Environmental factors especially diet, physical activity and age, can also interact with genetic predisposition to affect disease prevalence and severity (Stern, 2000). T2DM is preceded by the development of insulin resistance in target tissues, but the molecular causes of its initiation and progression are still unclear.

1.13.5 Insulin resistance

In the initial stages of insulin resistance, islets initially compensate for the loss of sensitivity by expanding β-cell mass and insulin secretory capacity. Eventually this heightened demand cannot be met resulting in loss of β-cells and reduction in circulating insulin levels. This is despite continuing peripheral insulin resistance, and the consequence is chronic hyperglycaemia and overt T2DM (Stumvoll et al., 2005).

Insulin resistance is not only a fundamental aspect of the etiology of type 2 diabetes, but is also linked to a wide array of other conditions including hypertension, hyperlipidemia, atherosclerosis and polycystic ovarian disease (Kahn and Flier, 2000). It is characterised by defects at many levels including decreases in receptor concentration and kinase activity, concentration and phosphorylation of insulin receptor substrate proteins, phosphatidylinositol 3-kinase (PI3K) activity, glucose transporter translocation and the activity of intracellular enzymes (Saltiel and Kahn, 2001).

A combination of both genetic and environmental factors can profoundly influence insulin sensitivity. A strong genetic component for insulin resistance is suggested by the concordance between monozygotic twins and increased prevalence in first-degree relatives of affected individuals (Kahn et al., 1996). With regards to environmental factors, although obesity is the predominant risk factor for the onset of insulin resistance, other environmental factors such as physical inactivity also contribute. The precise mechanisms whereby obesity causes insulin resistance are complex and not completely understood.

1.14 The role of insulin in peripheral glucose homeostasis

To understand the cellular and molecular mechanisms responsible for T2DM, it is necessary to conceptualise the framework within which glycaemia is controlled (Figure 1.5).

1.14.1 Pancreatic islet function and glucose uptake

Plasma glucose levels are tightly regulated between 4 and 7 mM in normal individuals (DeFronzo, 2004). This narrow range is governed by a balance between glucose gut absorption, hepatic glucose production and uptake of glucose by peripheral tissues and organs. The balance between the utilisation and production of glucose is maintained at equilibrium by the opposing actions of insulin and glucagon. Increasing blood glucose levels result in the release of insulin from β-cells, which stimulates glucose transport into muscle and fat via GLUT4 glucose transporter mechanisms, whilst inhibiting hepatic glucose production (Kahn and Flier, 2000). Decreasing glucose levels result in the release of glucagon from the α-cells within the islets of Langerhans. This in turn results in the release of glucose stores and newly synthesised glucose into the bloodstream. Thus, the co-ordinated action of insulin and glucagon ensure that glucose homeostasis is maintained throughout a wide variety of physiological states (DeFronzo, 2004).

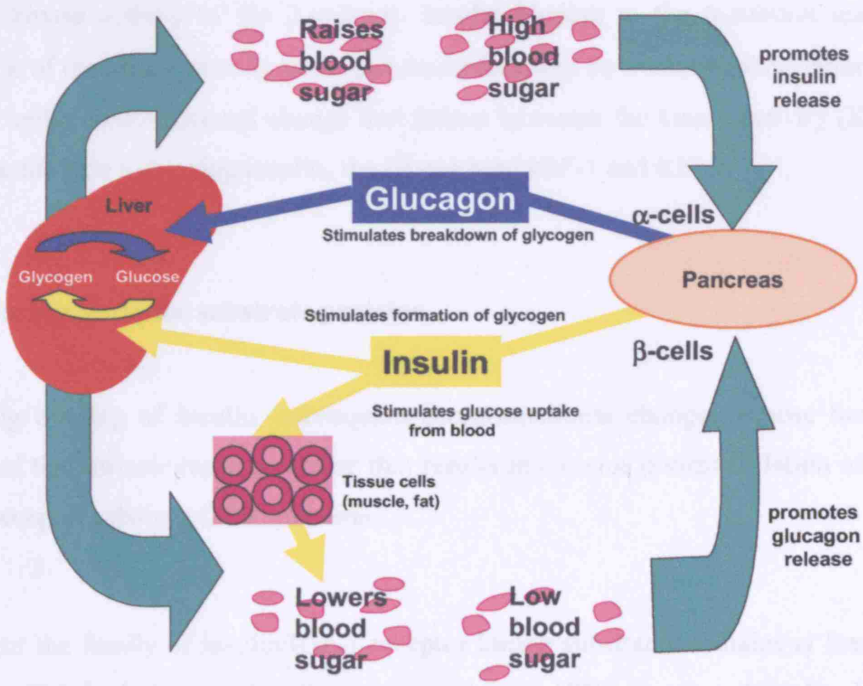

Figure 1.5: Regulation of plasma blood glucose by opposing actions of insulin and glucagon.

1.15 Insulin receptor signalling pathways

The binding of insulin to its receptor induces a cascade of intracellular signalling events that regulate key cellular functions, including glucose transport and oxidation, synthesis of glycogen, triglyceride and protein, and also regulation of gene expression (Nandi et al., 2004).

1.15.1 The insulin receptor family

The insulin receptor (IR) is present in virtually all vertebrate tissues although the level of expression varies. It belongs to a subfamily of receptor tyrosine kinases (RTKs) that includes the insulin like growth factor 1 (IGF-1) receptor and the insulin receptor-related receptor (IRR). These receptors are tetrameric proteins consisting of two alpha (α) and two beta (β) subunits, that function as an allosteric enzyme in which the α-subunit inhibits the tyrosine kinase activity of the β-subunit. Insulin binding to the α-subunit leads to de-repression of the kinase activity in the β-subunit followed by transphosphorylation of the β-subunits and a conformational change that further increases the kinase activity (Kido et al., 2001). In addition to binding insulin, the IR can bind IGF-1 and IGF-2.

1.15.2 Insulin receptor substrate proteins

Following binding of insulin, subsequent cconformational changes expose the catalytic domain of the intrinsic receptor kinase that results in tyrosine phosphorylation of cytosolic insulin receptor substrate (IRS) proteins.

At present the family of insulin/IGF-1 receptor kinase substrates contains at least thirteen members. This includes four insulin receptor substrate (IRS) proteins, three Src-Homology Collagen (SHC) proteins, growth factor receptor bound-2 (Grb-2) associated binder-I (Gab-1), and five members of the p62dok family (DOK1, DOK2, DOK3, DOK4 and DOK5) (Van Obberghen et al., 2001).

1.15.2.1 Irs proteins

The insulin receptor substrate (IRS) proteins represent key elements in insulin and IGF action. The IRS1 and IRS2 proteins are 185 kDa and 190 kDa in size respectively. Both are widely expressed in humans and mice. IRS3, a 60 kDa protein is largely restricted to adipose tissue. Expression of IRS4, a 160 kDa protein, is restricted to the thymus, brain, kidney and possibly β-cells (Van Obberghen et al., 2001).

IRS proteins lack intrinsic catalytic activity but are composed of multiple interaction domains and phosphorylation motifs (Van Obberghen et al., 2001) The four IRS proteins share in common an NH2 terminal pleckstrin homology (PH) domain followed by a phosphotyrosine binding (PTB) domain. Both the PH and PTB domains are highly conserved in each IRS protein. In addition, each IRS protein contains a poorly conserved domain of variable length containing several potential tyrosine phosphorylation sites in the COOH terminus (Figure 1.6).

The PH domains are believed to bind to acidic motifs in various proteins or to phospholipids in cell membranes. The PTB domains recognise N-P-x-Y motifs in proteins. Concerning the COOH terminus domain, insulin, IGF-1 and certain cytokine receptors phosphorylate IRS proteins at specific Y-x-x-M motifs within this domain. These motifs serve as docking sites for proteins that contain SH2 (Src-homology-2) domains. Phosphorylation of the tyrosine residues of IRS proteins increases the affinity with which they bind other signalling molecules. Each tyrosine phosphorylated motif of the IRS proteins is able to bind to a specific signalling molecule, and thus different protein complexes can be formed resulting in the engagement of various signalling pathways (White, 2002).

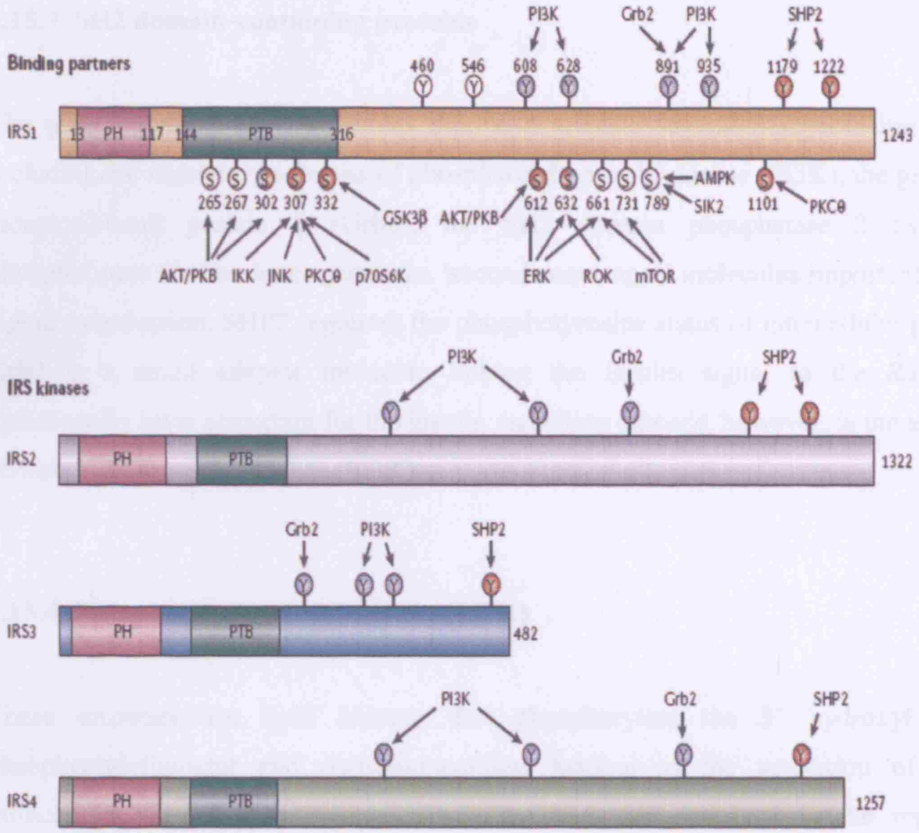

Figure 1.6: Structure and interacting partners of the insulin-receptor substrates. The four insulin-receptor substrate (IRS) isoforms, IRS1, IRS2, IRS3 and IRS4, share a pleckstrin-homology (PH) domain (magenta), a phosphotyrosine-binding (PTB) domain (dark green) and several sites of phosphorylation on tyrosine and serine residues. The positions of the tyrosine residues (Y) that are phosphorylated by the IR and the downstream-signalling proteins that bind to these sites are shown. The positions of the serine residues (S) and the kinases responsible for their phosphorylation are also shown. Blue circles represent sites of positive regulation, whereas red circles represent sites of negative regulation. Circles with both colours depict sites in which the regulation has been reported to be either positive or negative under various conditions. White circles represent sites in which the effect of phosphorylation is currently unknown. phosphatidylinositol 3-kinase (PI3K), growth-factor-receptor-bound protein-2 (Grb2), Src-homology-2 (SH2) domain-containing tyrosine phosphatase-2 (SHP2), AKT, IκB kinase (IKK), c-Jun-N-terminal kinase (JNK), protein kinase Cθ (PKCθ), p70 ribosomal protein S6 kinase ($p70^{S6K}$), glycogen synthase kinase-3 β (GSK3β). Adapted from Taniguchi et al., 2006.

1.15.3 SH2 domain-containing proteins

The phosphorylated IRS molecules bind and activate several SH2 containing proteins, including the regulatory subunits of phosphatidylinositol 3-kinase (PI3K), the growth factor receptor-bound protein 2 (Grb2), the SH2 domain phosphatase 2 (SHP2), and phospholipase C. The latter generates 'second messenger' molecules important for insulin signal transduction. SHP2 regulates the phosphotyrosine status of intracellular proteins and Grb2 is a small adaptor molecule linking the insulin signal to the *Ras* pathway. Functionally most important for the insulin signalling cascade, however, is the activation of phosphatidylinositol 3-kinase (PI3K).

1.15.4 Phosphatidylinositol 3-kinase (PI3K)

These enzymes are lipid kinases that phosphorylate the 3' hydroxyl group of phosphoatidylinoistol and phosphoinositides leading to the activation of numerous intracellular signalling pathways. These pathways are involved in the regulation of functions as diverse as cell metabolism, vesicle trafficking, survival and polarity. Numerous PI3Ks have been identified using both biochemical approaches and PCR-based cloning strategies. They are divided into three classes (I-III) based on both their substrate preference and sequence homology (Figure 1.7).

Class I PI3Ks are the main type involved in insulin signalling and consist of two groups: class IA and class IB. This classification depends on the receptor types to which they couple. Class IA PI3Ks are activated by RTKs whereas class IB PI3Ks are activated by GPCRs (Katso et al., 2001)

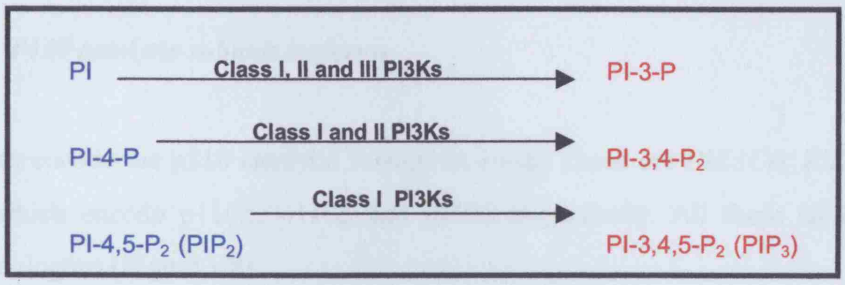

Figure 1.7: There are three classes (I–III) of PI3K which show distinct substrate preferences. *In vivo,* class I PI3Ks generate phosphatidylinositol-3,4,5-trisphosphate (PIP_3) from phosphatidylinositol-4,5-bisphosphate (PIP_2). Class III PI3Ks generate phosphatidylinositol-3-phosphate (PI-3-P) from phosphatidylinositol (PI). Class II PI3Ks preferentially generate PI-3-P and phosphatidylinositol-3,4-biphosphate(PI-3,4-P_2) *in vitro.*

1.15.5 Class IA PI3Ks

Class IA PI3K is a heterodimer that consists of a p85 regulatory subunit and a p110 catalytic subunit. In mammals there are numerous isoforms of each subunit. It is not currently known if specific catalytic and regulatory subunit interactions mediate distinct physiologic outputs. The main role of class IA PI3Ks seems to be the direction of energy into cell growth and proliferations.

1.15.5.1 P85 regulatory subunit isoforms

Three genes: *PI3KR1, PI3KR2* and *PI3KR3* encode the p85α, p85β and p55γ isoforms of the p85 regulatory subunit respectively. The *PI3KR1* gene has also been shown to give rise to two shorter isoforms p55α and p50α by alternative transcription-initiation sites. The structures of the class IA p85 regulatory isoforms are shown in Figure 1.8. The p85 regulatory subunit is vital in mediating the activation of class IA PI3K by RTKs, as the SH2 domains bind to phospho-tyrosine residues in the sequence context pY-x-x-M on activated RTKs or adaptor molecules such as IRS1. This binding results in the removal of the basal inhibition of p110 by p85 and the subsequent recruitment of the p85-p110 heterodimer to its substrate (PIP_2) at the plasma membrane.

1.15.5.2 P110 catalytic subunit isoforms

Three genes encode the p110 catalytic subunit isoforms. These are *PIK3Cα, PIK3Cβ* and *PIK3Cδ*, which encode p110α, p110β and p110δ respectively. All these isoforms are highly homologous (Figure 1.8).

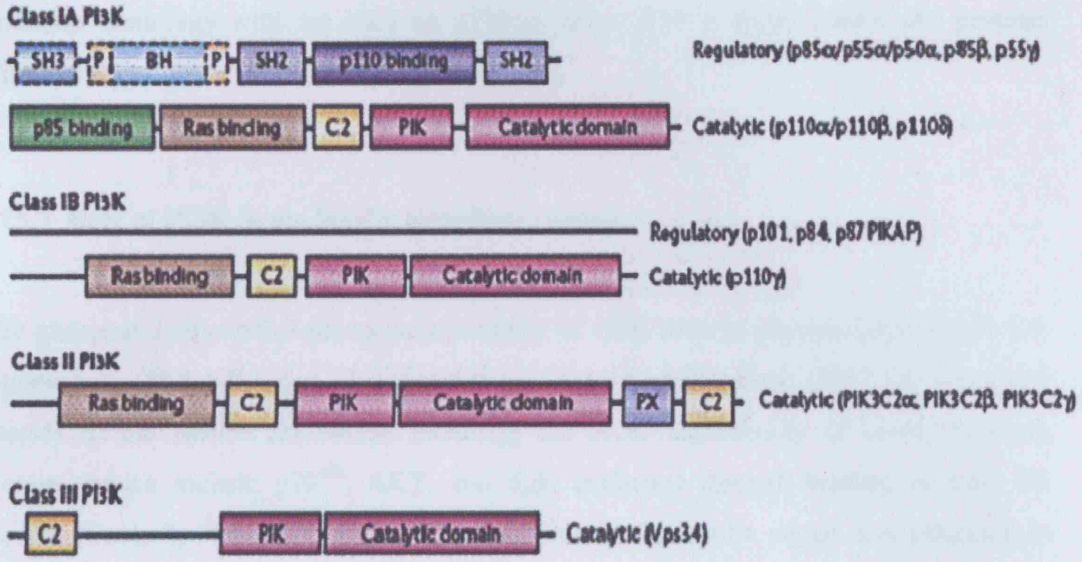

Figure 1.8: Schema depicting the domain structures of various PI3K isoforms. Class IA PI3K is a heterodimer that consists of a p85 regulatory subunit and a p110 catalytic subunit. The class IA p85 regulatory isoforms have a common core structure consisting of a p110-binding domain (also called the inter-SH2 domain) flanked by two Src-homology 2 (SH2) domains. Class IB PI3K is a heterodimer consisting of a p101 regulatory subunit and a p110γ catalytic subunit. Although p110γ shares extensive homology with the class IA p110 proteins, p101 is distinct from p85 proteins. Class II PI3Ks consist of only a p110-like catalytic subunit. The three isoforms of class II PI3Ks share significant sequence homology with the class I p110 subunits. Class II PI3Ks have an extended divergent N terminus, and additional domains at the C terminus. Class III PI3Ks consist of a single member, Vps34. Adapted from Engelman et al., 2006.

1.15.6 Class IB PI3Ks

This class of PI3Ks are not regulated by RTKs, as they do not possess a p85 family regulatory subunit. However, similarly to the class IA kinases they are also heterodimers consisting of a p101 regulatory subunit and a p110γ catalytic subunit. The p101 regulatory subunit facilitates the activation of the p110γ subunit of the heterodimer complex by direct interaction with Gβγ complexes of heterotrimeric G proteins. Although p110γ shares extensive homology with the class IA p110 proteins, p101 is distinct from p85 proteins (Figure 1.8).

1.15.7 Role of PI3K in the insulin signalling cascade

The phosphatidylinositol-3-phosphates products of PI3K such as phosphatidylinositol-3,4-biphosphate (PI-3,4-P_2) and phosphatidylinositol-3,4,5-triphosphate (PIP_3) recruit serine kinases to the plasma membrane including the AGC superfamily of serine/threonine kinases (which include $p70^{s6k}$, AKT, and SgK isoforms) through binding to their PH domain (Cantrell, 2001). These play a central role in the insulin signal diversification to downstream pathways relating to carbohydrate metabolism and lipolysis, as well as to gene expression, transcription and protein turnover (Shepherd et al., 1998).

1.15.8 AKT and PDK-1

The binding of PIP_3 to the PH domain of the cytosolic serine/threonine kinase AKT (a 57 kDa protein also known as protein kinase B, PKB) and to the 63 kDa phosphoinositide-dependent kinase-1 (PDK-1) results in the co-localisation of these two proteins at the membrane (Cantrell, 2001). During this co-localisation, PDK-1 phosphorylates and activates AKT which in turn phosphorylates a variety of substrates that enable the control of various biological signalling cascades such as glucose transport, protein synthesis, cell proliferation, cell survival, glycogen synthesis and inhibition of lipolysis and gene expression (White, 2002).

1.15.9 Mitogenic insulin effects

In addition to its metabolic effects, insulin plays a major role in regulating cell growth, differentiation, and apoptosis (Shepherd et al., 1998; Vanhaesebroeck and Alessi, 2000). The signal for these responses is initially transmitted through phosphorylated IRS proteins but then diversifies.

One main branch of the cascade follows the described PI3K pathway, with AKT exerting an anti-apoptotic effect when constitutively over-expressed (Sabbatini and McCormick, 1999). AKT phosphorylates the anti-apoptotic protein BAD, activates the IkB kinases (IKKs) that liberate the cell survival transcription factor NF-κB, and also promotes the nuclear exclusion of forkhead transcription factors which subsequently reduce transcription of the apoptosis factor Fas ligand (Vanhaesebroeck and Alessi, 2000). AKT1 appears to be responsible for these processes, as a targeted deletion of this isoform leads to dwarfism and increased apoptosis in mice (Chen et al., 2001; Cho et al., 2001).

A second major branch of mitogenic insulin signalling is the Grb2/SOS/Ras and Raf-1/ MEK/ERK serine kinase cascade (Tomlinson, 1999). Although largely distinct from the PI3K pathway, there is cellular communication between the two. Following association with an IRS protein, a complex of Grb2 with the Son of Sevenless (SOS) exchange protein activates the small, membrane-bound G-protein Ras by exchanging GDP for GTP. Once activated Ras operates as a molecular switch stimulating a serine kinase cascade through the stepwise activation of Raf, MAP kinase kinase (MEK) and MAP kinase (ERK) (Roberts, 1992). Activated ERK can translocate into the nucleus where it catalyses the phosphorylation of transcription factors (e.g. elk1, c-*fos*), initiating a transcriptional programme that leads to cellular proliferation or differentiation.

Emerging consensus is that the acute metabolic effects of insulin require activation of the IRS to PI3K pathway, where as the Ras-MAPK pathway plays a role in certain tissues to stimulate the actions of insulin on growth proliferation. Figure 1.9 is a summary of insulin signalling transduction pathways.

1.15.8.1 AKT mediated effects on glucose homeostasis and protein synthesis

Activated AKT plays an important and diverse role in glucose homeostasis. Three separately encoded proteins are currently known: AKT1, AKT2, and AKT3. The AKT2 isoform mediates the insulin-dependent translocation of GLUT-4 molecules from intracellular storage vesicles into the plasma membrane, thus facilitating glucose influx into the cell and lowering plasma glucose levels (Bae et al., 2003; Cho et al., 2001). Conversely, its absence leads to insulin resistance and hyperglycaemia (Cho et al., 2001). AKT inactivates glycogen synthase kinase 3 (GSK3) by phosphorylation, which in turn activates glycogen synthase and promotes glucose storage in liver and skeletal muscle (Summers et al., 1999). AKT also downregulates phosphoenolpyruvate carboxykinase (PEPCK), a key enzyme of gluconeogenesis, thus reducing HGP (Gabbay et al., 1996; Summers et al., 1999).

The FOXO forkhead transcription factors are also direct targets for AKT. Their phosphorylation leads to exclusion from the nucleus and thus inhibition of the transcription of the genes involved in gluconeogenesis, ketogenesis, and fatty acid oxidation (Wolfrum et al., 2004). Several studies have shown a role for FOXO1 in mediating the metabolic actions of insulin, including hepatic gluconeogenesis, skeletal muscle glucose disposal, adipocyte differentiation and pancreatic β-cell growth (Kitamura et al., 2002; Furuyama et al., 2003; Nakae et al., 2003; Puigserver et al., 2003; Matsumoto et al., 2006; Naimi et al., 2007).

In addition, AKT can also regulate protein synthesis by inhibiting the activities of Tuberous Sclerosis-1 and 2 (TSC1-TSC2) enzymes (Garami et al., 2003). TSC-1 and TSC-2 have an inhibitory role on the mammalian Target of Rapamycin (mTOR), which mediates protein synthesis by its stimulatory effects upon elongation factor-4E binding protein (4E-BP1) and the p70 ribosomal s6 protein kinase ($p70^{s6k}$) (Garami et al., 2003). The $p70^{s6k}$ protein is responsible for phosphorylation of the 40S ribosomal protein S6, and thereby regulates the translation of several hundred mRNAs.

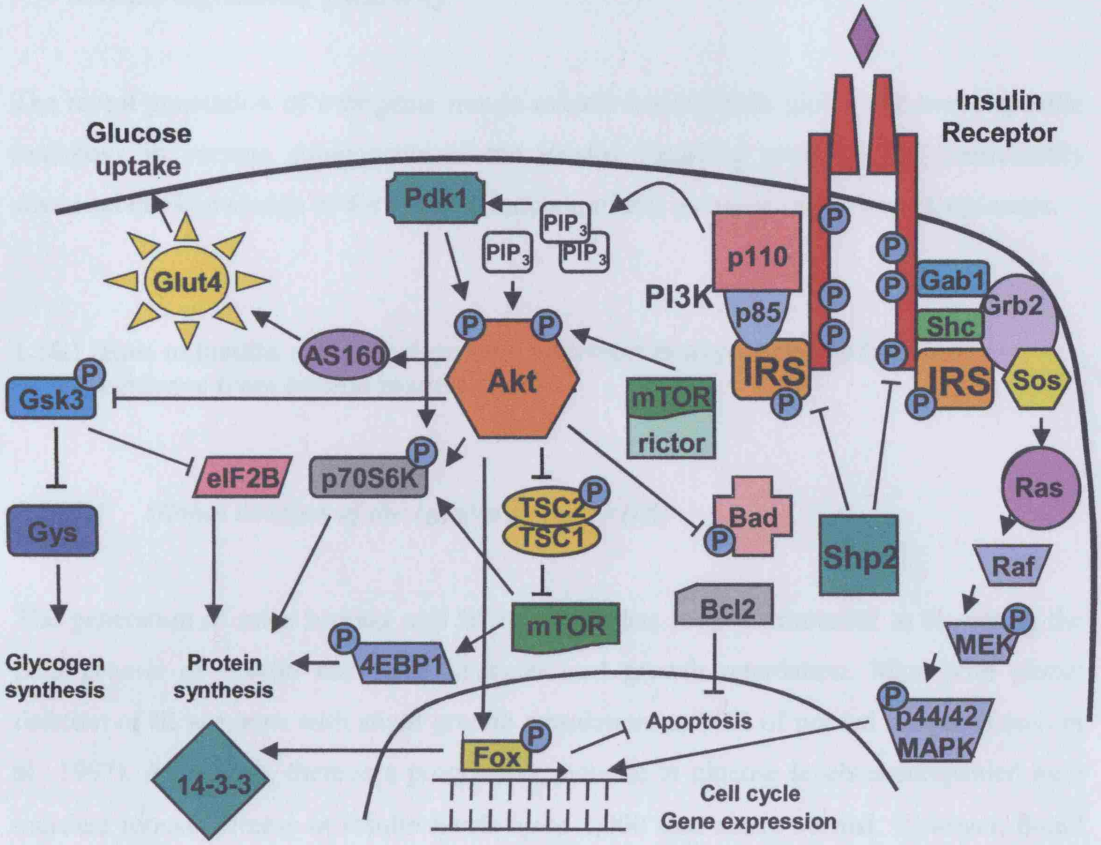

Figure 1.9: Insulin signalling cascade. Following ligand binding, the activated insulin receptor recruits insulin receptor substrate (IRS) and other molecules (Grb2, Gab1, Shc). These scaffold proteins initiate a signalling cascade via Sos- Ras-Raf-MEK to activate p44/42 MAPK, which regulates gene transcription related to cell proliferation and apoptosis. p110 recruitment to Irsbound p85 activates PI3K and generates PIP_3 molecules. This leads to Pdk1-mediated AKT activation, which diversifies the insulin signal. Glucose transport is enhanced by AS160-mediated Glut4 translocation, and glycogen synthesis is stimulated by Gsk3 inhibition. AKT increases protein synthesis directly by activating $p70^{S6K}$ and indirectly through TSC1:TSC2 complex phosphorylation, the mTOR-4EBP1 pathway, and the Gsk3-associated de-repression of eIF2B. AKT phosphorylates nuclear Fox transcription factors, leading to their exclusion from the nucleus. Fox proteins control gene expression, elements of the cell cycle and influence apoptosis. AKT also regulates apoptosis through Bcl2-related proteins.

1.16 Murine models of obesity: insights into the role and function of the insulin signalling pathway

The recent generation of transgenic mouse models bearing both global and tissue-specific mutations in various components of the insulin signalling pathway has considerably advanced our knowledge of the role and function of this pathway and its key components.

1.16.1 Role of insulin receptor signalling pathways in hypothalamic function: evidence from animal models

1.16.1.1 Global deletion of the Insulin Receptor (IR)

The generation of mice bearing null IR mutations has been instrumental in dissecting the pathogenesis of insulin resistance, diabetes and growth retardation. Mice with global deletion of IR are born with slight growth retardation, at 90% of normal weight (Louvi et al., 1997). After birth, there is a progressive increase in glucose levels accompanied by a transient robust increase in insulin levels up to 1,000 fold above normal. However, β-cell failure occurs within a few days characterised by extensive degranulation of β-cells (Nakae et al., 2001). Mice eventually die of diabetic ketoacidosis. Thus the insulin receptor is necessary for postnatal fuel homeostasis but not for pre-natal growth and metabolic control (Nandi et al., 2004).

1.16.1.2 Neuronal deletion of the Insulin Receptor

In the CNS, insulin receptors are expressed at high levels in many areas of the brain including the olfactory bulb, the hypothalamus and the pituitary. Although neurons are known to metabolise glucose in an insulin independent manner, the generation of mice with global neuronal deletion of the IR has helped address the physiological role of insulin signalling in the brain.

Mice with global neuronal-specific ablation of the IR (*NIRKO* mice) were generated using the Cre/LoxP system (Bruning et al., 2000). Inactivation of the IR had no effect on brain development or neuronal survival. However, female *NIRKO* mice were hyperphagic, with both male and female *NIRKO* mice demonstrating DIO. Consistent with this, both sexes exhibited about a two-fold increase in perigonadal WAT, with concordant increases in plasma leptin levels. In addition, *NIRKO* mice developed mild insulin resistance, had elevated plasma insulin levels and hypertriglyceridemia. Surprisingly, both male and female mice had subfertility. Taken together, these results implicate CNS insulin receptor signalling in the regulation of energy disposal, fuel metabolism and reproduction.

The use of anti-sense technology has also highlighted the role of insulin signalling in the hypothalamus (Obici et al., 2002a). In this study, anti-sense oligodeoxynucleotides directed against the IR were injected directly into the third cerebral ventricle of rats. Following a seven day infusion, hypothalamic IR levels decreased by 80% in the ARC region of the hypothalamus. This selective decrease in hypothalamic IRs was accompanied by rapid-onset hyperphagia and increased fat mass. In addition, during insulin clamp studies, physiological hyperinsulinaemia decreased glucose production by 25% in rats treated with the anti-sense oligodeoxynucleotides in contrast to 55% in those treated with control oligodeoxynucleotides.

Taken together, these studies indicate that insulin receptors in discrete areas of the hypothalamus have a physiological role in the control of food intake, fat mass, and hepatic action of insulin.

The use of conditional gene targeting has allowed further dissection of the role of insulin receptor signalling in various insulin target tissues including muscle and liver. Table 1.4 below summarises the various phenotypes of the tissue-specific insulin receptor knockouts that have been generated.

Tissue specific insulin receptor knockout	Phenotype	Reference
Global	Diabetic ketoacidosis and subsequent death	Louvi et al, 1997
Muscle	Dyslipidaemia	Bruning et al., 1998
Cardiac Muscle	Reduced heart size and performance	Belke et al., 2002
Muscle/adipose tissue	Impaired glucose tolerance	Lauro et al., 1998
Adipocyte	Protection against obesity and increased longevity	Bluher et al., 2002; Bluher et al., 2003
Liver	Moderate insulin resistance and hyperglycaemia	Michael et al., 2000
β-cell	Impaired glucose tolerance	Kulkarni et al., 1999
Vascular endothelium	Protection from hypoxia-Induced neovascularisation	Vicent et al., 2003

Table 1.4: Summary of the phenotypic effect of the deletion of the insulin receptor in various tissues. Adapted from Nandi et al., 2004.

1.16.2 Different roles of the IRS proteins: evidence from animal models

Gene deletion studies in mice have shown that despite their close homology, the four IRS proteins serve different though complementary roles in insulin/IGF-1 signalling (Table 1.5 and Figure 1.10).

1.16.2.1 Irs1 null mice

Disruption of *Irs1* in mice results in both pre- and post natal growth retardation (Araki et al., 1994). In addition, mice exhibit insulin resistance in peripheral tissues and impaired glucose tolerance. However, diabetes does not develop in these mice as insulin secretion increases to compensate for the mild resistance to insulin. Altogether, this suggests an important role of IRS1 in both insulin and IGF-1 actions.

1.16.2.2 Irs2 null mice

Irs2 null mice exhibit mild peripheral insulin resistance and β-cell deficiency at birth (Withers et al., 1998). Subsequent β-cell failure in the face of continued peripheral insulin resistance causes overt fasting hyperglycaemia without ketoacidosis, a common characteristic of human T2DM. The early β-cell failure was found to be a result of reduced IRS2-mediated IGF-1 signalling causing defects in β-cell development and survival (Withers et al., 1999). The metabolic phenotye showed marked sexual dimorphism, whereby male animals developed overt diabetes from 8-10 weeks of age and females displayed compensatory hyperinsulinaemia for more than one year.

In addition to the role of IRS2 signalling in suppression of hepatic gluconeogenesis and the regulation of lipolysis and glycogen metabolism in skeletal muscle, IRS2 also plays complex roles in neuroendocrine function (Burks et al., 2000c). Independent of the diabetic phenotype and despite having elevated leptin levels, *Irs2* null females mice are hyperphagic and develop obesity (Burks et al., 2000c).

These findings not only suggest the presence of leptin resistance but also that CNS insulin action or components of the insulin signalling pathways are also necessary for intact neuronal responsiveness to leptin. Indeed, STAT3 phosphorylation in response to leptin is defective in *Irs2* null mice, suggesting some signalling convergence between leptin and insulin (Burks et al., 2000c). These findings support the hypothesis of potential cross talk

between insulin and leptin signalling in the CNS, with IRS2 implicated as a convergence point between the two pathways. In contrast to *Irs1* KO mice, *Irs2* KO mice have defective growth in only some tissues, including certain regions of the brain, islets and retina. Finally, *Irs2* null females are infertile, and have small anovulatory ovaries with reduced number of follicles (Burks et al., 2000c).

1.16.2.3 Irs3 and Irs4 null mice

Irs3 null and *Irs4* null mice have normal or near normal growth and metabolism. Ablation of *Irs3* is devoid of a clear phenotype (Bjornholm et al., 2002). Ablation of *Irs4* is associated with modest growth retardation and insulin resistance (Bjornholm et al., 2002; Fantin et al., 2000).

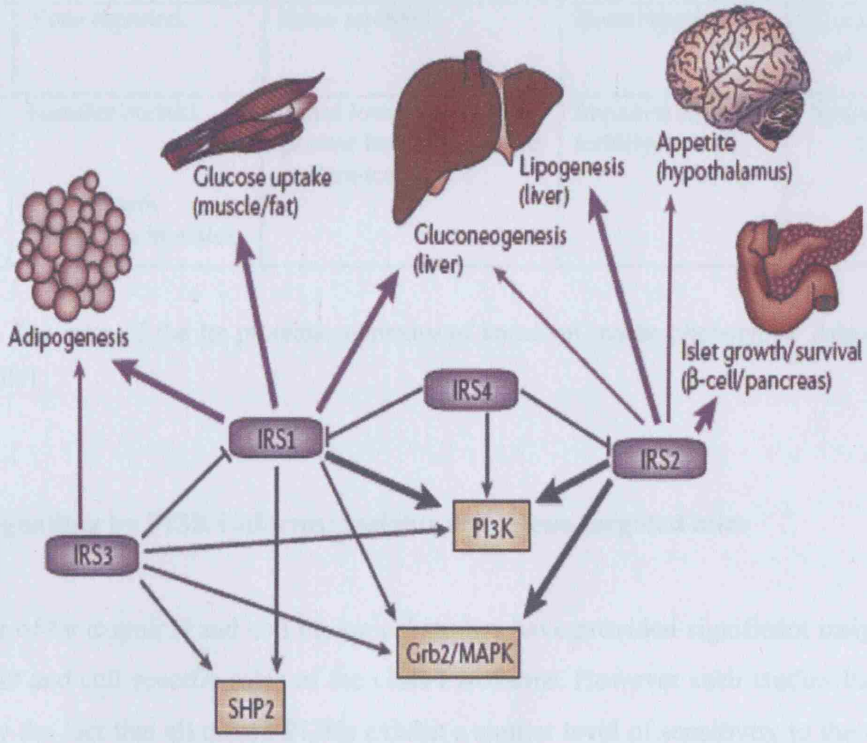

Figure 1.10: Isoform-specific functions of IRS proteins. Summary of the relative contribution of each insulin-receptor substrate (IRS) isoform (purple boxes) to the biological actions that are regulated by insulin (black arrows), as determined by knockdown and knockout studies. Adapted from Taniguchi et al., 2006.

IRS protein	Development and growth	Metabolic phenotype	Neuroendocrine phenotype	References
IRS1	Intrauterine and post-partum growth retardation (~ 40%).	Insulin resistance in skeletal muscle *in vivo*. Impaired glucose uptake in muscle and fat *in vitro*.	None reported.	Araki et al., 1994
IRS2	Intrauterine and post-partum growth retardation (~ 10%). Impaired β-cell development.	Hypertriglyceridaemia. Insulin resistance *in vivo* in liver, muscle and fat. Normal glucose uptake in muscle and fat *in vitro*.	Female infertility. Hyperphagia and obesity. Hyperleptinaemia.	Withers et al., 1998 Burks et al., 2000c
IRS3	None reported.	None reported.	None reported.	Bjornholm et al., 2002
IRS4	Females normal. Mild growth retardation in males.	Males lower fasting glucose but mild glucose intolerance.	Impaired female fertility.	Fantin et al., 2000

Table 1.5: The roles of the Irs proteins: summary of knockout mouse phenotypes. Adapted from Withers, 2001.

1.16.3 Signalling by PI3K isoforms: insights from gene-targeted mice

A number of biochemical and cell biological studies have provided significant insights into the distinct and cell specific roles of the class I isoforms. However such studies have been limited by the fact that all class I PI3Ks exhibit a similar level of sensitivity to the classical PI3K inhibitors wortmannin and LY294002. Other approaches have therefore been taken, such as the microinjection of isoform-specific neutralising antibodies. These studies have also had limited success, as not all cells are amenable to microinjection, and so do not allow

the investigation of specific isoform functions in different organs or other physiological settings involving live animals.

Nonetheless, our understanding of the *in vivo* function of the various isoforms of class I PI3Ks has been expanded considerably in recent years with the use of gene deletion studies in mice. These studies have highlighted the key role of class IA PI3K signalling in the context of the regulation of growth and metabolism. The dysregulation of this pathway is crucial for the pathophysiology of a number of human diseases, most notably in T2DM and cancer.

1.16.3.1 Targeted disruption of the catalytic subunits

All class I catalytic isoforms have been inactivated by gene targeting. A description of studies focusing on p110δ and p110γ isoforms, predominantly expressed in cells of the immune system, are beyond the scope of this work. However, the results of studies targeting the p110α and p110β isoforms, both of which have broad tissue distribution, are summarised in Table 1.6 below. These studies indicate an important role for PI3Ks during embryonic development as both the *p110α* null (Bi et al., 1999) and *p110β* null animals (Bi et al., 2002) were embryonically lethal. Interestingly, despite the embryonic lethality of *p110α* null and *p110β* null mice, animals that are heterozygous for deletion of both the p110α and p110β alleles ($p110\alpha^{+/-}p110\beta^{+/-}$) are normal compared to controls (Brachmann et al., 2005). These studies indicate non-redundant roles for p110α and p110β, since lacking one copy of each gene did not replicate the phenotypes seen when both copies of either gene is targeted.

With regards to the function of the catalytic subunits in normal metabolic function, the study of Foukas and colleagues demonstrated a critical role for p110α in growth factor and metabolic signalling (Foukas et al., 2006). Mice heterozygous for a p110α kinase dead knockin exhibited reduced somatic growth, hyperinsulinaemia, glucose intolerance, hyperphagia and increased adiposity. The explanation for the metabolic phenotype

displayed by these mice stems from the highly selective recruitment and activation of p110α to IRS signalling complexes. To date, no groups have replicated the studies of Foukas et al with regards to the p110β catalytic subunit, and so the role of this isoform in the regulation of metabolism is still unknown.

Targeted subunit	Viability	Metabolic Phenotype	Biochemical Features	Reference
p110α KO (homozygous)	Embryonic lethal. [E10.5]	Not applicable.	Increased expression of p85.	Bi et al., 1999
p110β KO (homozygous)	Embryonic lethal. [E3.5]	Not applicable.	Not applicable.	Bi et al., 2002
p110α KI (heterozygous)	Viable.	Reduced somatic growth. Hyperinsulinaemia. Glucose tolerance. Hyperphagia. Increased adiposity.	Severely blunted signalling via IRS proteins.	Foukas et al., 2000
$p110\alpha^{+/-}p110\beta^{+/-}$ KO (heterozygous)	Viable.	Normal.	Normal.	Brachmann et al., 2005

Table 1.6: Metabolic phenotypes of mice with targeted PI3K catalytic subunits. KO, Knockout, KI, knockin. Adapted from Vanhaesebroeck et al., 2005.

1.16.3.2 Targeted disruption of the regulatory subunits

To date, four mouse lines with targeted deletion of the class IA PI3K regulatory subunits have been generated. The resulting phenotypes of these four models are summarised in the below Table 1.7. It should be taken into account that deletion of class IA regulatory subunits often alters the PI3K subunit profile in cells, and as consequence it is very difficult to ascertain the roles of the various regulatory subunit isoforms.

Targeted Subunit	Metabolic Phenotype	Biochemical features		
		Changes in PI3K subunit expression	AKT Ser473 phosphorylation upon insulin/IGF-1 stimulation	Lipid kinase activity - levels upon insulin/IGF-1 stimulation
p85α p55α p50α (pan p85α) homozygous (perinatal lethality)	Hypoglycaemia. Hypoinsulinaemia.	Increased p85β. Decreased p110α. Increased p110β.	Liver and skeletal muscle unaffected. MEFs: decreased upon insulin and IGF-1 stimulation. ES cells: decreased upon IGF-1.	Liver and muscle: decreased pY-associated activity. Adipocytes: decreased. MEFs: decreased PIP_3 levels and pY-associated activity *in vivo* upon IGF-1 stimulation.
p85α p55α p50α (pan p85α) heterozygous	Increased glucose tolerance. Increased insulin sensitivity.	Increased p85β. p110α unaffected. p110β unaffected.	Liver and skeletal muscle: increased upon intravenous insulin MEFs: increased upon IGF-1.	Liver and muscle: increased pY-associated activity. MEFs:increased PIP_3 levels *in vivo* upon IGF-1 stimulation.
p85α only (still express p55α and p50α)	Increased insulin sensitivity Hypoglycaemia.	Increased p55α and increased p50α in muscle and fat cells. p110α and p110β unaffected	Adipocytes: not reported.	Adipocytes: increased PIP_3 levels. Muscle and adipocytes: decreased pY-associated activity. Muscle: increased IRS2-associated activity and decreased pY- and IRS1-ssociated activity.
p55α and p50α (still express p85α)	Increased insulin sensitivity.	In muscle: decreased p85α In adipocyte and liver: p85α unaffected	Muscle: increased upon insulin stimulation. Isolated adipocytes: not affected upon insulin stimulation.	
p85β	Increased insulin sensitivity. Hypoglycaemia. Hypoinsulinaemia.	p85α, p55α, p50α, 110α and p110β not affected	Muscle: increased upon insulin stimulation Liver: not affected upon insulin stimulation	Muscle: increased IRS2-associated activity.

Table 1.7: Viability and metabolic phenotypes of mice with targeted regulatory subunits. pY denotes tyrosine phosphorylation. Adapted from Vanhaesebroeck et al., 2005.

1.16.3.3 Effect of targeting of regulatory subunits on p110 catalytic subunits and other non-targeted regulatory subunits

Data suggests that p110 isoforms do not demonstrate a binding specificity for distinct regulatory subunits (Vanhaesebroeck et al., 2005). As a result, deletion of regulatory subunits interferes with the ability of all catalytic subunits to become recruited to pY (phosphorylated tyrosine), with the level of impact being relative to the expression level of the targeted regulatory subunit. This is evident when comparing the effects of deletion of p85α with the effects of p85β deletion, on the level of p110 expression levels. The p85α isoform is widely expressed and is the most abundant class IA regulatory subunit. Upon its deletion (pan-85α null animals), the expression levels of all isoforms is severely reduced (Fruman et al., 2000). In contrast, the deletion of p85β (expressed at considerably lower levels) has no affect on the expression of other Class IA subunits (Ueki et al., 2002). These findings are consistent with the suggested role of the regulatory subunits in the stabilisation of the p110 catalytic subunits (Ueki et al., 2002).

With regards to the effect on regulatory subunits, targeting of the various products of the *PIK3R1* gene also changes the expression pattern of non-targeted regulatory subunits. Due to the likelihood of the various regulatory subunits having distinct biological and signalling functions, interpretation of any observed phenotype in transgenic lines targeting regulatory subunits is further complicated. In addition, it is possible that the removal of one regulatory subunit isoform results in the facilitation of recruitment of other isoforms even if not upregulated (Vanhaesebroeck et al., 2005).

1.16.4 Role of signals downstream of AKT in the hypothalamic regulation of energy homeostasis

1.16.4.1 Role for $p70^{s6k}$

Previous studies have indicated a key role for $p70^{s6k}$ (an effector of mTOR) in the regulation of glucose homeostasis. Mice null for this kinase are hypoinsulinaemic, glucose intolerant and have reduced β-cell mass (Pende et al., 2000). These animals exhibit normal fasting blood glucose levels, indicating an increased sensitivity to insulin. With regards to hypothalamic function, Um and colleagues have since reported that

$p70^{s6k}$ mice are protected against age related obesity and DIO due to an enhancement in β-oxidation (Um et al., 2004). These animals remain insulin sensitive due to the apparent loss of a negative feedback loop from $p70^{s6k}$ to IRS1. In contrast, on HFD both WT mice and *ob/ob* mice display significant increases in $p70^{s6k}$ activity and increases in IRS1 phosphorylation. This study therefore suggests that under conditions of nutrient satiation, $p70^{s6k}$ has the ability to negatively regulate insulin signalling and thus energy homeostasis (Um et al., 2004).

1.16.5 Role for mTOR

A recent study has implicated a key role for the serine-threonine kinase, mTOR, in the regulation of food intake (Cota et al., 2006). Cota and colleagues demonstrated co-localisation of mTOR with NPY and POMC in the ARC, and that changes in expression level of this protein correlate with the energy status of the animal. For example, following a 48-h fast, mTOR levels are considerably lowered in the ARC compared to fed conditions. Administration of L-Leucine (a branched amino acid shown to stimulate mTOR activity) directly into the ARC of mice, resulted in significant reductions in food intake. The use of rapaymcin (an mTOR inhibitor) proved that this anorexia was dependent on hypothalamic mTOR signalling. The anorexigenic effects of ICV leptin treatment were also shown to be associated with increased hypothalamic mTOR activity. Taken together, these findings highlight an important role for hypothalamic mTOR signalling in food intake and energy balance regulation, and indicate that the anorexigenic effects of CNS adiposity signalling may be mTOR dependent.

1.17 Role for insulin signalling pathways in the regulation of reproduction

Recent studies have highlighted a role for the insulin signalling pathway in the regulation of reproductive function. Both male and female *NIRKO* animals display subfertility and impaired breeding performance, as indicated by timed mating studies (Bruning et al., 2000). This reduction in male fertility was found to be due to impaired spermatogenesis caused by reductions in luteinising hormone (LH). Ovaries from female *NIRKO* mice contained reduced numbers of antral follicles and corpora lutea, also due to reduced

levels of LH. As already described, IRS proteins have been shown to mediate the effects of the insulin receptor upon cellular and whole body physiology including reproduction (Withers, 2001). Mice lacking *Irs1* display only mild defects in reproductive function (Burks et al., 2000c; Withers, 2001). However, female *Irs2* null mice are infertile due to reduced pituitary LH levels and gonadotroph cell number and reduced gonadotrophin-stimulated ovulation. In addition, females exhibit markedly reduced numbers of ovarian follicles and corpora lutea (Burks et al., 2000c).

Insulin also stimulates GnRH secretion *in vivo* and ICV administration of insulin restores reproductive behaviour in diabetic rats (Burcelin et al., 2003; Kovacs et al., 2003). *In vitro* studies using immortalised GnRH neuronal cell lines have suggested that insulin regulates GnRH expression acting through the MAP kinase pathway (Salvi et al., 2006). Insulin signalling has also been shown to have complex roles in ovarian function including the regulation of ovarian steroidogenesis, follicular development and granulosa cell proliferation (Adashi et al., 1997; Poretsky et al., 1999; Willis et al., 1996). The strong association of insulin resistance and ovarian dysfunction in the polycystic ovarian syndrome also suggests a role for insulin signalling in ovarian function (Franks et al., 1999). CNS insulin signalling pathways therefore play a role in regulating female reproductive function in rodents.

1.18 Leptin receptor signalling cascade

The leptin receptor (LepR) belongs to the type 1 cytokine family which consist of a single membrane-spanning domain. Currently six leptin receptor isoforms are known to exist: Ob-Ra, Ob-Rb, Ob-Rc, Ob-Rd, Ob-Re and Ob-Rf. Each of these isoforms has an identical extracellular ligand-binding domain at the amino terminus but differ at the carboxyl terminus. Only the Ob-Rb (the long receptor isoform) contains intracellular motifs which are necessary for signal transduction (Banks et al., 2000).

Upon leptin binding the receptor recruits and activates a member of the janus kinase (JAK) family, primarily JAK2 (Banks et al., 2000). Once activated, JAK2 phosphorylates the intracellular domain of the leptin receptor, resulting in the creation of a binding site for the signal transducers and activators of transcription (STAT) molecules. In response to leptin stimulation, activated STAT3 translocates to the nucleus where it functions as a

transcription factor to stimulate transcription of target genes that mediate some of leptins cellular effects (Banks et al., 2000). A family of proteins known as suppressor of cytokine signalling (SOCS) molecules provide intracellular negative feedback to this signalling system and are synthesised in response to STAT3 activation following leptin stimulation. Leptin receptor activation is also known to activate ERK-regulated pathways (Banks et al., 2000). Figure 1.11 is a summary of the leptin receptor signalling cascade.

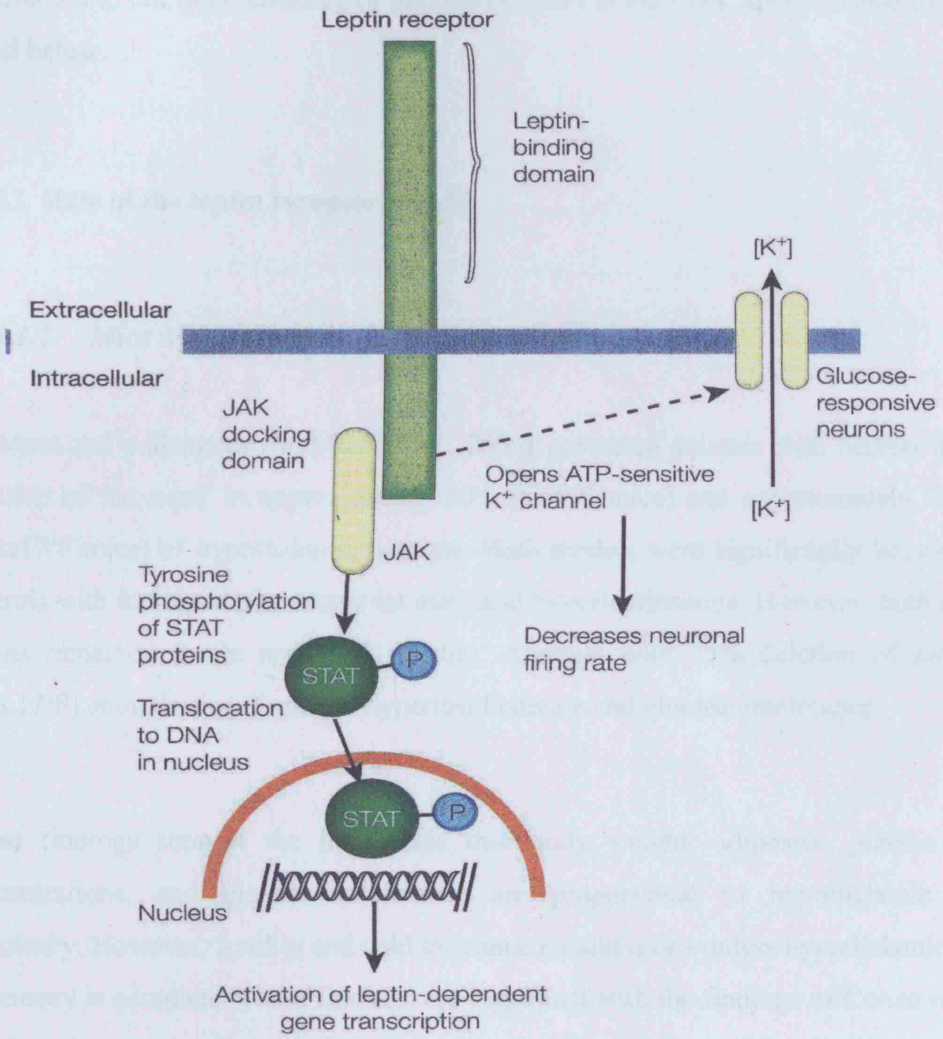

Figure 1.11: Leptin signalling pathways. The long form of LepR contains intracellular motifs required for signal transduction. Upon leptin binding the receptor recruits and activates JAK2. Activated, JAK2 phosphorylates the intracellular domain of the leptin receptor, creating a binding site for STAT molecules. In response to leptin stimulation, activated STAT3 translocates to the nucleus where it activates leptin-dependent gene transcription. Adapted from Banks et al., 2000.

1.19 Murine models of obesity and T2DM: insights into role and function of the leptin signalling pathway

Much of our current understanding of both the cellular and molecular activities of leptin has been derived from studies of murine models of obesity and diabetes. These models include the spontaneously occurring mutants *ob/ob* and *db/db*, as well as a number of models generated by gene-targeting approaches. A selection of these, which have contributed to our understanding of the role of leptin in the CNS, are described in further detail below.

1.19.1 Role of the leptin receptor (LepR)

1.19.1.1 Mice with neuronal deletion of the LepR

McMinn and colleagues (McMinn et al., 2005) generated animals with neuron-specific deletion of the *LepR* in approximately 50% (C F/F mice) and approximately 75% (C Delta17/F mice) of hypothalamic neurons. Both models were significantly heavier than controls with increased percentage fat mass and hyperleptinaemia. However, both mutant strains remained fertile and cold tolerant. Animals with 75% deletion of *LepR* (C Delta17/F) animals also displayed hyperinsulinaemia and glucose intolerance.

These findings support the hypothesis that body weight, adiposity, plasma leptin concentrations, and glucose intolerance are proportional to hypothalamic LepR deficiency. However, fertility and cold tolerance remain intact unless hypothalamic LepR deficiency is complete. These findings are consistent with the findings of Cohen et al, in which animals were generated with neuron specific deletion of LepR. The extent of obesity in these animals was negatively correlated with the level of LepR expression in hypothalamus (Cohen et al., 2001). In support of this, de Luca and colleagues found that expression of LepR specifically in the brain of *db/db* animals results in reversal of the obesity, diabetes and infertility phenotype (de Luca et al., 2005).

1.19.1.2 Animals with disrupted LepR-Stat3 signalling

The activation of the transcription factor STAT3 is known to be mediated by Tyr 1138. Bates and colleagues generated a model with specific disruption of the LepR-STAT3 signal, by replacing the gene encoding the *LepR* with one in which the Tyr 1138 is replaced with a serine residue (Bates et al., 2004). They found that similarly to *db/db* animals, mice homozygous for this mutation (*s/s* mice) were hyperphagic and obese. However, unlike *db/db* mice, these animals are fertile, long and less hyperglycaemic. In addition, unlike *db/db* mice which display elevated hypothalamic NPY expression and suppressed expression of the hypothalamic melanocortin system, *s/s* mice display only the latter (Bates et al., 2003). These studies indicate that LepR-STAT3 signalling mediates the effects of leptin on melanocortin production and body energy homeostasis, whereas distinct LepR signals regulate NPY and the control of fertility, growth and glucose homeostasis.

1.19.2 Role of STAT3

Mice with global deletion of *Stat3* die early in embryogenesis, prior to gastrulation (Takeda et al., 1997). However the use of conditional alleles of this gene have allowed analysis of its role in a tissue specific manner. The models that are of particular relevance to this thesis are described below.

1.19.2.1 Mice with mice with neural-specific disruption of Stat3

Gao and colleagues generated animals with neuronal specific disruption of *Stat3* by crossing *Stat3lox* animals with mice expressing a neuron specific cre recombinase (Gao et al., 2004). These *Stat3(N-/-)* mice had no apparent developmental abnormalities but were found to be susceptible to neonatal lethality. *Stat3(N-/-)* animals also exhibited a hyperphagic, obese, diabetic, hyperleptinaemic and infertile phenotype. Treatment with a melanocortin-3/4 receptor agonist was found to abrogate the hyperphagia of these animals. *Stat3(N-/-)* animals also had reduced energy expenditure and displayed hypothermia following fasting or cold stress. With regards to neruropeptide expression, *Stat3(N-/-)* animals also exhibited a marked reduction in *Pomc* expression, with an

increase in *Npy* and *Agrp* expression. These studies thus indicate an essential role for STAT3 in the CNS regulation of energy homeostasis and reproduction.

1.20 Potential convergence of insulin and leptin signalling pathways

Several lines of evidence indicate potential cross-talk between insulin and leptin signalling pathways in the control of glucose homeostasis, body adiposity and reproductive function.

1.20.1 Cell culture studies

Soon after the discovery of leptin, it was shown to modify the actions of insulin in various model systems. A potential site of intracellular interaction for both insulin and leptin action involves the enzyme PI3K, although generally considered a downstream effector of IRS1 and IRS2 signalling.

Studies in hepatocyte cell lines have demonstrated that leptin enhanced insulin-induced association of IRS1 with PI3K and increased PI3K activity (Cohen et al., 1996; Kellerer et al., 1997; Zhao et al., 2000). The assessment of IRS-mediated PI3K signalling in the liver and muscle of *ob/ob* mice indicated that these mice exhibited reduced *Irs1* and *Irs2* expression, leading to a differential decrease in IRS-PI3K signalling in these tissues (Kerouz et al., 1997). Subsequent studies in hepatocytes have demonstrated that leptin activates PI3K via tyrosine phosphorylation of IRS1 and IRS2, leading to activation of downstream targets such as AKT and phosphodiesterase 3B (PDE3B) (Zhao et al., 2000). Thus, leptin action in hepatocytes appears to involve signalling through IRS-PI3K pathways. Similar findings have been made in both muscle precursor cell lines (Kellerer et al., 1997) and in cultured pancreatic β-cells (Harvey et al., 2000).

1.20.2 *In vivo* studies

The first *in vivo* studies to support a hypothesis for the potential overlapping actions of insulin and leptin (Figure 1.12), found that the administration of leptin improves glucose homeostasis in both normal rodents (Sivitz et al., 1997) and models of leptin deficiency

(Halaas et al., 1995; Schwartz et al., 1996a). More importantly, these improvements were via mechanisms independent of effects on food intake. In further support for potential convergence between insulin and leptin signalling, Kim and colleagues (Kim et al., 2000) found that both hormones, when infused intravenously in rodents, were able to activate STAT molecules to differing degrees in several tissues. Furthermore, they observed that leptin, like insulin, is capable of activating IRS-PI3K pathways in adipose tissue and liver (albeit to a lesser extent than insulin).

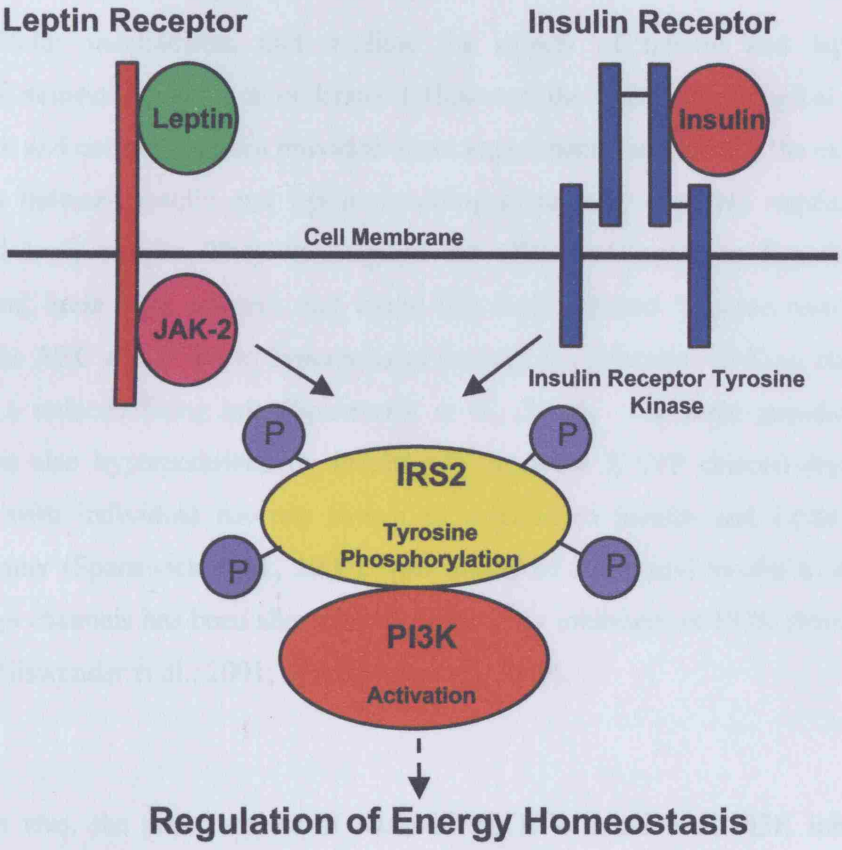

Figure 1.12: Potential cross-talk between insulin and leptin intracellular signalling via PI3K. The insulin receptor tyrosine kinase catalyses the tyrosine phosphorylation of IRS2, which associates with PI3K, resulting in activation of PI3K activity and downstream signal transduction. It is hypothesised that JAK2 can act through a similar, IRS dependent mechanism to activate PI3K. Both the leptin and insulin receptors interact with numerous other signal transduction pathways (not shown) but could be involved in the regulation of energy homeostasis.

1.20.3 Direct evidence for cross-talk between insulin and leptin signalling in the CNS

Convergence between insulin and leptin signalling pathways in the hypothalamic regulation of energy homeostasis is implicated by the concentration of insulin and leptin receptors in the ARC. In addition, these hormones exert similar effects on neuropeptide gene expression and are generated in proportion to body fat stores, thus linking changes in body fat mass to adaptive adjustments of feeding behaviour.

The intracellular mechanisms that mediate the effects of insulin and leptin in hypothalamic neurons are not well understood. However, the electrophysiological studies of Spanswick and colleagues have provided direct experimental support for the existence of cross-talk between insulin and leptin signalling systems in the CNS regulation of appetite and body weight. They investigated the effects of leptin on hypothalamic neurons in rat brain slice cultures and found that leptin caused 'glucose responsive' neurons in the ARC and VMH to hyperpolarise through the activation of K_{ATP} channels, resulting in a reduced firing rate (Spanswick et al., 2000). The same population of neurons were also hyperpolarised by insulin via the same KATP channel-dependent mechanism, with individual neurons shown to respond to insulin and leptin in an identical manner (Spanswick et al., 2000). This ability of leptin and insulin to activate neuronal K_{ATP} channels has been shown to be blocked by inhibitors of PI3K (Mirshamsi et al., 2004; Niswender et al., 2001; Spanswick et al., 2000).

Moreover, *in vivo,* the pre-treatment of rats with an ICV infusion of PI3K inhibitors (LY294002 or wortmannin) was found to completely block the ability of both ICV leptin and insulin to reduce food intake. Recent studies have also implicated a role for PI3K in mediating the reported effects of leptin on glucose homeostasis in the hypothalamus, and suggest that hypothalamic leptin signalling is an important determinant of glucose metabolism and that the underlying neuronal mechanism involves PI3K (Morton et al., 2005).

These studies therefore highlight the role of PI3K activation, a signalling molecule that classically mediates insulin action in peripheral tissues, in mediating the anorexigenic

effects of both insulin and leptin in the hypothalamic regulation of energy homeostasis. It should be noted that even though insulin and leptin signalling converge at the level of PI3K, the two hormones appear to elicit distinct signalling events downstream of PI3K. Unlike insulin, the ICV injection of leptin results in only a transitory phosphorylation of IRS proteins and association of IRS with PI3K, but does not result in activation of AKT in whole hypothalamic extracts (Carvalheira et al., 2005). In contrast to this transitory effect of leptin on IRS phosphorylation, leptin has been shown to robustly activate the MAPK pathway under the same experimental conditions.

1.20.4 Evidence for the modulation K_{ATP} channel activity by PI3K generated PIP_3 in hypothalamic neurons

The above mentioned studies have highlighted the role of activated PI3K in the regulation of cell excitability via stimulation of K_{ATP} channels channels in the brain. It is postulated that this might provide a potential molecular mechanism for mediating the central effects of insulin and leptin on energy and glucose homeostasis.

Three mechanisms for the modulation of K_{ATP} channel activity by PI3K generated PIP_3 have been proposed (summarised in Figure 1.13): (1) PIP_3 increases the probability that K_{ATP} channels are open, which indirectly lowers the ability of ATP to inhibit the channels (Baukrowitz et al., 1998; Shyng and Nichols, 1998), (2) PIP_3 directly decreases ATP binding to the channel (MacGregor et al., 2002) and (3) PIP_3 activates degradation of the local actin filaments around K_{ATP} channels (Mirshamsi et al., 2004).

However, the hypothesis that the hypothalamic regulation of energy homeostasis of both insulin and leptin is via the alteration of the electrical activity of their target neurons should be viewed with caution. More detailed investigations have demonstrated that only 45% of unidentified ARC neurons follow this pattern (Mirshamsi et al., 2004), and that activation of hypothalamic K_{ATP} channels by insulin is abolished in obese rats. In addition, it has been shown that in identified POMC neurons, leptin stimulates while insulin inhibits electrical activity (Choudhury et al., 2005). This is despite the findings of a recent study, discussed in further detail below, that both insulin and leptin stimulate PI3K in POMC neurons.

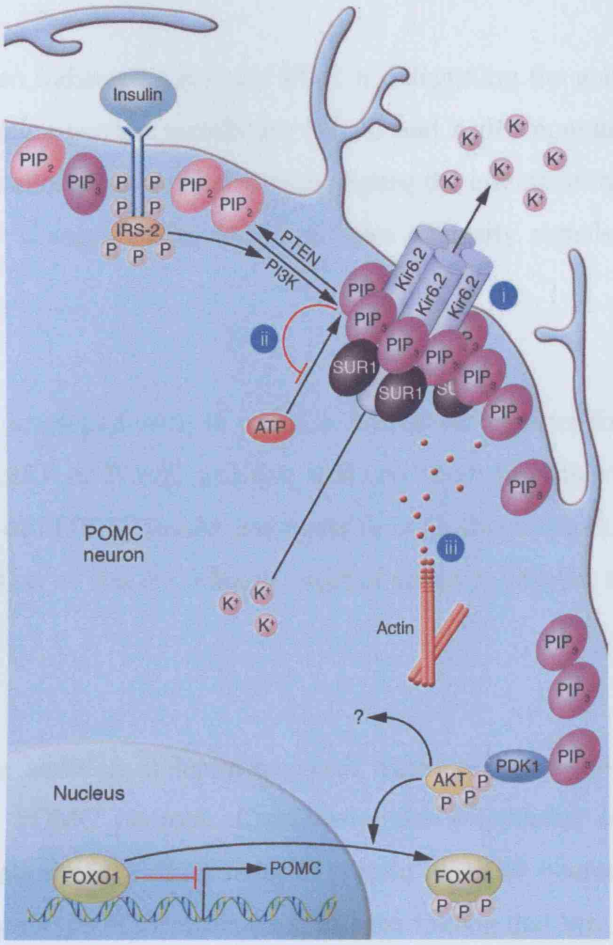

Figure 1.13: Generation of PIP_3 leads to K_{ATP} channel opening and consecutive cell hyperpolarisation. Insulin activates PI3K, which phosphorylates PIP_2 on position 3' in the inositol ring, generating PIP_3. The lipid phosphatase PTEN antagonises this by dephosphorylating PIP_3 to generate PIP_2. PIP_3 accumulation leads to activation of K_{ATP} channels and, thus, to potassium outflow. This leads to membrane hyperpolarisation and silencing of the neuron. Three different mechanisms for channel opening have been suggested: (i) PIP_3 binding to the KIR6.2 subunit of the potassium channel increases the probability that the channel is open, which indirectly lowers inhibition by ATP; (ii) PIP_3 competes with ATP for binding to the KIR6.2 subunit, thereby lowering ATP's ability to close the channel; and (iii) PIP_3 activates degradation of the local actin cytoskeleton. Adapted from Plum et al., 2006.

1.20.5 Direct evidence for cross-talk between insulin and leptin signalling in distinct hypothalamic neuronal populations

Recent work has also indicated a role for PI3K in integrating the action of insulin and leptin on hypothalamic neurons, namely the POMC and AgRP populations of the ARC. Although both populations are implicated as mediating the effects of insulin and leptin, it is still unclear how changes in the levels of these adiposity signals are perceived or integrated by them.

Xu and colleagues developed mice in which a fluorescent reporter for PI3K activity is targeted to either AgRP or POMC neurons, and used 2-photon microscopy to measure dynamic regulation of PI3K by insulin and leptin in brain slices (Xu et al., 2005b). PI3K was chosen as a marker as it is the primary target of action by insulin, with leptin thought to act similarly.

They found that the addition of leptin triggered membrane accumulation of the PI3K reporter protein in POMC neurons. Conversely, the withdrawal of leptin triggered membrane accumulation of the PI3K reporter protein in AgRP neurons, consistent with the neuropeptide phenotype of these neurons, and the finding that low leptin levels result in their activation. With regards to insulin, the addition of this compound resulted in membrane accumulation of the PI3K reporter protein in POMC neurons.

Surprisingly, leptin and insulin had opposite effects on AgRP neurons, with membrane accumulation of the reporter protein inhibited by leptin but stimulated by insulin. This activation of PI3K by insulin in AgRP neurons is the opposite of what would be predicted for a physiologic adiposity signal. The use of inhibitors of synaptic transmission showed that leptin directly activates PI3K in POMC neurons, but the effect of leptin withdrawal in activating PI3K in AgRP neurons requires synaptic transmission and therefore must be mediated indirectly. In the case of insulin, synaptic transmission was not required to mediate the activation of PI3K in either AgRP or POMC neurons. The authors also demonstrate that the leptin-induced PI3K activation in POMC neurons is independent of STAT3 function.

Taken together, these results suggest a fundamental difference in the way POMC and AgRP neurons modulate PI3K activity in response to leptin. This is not only in direction of modulation but also in the underlying mechanism, with leptin having a primary effect on POMC neurons but a secondary effect on AgRP neurons (Figure 1.14). This study indicates that the functions of both insulin and leptin on energy balance do not overlap completely.

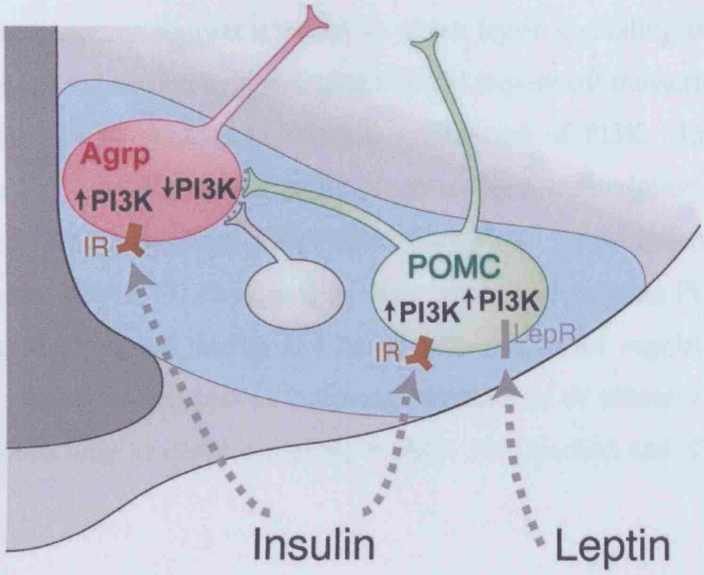

Figure 1.14: Unifying mechanism for leptin modulation of key arcuate nucleus neurons in which PI3K activity is a mediator and/or marker of neuronal activation and neuropeptide release in both AgRP (pink) and POMC (green) neurons. The effects of insulin on PI3K activity are direct in both neuronal subtypes, but the effects of leptin on PI3K activity in AgRP neurons require synaptic transmission from POMC or other inhibitory presynaptic neurons. IR, insulin receptor; LepR, leptin receptor. Adapted from Xu et al., 2005b.

1.20.6 Role for FOXO1 as an alternative mechanism for the interaction of insulin and leptin signalling at the level of hypothalamic neuropeptide expression

Although the above highlighted studies do indicate a role for PI3K in mediating the anorexigenic effects of insulin and leptin on energy homeostasis, little is known of the signals downstream of PI3K. Leptin has recently been shown to inhibit the hypothalamic expression of NPY and AgRP in a mechanism that requires intact PI3K signalling (Morrison et al., 2005). The anorexigenic effects of leptin are known to be mediated by

STAT3, but little is known of the potential interaction of the PI3K and STAT3 dependent actions of leptin. FOXO1 is known to control metabolism and cellular differentiation in a PI3K-dependent manner (Accili and Arden, 2004). Two groups have recently investigated whether this control is via the regulation of neuropeptide-dependent food intake (Kim et al., 2006; Kitamura et al., 2006).

The results of these studies suggest a model in which leptin signalling through JAK2-STAT3 inhibits *Agrp* expression by squelching FOXO1-dependent transcription of *Agrp*, and that this inhibition of FOXO1 function is independent of PI3K. In other words, activation of the PI3K-AKT pathway could decrease *Agrp* transcription by inhibiting FOXO1 activity, while promoting STAT3-mediated *Pomc* transcription by reducing FOXO1 antagonism of STAT3. Thus, despite many studies implicating PI3K as a direct point of convergence between insulin and leptin pathways in the regulation of energy homeostasis, these findings suggest an additional mechanism of interaction, namely by transcriptional squelching of distal effectors; FOXO1 (for insulin) and STAT3 (leptin) (Figure 1.15).

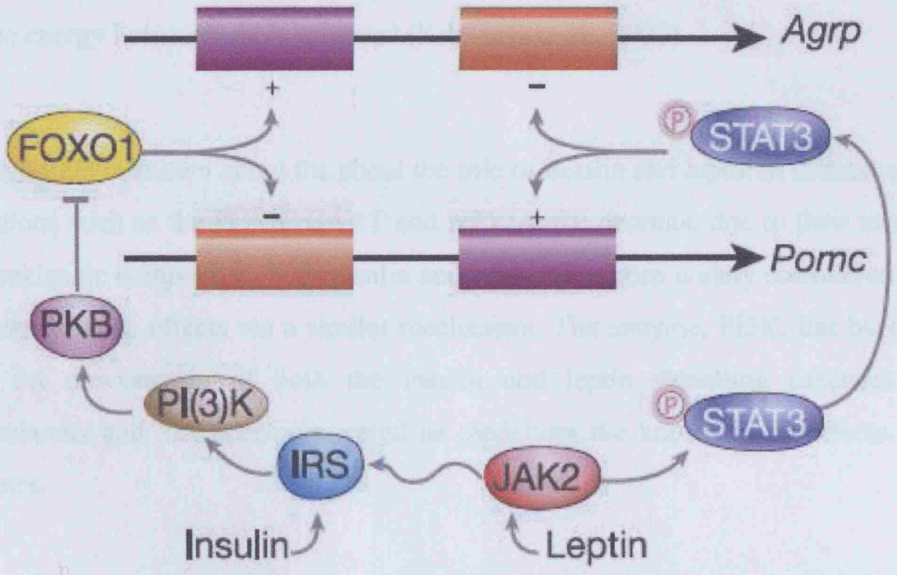

Figure 1.15: Model for the reciprocal regulation of *Pomc* and *Agrp* gene transcription via FOXO1 and STAT3. Adapted from Morton et al., 2006.

1.21 Summary

The use of animal models has provided significant evidence for the role of leptin and insulin action in the CNS regulation of food intake, energy expenditure, reproductive function and peripheral glucose homeostasis. Both hormones circulate in proportion to body fat stores and are proposed to regulate energy homeostasis via their ability to elicit key effector pathways in the CNS resulting in a response where by feeding behaviour, autonomic outflow and substrate metabolism are adjusted in ways that promote homeostasis of both energy stores and fuel metabolism.

Recent evidence has suggested a key role for the ARC in the regulation of energy homeostasis, and specifically the POMC/CART and NPY/AgRP neurons within this region. Upon entering the ARC, insulin and leptin are proposed to bind to their corresponding receptors present on the first-order NPY/AgRP and POMC/CART neurons. These first order neurons subsequently control food intake and energy homeostasis via interactions with second order neurons located in other hypothalamic regions involved in food intake and energy homeostasis. Thus, a mechanism which allows transduction of peripheral signals into behavioural and metabolic responses to regulate energy homeostasis is achieved (Schwartz et al., 2000).

Although little is known about the about the role of insulin and leptin in distinct neuronal populations such as the POMC/CART and NPY/AgRP neurons, due to their similarities as anorexigenic compounds, both insulin and leptin have been widely considered to exert their anorexigenic effects via a similar mechanism. The enzyme, PI3K, has been shown to be act downstream of both the insulin and leptin signalling cascades in the hypothalamus and has been implicated as mediating the anorexigenic effects of both hormones.

1.22 Aims

In addition to the important role for insulin signalling in the classical peripheral target tissues such as liver, muscle and fat, it is now evident that the brain is also a key target for insulin action. Recent evidence has indicated that intact CNS insulin receptor signalling is required for both energy homeostasis and peripheral glucose homeostasis (Bruning et al., 2000; Obici et al., 2002a; Obici et al., 2002b; Plum et al., 2006). More specifically, a key role for IRS2 mediated signalling pathways in the CNS has been implicated by the phenotype of the *Irs2* null mouse. In addition to the insulin resistance, β-cell failure and subsequent diabetic phenotype of *Irs2* null mice (Withers et al., 1998), these animals also display a phenotype of hypothalamic dysfunction (obesity, hyperphagia, subfertility), and resistance to the anorexigenic effects of peripherally administered leptin (Burks et al., 2000c). However, these studies have raised a number of key points:

- The identity of the neuronal populations mediating the effects of insulin on food intake and body weight regulation is unknown.

- Although the severe impaired glucose homeostasis of *Irs2* null animals is thought to be due to deletion of *Irs2* in the β-cell, the relevant contribution of CNS IRS2 mediated insulin signalling to this phenotype, if any, is unclear.

- It remains unclear whether deletion of *Irs2* in the ovary is solely responsible for the infertility of female *Irs2* null animals, or if the deletion of *Irs2* in the CNS also contributes to this phenotype.

- The resistance of *Irs2* null animals to the anorexigenic effects of leptin indicate that IRS2 may be a point of convergence between insulin and leptin signalling pathways in the CNS.

The enzyme PI3K is known to be a major downstream effector of insulin signalling, and has been implicated as a potential point of convergence between insulin and leptin signalling cascades in the hypothalamic regulation of energy and glucose homeostasis (Mirshamsi et al., 2004; Morton et al., 2005; Niswender et al., 2001; Spanswick et al., 2000). Although several classes of PI3K exist, it is the class IA isoforms that are considered to be the main class involved in mediating the effects of insulin (Katso et al., 2001). In support of this, a recent *in vivo* study has highlighted the key role for the p110α catalytic subunit (a member of class IA) signalling in the context of the regulation of growth and metabolism (Foukas et al., 2006).

The aim of this thesis was to investigate the role of insulin signalling pathways in the hypothalamic regulation of energy homeostasis. More specifically, the roles of IRS2 and p110β pathways in neurons of the ARC (namely the AgRP and POMC populations) implicated as key targets of insulin in the hypothalamic regulation of energy homeostasis were studied. To do so, the following mouse lines were generated:

1. Mice with *Irs2* deletion in all neurons
2. Mice with *Irs2* deletion in POMC neurons
3. Mice with *Irs2* deletion in AgRP neurons
4. Mice with *p110β* deletion in POMC neurons
5. Mice with *p110β* deletion in AgRP neurons

It was predicted that the phenotypic characterisation of these transgenic lines would address the outstanding queries regarding the role of hypothalamic IRS2 mediated insulin signalling pathways in the regulation of energy homeostasis, glucose homeostasis and reproductive function. In addition, these studies were predicted to assess the contribution of the p110β isoform in the PI3K effects on metabolic function and enable the validation of a role for PI3K as a potential mechanism of mediating the anorexigenic effects of both insulin and leptin.

Chapter 2
Methods and materials

2 Methods and Materials

2.1 Conditional gene targeting using the *Cre-loxP* system

The animal models described in this thesis were generated with the use of conditional gene targeting technology. Conditional gene targeting refers to a gene modification in the mouse that is restricted to either certain cell types (tissue-specific), to a stage within development (temporally specific), or both (Lewandoski, 2001). To date, the *cre-loxP* system is the best characterised system for the achievement of conditional gene inactivation in mice (Wilson and Kola, 2001). *Cre-loxP* technology was introduced in the 1980's (Sauer and Henderson, 1988; Sternberg and Hamilton, 1981) and patented by DuPont Pharmaceuticals. It has been successfully applied in yeasts, plants, mammalian cell cultures, and mice (Araki et al., 1987).

The *cre-loxP* system is compromised of two components: the *cre* recombinase enzyme and a small stretch of DNA recognised by the recombinase (*loxP* site) (Stark et al., 1992; Van Duyne, 2001). The *cre* recombinase is produced by the bacteriophage P1 and is a member of the λ integrase superfamily of site-specific recombinases that cleave DNA at a distinct target sequence and ligate it to the cleaved DNA of a second identical site to generate a contiguous strand. This recombination is carried out with absolute fidelity such that not a single nucleotide is gained or lost overall. The *loxP* site is a 34 bp, as size that is unlikely to occur at random in even the largest vertebrate genome and yet small enough to be effectively neutral towards gene expression when positioned in chromosomal DNA for genetic manipulations.

Two separate mouse strains are typically generated and intercrossed for a conditional gene targeting experiment (Figure 2.1). One mouse strain expressed the *cre* recombinase in selected tissues, depending on which promoter has been selected to drive recombinase expression. This strain is mated with a strain that carries the gene of interest flanked (floxed) by the *loxP* sites. The location of the *loxP* sites has to be appropriately chosen such as that the function of the gene is not affected and that deletion of the floxed gene segment will lead to inhibition of transcription and/or translation of the gene of interest, or to the synthesis of a non-functional protein. It is important to note, that in offspring, cells expressing the recombinase delete the target gene segment whereas the target gene

remains functional in cells of all other tissues where cre is not expressed. However, a potential limitation of this *cre-loxP* system is that if the gene promoter chosen to drive the cre is expressed in cells/tissues other than the cells/tissue of interest, the targeted gene will also be inactivated in these populations. This should thus be taken into consideration upon interpretation of any resultant phenotypes generated.

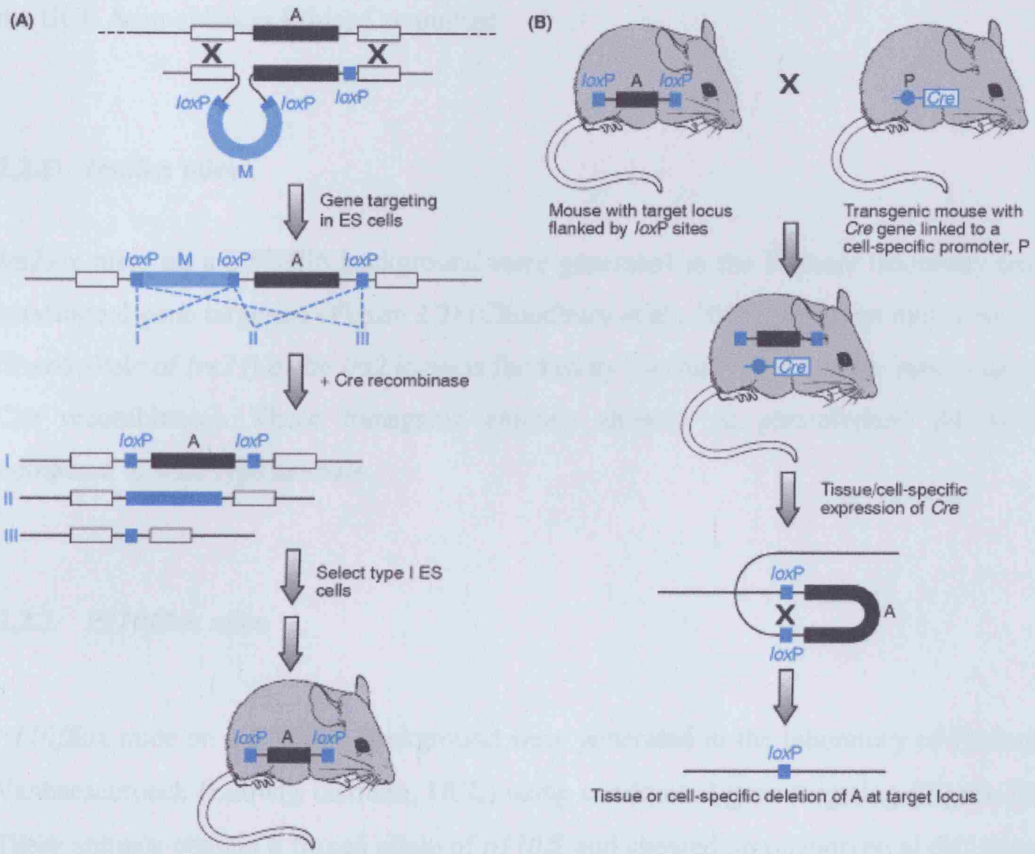

Figure 2.1: Gene targeting using the *cre-lox*P recombination system to inactivate a gene in a desired cell type. (A) Schema of a standard homologous recombination method using mouse ES cells, in which three *loxP* sites are introduced along with a marker M at a target locus A (typically a small gene or an internal exon which if deleted would cause a frameshift mutation). Subsequent transfection of a *cre* recombinase gene and transient expression of this gene results in recombination between the introduced *loxP* sites to give different products. Type I recombinants are used to generate mice in which the target locus is flanked by *loxP* sites. Such mice can be mated with previously constructed transgenic mice (B) that carry an integrated construct consisting of the *cre* recombinase gene linked to a tissue-specific promoter. Offspring that contain both the *loxP*-flanked target locus plus the *cre* gene will express the *cre* gene in the desired tissue type, and the resulting recombination between the *loxP* sites in these cells results in tissue-specific inactivation of the target locus A. Adapted from Strachan and Read, 1999.

2.2 Animals

Animals were housed in specific-pathogen free barrier facilities and maintained under a controlled environment (temperature 21-23 °C, 12-h light-dark cycle, lights on at 07:00) with *ad libitum* access to food (RM1 diet SDS UK Ltd) and water. All animal procedures were approved by the British Home Office Animals Scientific Procedures Act 1986 and the UCL Animal Users Ethics Committee.

2.2.1 *Irs2lox* mice

Irs2lox mice on a C57/Bl6 background were generated in the Withers laboratory using conditional gene targeting (Figure 2.2) (Choudhury et al., 2005). These animals contain a floxed allele of *Irs2* (i.e. the *Irs2* locus is flanked by two *loxP* sites that are target sites for Cre recombinase). These transgenic animals showed no phenotypical differences compared to wild type animals.

2.2.2 *P110βlox* mice

P110βlox mice on a C57/Bl6 background were generated in the laboratory of Professor Vanhaesebroeck (Ludwig Institute, UCL) using conditional gene targeting (Figure 2.3). These animals contain a floxed allele of *p110β*, and showed no phenotypical differences compared to wild type animals.

It is important to note that exons 19 and 20 of the *p110β* kinase domain were floxed. Thus, removal of these exons following Cre-mediated recombination results in the splicing of exon 18 and exon 21, creating an out-of-frame fusion protein in which the normal C-terminus is not retained. However, mutant p110β protein still retains its ability to associate with regulatory subunits, thus maintaining the stoichiometry within the tissue/cell of interest.

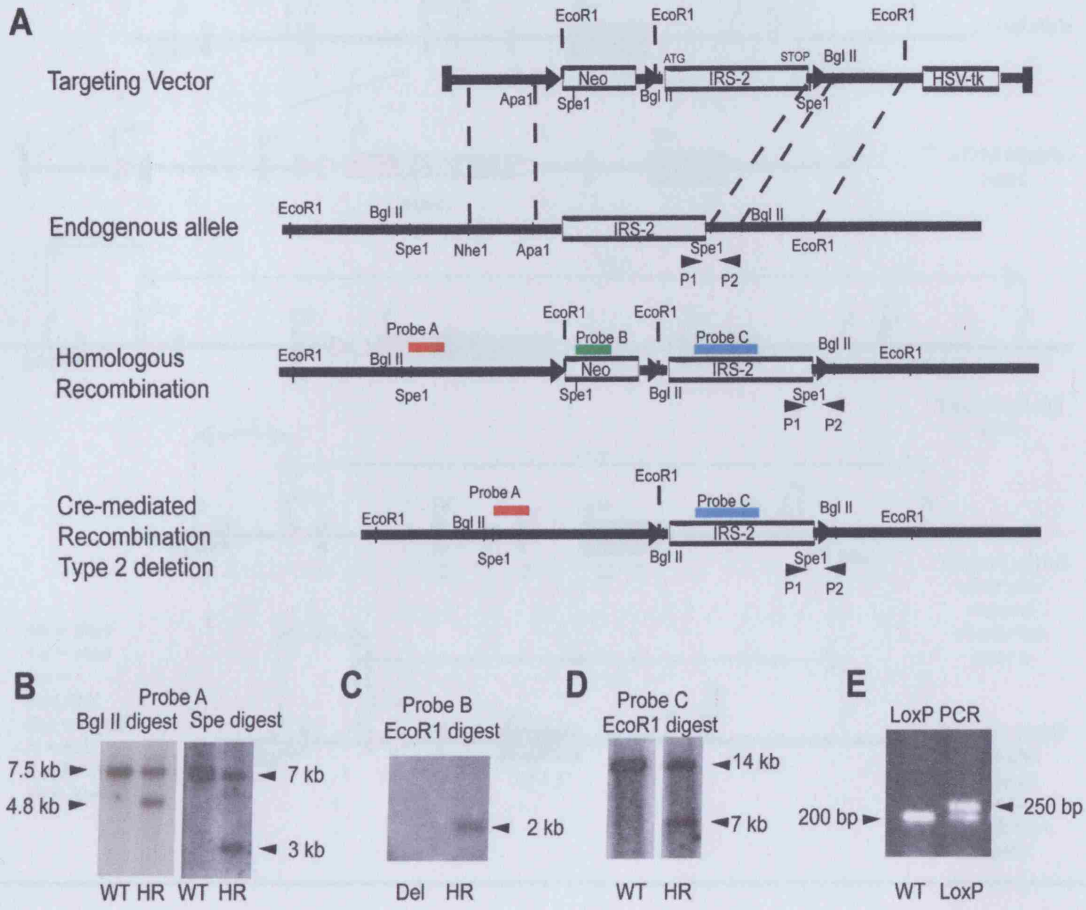

Figure 2.2: Generation of *Irs2lox* mice. (A) Schema of targeting construct design, simplified restriction map of the *Irs2* locus, the locus after homologous recombination and the deletion of neomycin cassette (Neo), and Southern blotting and PCR genotyping strategies used to identify these events. External probe A was used to identify homologous recombination (HR), probe B to detect the selection cassette, and probe C to detect the coding region of IRS2. HSV-tk, herpes simplex virus thymidine kinase. (B) Southern blot analysis with probe A demonstrating homologous recombination after targeting. (C and D) Southern blots using probe B after Cre-mediated recombination demonstrating deletion (Del) of the neomycin cassette and using probe C to demonstrate retention of IRS2 coding region confirming type 2 recombination. (E) PCR analysis with primers P1 and P2 of HR clone that has lost the neomycin cassette, but retained the *loxP* site downstream of the IRS2 coding region.

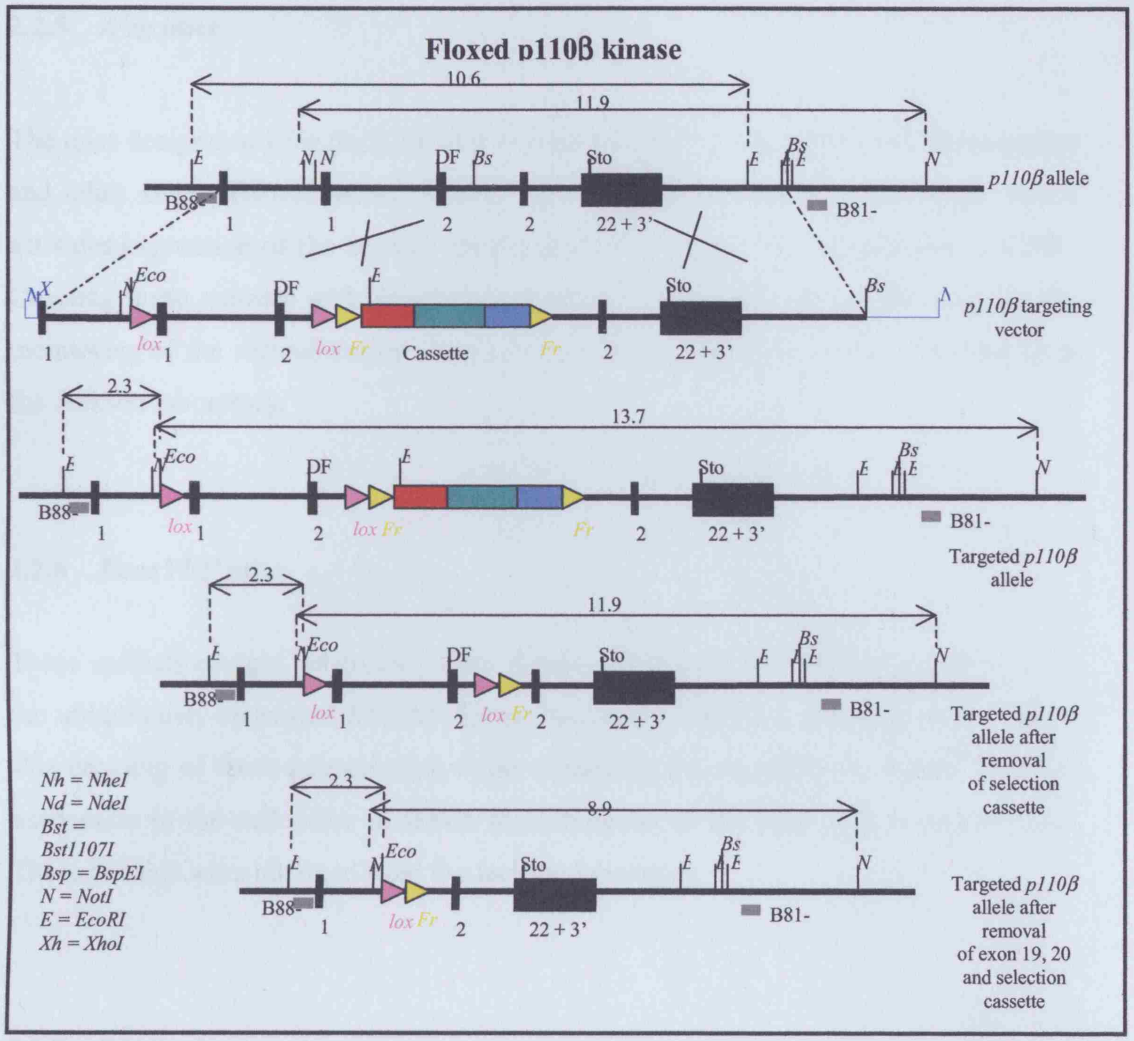

Figure 2.3: The targeting construct, showing a simplified restriction map of the *p110β* locus, the locus after homologous recombination, and the deletion of the selectable marker following *in vitro* Cre-mediated recombination.

2.2.3 *NesCre* mice

NesCre mice on a C57/Bl6 background (Tronche et al., 1999) were obtained from the Jackson laboratory.

2.2.4 *POMCCre* and *AgRPCre* mice

POMCCre and *AgRPCre* animals (Xu et al., 2005a; Xu et al., 2005b), both on a FVB/N-C57BL/6J mixed background, were obtained from Dr. G. Barsh, Stanford University.

2.2.5 *Z/eg* mice

The mice designated Z/eg (lacZ/EGFP), express lacZ throughout embryonic development and adult stages (Novak et al., 2000). Cre excision, removes the lacZ gene, which activates expression of the second reporter, enhanced green fluorescent protein (eGFP). Crossing these animals with those expressing the Cre-recombinase enzyme allows the monitoring of the recombination event of *loxP* sites. These animals were obtained from the Jackson laboratory.

2.2.6 *RosaYFP* mice

These animals contain enhanced yellow fluorescent protein (eYFP) cDNA inserted into the ubiquitously expressed *ROSA26* locus, flanked by *loxP* sites (Srinivas et al., 2001). The crossing of these animals with those expressing Cre-recombinase, results in eYFP expression in the cell/tissue in which recombination of the *loxP* sites is taking place. These animals were obtained from the Jackson laboratory.

2.2.7 *R26R* mice

Gt(Rosa)26Sortm1Sor allele (*R26R*) mice contain a *LacZ* gene inserted into the ubiquitously expressed *ROSA26* locus, flanked by *loxP* sites (Soriano, 1999). The crossing of these animals with those expressing Cre-recombinsase, results in expression of LacZ in the cell/tissue in which recombination of the *loxP* sites is taking place. These animals were obtained from the Jackson laboratory.

2.3 Generation of *NesCreIrs2lox* mice

Irs2lox mice were crossed with *NesCre* mice, to obtain mice heterozygote for *Irs2lox* and positive for the *NesCre* transgene. These were then crossed with *Irs2lox* heterozygote mice to obtain *NesCreIrs2KO* animals and all other genetic combinations.

2.4 Generation of *POMCCreIrs2lox* mice

Irs2lox mice were crossed with *POMCCre* mice, to obtain mice heterozygote for *Irs2lox* and positive for the *POMCCre* transgene. These were then crossed with *Irs2lox* heterozygote mice to obtain *POMCCreIrs2KO* and all other genetic combinations.

2.5 Generation of *AgRPCreR26RIrs2lox* mice

Ectopic *lacZ* expression has been found in approximately 30% of *AgrpCreR26R* mice (Kaelin et al., 2004). To ensure that no mice in which germline deletion of *Irs2* were studied, *AgRPCre* and *R26R* mice were intercrossed to produce *AgrpCreR26R* animals. These were crossed with *Irs2lox* homozygote mice to generate *AgrpCreR26Irs2lox*$^{+/-}$ mice. These were crossed with *Irs2lox* heterozygote mice to obtain *AgRPCreR26RIrs2KO* mice (hereby referred to as *AgRPCreIrs2KO)* and all other possible combinations.

2.6 Generation of *POMCCreR26RIrs2lox* mice

POMCCreIrs2KO mice were crossed with animals carrying the *R26R* allele. These were then intercrossed, to obtain *POMCCreR26RIrs2KO* mice and other mice of intermediary genotypes.

2.7 Generation of *POMCCrep110βlox* mice

P110βlox mice were crossed with *POMCCre* mice, to obtain mice heterozygote for *p110βlox* and positive for the *POMCCre* transgene. These were then crossed with *p110βlox* heterozygote mice, to obtain *POMCCrep110βKO* and all other genetic combinations.

2.8 Generation of *AgRPCrep110βlox* mice

P110βlox mice were crossed with *AgRPCre* mice to obtain mice that were heterozygote for *p110βlox* and positive for the *AgRPCre* transgene. These animals were crossed with *p110βlox* heterozygote mice, to obtain *AgRPCrep110βKO* and all other genetic combinations.

2.9 Generation of *POMCCrep110βloxZ/eg* mice

POMCCrep110βKO mice were crossed with animals carrying the Z/eg transgene to give *POMCCrep110βlox*$^{+/-}$*Z/eg* mice. These were intercrossed to obtain *POMCCrep110βKOZ/eg* mice and other animals of intermediary genotypes.

2.10 Generation of *AgRPCrep110βKOYFP* mice

AgRPCrep110βKO mice were crossed with mice positive for the *Rosa26YFP* transgene to obtain *AgRPCrep110βflox*$^{+/-}$*YFP* animals. These were then intercrossed to obtain *AgRPCrep110βKO YFP* mice and other mice of intermediary genotypes.

2.11 Genotyping strategies

Mice were tail tipped (~ 2 mm) at around 14 days of age, using ethyl chloride spray as a local anaesthetic. Polymerase chain reaction (PCR) genotyping was then carried out upon extracted DNA, in order to determine the genotype of each mouse.

2.11.1 DNA extraction of tail tips

Each tail tip was placed in a 1.5 ml eppendorf tube and 600µl 0.1M NaOH added. Tubes were heated at >100°C for 10 minutes and then left to stand at room temperature (RT) for 10 minutes. 100µl 1M Tris (pH 6.8) was then added and 1µl of the resulting mixture was used for PCR genotyping. The PCR strategies for detecting the genotypic status of the various genes of interest differed. The details of these strategies are outlined below.

2.11.2 *NesCre* genotyping

NesCre genotyping was performed using the following primers: Cre 1084 5' GCG GTC TGG CAG TAA AAA CTA TC 3', Cre 1085 5' GTG AAA CAG CAT TGC TGT CAC TT 3' together with internal positive control primers for the *IL2* gene: IL2 forward and IL2 reverse (5' TAGGCCACAGAATTGAAAGATCT 3' and 5' GTAGGTGGAAATTCTAGCATCATCC 3' respectively).

PCR reaction mixture

Reddymix	9 µl
Cre1084	0.75 µl
Cre1085	0.75 µl
IL2F	0.25 µl
IL2R	0.25 µl

10 µl of this mixture was added to 1 µl of DNA.

PCR profile

94 °C for 3mins

94 °C for 30 secs
60 °C for 30 secs
72 °C for 1 min
x 30

72 °C for 10 mins

Samples stored at 4 °C until analysis.

PCR product analysis

This resulted in a 324 bp IL2 internal control product in all samples. For samples that were *NesCre* positive, a 100 bp product was also generated (Figure 2.4).

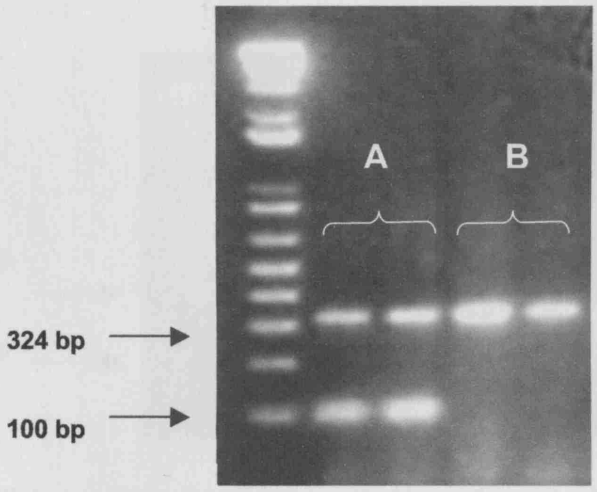

Figure 2.4: *NesCre* genotyping. Samples A are present and samples B are negative for the *Cre* allele.

2.11.3 *POMCCre* genotyping

POMCCre genotyping was performed using the following primers: PC1 5' AGTGTTGGCTCAATGTCCTTCCTG 3' and PAC2 5' CCGCATAACCAGTGAAACAGCATTG 3' together with internal positive control primers for the *IL2* gene: IL2 forward 5' CTAGGCCACAGAATTGAAAGATCT 3' and IL2 reverse 5' GTAGGTGGAAATTCTAGCATCATCC 3'.

PCR reaction mixture

Reddymix	9 µl
PC1	0.75 µl
PAC2	0.75 µl
IL2F	0.25 µl
IL2R	0.25 µl

10 µl of this mixture was added to 1 µl of DNA.

PCR profile

94 °C for 4 mins

94 °C for 30 secs
55 °C for 30 secs
72 °C for 1 min
x 30

72 °C for 7 mins

Samples stored at 4 °C until analysis.

PCR product analysis

This resulted in a 324 bp IL2 internal control product in all samples. For samples that were *POMCCre* positive, a 500 bp product was also generated (Figure 2.5).

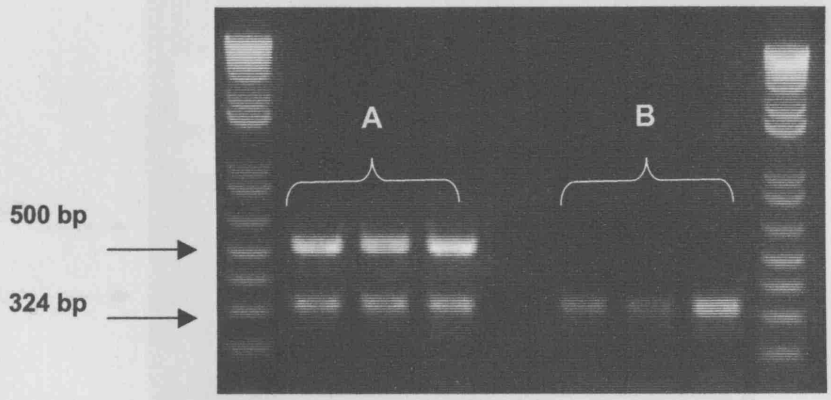

Figure 2.5: *POMCre* genotyping. Samples A are positive and samples B are negative for the *Cre* allele.

2.11.4 *AgRPCre* genotyping

AgRPCre genotyping was performed using the following primers: AC1 5' GTACCCTAAGGATGAGGAGAGAC 3' and PAC2 5 'CCGCATAACCAGTGAAACAGCATTG 3' together with internal positive control primers for the *IL2* gene: IL2 forward 5' CTAGGCCACAGAATTGAAAGATCT 3' and IL2 reverse 5' GTAGGTGGAAATTCTAGCATCATCC 3'.

PCR reaction mixture

Reddymix	9 µl
AC1	0.75 µl
PAC2	0.75 µl
IL2F	0.25 µl
IL2R	0.25 µl

10 µl of this mixture was added to 1 µl of DNA.

PCR profile

94 °C for 4 mins

94 °C for 30 secs
55 °C for 30 secs
72 °C for 1 min
x 30

72 °C for 7 mins

Samples stored at 4 °C until analysis.

PCR product analysis

This resulted in a 324 bp IL2 internal control product in all samples. For samples that were *AgRPCre* positive, a 500 bp product was also generated (Figure 2.6).

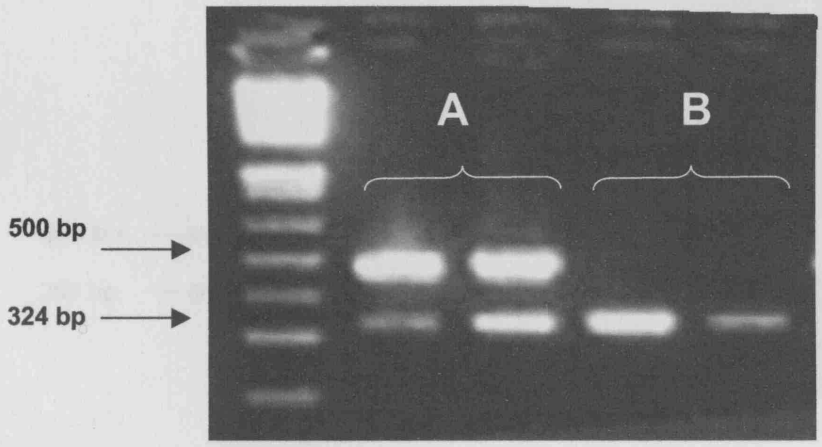

Figure 2.6: *AgRPCre* genotyping. Samples A are present and samples B are negative for the Cre allele.

2.11.5 *Irs2lox* genotyping

Irs2lox genotyping was performed using primers that flank the 3' loxP site: loxP forward 5' ACTTGAAGGAAGCCACAGTCG 3' and loxP reverse 5' AGTCCACTTTCCTGACAAGC 3'.

PCR reaction mixture

Reddymix	9 µl
PF	0.5 µl
PR	0.5 µl

10 µl of this mixture was added to 1µl of DNA.

PCR profile

94 °C for 1 min

94 °C for 30 secs
53 °C for 30 secs
72 °C for 1 min
x 30

72 °C for 10 mins

Samples stored at 4 °C until analysis.

PCR product analysis

This resulted in a 200 bp product for the wild-type allele and/or a 250 bp product for the *Irs2lox* allele (Figure 2.7).

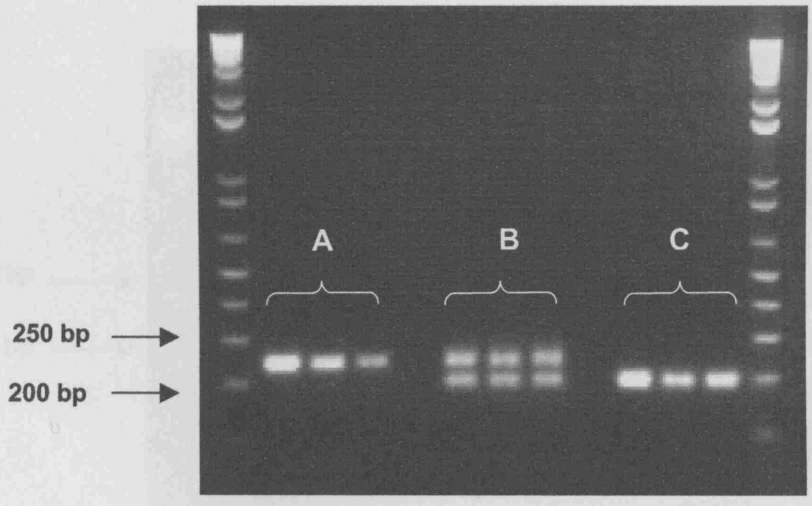

Figure 2.7: *Irs2lox* genotyping. Samples A are homozygote for the *Irs2lox* allele. Samples B are heterozygote for the *Irs2lox* allele. Samples C are wild-type for the *Irs2lox* allele.

2.11.6 *R26R* genotyping (LacZ and YFP)

R26R genotyping was performed using the following three primers: Rosa A 5′-AAAGTCGCTCTGAGTTGTTAT-3′, Rosa B 5′GCGAAGAGTTTGTCCTCAACC-3′ and Rosa C 5′-GGAGCGGGAGAAATGGATATG-3′.

PCR reaction mixture

Reddymix	21 µl
Rosa A	1 µl
Rosa B	1 µl
Rosa C	1 µl

24 µl of this mixture was added to 1 µl of DNA.

PCR profile

94 °C for 2 mins

93 °C for 30 secs
58 °C for 30 secs
65 °C for 1 min
x 40

72 °C for 10 mins

Samples stored at 4 °C until analysis.

PCR product analysis

This resulted in a 550 bp wildtype band and/or a 250 bp transgene band (Figure 2.8).

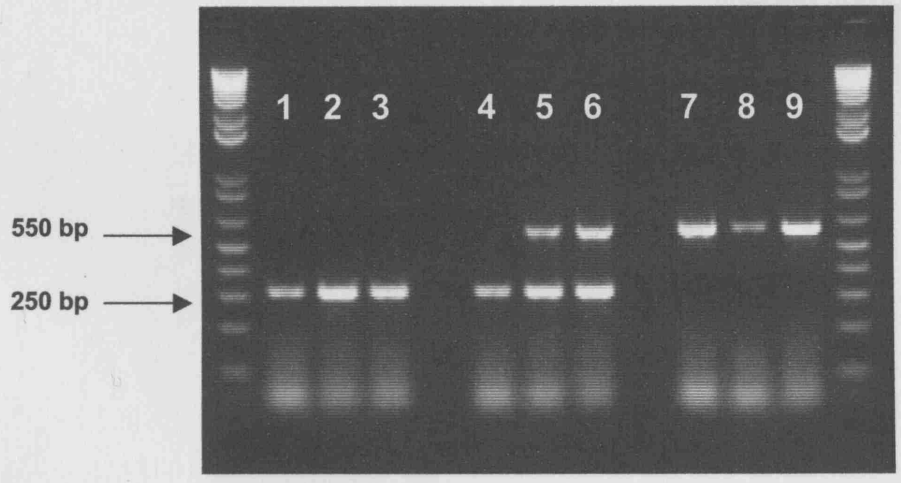

Figure 2.8: *R26R* genotyping. Samples 1-4 are homozygote for the *R26R* allele. Samples 5 and 6 are heterozygote for the *R26R* allele. Samples 7-9 are wild-type for the *R26R* allele.

2.11.7 *Irs2* deletion

Irs2 deletion was analysed using primers located ~1.1 kb upstream of the 5' loxP site (DF 5' GGGAACCTGACAAGTGAATG 3') and ~0.2 kb downstream of the 3' loxP site (loxP 5' AGTCCACTTTCCTGACAAGC 3').

PCR reaction mixture

Reddymix	44 µl
DF	2 µl
PR	2 µl

48 µl of this mixture was added to 2 µl of DNA.

PCR profile

95 °C for 3 mins

95 °C for 1 min
52 °C for 1 min
72 °C for 1 min
x 30

72 °C for 7 mins

Samples stored at 4 °C until analysis.

PCR product analysis

The presence of a 1.3kb product indicated that recombination had occurred between the *loxP* sites (Figure 2.9).

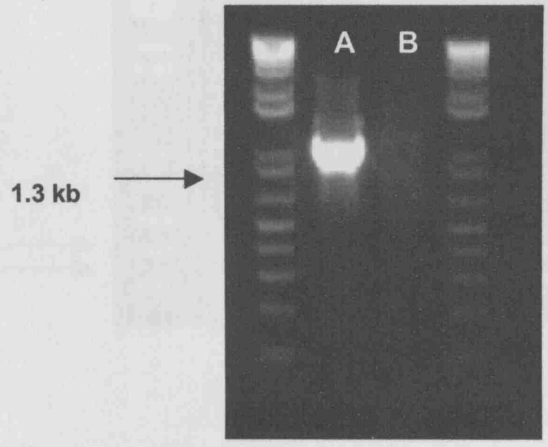

Figure 2.9: PCR for *Irs2* deletion. Sample A is positive and sample B is negative for deletion of *Irs2*.

2.11.8 *P110βlox* genotyping

P110βlox genotyping was performed using the following two primers: B3: 5' AGTGAACGCTATGCATCACACCAGC 3' and B98: 5' AAGTACAAACATCCAAGCAA 3'

PCR reaction mixture

ddH_20	17.875 µl
Titanium Buffer	2.5 µl
dNTPs (2.5 mM)	2 µl
B3	1 µl
B98	1 µl
Titanium Taq	0.125 µl

25 µl of this mixture was added to 3 µl of DNA.

PCR profile

94 °C for 3 mins

94 °C for 30 secs
65 °C for 30 secs
72 °C for 1 min 30 secs
x 35

72 °C for 7 mins

Samples stored at 4 °C until analysis.

PCR product analysis

This resulted in a 304 bp product for the wild-type allele and/or a 372 bp product for the *p110βlox allele* (Figure 2.10).

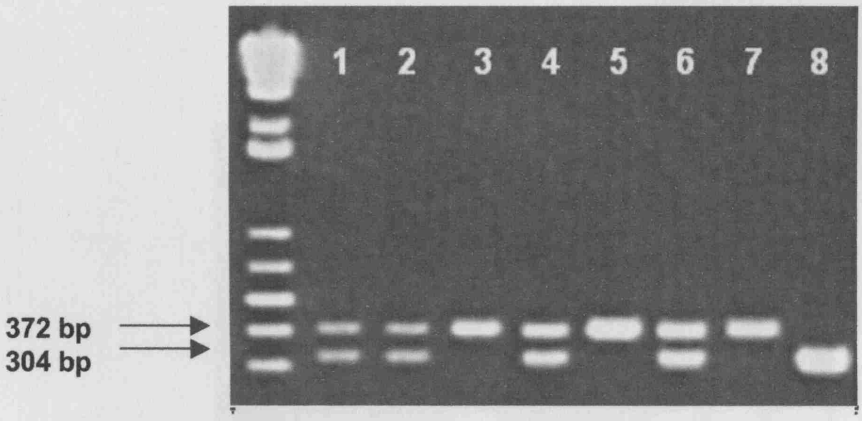

Figure 2.10: *P110βlox* genotyping. Samples 1, 2, 4 and 6 are heterozygote for the *p110βlox* allele. Samples 3, 5 and 7 homozygote for the *p110βlox* allele. Sample 8 is WT for the *p110βlox* allele.

2.11.9 *Z/eg* genotyping

Z/eg genotyping was performed using the following two primers: Z/eg forward 5' CCTCTGCCAAAAATTATGGGG 3' and Z/eg reverse 5' ACTATGGTTGCTGACTAATTG 3'.

PCR reaction mixture

Reddymix	22 µl
ZF	2 µl
ZR	2 µl

24 µl of this mixture was added to 1 µl of DNA.

PCR profile

94 °C for 1 min

94 °C for 30 secs
55 °C for 30 secs
72 °C for 1 min 30 secs
x 29

72 °C for 10 mins

Samples stored at 4 °C until analysis.

PCR product analysis

This resulted in a 750 bp product if samples were positive for the *Z/eg* allele (Figure 2.10).

Figure 2.11: *Z/eg* genotyping. Samples 1,4 and 5 are negative for presence of the Z/eg allele. Samples 2, 3, 6, 7 and 8 are positive for the Z/eg allele.

2.12 LacZ staining on earpunches

Tissue from ears was taken from mice using standard ear punchers. The tissue was incubated in the dark overnight at 37° C in β-galactosidase stain solution (1 x PBS, 2mM $MgCl_2$, 0.01% sodium deoxycholate, 0.02% Nonidet P-40, 5mM potassium ferricyanide and 5mM potassioum ferrocyanide) containing a 1:40 dilution of X-gal (40mg/ml). The presence of blue staining of the tissue indicated β-galactosidase activity and therefore, ectopic Cre expression.

2.13 *In vivo* physiological studies

2.13.1 Investigation of body weights

All body weights were recorded during the early light phase between 9am and 12pm using a Sartorius BP60 balance (Sartoruis, Goettingen, Germany) recording to the nearest 0.01g.

2.13.2 Body length

Body length (naso-anal distance) was measured in cm using a standard ruler, either post-mortem or in anaesthetised mice with the observer blinded to the genotype.

2.13.3 Feeding studies

2.13.3.1 Analysis of food intake

For analysis of food intake mice, were singly housed and allowed to acclimatise for a week. Each individual was then given a pre-weighed amount of food (~100g) and allowed *ad libitum* feeding. Food intake and body weight were measured for seven days at the ages indicated. Food was weighed daily in the early light phase (8am-10am) unless otherwise stated.

2.13.3.2 Response to fasting

Singly housed animals were exposed to two 16 hour (h) overnight fasts (at least 4 days apart) in a two week period preceding the study to acclimatise them. Two evenings before the study, the animals were removed into a clean cage to ensure that no small food pieces were present among the bedding. The evening before the study (at approximately 5pm), food was removed from the cages and the mice fasted for approximately 16-h overnight. In the early light phase (8am-9am) approximately 75g of food was weighed, recorded and given to each animal. The food was then weighed after 1-h, 2-h, 4-h, 8-h and 24-h post-refeeding. The body weight of the mice was also recorded. All measurements were made with a Sartorius BP60 balance (Sartoruis, Goettingen, Germany) recording to the nearest 0.01g.

2.14 High fat diet (HFD) feeding

Animals were weighed at 6 weeks of age. Controls and knockouts (KOs) were each divided into two body-weight matched groups. A control and KO group were maintained on a standard chow diet (4.3% fat, RM1, Special Diet Services). The remaining control and KO groups were placed on HFD consisting of 45% fat, 35% carbohydrate and 20% protein (Research Diets, New Brunswick, NJ, USA). All groups were weighed (between 9am and 11am) once a week, for the number of weeks indicated.

2.15 Response to peripheral MTII treatment

Mice were singly housed at least two weeks before the study. The week preceeding the study, animals were handled and sham injected with saline (100 µl) each morning (at approximately 9 am). Two evenings prior to the study, animals were removed into a clean cage to ensure that no small pieces of food remained within the bedding. The evening before the study (at approximately 5 pm), food was removed from the cages and the mice were fasted for approximately 16-h overnight. The MTII (5 mg) (Bachem) was reconstituted in 10ml of sterile PBS resulting in a final concentration of 0.5 µg/µl, and made the morning of the study.

In the early light phase (8am-9am), animals were injected intraperitoneally (i.p.) with 100 µl of saline or 50 µg of MTII (in a volume of 100 µl). Immediately after injections, animals were returned to their home cage containing a known amount of chow (~75g). Food was then reweighed at 1-h, 2-h, 4-h, 8-h and 24-h post-injection using a Sartorius BP60 balance (Sartoruis, Goettingen, Germany) recording to the nearest 0.01g. The study was performed in a cross-over design with each animal acting as its own control. Thus, following a week washout period, the study was repeated with animals that had received MTII in the first phase now receiving saline and vice versa.

2.16 Response to peripheral leptin treatment

Animals were singly housed for at least two weeks prior to the study. For 10 days prior to the study, animals were handled and sham injected with 100 µl saline on a daily basis (at approximately 6pm). The daily food intake and body weight of each mouse was also measured each evening to ensure that animals were not stressed and were eating normally. Two days prior to the study, animals were removed into a clean cage to ensure no small pieces of food remained within the bedding.

On the first day of the study (day 0), the animals were weighed in the afternoon (at approximately 4pm) and the food was removed from each cage. The control animals were then divided into two body-weight matched groups: one to receive leptin and the other to receive the vehicle control. KO animals were also randomly divided into two body-weight matched groups, each to receive the different treatment. The protocol that was used is summarised below:

Day 0- each mouse was injected i.p. with either 100 µl of vehicle or leptin (R&D Systems Inc., MN, USA), at a dose equivalent to 5 µg/g) at approximately 6pm. To each cage, a pre-weighed amount of food was then added. The next day (day 1), food was measured at 9am and again at approximately 4pm, at which point it was removed from the cage into a sealed bag. Body weights were also measured at approximately 4pm in order to calculate the injection dose for the evening. Mice were injected with either leptin or vehicle (as before) at around 6pm. Following the injections, the food from the sealed

bag was returned to each cage. On day 2, the steps of day 1 were repeated. On day 3, the food and body weight of each animal was recorded at approximately 9am and 6pm.

This study was designed as a cross-over experiment, so that each animal served as its own control. Thus, following a one week washout period, the study was carried out on the same animals. All the animals that received vehicle control in the first week of the study received leptin, and vice versa.

2.17 Analysis of body composition

Three methods were used to determine the body composition of the various animal models studied: magnetic resonance imaging (MRI), dual-energy x-ray absorptiometry (DEXA) scanning and weighing of fat pads.

2.17.1 Magnetic resonance imaging (MRI)

Mice were scanned using a 4.7T Varian system (post-mortem). Whole body images (between 50-60 slices; 2 mm thick) were obtained for each mouse using a spin-echo sequence (TR4500/TE20). Semi-automatic image segmentation software (sliceOmatic v4.2, Tomovision) was used to separate and quantify respective tissue volumes (Ross et al., 1991). For adipose tissue, the volume was multiplied by a correction factor of 0.9 in order to account for hydration (Tang et al., 2002). This work was carried out by Dr. Po Wah in the laboratory of Professor Jimmy Bell, Imperial College London.

2.17.2 Dual-energy X-ray absorptiometry (DEXA) scanning

Mice were terminally anaesthetised and their body composition analysed using a DEXA scanner. This study employed the PIXImus DEXA scanner (Lunar, GE Healthcare, USA) specifically designed to study the skeleton of small rodents. DEXA scanning works on the principle that X-rays reflect from bone in a density dependent manner. The PIXImus system exposes the entire animal to a cone shaped beam of high energy (80 kV)

and low energy (55 kV) x-rays. A CCD (charged couple device) camera detects the radiation hitting a luminescent panel below the test subject. The varied compositions of bone mineral, fat and lean tissue means they differentially absorb or reflect the dual energy X-rays. Thus, by digitally processing the detected radiation, the PIXImus can calculate the relative quantities of bone, fat and lean tissue along the x-ray path. During each scan, the dual x-ray exposure is performed four times and on completion, the data is collated to produce a 'summary' image, the density of which is compared to a standard object (mouse phantom) used to calibrate the instrument. All data was analysed using the PIXImus software (version 1.8, Lunar, GE Healthcare, USA).

2.17.3 Analysis of adiposity by fat pad weights

Animals were sacrificed by either cervical dislocation or terminal anaesthesia (see below). As an indicator of total body white adipose tissue (WAT) mass, the gonadal fat pad and mesenteric fat depots were carefully dissected out, pooled and weighed. With regards to brown adipose tissue (BAT), the two depots on the dorsal aspect of the thorax (between the scapulae) were dissected out. All weights were measured to the closest 0.0001g.

2.18 Metabolic studies

2.18.1 Determination of fasting blood glucose (FBG) levels

Mice were fasted for approximately 16-h overnight, and blood glucose levels were determined during the early light phase (8am-10am) via tail vein bleeds using a Glucometer Elite glucometer (Bayer). Ethyl chloride was used as a local anaesthetic.

2.18.2 Determination of glucose homeostasis by intra-peritoneal glucose- tolerance tests

Mice were fasted for 16-h and blood glucose levels determined as described above. Mice were then injected i.p. with 1.5 g $kg^{-1}$of D-glucose, and blood glucose measured at 15, 30, 60 and 120 minutes post-injection.

2.18.3 Determination of fasting insulin and leptin levels

Blood samples taken from animals following a 16-h overnight fast were centrifuged at 10,000 rpm for 15 minutes at 4 °C. The plasma was then immediately removed and frozen at -80 °C until assayed. Plasma insulin levels were measured using an ultrasensitive rat insulin ELISA (CrystalChem Inc.) with mouse insulin standards. Plasma leptin levels were measured using a mouse leptin ELISA (CrystalChem Inc.). All samples were assayed in duplicate and in one assay to avoid inter-assay variation.

2.18.4 Determination of resting metabolic rate and activity

Resting metabolic rate (RMR) was studied in male mice (ages indicated in result sections) at 30 ± 0.1°C (thermoneutral), 22 ± 0.1°C (housing temperature) or both temperatures by openflow respirometry using a paramagnetic oxygen analyser (Series 1100, Servomex Group Ltd, Crowborough, Sussex, U.K.) as previously described (Selman et al., 2001). Free access to food and water was permitted prior to metabolic measurements.

In brief, mice were weighed (0.01g, Sartorius) and rectal body temperature measured (2751-K, Digitron Instrumentation Ltd, U.K.) in advance of being placed individually within an airtight Perspex chamber inside a temperature-controlled incubator (INL-401N-010, Gallenkamp, U.K.). Silica gel dried air was pumped through the system (Charles Austin Pump Ltd, U.K) at 600-800mls min^{-1} (DM3A, Alexander Wright Flow Meter, U.K.), re-dried and a sub-sample (~150mls min^{-1}) passed through the oxygen analyser. Energy expenditure was calculated using the Weir equation (Weir, 1949) with all samples corrected for standard temperature and pressure (McLean and Speakman,

2000) and downloaded directly on to a microcomputer. The lowest 10 consecutive readings in oxygen concentration (equivalent to 5 minutes in the chamber) were taken as an estimate of the RMR (mls O2 min^{-1}). A general-linear model was used to control for observed body mass differences between groups. This work was carried out by Dr. Colin Selman (UCL), in collaboration with the laboratory of Professor John Speakman, University of Aberdeen.

2.19 Harvesting of tissues

2.19.1 Blood collection

Two differing methods were used for the collection of plasma. Samples were collected from live mice via tail bleed using a capillary blood collection system (Sarstedt, Nümbrecht, Germany). An alternative terminal approach involved the decapitation of dead animals (killed by cervical dislocation) and collection of blood. All samples were allowed to clot, and then placed on ice until centrifugation at 10,000 rpm for 15 minutes at 4 °C. Plasma was immediately separated and stored at –80 °C until analysis. If samples were required in a fasted state, animals were fasted for 16-h overnight, prior to blood collection.

2.19.2 Harvesting of brain and hypothalamus

Mice were either terminally anaesthetised (as previously described) or killed by cervical dislocation. In the case of terminal anaesthesia, animals were subjected to an i.p. injection with an overdose of Sodium pentobarbitone (Euthatal; Rhône Mérieux, Harlow, UK) at a dose of 500 mg kg^{-1} body weight. The head was then removed, the brain dissected out of the skull, and snap frozen in liquid nitrogen. If required, following removal of the brain from the skull, the hypothalamus was rapidly dissected and snap frozen in liquid nitrogen. As before, if samples were required in a fasted state, animals were fasted for 16-h overnight prior to dissection.

If fixed brains were required, mice were terminally anaesthetised and brains harvested following transcardiac perfusion with phosphate-buffered saline (PBS) and 4%

paraformaldehdye (PFA), using a Marlow Watson peristaltic pump. Brains were post-fixed overnight in 4% PFA, and then transferred to 30% sucrose and subsequently frozen after 48-h.

2.19.3 Harvesting of other tissues

Mice were either terminally anaesthetised (as described above) or killed by cervical dislocation. Peripheral tissues (including samples of liver, quadricep muscles, fat and ovaries were rapidly dissected and snap frozen in liquid nitrogen for subsequent analysis. If required, pituitaries were harvested, and either snap frozen or homogenised in 1M urea in PBS and stored at –80 °C prior to analysis. The pancreas was removed and fixed in 4% PFA. If tissue samples were required in a fasted state, animals were fasted for 16-h overnight prior to dissection.

2.20 DNA, RNA and protein extraction from tissues

2.20.1 DNA extraction from tissue

Tissue was placed in 525 µl lysis buffer (50 mM Tris pH8, 100 mM EDTA, 100 mM NaCl, 1% SDS) with 35 µl Proteinase K (10 mg/ml) and incubated overnight at 55 °C. Follwing this, 2 µl of RNase A (0.2mg/ml) was added and the mixture incubated at 37 °C for 1-h. 500 µl 5M NaCl was added, and the solution mixed gently and then 700 µl chloroform:isoamylalcohol (24:1) added. Samples were mixed gently for 2-h at room temperature, and centrifuged at 10,000 rpm for 10 minutes to and the upper aqueous phase removed to a new tube. 700 µl isopropanol was added to precipitate the DNA, which was pelleted by centrifuging at 10,000 rpm for 10 minutes. The DNA pellet was then washed with 70% ethanol and resuspended in 200 µl TE buffer.

2.20.2 mRNA extraction and quantification

Throughout handling of tissue and the extraction process, standard precautions were taken to reduce the risk of RNAse contamination. Bench surfaces, tools, and pipettes

were treated with RNAse inhibitor spray (RNase*Zap*; Ambion, Huntingdon, UK), filtered pipette tips used, and gloves frequently changed. 100 mg of tissue was homogenised on ice in a 5 ml flat-bottom universal container at 12,000 rpm with a Turrax T25 dispersing tool in 1 ml of a phenol/guanidine isothiocyanate solution according to the manufacturer's instructions (TRIZOL; Invitrogen, Paisley, UK). The precipitated RNA was resuspended in 60 µl of nuclease-free H_2O (Promega, Southampton, UK).

RNA quantification and analysis of purity were determined by measuring the absorbances at 260 nm and 280 nm in a CE 2041 spectrometer (Cecil Instruments, Cambridge, UK). RNA concentration was adjusted to 100 ng/µl with nuclease-free H_2O.

2.20.3 Protein extraction and quantification

Protein lysis buffer (10mM Tris, 5mM EDTA, 50mM NaCl, 30mM $Na_2H_2P_2O_7$, 1% Triton X-100, 50mM NaF, 0.1mM Na_3VO_4, adjusted to pH 7.6) was freshly prepared by dissolving a protease inhibitor mixture tablet (MiniComplete; Roche Diagnostics, Lewes, UK) per 10 ml of buffer, and by adding PMSF to a final concentration of 1mM immediately prior to use. Tissue (300-500mg) was homogenised on ice in 1 ml of lysis buffer in a 5 ml flat-bottom universal container at 12,000 rpm with a Turrax T25 rotor-stator dispersing tool (IKA, Staufen, Germany). The lysate was incubated on ice for 30 minutes to increase protein solubilisation, and transferred to a 1.5 ml tube. Following centrifugation at 10,000 rpm for 20 minutes at 4 °C, the clear phase between the lipid-containing upper phase and the sedimented insoluble tissue components was transferred to a new reaction tube. Protein concentration was determined by a Bradford reaction assay (BioRad, Hemel Hempstead, UK).

2.21 Immunoprecipitation and western blotting

Protein was extracted as described above (2.19.3) from snap frozen samples.

2.21.1 Immunoprecipitation of IRS2

For the immunoprecipitation of IRS2, 10 µl of anti-IRS2 sheep polyclonal antibody (generated by the Withers laboratory) was incubated with 2 mgs of lysate at 4 °C, on a rotary mixer overnight (total volume of 1 ml). Following overnight incubation with antibody, samples had 100 µl total bead volume of pre-washed protein-A agarose (Roche Diagnostics) added to them using a wide-orifice tip. The samples were incubated for a further 120 minutes at 4 °C. Immunoprecipitations were then clarified by gentle centrifugation and washed twice with 750 µl of 1 x lysis buffer. Samples were then denatured in 20 µl of 2x SDS-sample buffer (125mM Tris pH 6.8, 20% glycerol, 4% SDS, 1% bromophenol blue, 200mM β-mercaptoethanol) at 100 °C for 5 mins. Following centrifugation at 10,000 rpm for 2 minutes, the supernatant was used for SDS-polyacrylamide gel electrophoresis and subsequent immunoblotting.

2.21.2 Immunoblotting

Polyacrylamide gel electrophoresis was performed using the Mini-Protean electrophoresis system (BioRad). Lysates were resolved on 7.5% SDS-PAGE gels, immersed in running buffer (25mM Tris, 192mM glycine, 0.1% SDS). 20 µl of recovered immunoprecipitate was loaded per lane and 10 µl of a coloured molecular weight marker was also loaded to indicate protein size (Rainbow; Amersham, Little Chalfont, UK). Electrophoresis was performed at 100V for 60-90 minutes. Proteins were transferred from the gel to a polyvinylidene-difluoride membrane (Amersham) in transfer buffer [25mM Tris, 192mM glycine, 20% methanol (vol/vol)] at 100V for 90-120 minutes.

The membrane was incubated in blocking solution consisting of 5% non-fat dried milk in TNT buffer (50mM Tris pH 8.0, 150mM NaCl, 0.1% Tween 20) at room temperature for 60 minutes to reduce non-specific binding of antibody. Primary antibody (anti-IRS2 sheep polyclonal antibody generated by the Withers laboratory) was diluted to a concentration of 1:1,000 with blocking solution, in which the blot was incubated at 4 °C for approximately 16-h. The membrane was washed three times in TNT buffer for 5 minutes and incubated at room temperature for 1-h in HPO-conjugated polyclonal sheep anti-mouse antibody (Amersham, NA 931) (1:10,000 in blocking solution).

Following a further three 5 minute washes in TNT buffer, the blot was analysed by application of a chemiluminescence detection kit (ECL Plus; Amersham) and autoradiography (Hyperfilm ECL; Amersham). Exposed films were quantified with self-calibrating GS 800 densitometer and proprietary software (Quantity One 4.5; BioRad).

2.22 Gene expression studies

RNA was extracted as described in section 2.19.2 from hypothalamic samples snap frozen at the time of dissection, and realtime PCR (RT-PCR) was performed to analyse the gene expression of various feeding neuropeptides.

2.22.1 Reverse transcription

Once extracted, mRNA was reverse transcribed in order to generate complementary DNA (cDNA) template for RT-PCR quantification. The TaqMan Retrotranscription Kit (Applied Biosystems) was used. Briefly, each sample contained 2.5 µl of RT Buffer (10X), 5.5 µl of $MgCl_2$, 5 µl of dNTPs, 1.25 µl of oligo-DT, 0.5 µl of RNAse inhibitor, 0.5 µl of reverse transcriptase with 1 µg of RNA used as a template. Each reaction was set-up in 0.2 ml reaction tubes (BioRad) and the the total volume in each tube made up to 25 µl with nuclease free water. Samples were incubated at 37 °C for 60 minutes, and the reverse transcriptase subsequently inactivated by heating the samples to 95 °C for 5 minutes. The resulting cDNA was then stored at –20 °C until PCR analysis.

2.22.2 Real-time polymerase chain reaction

Quantitative PCR was performed with the TaqMan system (Applied Biosystems). Proprietary sequence Taqman Gene Expression assay FAM/TAMRA primers (Applied Biosystems, Foster City, CA, USA) were used: AgRP (Mm00475829_g1), CART (Mm0048986_m1) HPRT (hypoxanthine guanine phosphoribosyl transferase, Mm99999915_g1), NPY (Mm00445771_m1), and POMC (Mm00435874_m1).

The reactions were carried out in a 25 µl reaction volume in an ABI Prism 7900 HT thermocycler (Applied Biosystems). The manufacturer's recommended cycling conditions were employed, which consisted of 50 °C for 2 min and subsequent 95 °C for 10 min, followed by 40 cycles of 95 °C for 15 sec and 60 °C for 1 min, with all temperature changes occurring at maximum ramp speed. For the melting curve, two subsequent steps of 95 °C for 15 sec and 60 °C for 15 sec also occurred at maximum ramp speed and were followed by a slow 2% temperature ramp step to 95 °C. The integrated 488 nm Argon laser excitation/detection system used SDS 2.1 software (Applied Biosystems).

2.23 Immunocytochemistry on hypothalamic sections

Thirty µm sections were cut from frozen perfused brains using a sliding microtome and samples and stored at –20 °C in cryoprotectant before use. Samples were washed 3 times in potassium phosphate buffered saline (KPBS) pH 7.4 and then blocked with 2% chicken serum in KPBS/0.4% Triton X-100 for 1-h at room temperature. Samples were then incubated with primary antibodies in KPBS/0.4% Triton X-100 for 48-h at 4 °C. The primary antibodies used were rabbit anti-IRS2 antibody (Upstate) and mouse monoclonal anti-lacZ (Abcam). Slices were then washed 4 x 10 min at room temperature with KPBS, and incubated with appropriate secondary antibodies (fluorescently labelled) for 1-h in KPBS/0.4% Triton X-100 at room temperature before being washed 4 x 10 min in KPBS at room temperature. The fluorescently labelled secondary antibodies used were chicken anti-rabbit IgG-AlexaFluor 594 (red) conjugate and chicken anti-mouse IgG-AlexaFluor 488 conjugate (green) (Molecular Probes). Slices were mounted on polylysine-coated microscope slides and cover-slipped with buffered glycerol.

2.24 Pancreatic immunocytochemistry (ICC) and measurement of islet mass and number

Animals were killed by terminal anaesthesia or cervical dislocation. The pancreas was then removed, cleared of fat and lymph nodes and fixed in 4% PFA, embedded in paraffin and cut into 5 µm sections. Sections were treated with 0.01M citrate buffer for 10 min at 95 °C and incubated with blocking solution consisting of PBS buffer with 5 %

normal chicken serum and 2 % BSA for 30 min. A cocktail of primary antibodies in blocking buffer containing mouse anti-insulin antibody (clone K36aC10, Sigma-Aldrich) and rabbit anti-glucagon (Abcam Ltd) was applied for 2-h at RT or overnight at 4 °C. The sections were subsequently incubated chicken anti-rabbit IgG-AlexaFluor 594 (red) conjugate and chicken anti-mouse IgG-AlexaFluor 488 conjugate (green) (Molecular Probes) for 2-h at RT. Transmitted light and fluorescent images were captured with Metamorph software using a Zeiss Axiophot 2 microscope or with SimplePCI software using an Olympus BX51 microscope equipped with Hamamatsu 95 black and white camera.

For quantification of β-cell area and islet number, five pancreases were analysed per genotype. For each pancreas four sections, at least 150 μm apart, were analysed. For each section, the total area occupied by insulin-positive cells was scored using Simple PCI software, together with the number of islets on the section. Results are expressed as the percentage of the total islet area and the mean islet density for each pancreatic section. This work was carried out by Dr. Marc Claret (UCL).

2.25 Reproductive studies

2.25.1 Superovulation studies

Female mice, at approximately 8-10 weeks of age, were given an i.p. injection of 10 IU pregnant mare's serum (PMSG, Folligon, Intervet Inc). This was followed 46 hours later by 8 IU of human chorionic gonadotropin (Chorulon, Intervet Inc). Oocytes were flushed from the oviduct 14-16 hours after the second injection. This work was carried out with Dr. Irina Neganova (UCL).

2.25.2 Oestrous cycle progression

To monitor the oestrous cycles of *NesCreIrs2KO* and control animals, mice were vaginally smeared on a daily basis for complete cycles. The smears were spread onto

glass slides, which were then stained with Giemsa stain. This work was carried out with Dr. Irina Neganova (UCL).

2.25.3 Analysis of reproductive hormone levels

2.25.3.1 Serum levels of oestrogen and progesterone at dioestrous

Blood samples were collected as previously described (2.18.1). Samples were left to coagulate at 4 °C overnight, centrifuged with the serum collected and frozen at -20 °C. Serum oestrogen and progesterone levels were measured using immunofluorometric assays (Delfia, Perkin Elmer, Turku, Finland).

2.25.3.2 Piuitary hormone levels

Pituitaries were harvested during dioestrous. They were homogenised in 1ml of 1M urea in PBS and stored at -80 °C prior to analysis. Radioimmunoassays (RIAs) for pituitary luteinizing hormone (LH), follicle stimulating hormone (FSH) and prolactin were performed as previously described. This work was carried out in collaboration with the laboratory of Professor Stephen Bloom, Imperial College London.

2.25.4 Ovarian histomorphometric analyses

Ovaries were fixed in 10% buffered formalin, embedded in paraffin and cut into 5 μm sections. For histomorphometric analysis sections were stained with haematoxylin-eosin. Follicles, classified according to their diameter and number of granulosa cell layers, were counted in every tenth section, starting from the fifth section, through the entire ovary. Only follicles with a clearly visible oocyte nucleus were counted to avoid double counting. Atretic follicles were defined on the following morphological criteria: follicle and oocyte shape, localisation of the oocyte in the follicle, presence of a degenerated oocyte, altered zone pellucida, the presence of granulosa cells inside zone pellucida, presence of more than 3 pynknotic nuclei in granulosa cells and macrophage invasion. Follicle growth, follicle and oocyte size (diameter) and total follicular and antral cavity

area were measured using LUCIA software (Nikon UK, Kingston-upon-Thames, UK). This work was carried out by Dr. Irina Neganova (UCL).

2.25.5 Timed matings

At 6 weeks of age, six female *NesCreIrs2KO* animals and six controls were pair mated with wildtype C57/Bl6 males for the duration of 12 weeks. Fertility was assessed by daily monitoring of pregnancies, litter and pup number.

2.26 Suppliers

General laboratory chemicals were purchased from Sigma-Aldrich, Gillingham, UK, except where stated otherwise.

2.27 Data handling and statistics

All data was expressed as an average ± S.E.M. for all data points. Standard error of the means, and all other statistical tests were performed using GraphPad Prism Version 4. Paired and unpaired t-tests and 2-way ANOVA with Bonferroni post-tests were performed as appropriate.

Chapter 3

Phenotypic characterisation of *NesCreIrs2KO* animals

3 Characterisation of *NesCreIrs2KO* animals

An important role for IRS2 in energy homeostasis, glucose homeostasis and reproduction has been implicated by studies of animals with global deletion of this gene. *Irs2* null mice are insulin resistant, display β-cell failure and as a result develop diabetes (Withers et al., 1998). A key role for IRS2 in the CNS regulation of energy homeostasis is also suggested by the obesity and hyperphagia of these animals (Burks et al., 2000c). These findings implicate a significant role for CNS insulin signalling in the regulation of energy homeostasis and are supported by the hypothalamic dysfunction and impaired glucose homeostasis displayed by *NIRKO* animals (Bruning et al., 2000).

To investigate the role of IRS2 in the CNS regulation of energy homeostasis and glucose homeostasis in a tissue-specific manner, mice with specific deletion of *Irs2* in the CNS were generated. To do so, *NesCre* animals (which expresses Cre recombinase under the control of a rat nestin promoter) were crossed with *Irs2lox* animals (animals with a conditional allele of *Irs2*).

3.1 Proof of *Irs2* deletion

Nestin, an intermediate filament protein, is expressed in the central and peripheral nervous system by embryonic day 11. *NesCre* transgenic animals have been used extensively in recent years (Bruning et al., 2000; Lendahl et al., 1990; Tronche et al., 1999). Despite this, before the commencement of investigations, studies aimed at confirming the lack of *Irs2* expression in the CNS of *NesCreIrs2KO* animals were performed.

Indeed, the use of various methods demonstrated the deletion of *Irs2* at the DNA, mRNA and protein levels in the hypothalami of *NesCreIrs2KO* animals but not controls (Figure 3.1). Thus, the use of *NesCreIrs2KO* animals as a valid model for the study of IRS2 mediated signalling pathways in the CNS was confirmed. Therefore, a series of systematic analyses to investigate the hypothalamic function, glucose homeostasis and reproductive function of *NesCreIrs2KO* animals and controls were undertaken.

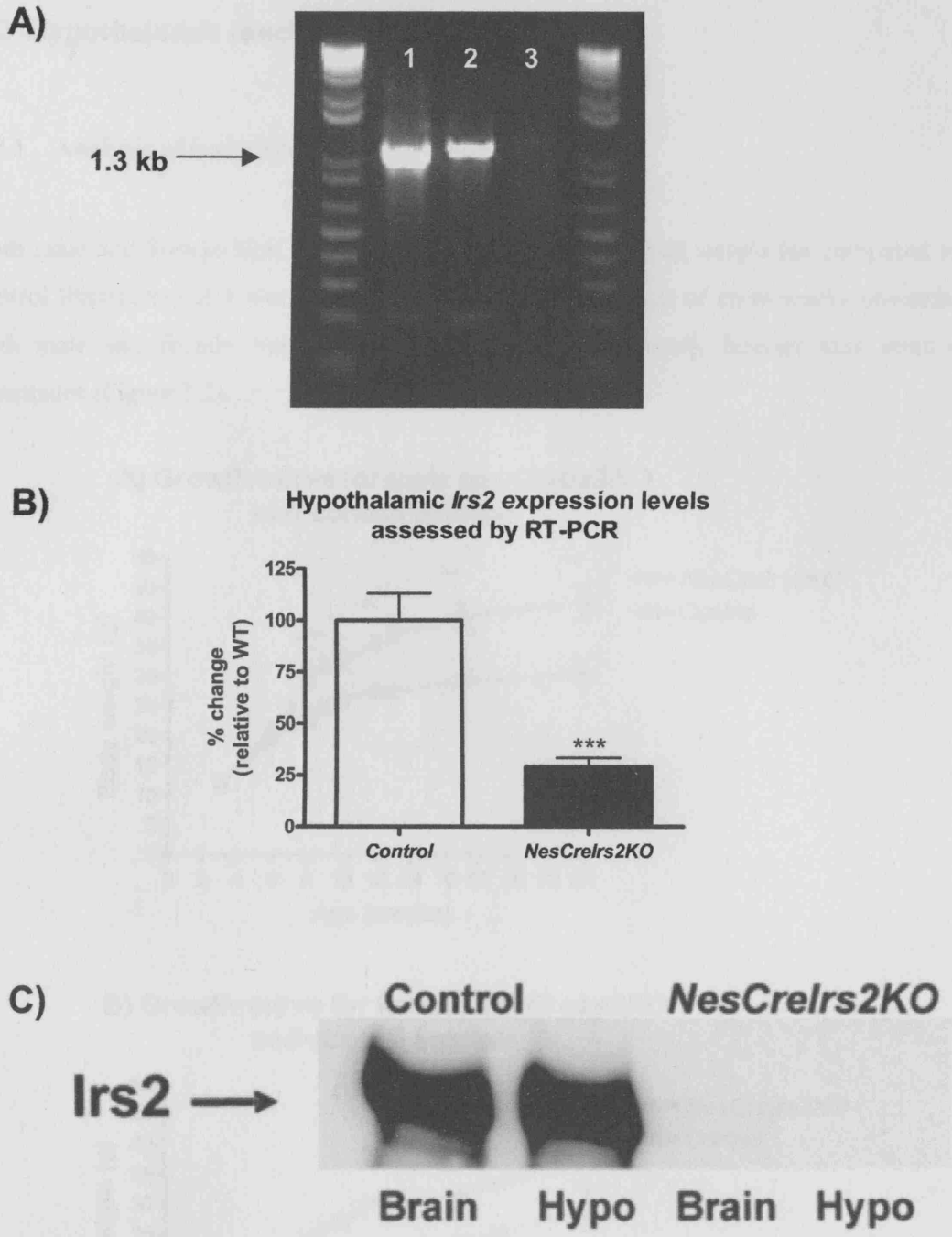

Figure 3.1: A) PCR analysis of *Irs2* deletion in DNA extracted from: 1) *NesCreIrs2KO* whole brain, 2) *NesCreIrs2KO* hypothalami and 3) wild-type brain. A 1.3kb band in samples 1 and 2 confirms deletion of *Irs2.* B) Gene expression analysis of hypothalamic *Irs2* levels in control and *NesCreIrs2KO* animals. *NesCreIrs2KO* mice display signficiantly reduced IRS2 levels compared to WT (*** $P<0.0001$). C) Immunoprecipitation and western blotting analysis of IRS2 in whole brain and hypothalamic lysates. No IRS2 protein was detected in samples from *NesCreIrs2KO* animals, confirming the deletion of the *Irs2* gene in the brain of these animals.

3.2 Hypothalamic function

3.2.1 Analysis of body weight

Both male and female *NesCreIrs2KO* animals, were of normal weight (as compared to control littermates) at 3 weeks of age. However, from the age of eight weeks onwards, both male and female *NesCreIrs2KO* mice were significantly heavier than control littermates (Figure 3.2).

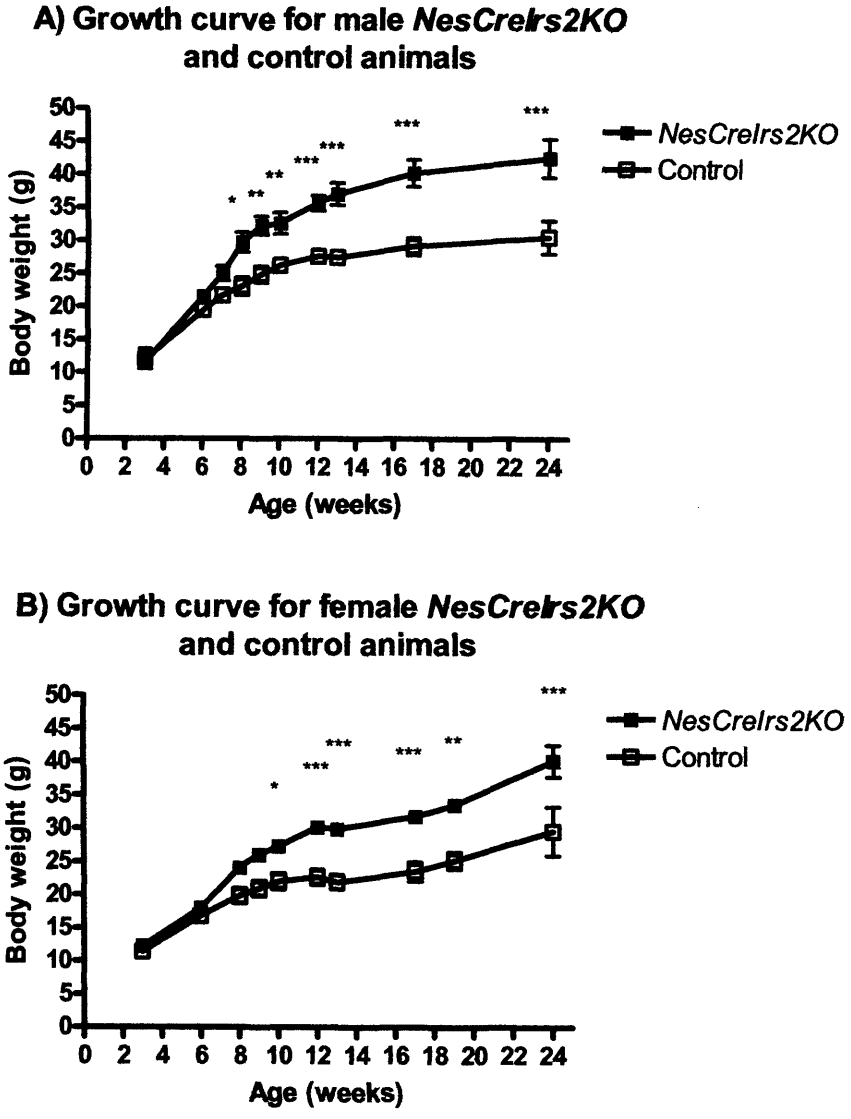

Figure 3.2: Growth curve for A) male *NesCreIrs2KO* and control animals and B) female *NesCreIrsKO* and control animals. Data represent the mean ± SEM for 6-12 animals of each genotype. * $P < 0.05$, ** $P < 0.01$, *** $P < 0.001$.

3.2.2 Analysis of body composition by MRI scanning

In order to determine whether the increased body weight of *NesCreIrs2KO* animals was due to changes in lean tissue mass, fat mass or a combination of both these factors, the body composition of 7-month-old males was analysed using MRI scanning. Male *NesCreIrs2KO* animals displayed an almost two-fold increase in fat mass, as compared to controls (Figure 3.3). No difference in lean tissue mass was detected in these animals.

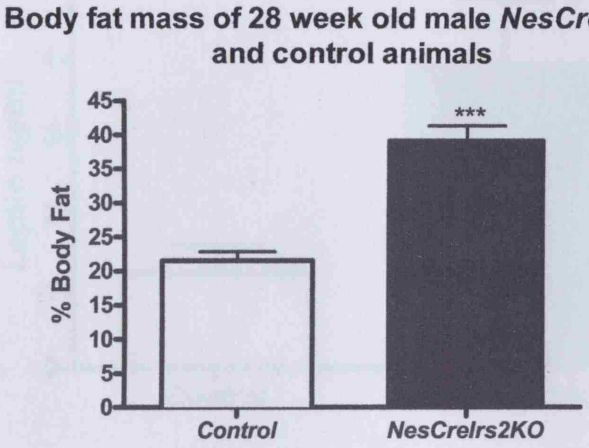

Figure 3.3: Body fat mass of 28-week-old male *NesCreIrs2KO* and controls as revealed by MRI scanning. Data represent the mean ± SEM for 4 animals of each genotype. *** $P < 0.001$.

Figure 3.4: Photograph of male *NesCreIrs2KO* (left) and control (right) at 12 months of age.

3.2.3 Plasma leptin levels

Consistent with their increased body weight at this age, at 12-week-old male *NesCreIrs2KO* animals had significantly raised fasting plasma leptin as compared to control animals (Figure 3.5).

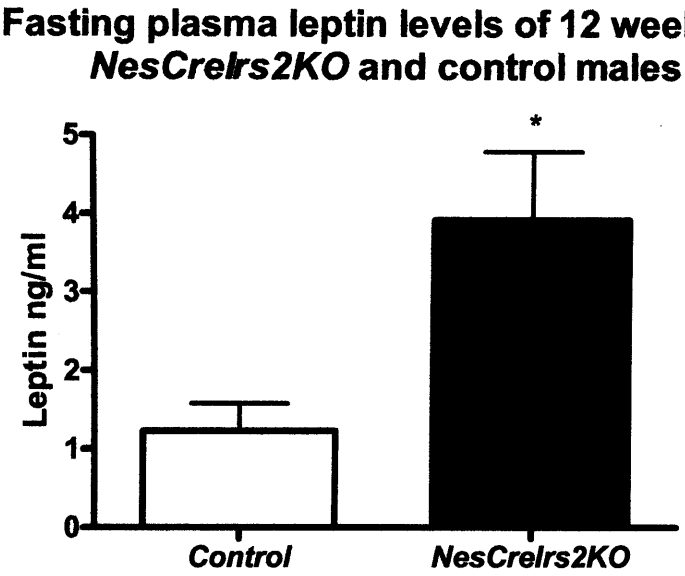

Figure 3.5: Fasting plasma leptin levels were measured on male *NesCreIrs2KO* and control mice at 12 weeks of age following a 16-h overnight fast. Data represent the mean ± SEM for 8 animals of each genotype. * $P < 0.05$.

3.2.4 Analysis of feeding behaviour

The increased adiposity of *NesCreIrs2KO* animals compared to controls could be a result of increased energy intake (i.e. food intake), decreased energy expenditure or indeed a combination of these two defects. In order to ascertain the contribution of feeding to the obese phenotype of *NesCreIrs2KO* animals, both the daily food intake of these animals and their feeding response to fasting were analysed.

3.2.4.1 Analysis of food intake

At 12 weeks of age, male and female *NesCreIrs2KO* mice were significantly hyperphagic compared to controls (Figure 3.6). This suggests that the increased body adiposity of these animals was partly due to their increased caloric intake.

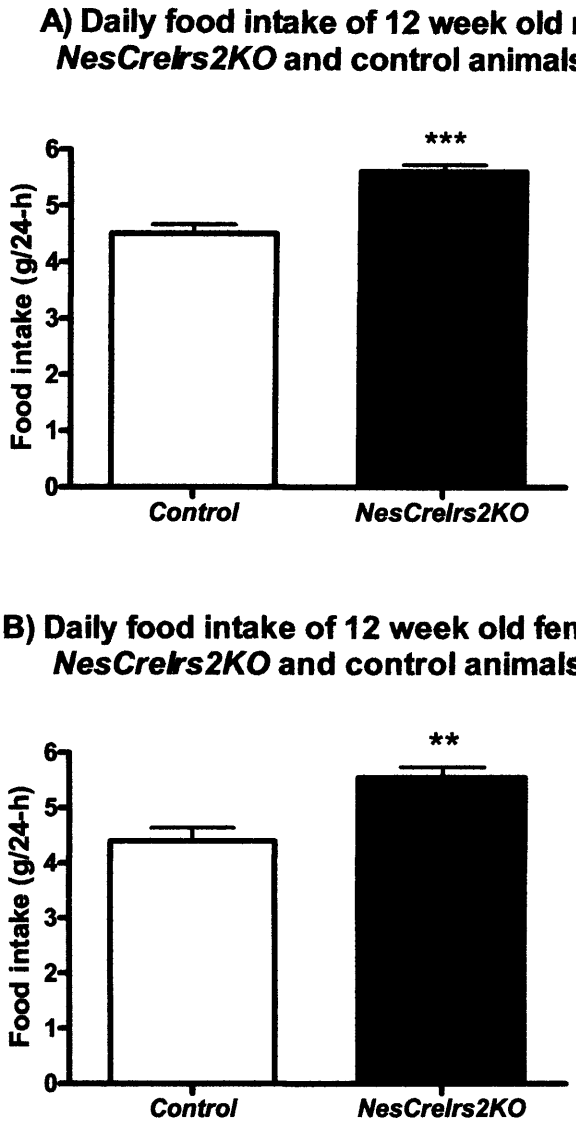

Figure 3.6: The daily (24-h) food intake was measured in: A) males at 12 weeks of age, B) females at 12 weeks of age. Data represent the mean ± SEM for 8-16 animals of each genotype. ** $P < 0.01$, *** $P < 0.001$.

3.2.4.2 Response to fasting

No increases in the food intake of *NesCreIrs2KO* animals at 5 months of age were detected following an overnight fast at 1, 2, 4 or 8 hours post re-feeding. However, both male and female *NesCreIrs2KO* animals exhibited an increase in 24-hour food intake (Figure 3.7), indicating an abnormality in feeding regulation during the dark phase. The hyperphagia exhibited by *NesCreIrs2KO* animals, suggests defects in long-term feeding regulation, governed by factors such as insulin and leptin.

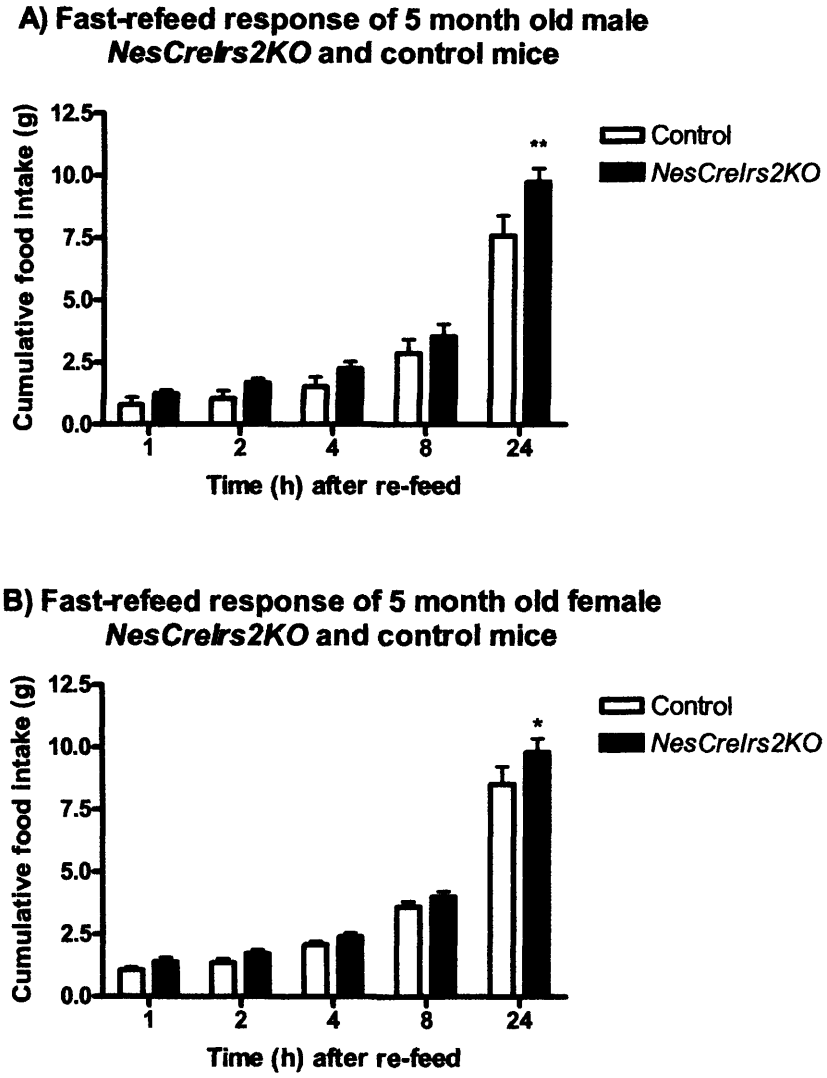

Figure 3.7: Re-feeding response in A) 5 month old male mice and B) 5 month old female mice. Following a 16-h overnight fast, approximately 50 g of food was weighed and given to each animal. The food was then weighed after 1-h, 2-h, 4-h, 8-h and 24-h. Data represent the mean ± SEM for 6-8 animals of each genotype. * $P < 0.05$, ** $P < 0.01$.

3.2.5 Metabolic Rate

In order to determine whether the obese phenotype of *NesCreIrs2KO* animals was due solely to the hyperphagia of these animals, or also partly due to impairments in energy expenditure, the metabolic rate of 12-week-old *NesCreIrs2KO* mice and relevant controls was assessed.

No significant difference in metabolic rate was seen between *NesCreIrs2KO* mice compared to controls at 12 weeks of age at either thermoneutral (30 ± 0.1°C) and housing temperature (22 ± 0.1°C) (Table 3.1).

Genotype	**RMR (ml O^2/min)**		
	30 °C	**22 °C**	**Tb (°C)**
Control	0.52 ± 0.02	0.90 ± 0.07	37.6 ± 0.3
NesCreIrs2KO	0.62 ± 0.07	0.91 ± 0.09	37.6 ± 0.2

Table 3.1: Summary of analysis of metabolic rate in 12-week-old male *NesCreIrs2KO* and control animals. Data represent the mean ± SEM for 8 animals of each genotype. Resting metabolic rate (RMR) and body temperature (Tb).

3.2.6 Analysis of body length

Measurement of naso-anal body length of male animals at 12 weeks of age revealed that *NesCreIrs2KO* were significantly longer (~12.4% increase) than controls (Figure 3.8).

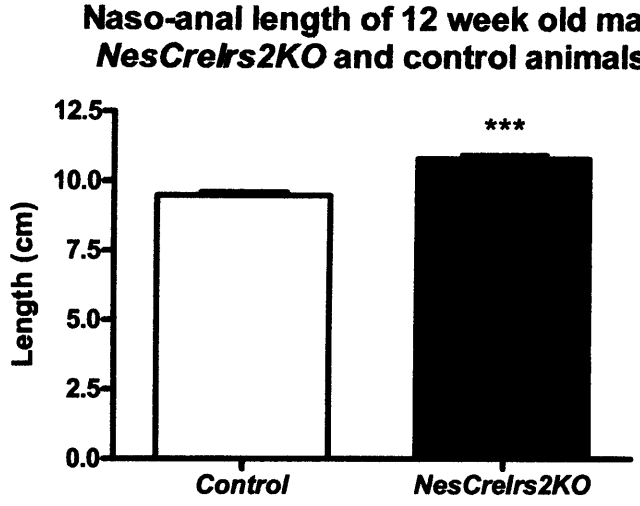

Figure 3.8: Naso-anal length was measured in male *NesCreIrs2KO* and control mice at 12 weeks of age. Data represent the mean ± SEM for 4-6 animals of each genotype. *** $P < 0.001$.

3.2.7 Response to leptin

In order to further analayse the defects relating to the obesity phenotype of *NesCreIrs2KO* animals, the sensitivity of these animals to the anorexigenic effects of peripherally administered leptin was assessed.

Leptin treatment (5mg/kg) inhibited food intake by 20% in both control and *NesCreIrs2KO* mice (Figure 3.9). In addition, following the treatment, control mice displayed a 1.09g loss in body weight, compared with a 1.3g loss of weight in *NesCreIrs2KO* mice. Taken together, these findings indicate that 12-week-old *NesCreIrs2KO* mice are not resistant to the anorexigenic effects of leptin.

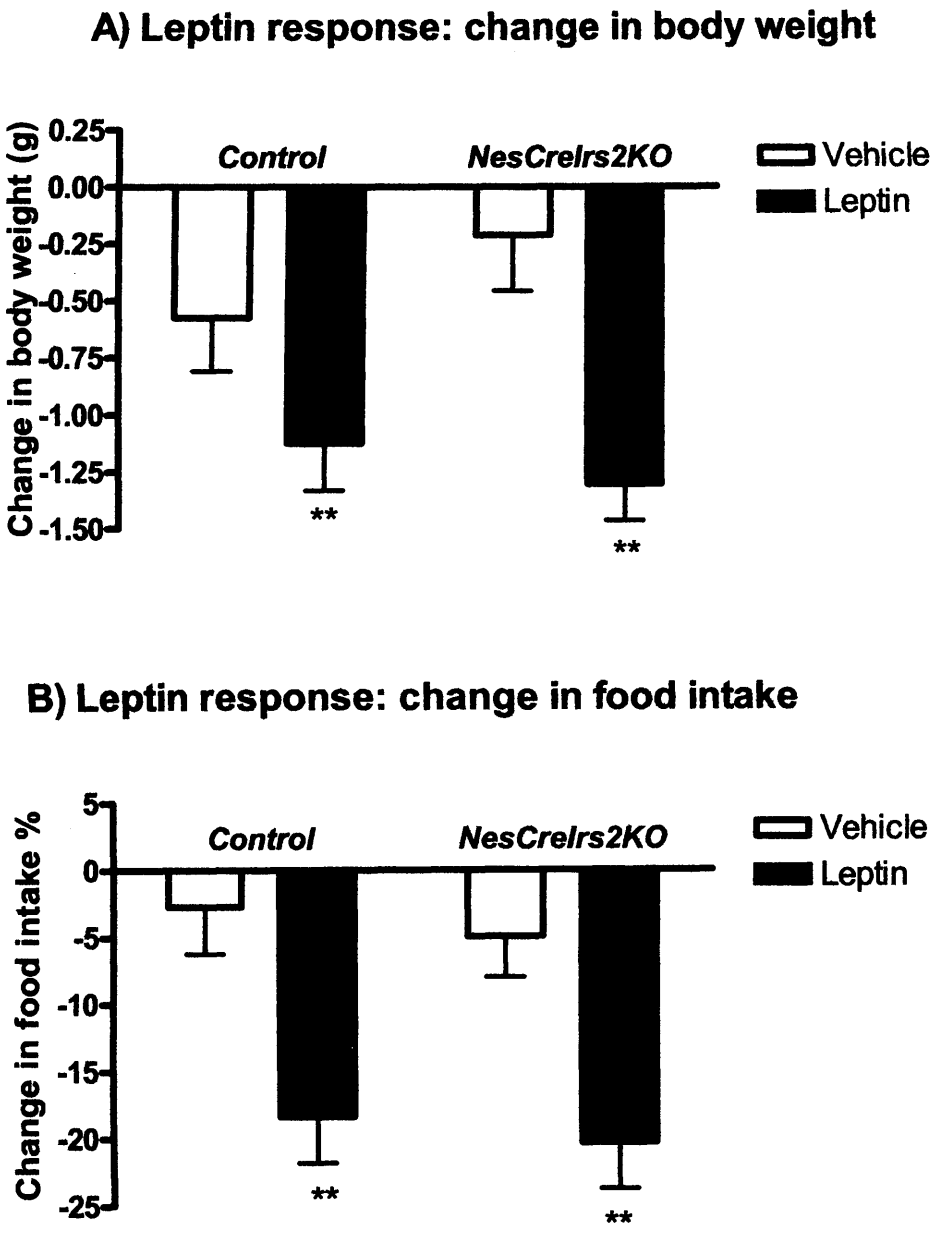

Figure 3.9: The response to 3 days of intraperitoneal leptin administration upon A) body weight and B) food intake was determined in acclimatised male *NesCreIrs2KO* and control mice at 12 weeks of age. Animals were injected once daily prior to the onset of the dark-phase with either leptin (5 mg/kg) or vehicle for three days in a cross-over design study. Both body weight and cumulative food intake were recorded. Data represent the mean ± SEM for 8 animals of each genotype. ** $P < 0.01$.

3.2.8 Analysis of hypothalamic neuropeptide expression

It was hypothesised that the deletion of *Irs2* in the brain of *NesCreIrs2KO* animals may have altered the expression levels of various neuropeptides involved in the regulation of food intake.

Analysis of the gene expression of hypothalamic neuropeptides of 12-week-old fasted *NesCreIrs2KO* and control animals, showed no significant differences in *Agrp, Cart* or *Npy* expression levels. However, almost a 50% reduction in hypothalamic *Pomc* gene expression in *NesCreIrs2KO* mice was detected (Figure 3.10).

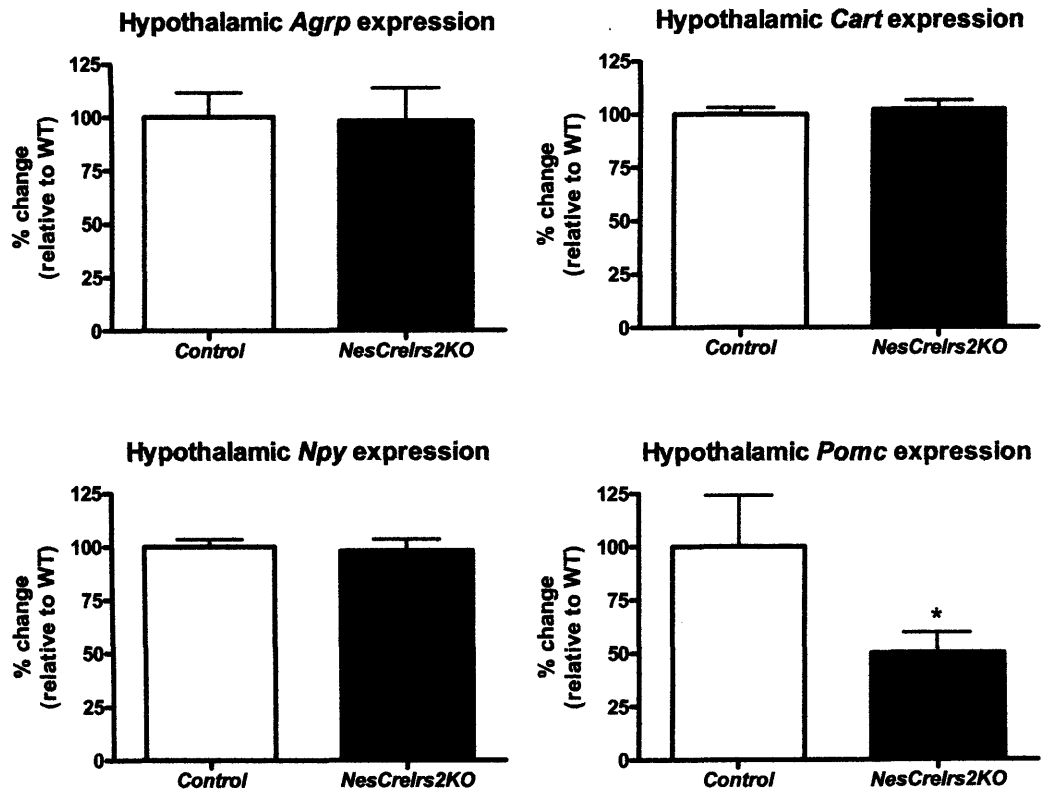

Figure 3.10: Summary of gene expression of hypothalamic *Agrp, Cart, Npy* and *Pomc* analysed in using RT-PCR. Data shown represents the % change neuropeptide concentration of *NesCreIrs2KO* animals as compared to control animals. Data represent the mean ± SEM for 6 animals of each genotype. * $P < 0.05$.

3.3 Glucose Homeostasis

A role for CNS insulin signalling in the regulation of peripheral glucose homeostasis and insulin action has been implicated by a number of studies. Of particular relevance is the study by Obici and colleagues (2002) in which anti-sense oligodeoxynucleotides were used to block hypothalamic insulin receptors (Obici et al., 2002a) and also the impaired glucose homeostasis of *NIRKO* mice (Bruning et al., 2000). Taken together, these studies suggest a signficiant role for CNS insulin signalling in the regulation of glucose homeostasis.

In order to investigate the role of IRS2 mediated insulin signalling pathways in the CNS regulation of glucose homeostasis, various studies were carried out on *NesCreIrs2KO* mice. A further aim of these studies was to assess the contribution of the CNS deletion of *Irs2* to the severe dysregulation of glucose homeostasis displayed by global *Irs2* null animals.

3.3.1 Fasting blood glucose (FBG) levels

By 12 weeks of age *NesCreIrs2KO* male mice were significantly hyperglycaemic, compared to controls, with this still evident at 6 months. However, blood glucose while increased, was still within normal limits.

Figure 3.11: FBG levels (mmol/L) of mice following a 16-h fast of A) males at 12 weeks of age and B) males at 6 months of age. Data represent the mean ± SEM for 8 animals of each genotype. * $P < 0.05$, ** $P < 0.01$.

3.3.2 Glucose tolerance

Glucose tolerance tests were performed on male *NesCreIrs2KO* and control mice at 12 weeks of age and 6 months of age. At both ages, male *NesCreIrs2KO* mice exhibited impaired glucose tolerance compared to controls.

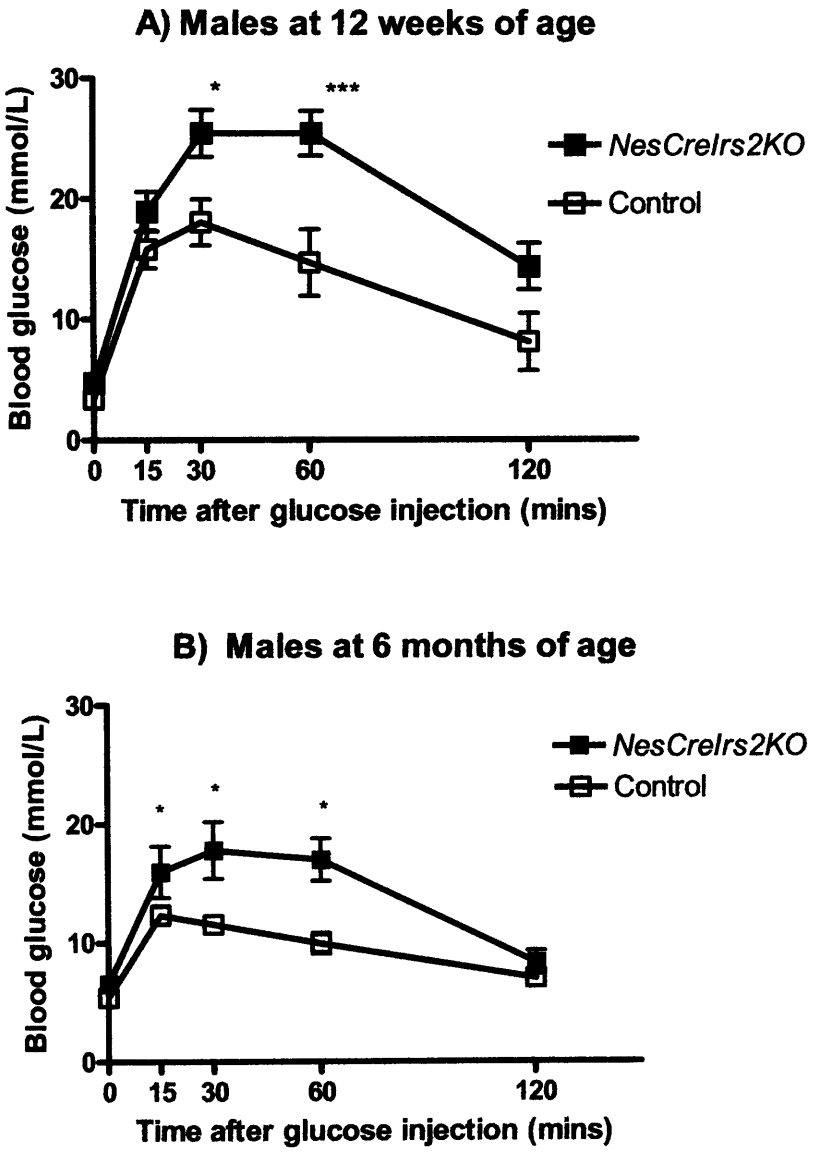

Figure 3.12: Glucose tolerance tests performed on male mice at A) 12 weeks of age and B) 6 months of age. Data represent the mean ± SEM for 7-9 animals of each genotype. * $P < 0.05$, ** $P < 0.01$, *** $P < 0.001$.

3.3.3 Fasting plasma insulin levels

In order to further understand the mechanisms of disordered glucose homeostasis in *NesCreIrs2KO* animals, the fasting plasma insulin levels of animals at 12 weeks of age were measured. This analysis revealed that *NesCreIrs2KO* animals were significantly hyperinsulinaemic; with more than a two-fold increase in basal levels, compared to control animals. This suggests the presence of insulin resiatnce in *NesCreIrs2KO* animals.

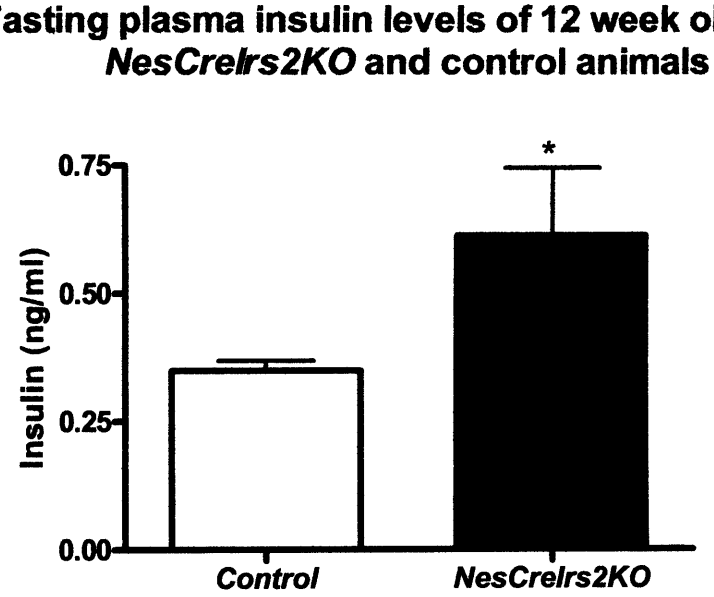

Figure 3.13: Fasting plasma insulin levels were measured on male *NesCreIrs2KO* and control mice following a 16-h overnight fast at 12 weeks of age. Data represent the mean ± SEM for 8-12 animals of each genotype. * $P < 0.05$.

3.3.4 Pancreatic islet mass and density

Analysis of islet size and density in male mice at 12 weeks of age showed that *NesCreIrs2KO* mice exhibited increased β-cell mass of almost double that of control animals. This provides further evidence of a compensatory response to insulin resistance in *NesCreIrs2KO* animals and is consistent with both the hyperinsulinaemia and obesity seen at the same age.

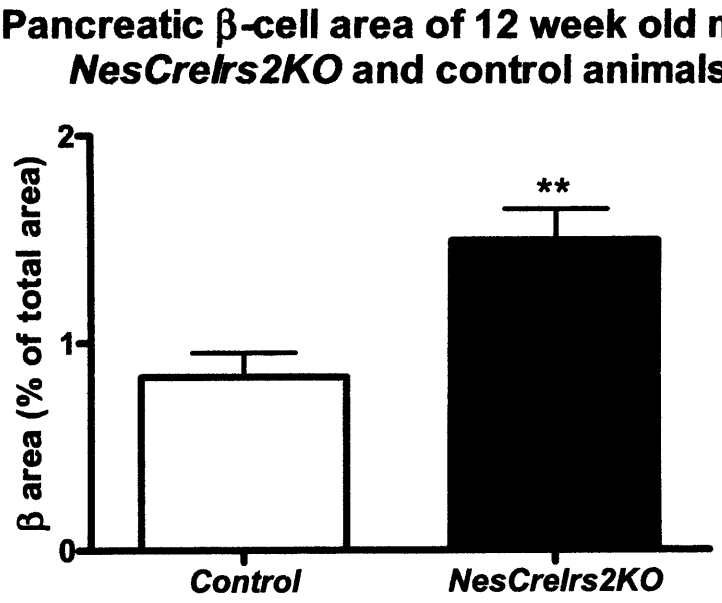

Figure 3.14: The percentage total pancreatic area occupied by β-cells in male *NesCreIrs2KO* and control animals at 12 weeks of age. Five pancreases were analysed per genotype at each time point and for each pancreas four sections were analysed. Data represent the mean ± SEM for 5 animals of each genotype. ** $P < 0.01$.

3.4 Assessment of reproductive function

Reproductive dysfunction is a feature of both the *NIRKO* mouse and *Irs2* null animals. *NIRKO* animals exhibited impaired spermatogenesis and ovarian follicle maturation due to the hypothalamic dysregulation of luteinising hormone. Global *Irs2* null females have small, anovulatory ovaries with reduced numbers of follicles. The plasma levels of luteinising hormone, prolactin and sex steroids were also reduced in these animals. Pituitaries were also decreased in size and contain reduced numbers of gonadotrophs. Taken together, these studies highlight a role for intact insulin signalling in the brain not only in the regulation of energy disposal and fuel metabolism, but also in the regulation of reproductive function.

The aim of this section of work was to investigate the reproductive function of *NesCreIrs2KO* animals, and to address the contribution of CNS *Irs2* signalling pathways to the infertility phenotype of the *Irs2* null mouse in a tissue specific manner. Males with global deletion of *Irs2* exhibited no reproductive defects. In addition, male *NesCreIrs2KO* animals were known to be fertile, as they were used as breeders prior to the commencement of studies aimed at assessing the fertility of these animals. Therefore the studies described in the following chapter were carried out solely on female animals.

3.4.1 Validation of *NesCreIrs2KO* females as model for studying the role of CNS IRS2 pathways in the regulation of reproductive function

Prior to the commencement of studies, it was vital to ensure that no *Irs2* deletion was occurring in non-CNS tissues that contribute to fertility (more specifically the pituitary and ovary). At both the DNA and mRNA levels, no *Irs2* deletion was detected in either tissue (Figure 3.15), confirming the use of *NesCreIrs2KO* animals as a valid model for studying the contribution of CNS IRS2 pathways to the regulation of female reproductive function. Thus, a series of studies designed to determine various physiological parameters of reproduction in *NesCreIrs2KO* females were performed.

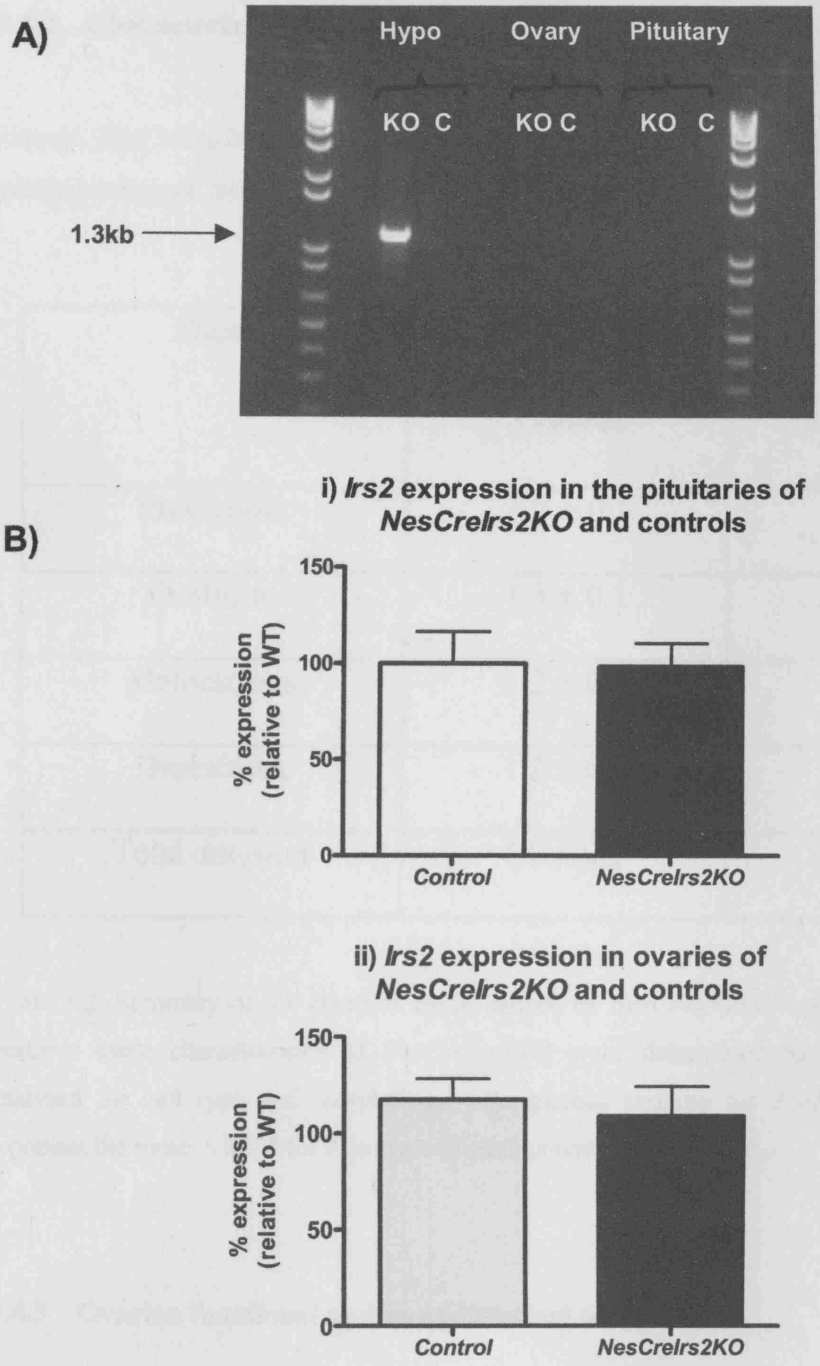

Figure 3.15: A) DNA was extracted from the hypothalami, pituitaries and ovaries of *NesCreIrs2KO* and control animals. PCR was performed to detect *Irs2* deletion in these samples. No bands were amplified in pituitary and ovarian samples, indicating no recombination of the *loxP* sites in these tissues. B) *Irs2* gene expression analysis by RT-PCR. i) Gene expression levels in the pituitaries of *NesCreIrs2KO* and controls, ii) gene expression levels in the ovaries of *NesCreIrs2KO* and controls. These analyses revealed that the pituitary and ovarian *Irs2* mRNA expression of *NesCreIrs2KO* animals were equivalent to that of control animals. Data represent the mean ± SEM for 12-17 animals of each genotype.

3.4.2 Characterisation of oestrous cycle

Female *NesCreIrs2KO* mice were found to have an extended oestrous cycle due to a mildly prolonged dioestrous phase (Table 3.2).

Phase	Duration (days)	
	Control	***NesCreIrs2KO***
Proestrous	1.2 ± 0.1	1.5 ± 0.2
Oestrous	1.3 ± 0.1	1.3 ± 0.2
Metoestrous	1.2 ± 0.1	1.4 ± 0.2
Dioestrous	1.2 ± 0.1	1.9 ± 0.2*
Total duration	4.9 ± 0.1	6.1 ± 0.2*

Table 3.2: Summary of the oestrous cycle pattern of *NesCreIrs2KO* and control females. The oestrous cycle characteristics of *NesCreIrs2KO* were determined by daily vaginal smears analysed for cell type and morphology with giemsa staining for 3 completed cycles. Data represent the mean ± SEM for 8 animals of each genotype. * $P < 0.05$.

3.4.3 Ovarian functional and morphological analyses

3.4.3.1 Ovarian function

No differences in the timing of ovulation and the numbers of oocytes recovered were seen when *NesCreIrs2KO* mice and control mice were super-ovulated (total oocytes recovered per animal: control 23.6 ± 2.3 vs *NesCreIrs2KO* 21.1 ± 2.1, n=5, p = N.S.

3.4.3.2 Ovarian morphological analysis

Haematoxylin-eosin staining of ovarian sections demonstrated the presence of follicles of all developmental stages and corpora lutea in *NesCreIrs2KO* and control mice (Figure 3.16), consistent with the normal response of *NesCreIrs2KO* animals to superovulation.

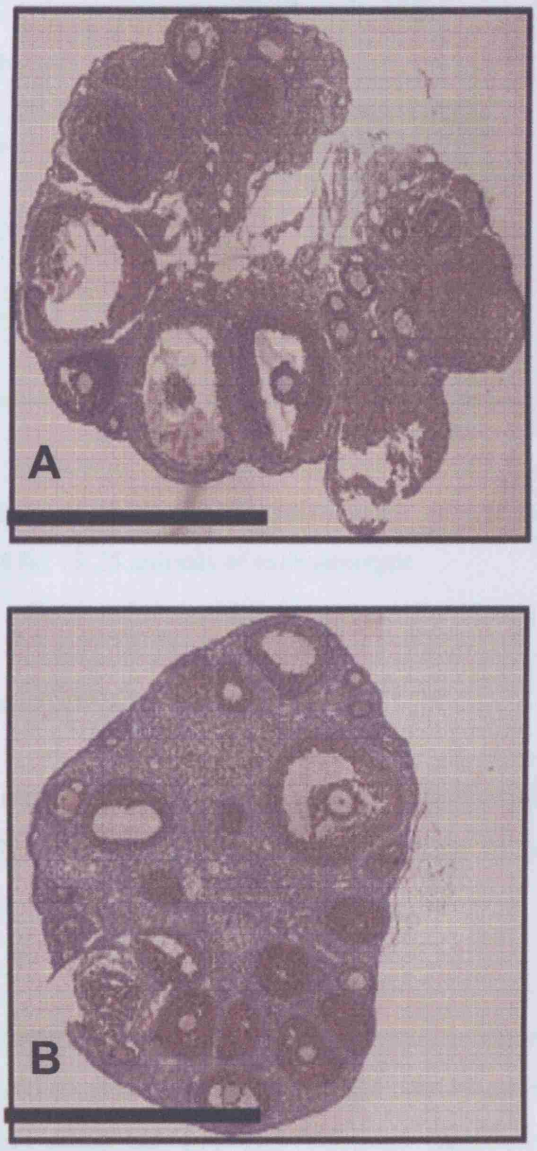

Figure 3.16: Ovarian anatomy in control and *NesCreIrs2KO* mice. Low magnification photomicrograph of: A) control and B) *NesCreIrs2KO* animals. Scale bars are 0.5 mm. It should be noted that the brown staining visible in the photomicrograph is peroxidase staining from independent immunohistochemistry studies.

3.4.3.3 Ovarian weights

Ovarian weights of *NesCreIrs2KO* animals at 12 weeks of age, were indistinguishable from those of control animals (Figure 3.17).

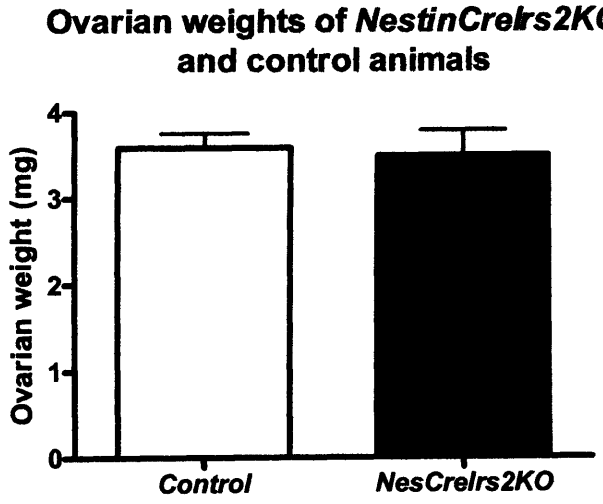

Figure 3.17: Ovarian weights of *NesCreIrs2KO* and control animals at 12 weeks of age. Data represent the mean ± SEM for 15-25 animals of each genotype.

3.4.4 Analysis of reproductive hormone levels

Pituitaries and blood were collected from *NesCreIrs2KO* and control animals during the dioestrous phase of the oestrous cycle, for the analysis of the levels of various reproductive hormones.

Analaysis of serum oestradiol and progesterone levels demonstrated no differences in the levels of these hormones between *NesCreIrs2KO* and control animals. With regards to pituitary hormones, the levels of LH and FSH in *NesCreIrs2KO* animals were comparable to controls. However, the level of prolactin in *NesCreIrs2KO* animals was significantly reduced compared to controls. These results are summarised in the table below (Table 3.3).

Hormone levels	Serum/pituitary levels	
	Control	*NesCreIrs2KO*
Oestradiol (nmol/L)	0.016 ± 0.002	0.017 ± 0.04
Progesterone (nmol/L)	4.198 ± 0.7	3.43 ± 1.0
LH (ng/ml)	300.6 ± 37.3	218.5 ± 34.3
Prolactin (ng/ml)	4048 ± 840.7	979.5 ± 126.9**
FSH (ng/ml)	43.78 ± 3.435	34.08 ± 4.579

Table 3.3: Summary of the dioestrous levels of serum oestradiol and progesterone, and reproductive pituitary hormones. Data represent the mean ± SEM for 8 animals of each genotype. ** $P < 0.01$.

3.4.5 Analysis of breeding performance by timed mating studies

In continuous mating studies, the average duration between litters and the size and number of litters over the study period were similar in *NesCreIrs2KO* and control mice (Table 3.4).

	Control	*NesCreIrs2KO*
Total number of litters	23	19
Total number of pups	172	137
Average no. of litters per female	3.833 ± 0.1667	3.167 ± 0.3073
Average no. of pups per litter	7.478 ± 0.6969	7.211 ± 0.7318
Average duration between litters (days)	26.06 ± 1.885	28.69 ± 2.725

Table 3.4: Summary of breeding performance of six female *NesCreIrs2KO* animals and six controls, pair mated with wildtype C57/Bl6 males. Performance was assessed by monitoring of the litter number and size, and also duration between litters. Data represent the mean ± SEM for 6 animals of each genotype.

3.5 Summary of hypothalamic function, glucose homeostasis and reproductive function of *NesCreIrs2KO* animals

3.5.1 Hypothalamic function

Studies into the hypothalamic function of *NesCreIrs2KO* mice showed that these animals had considerable abnormalities. Both sexes exhibited significantly increased body weight compared to controls, with an almost two-fold increase in adiposity. Consistent with this, *NesCreIrs2KO* mice were significantly hyperleptinaemic, yet remained senstive to the anorexigenic effects of peripherally administered leptin. In addition, *NesCreIrs2KO* animals were long and hyperphagic, but still had normal resting metabolic rate.

3.5.2 Glucose homeostasis

Studies investigating the glucose homeostasis of these animals, showed that *NesCreIrs2KO* mice were signficantly hyperglycaemic and demonstrated impaired glucose tolerance compared to control animals. In addition, *NesCreIrs2KO* animals displayed hyperinsulinaemia and increased pancreatic islet mass density

3.5.3 Reproductive function

Female *NesCreIrs2KO* mice were found to have an extended oestrous cycle due to a mildly prolonged dioestrous phase. The levels of serum oestradiol and progesterone levels during dioestrous were however normal. The analysis of pituitary hormones during dioestrous showed that although the levels of LH and FSH were comparable to controls, *NesCreIrs2KO* animals had significantly reduced prolactin levels. No differences in the timing of ovulation and the numbers of oocytes recovered were seen when *NesCreIrs2KO* mice and control mice were super-ovulated. Finally, timed matings between *NesCreIrs2KO* females and control males showed that these animals had normal breeding performance compared to control females.

Chapter 4

Phenotypic characterisation of *POMCCreIrs2KO* animals

4 Characterisation of *POMCCreIrs2KO* mice

The role of POMC/CART neurons in the regulation of energy homeostasis via the interaction with adiposity signals, such as insulin, has been widely considered essential in the regulation of energy homeostasis. POMC neurons have been implicated as mediating the anorexigenic effects of insulin on energy homeostasis. Insulin receptors are known to be present on POMC neurons indicating a role for insulin signalling in this neuronal population (Benoit et al., 2002). Administration of both insulin and leptin directly into the third ventricle of mice has been shown to result in increased hypothalamic expression of *Pomc* mRNA (Benoit et al., 2002; Brown et al., 2006). However, despite these findings, the physiological role of insulin signalling in POMC neurons is still unknown. Numerous studies have also implicated a role for the hypothalamic melanocortin system in the regulation of peripheral glucose homeostasis (Farooqi et al., 2003; Marks and Cone, 2001; Obici et al., 2001; Schwartz, 2001).

In order to fully address the role of IRS2 mediated insulin signalling in POMC neurons, a number of studies were carried out on *POMCCreIrs2KO* mice designed to assess the hypothalamic function and various parameters of glucose homeostasis of these animals.

4.1 Proof of *Irs2* deletion

POMCCre transgenic animals have been used extensively in recent years (Xu et al., 2005a; Xu et al., 2005b; Xu et al., 2007). Despite this, before the commencement of investigations, studies aimed at confirming *POMCCreIrs2KO* animals were lacking *Irs2* expression in the hypothalamus were performed. A PCR-based strategy showed that recombination of *Irs2lox* alleles was occurring in the hypothalami of *POMCCreIrs2KO* animals, and immunocytochemistry analysis demonstrated the deletion of *Irs2* specifically in POMC neurons (Figure 4.1). These studies therefore established *POMCCreIrs2KO* animals as a valid model for investigating the physiological role of IRS2 signalling in POMC neurons in the context of energy balance regulation. A number of studies were therefore carried out on *POMCCreIrs2KO* mice, designed to assess the hypothalamic function of these animals.

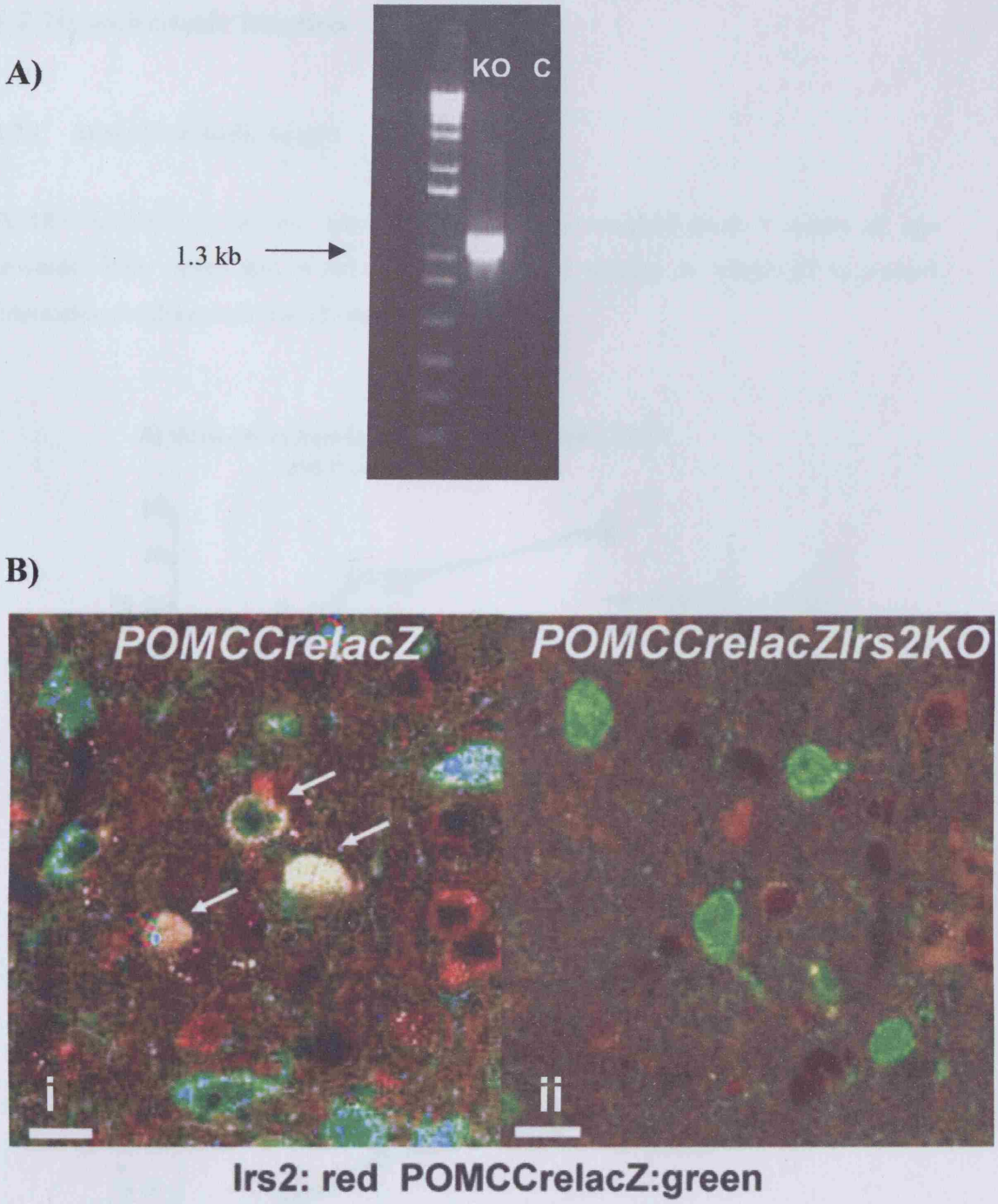

Figure 4.1: Studies proving deletion of *Irs2* in hypothalami of *POMCCreIrs2KO*. A) PCR analysis of *Irs2* deletion in DNA extracted from *POMCCreIrs2KO* and control hypothalami. A 1.3kb band in sample confirms deletion of *Irs2*. B) Proof of *Irs2* deletion in POMC neurons: i) co-localisation of POMCCreLacZ expression and IRS2 in *POMCCrelacZ* mice and ii) no co-localisation of POMCCreLacZ and IRS2 in *POMCCreIrs2KOlacZ* mice. Scale bars: 10 μm.

4.2 Hypothalamic function

4.2.1 Analysis of body weight

POMCCreIrs2KO mice and relevant controls were weighed from 5 weeks of age onwards. Both males and females were of normal weight, as compared to control littermates, at all ages studied (Figure 4.2).

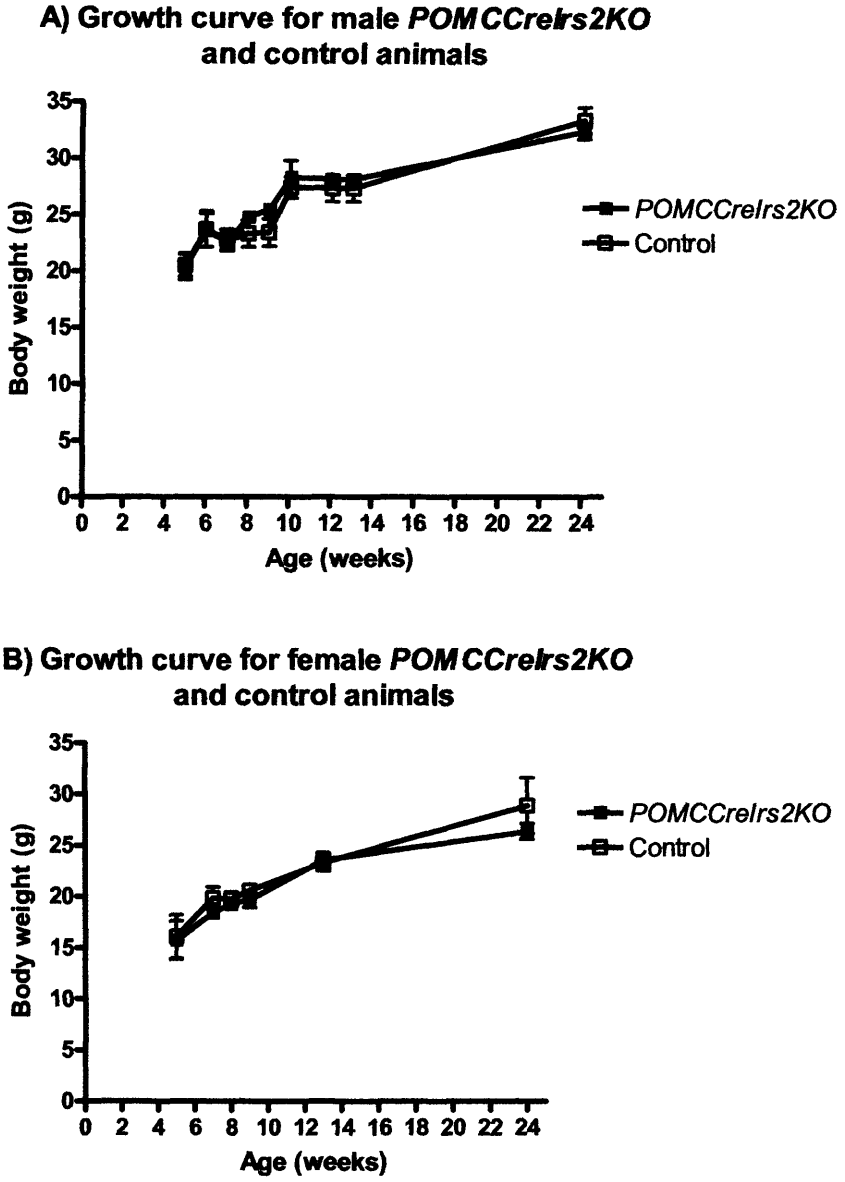

Figure 4.2: Growth curve for A) male *POMCCreIrs2KO* and control animals and B) female *POMCCreIrs2KO* and control animals. Data represent the mean ± SEM for 6-12 animals of each genotype.

4.2.2 Analysis of body composition by DEXA scanning

Analysis of the body composition of 6 month old male and female animals, showed no significant differences in fat mass, lean tissue mass and percentage fat mass between *POMCCreIrs2KO* and control animals of both sexes (Figure 4.3). These findings were conistent with the normal body weight of *POMCCreIrs2KO* animals at this age.

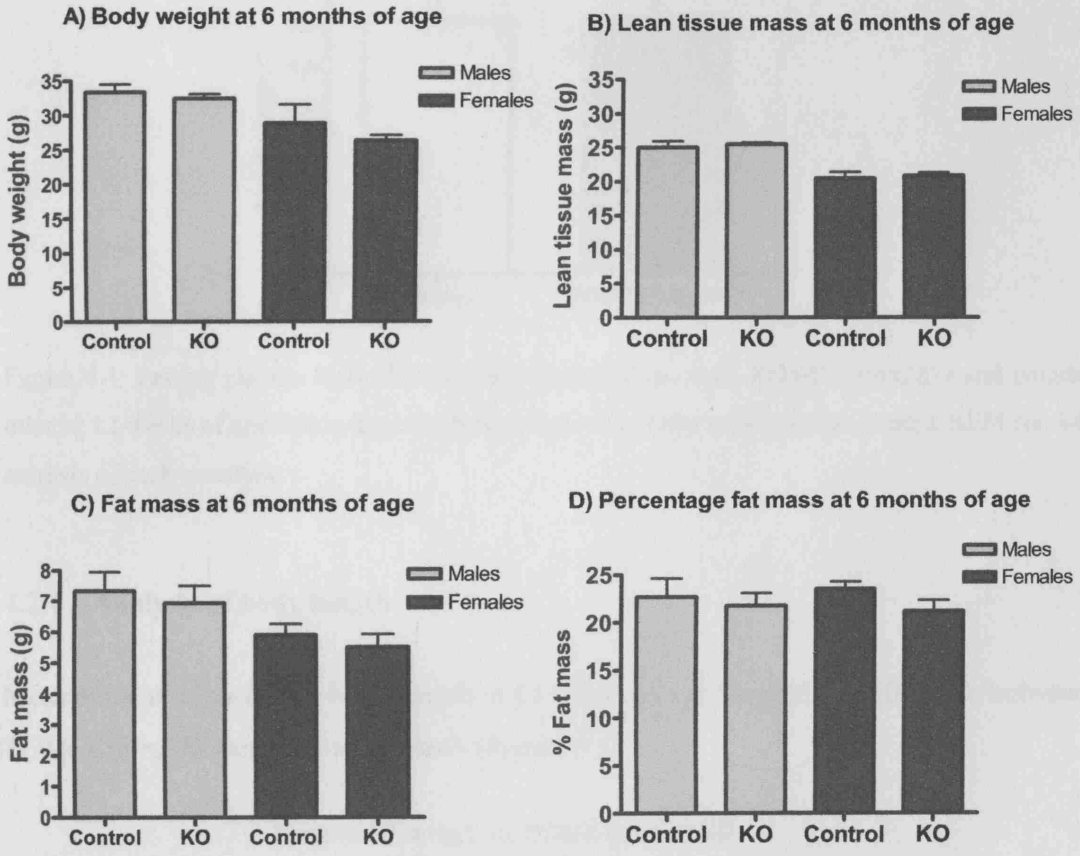

Figure 4.3: Analysis of body composition of 6 month old male and females by DEXA: A) body weight, B) lean tissue mass (g), C) fat mass (g), D) % fat mass. Data represent the mean ± SEM for 6 animals of each genotype.

4.2.3 Plasma leptin levels

Consistent with the lack of increased adiposity observed at this age, the fasting leptin levels of 12-week-old male *POMCCreIrs2KO* mice were indistinguishable from that of controls (Figure 4.4).

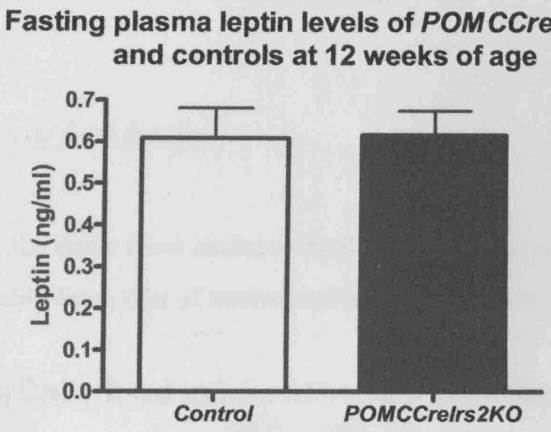

Figure 4.4: Fasting plasma leptin levels were measured on male *POMCCreIrs2KO* and control mice at 12 weeks of age following a 16-h overnight fast. Data represent the mean ± SEM for 6-8 animals of each genotype.

4.2.4 Analysis of body length

Measurement of naso-anal body length at 12 weeks of age showed no difference between *POMCCreIrs2KO* and control animals (Figure 4.5).

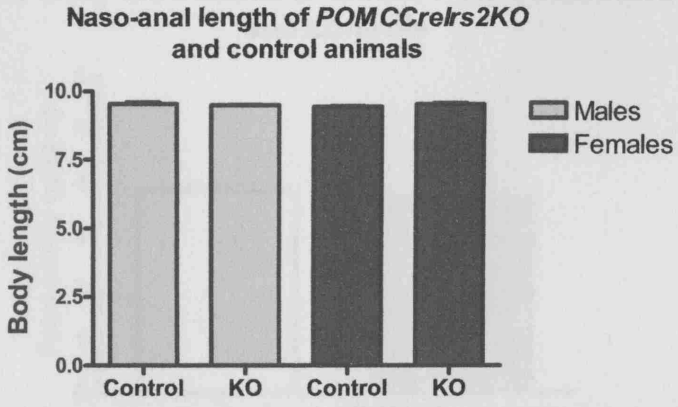

Figure 4.5: Naso-anal length (body length) was measured in male and female *POMCCreIrs2KO* mice at 12 weeks of age. Data represent the mean ± SEM for 8 animals of each genotype.

4.2.5 Analysis of feeding behaviour

Despite the lack of differences found in the body weight, body length and body composition of *POMCCreIrs2KO* compared to controls, the feeding behaviour of *POMCCreIrs2KO* animals was investigated. Studies undertaken included the analysis of food intake and re-feeding response to an overnight fast.

4.2.5.1 Analysis of food intake

At 8 weeks of age, the daily food intake of both male and female *POMCCreIrs2KO* mice were indistinguishable from that of control animals (Figure 4.6).

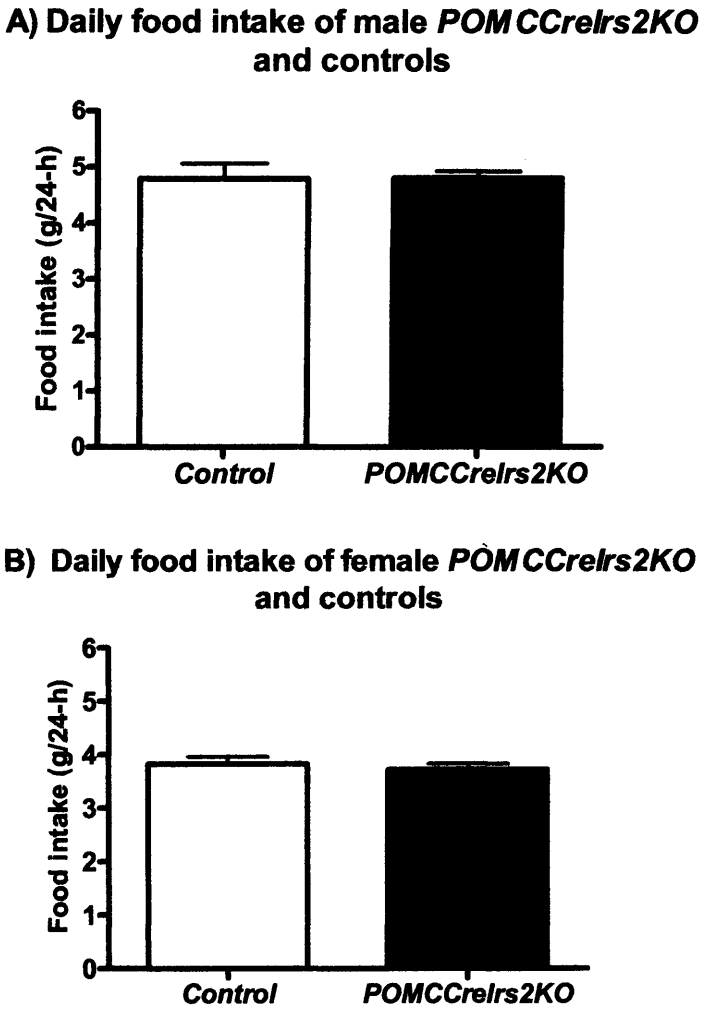

Figure 4.6: Daily food intake of A) male *POMCCreIrs2KO* and control animals and B) female *POMCCreIrs2KO* and control animals at 8 weeks of age. Data represent the mean ± SEM for 6-8 animals of each genotype.

4.2.5.2 Response to fasting

At 10 weeks of age, the feeding response of both male and female *POMCCreIrs2KO* mice was comparable to that of controls at all time points (Figure 4.7), indicating no impairment in short term feeding regulation mechanisms. These results were consistent with the normal daily food intake exhibited by these animals.

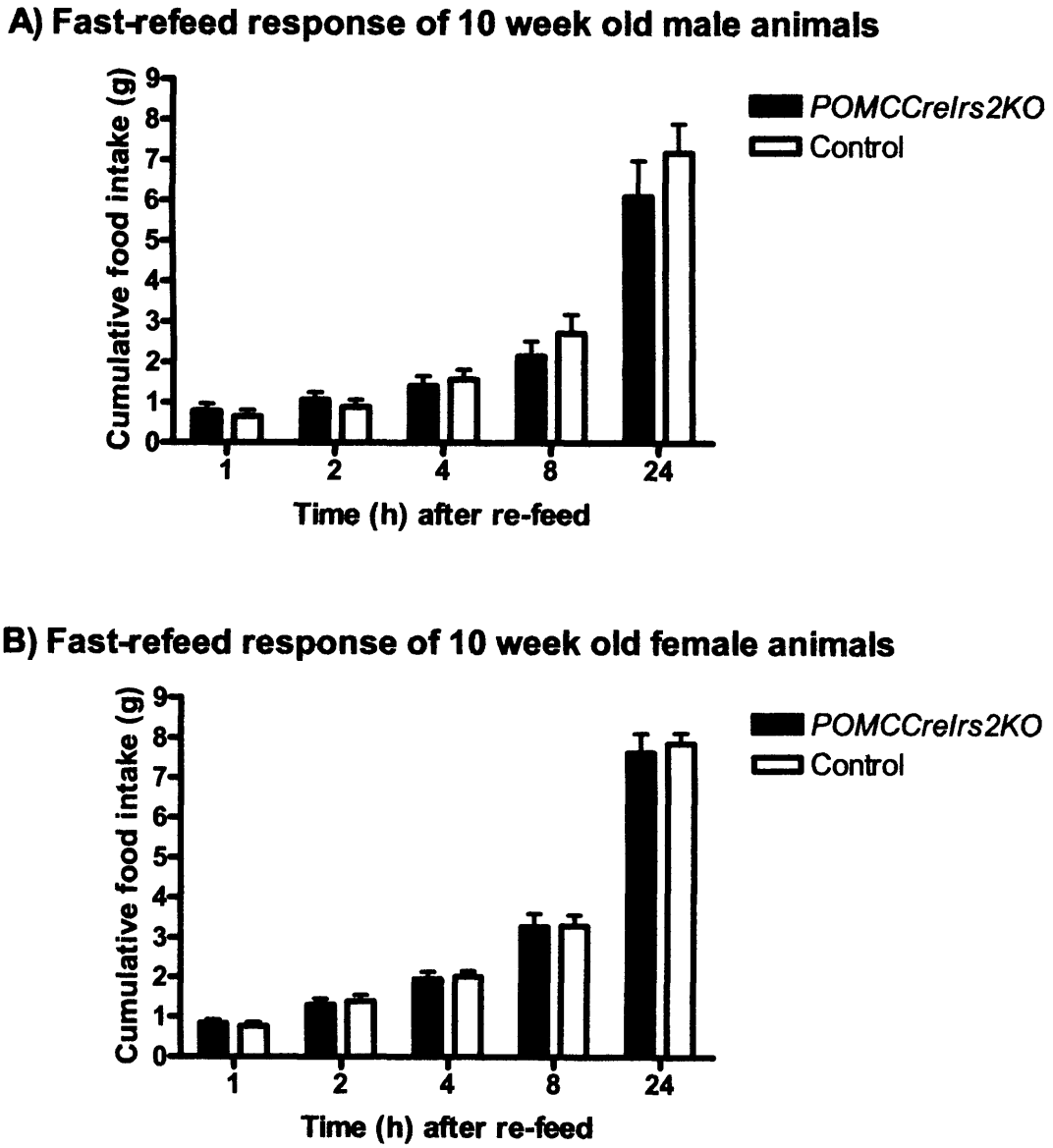

Figure 4.7: Re-feeding response following a 16-h overnight fast in 10 week old A) male *POMCCreIrs2KO* and controls and B) female *POMCCreIrs2KO* and controls. Data represent the mean ± SEM for 6-8 animals of each genotype.

4.2.6 High fat diet (HFD) trial

As can be seen from the results above, both male and female *POMCCreIrs2KO* displayed no difference in body weight compared to control animals, even at 6 months of age. Placing mice on a HFD has been shown to enhance any underlying obesity phenotype that may not be displayed on a standard chow diet (Bruning et al., 2000).

Male *POMCCreIrs2KO* and control mice were placed on a 12 week HFD trial from the age of 6 weeks, with the body weights of all mice measured once weekly throughout the trial. The body weights of *POMCCreIrs2KO* and control animals on a normal chow diet, were measured simultaneously. As expected both *POMCCreIrs2KO* and control animals gained more weight on the HFD, compared to mice of the same genotype on the standard diet. However, no differences in body weight were seen between *POMCCreIrs2KO* and control animals on the HFD (Figure 4.8).

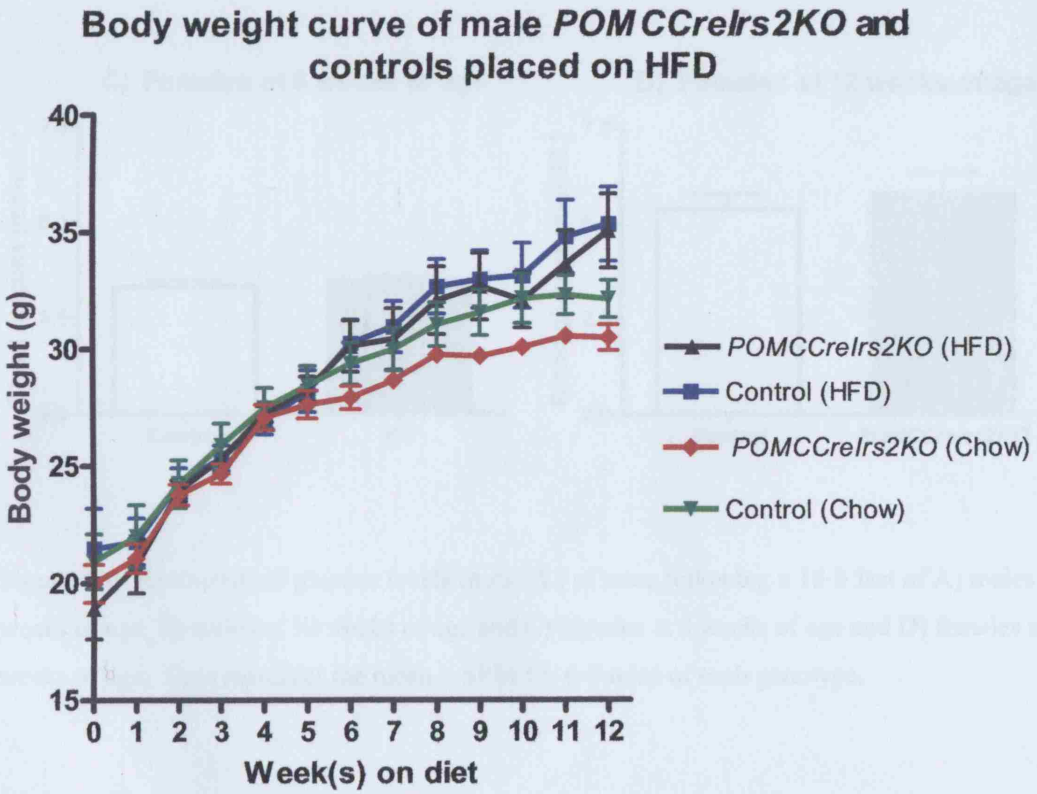

Figure 4.8: Body weight curve of male *POMCCreIrs2KO* and control mice on HFD and normal chow diet. Data represent the mean ± SEM for 6-9 animals of each genotype.

4.3 Glucose Homeostasis

4.3.1 Fasting blood glucose (FBG) levels

At both 8 and 12 weeks of age, male and female *POMCCreIrs2KO* mice had indistinguishable fasting blood glucose levels from control animals (Figure 4.9).

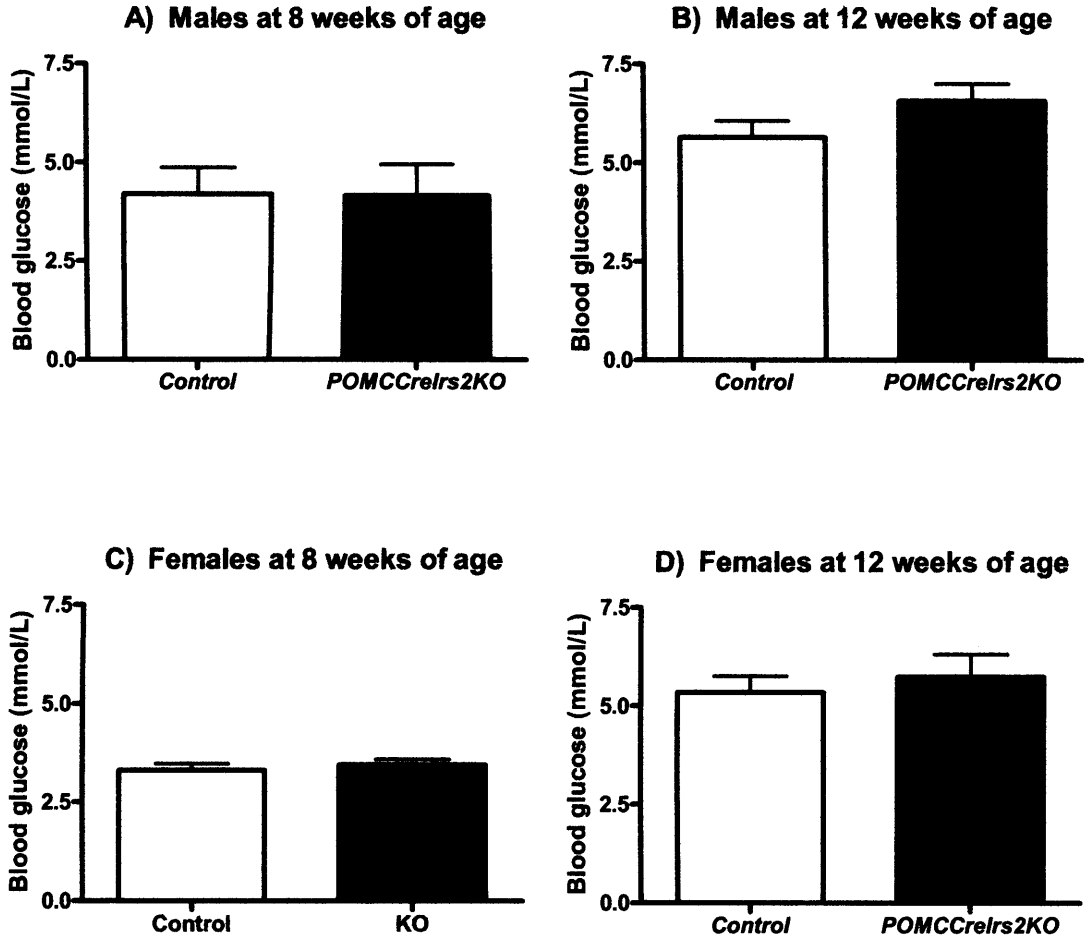

Figure 4.9: Fasting blood glucose levels (mmol/L) of mice following a 16-h fast of A) males at 8 weeks of age, B) males at 12 weeks of age and C) females at 8 weeks of age and D) females at 12 weeks of age. Data represent the mean ± SEM for 6-8 mice of each genotype.

4.3.2 Glucose tolerance

Glucose tolerance tests were performed on both male and female *POMCCreIrs2KO* and control mice at 8 and 12 weeks of age. At both ages, male and female *POMCCreIrs2KO* mice exhibited normal glucose disposal compared to controls (Figure 4.10).

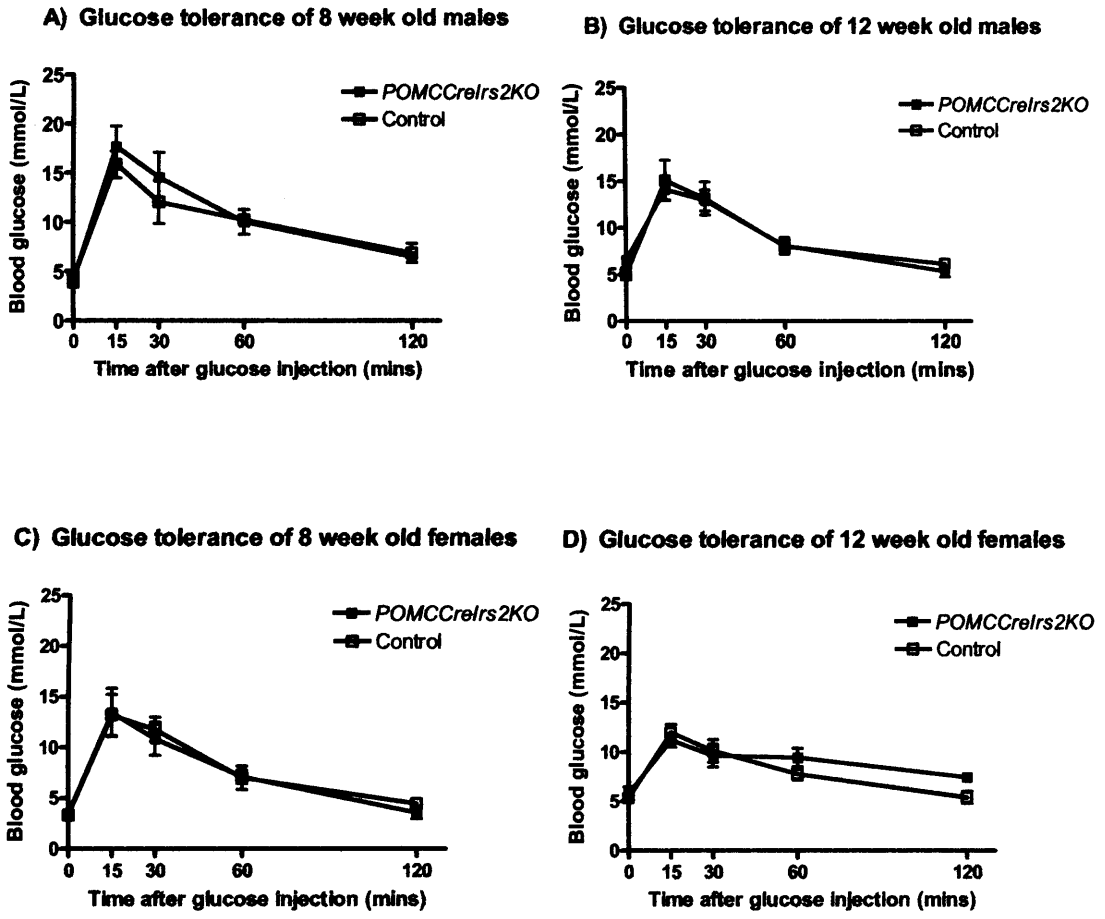

Figure 4.10: Glucose tolerance tests performed on: A) male mice at 8 weeks of age, B) male mice at 12 weeks of age, C) female mice at 8 weeks of age and D) female mice at 12 weeks of age. Data represent the mean ± SEM for 6-8 animals of each genotype.

4.3.3 Fasting plasma insulin levels

At 12 weeks of age male *POMCCreIrs2KO* mice had normal plasma insulin levels, as compared to control animals (Figure 4.11).

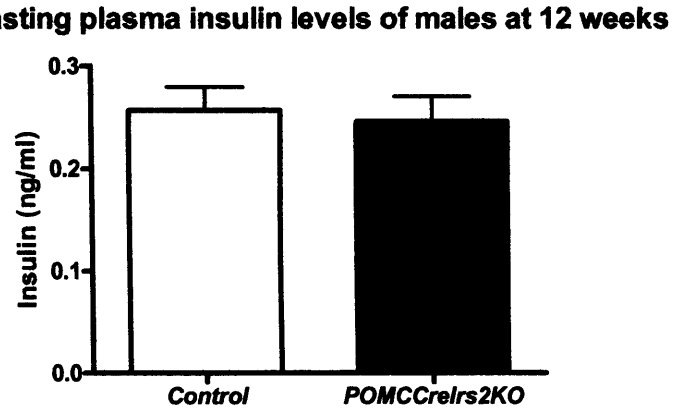

Figure 4.11: Fasting plasma insulin levels were measured on 12-week-old male *POMCCreIrs2KO* and control mice following a 16-h overnight fast. Data represent the mean ± SEM for 6 animals of each genotype.

4.4 Summary of hypothalamic function and glucose homeostasis of *POMCCreIrs2KO* animals

POMCCreIrs2KO animals exhibited normal body weight and body length compared to controls. Consistent with the lack of inceased adiposity, *POMCCreIrs2KO* animals had normal fasting leptin levels comnpared to controls. In addition, the daily food intake, fast-refeed response and sensitivity to DIO of *POMCCreIrs2KO* animals was comparable to controls.

With regards to glucose homeostasis, *POMCCreIrs2KO* animals exhibited normal fasting blood glucose levels, glucose tolerance and fasting insulin levels compared to control animals.

Chapter 5

Phenotypic characterisation of *AgRPCreIrs2KO* animals

5 Characterisation of *AgRPCreIrs2KO* mice

The dominant view in the field at the commencmnet of this work was that NPY/AgRP are primary first-order neurons that mediate the anorexigenic effects of insulin in the regulation of energy homeostasis. The ICV administration of insulin directly into the brain has been shown to inhibit expression of *Npy* and *Agrp* (Schwartz et al., 1992; Sipols et al., 1995). Although IRS2 has been shown to co-localise with NPY in the ARC (Pardini et al., 2006), the physiological role of insulin signalling in this NPY/AgRP neuronal population is still unknown.

In order to fully address the role of IRS2 mediated insulin signalling in AgRP neurons, a number of studies were carried out to assess various parameters of energy and glucose homeostasis in *AgRPCreIrs2KO* mice and controls.

5.1 Asessment of ectopic Cre expression in *AgRPCreIrs2KO* animals

Ectopic *lacZ* expression has been found in *AgRPCreR26R* mice with approximately 30% of these animals exhibiting widespread X-gal staining, affecting multiple brain regions as well as mesenchymal and epithelial tissues throughout the body (Kaelin et al., 2004).

To ensure that no mice in which germline deletion of *Irs2* were studied, ear punches were taken from all *AgRPCreIrs2KO* animals generated (all homozygous for the *R26R* transgene) and X-gal staining was performed. Animals positive for staining were excluded from all investigations described below.

5.2 Proof of *Irs2* deletion

Prior to commencement of phenotypic characterisation of *AgRPCreIrs2KO* animals, studies aimed at confirming the lack of *Irs2* expression in hypothalami of *AgRPCreIrs2KO* animals were undertaken. A PCR-based strategy did indeed

demonstrate that recombination of *Irs2loxed* alleles was occurring in the hypothalami of *AgRPCreIrs2KO* animals, and not controls (Figure 5.1).

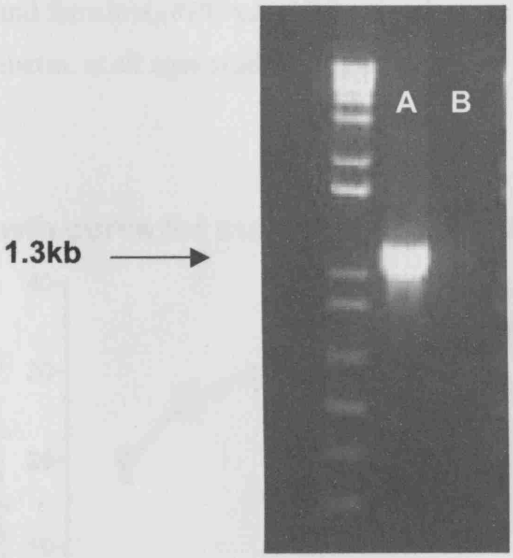

Figure 5.1: PCR analysis of *Irs2* deletion in DNA extracted from: A) *AgRPCreR26RIrs2KO* hypothalami and B) control hypothalami. A 1.3kb band in sample A confirms deletion of *Irs2* deletion. No band was amplified in sample B.

Despite proving deletion of *Irs2* was occurring in the hypothalami of *AgRPCreIrs2KO* animals, there was difficulty in demonstrating loss of *Irs2* expression in AgRP neurons. Immunocytochemical (ICC) studies proved unsuccessful due to the fact that no reliable antibodies against AgRP are currently available. As a result, the lack of IRS2 expression specifically in AgRP neurons could never be confirmed using this method. Alternative strategies aimed at expressing green fluorescent protein (GFP) in AgRP neurons (upon expression of Cre-recombinase in this cell type) also failed. This was due to the fact that the *AgRPCre*, *Irs2lox* and *Z/eg* alleles could never be genetically brought together, despite intensive breeding efforts. Although appropriate mating crossed were set-up, no *AgRPCreIrs2KOZ/eg* mice were ever generated (despite these crosses yielding offspring of all other intermediatory genotypes). However, the *AgRPCre* transgenic mouse line has been used in a number of studies and shown to be a reliable model (Kaelin et al., 2004; Xu et al., 2005b).

5.3 Hypothalamic function

5.3.1 Analysis of body weight

Both males and female *AgRPCreIrs2KO* animals were of normal weight, as compared to control littermates, at all ages studied (Figure 5.2).

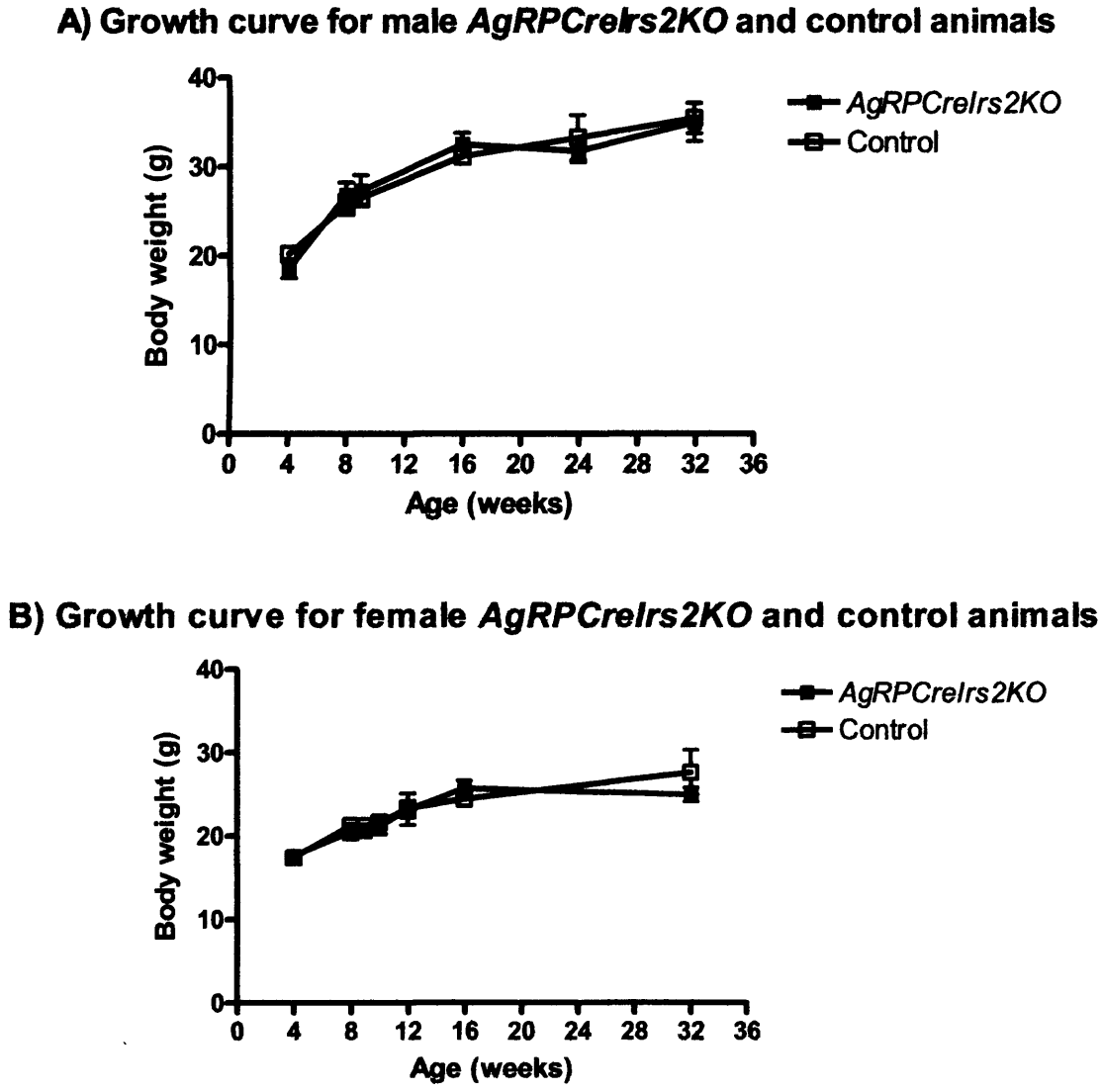

Figure 5.2: Growth curve for A) male *AgRPCreIrs2KO* and control animals and B) female *AgRPCreIrs2KO* and control animals. Data represent the mean ± SEM for 6-12 animals of each genotype.

5.3.2 Analysis of body composition by DEXA scanning

The body composition of 6-month-old males was assessed by DEXA scanning. Results showed no significant differences in fat mass, lean tissue mass, and percentage fat mass between *AgRPCreIrs2KO* and control animals (Figure 5.3).

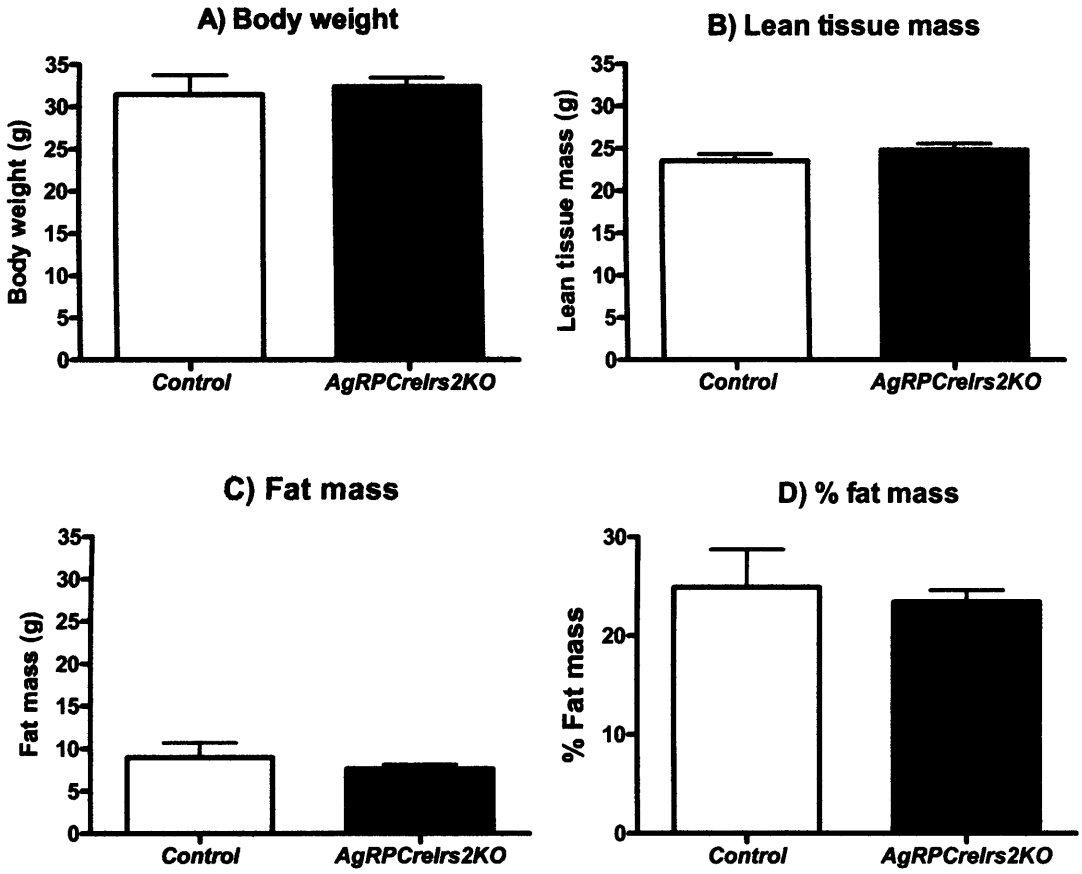

Figure 5.3: Analysis of body composition of 6 month old males by DEXA: A) body weight, B) lean tissue mass (g), C) fat mas (g), D) % fat mass. Data represent the mean ± SEM for 6 animals of each genotype.

5.3.3 Plasma leptin levels

Consistent with the lack of increased adiposity at 12 weeks of age, the fasting leptin levels of 12-week-old male *AgRPCreIrs2KO* animals were indistinguishable from controls (Figure 5.4).

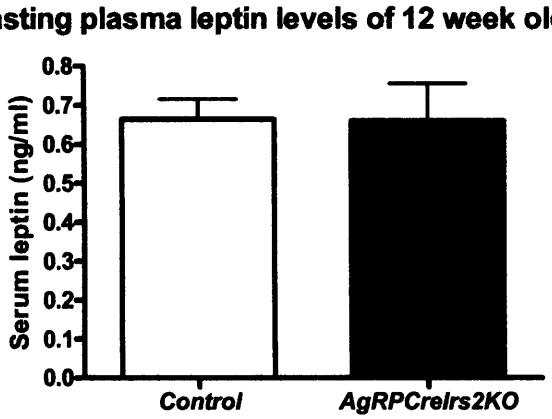

Figure 5.4: Fasting plasma leptin levels were measured on male *AgRPCreIrs2KO* and control mice at 12 weeks of age following a 16-h overnight fast. Data represent the mean ± SEM for 9 animals of each genotype.

5.3.4 Analysis of body length

Measurement of naso-anal body length in males at 6 months of age showed no significant difference between *AgRPCreR26RIrs2KO* and control animals (Figure 5.5).

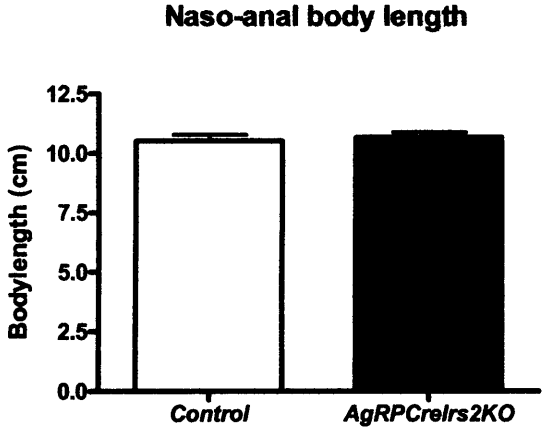

Figure 5.5: Naso-anal length (body length) was measured in male *AgRPCreIrs2KO* and control mice at 6 months of age. Data represent the mean ± SEM for 6 animals of each genotype.

5.3.5 Feeding behaviour

Despite the lack of differences found in the body weight, body length and body composition of *AgRPCreIrs2KO* animals compared to controls, the feeding behaviour of these animals was investigated. Studies undertaken included analysis of food intake and re-feeding response to an overnight fast.

5.3.5.1 Analysis of food intake

At 12 weeks of age, the daily food intake of both male and female *AgRPCreIrs2KO* mice was indistinguishable from that of control animals (Figure 5.6).

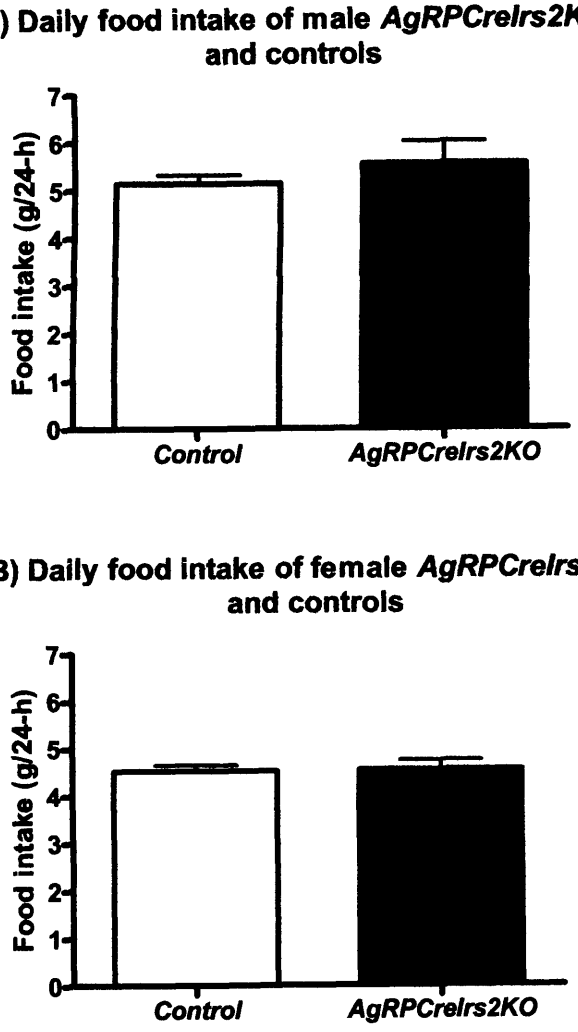

Figure 5.6: Daily (24-h) food intake was studied at 12 weeks of age in: A) male *AgRPCreIrs2KO* and control animals and B) female *AgRPCreIrs2KO* and control animals. Data represent the mean ± SEM for 6- 9 animals of each genotype.

5.3.5.2 Response to fasting

At 12 weeks of age, the feeding response of both male and female *AgRPCreIrs2KO* mice was comparable to that of controls at all time points measured, indicating no impairment in short term feeding regulation mechanisms. These results were consistent with the normal daily food intake exhibited by these animals (Figure 5.7).

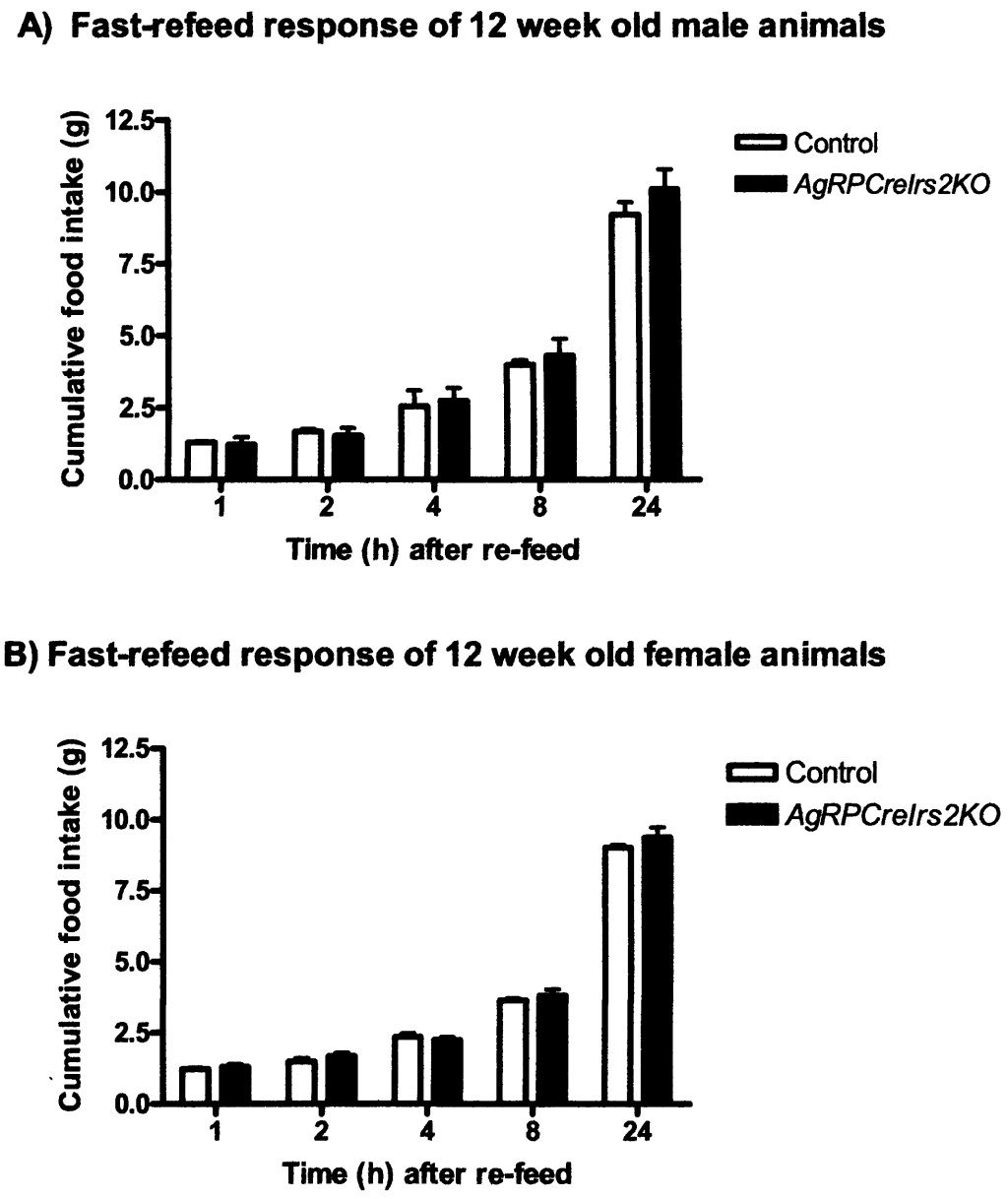

Figure 5.7: Re-feeding response following a 16-h overnight fast in A) 12 week old male mice and B) 12 week old female mice. Data represent the mean ± SEM for 6-9 animals of each genotype.

5.4 Glucose Homeostasis

In order to investigate the effect on glucose homeostasis of the deletion of IRS2 mediated insulin signalling in AgRP neurons, various metabolic studies were carried out on *AgRPCreIrs2KO* mice.

5.4.1 Fasting blood glucose (FBG) levels

At 12 weeks and 8 months of age, both male and female *AgRPCreIrs2KO* mice had indistinguishable FBG levels to control animals (Figure 5.8).

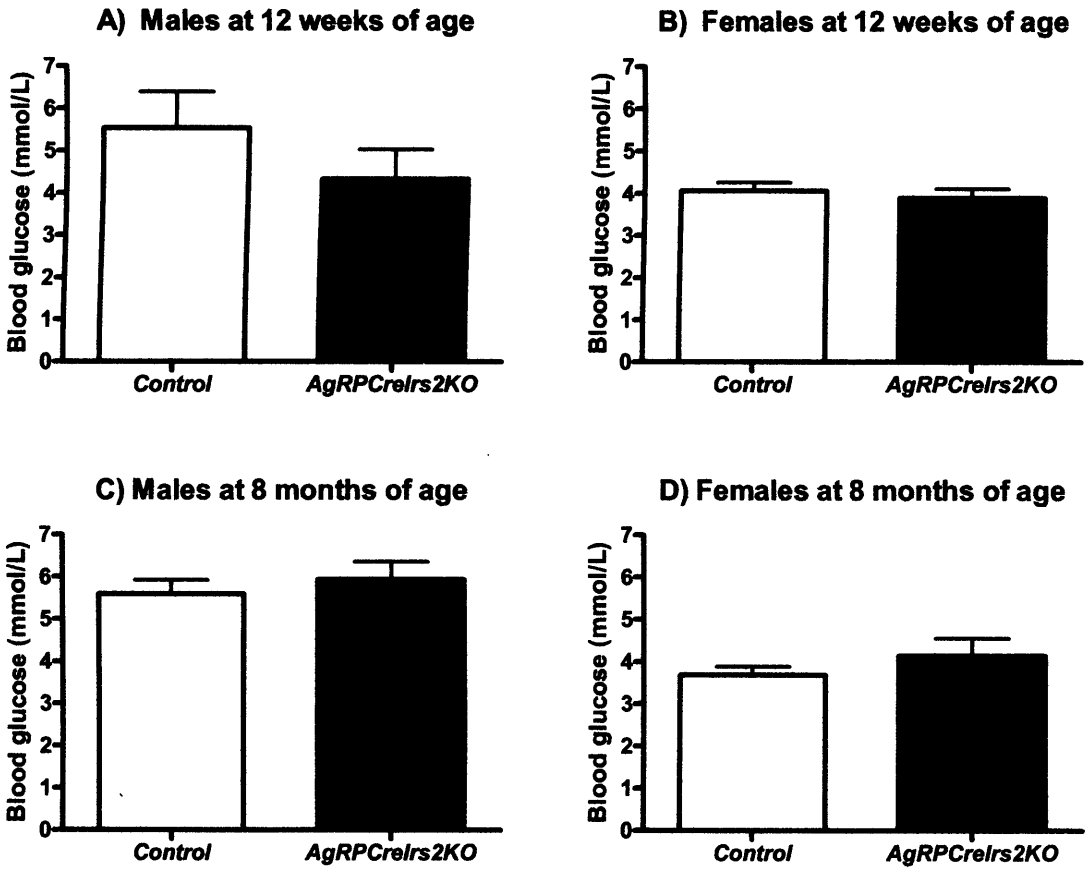

Figure 5.8: Fasting blood glucose levels (mmol/L) of A) males at 12 weeks of age, B) females at 12 weeks of age, C) males at 8 months of age and and D) females at 8 months of age. Data represent the mean ± SEM for 6-9 mice of each genotype.

5.4.2 Glucose tolerance

At 12 weeks of age, the glucose disposal of both male and female *AgRPCreIrs2KO* animals was comparable to controls (Figure 5.9).

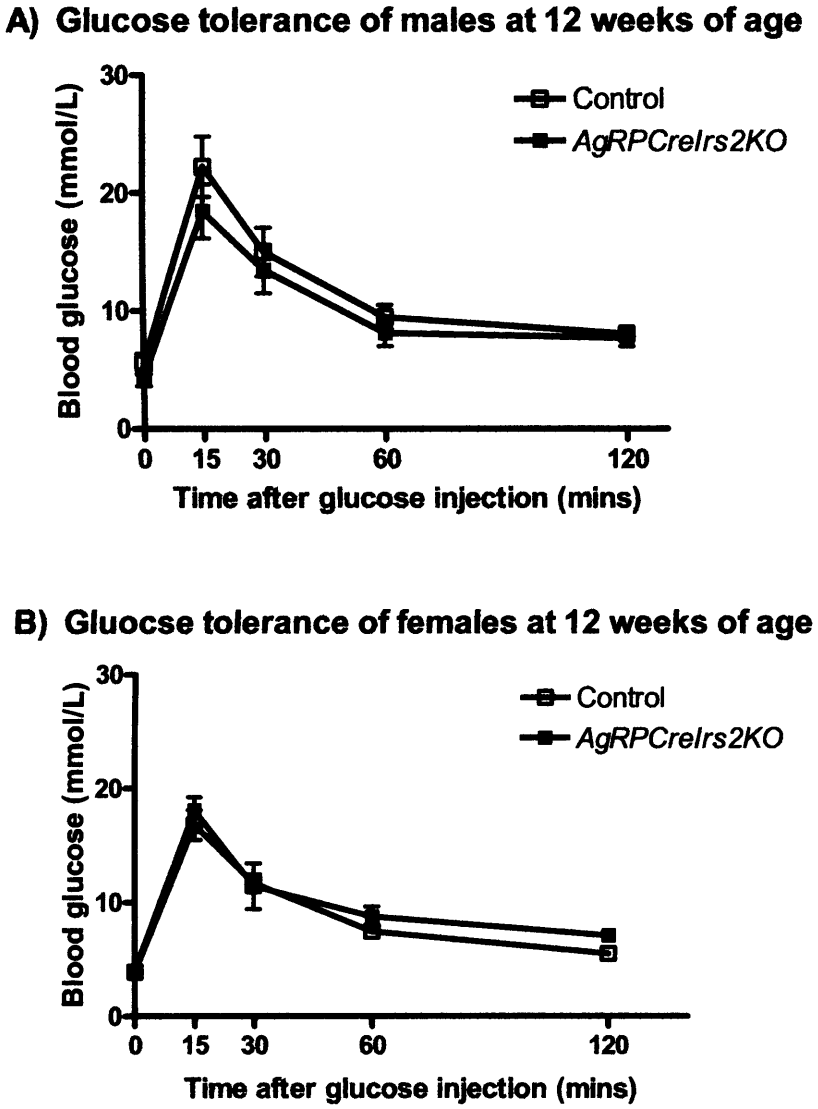

Figure 5.9: Glucose tolerance tests performed on: A) male mice at 12 weeks of age, B) female mice at 12 weeks of age. Following a 16 -h overnight fast and an intraperitoneal injection of D-glucose (1.5g/kg body weight), blood glucose levels were measured at the indicated time-points. Data represent the mean ± SEM for 6-9 animals of each genotype.

5.4.3 Fasting plasma insulin levels

At 12 weeks of age male *AgRPCreIrs2KO* mice had normal fasting insulin levels as compared to control animals (Figure 5.10).

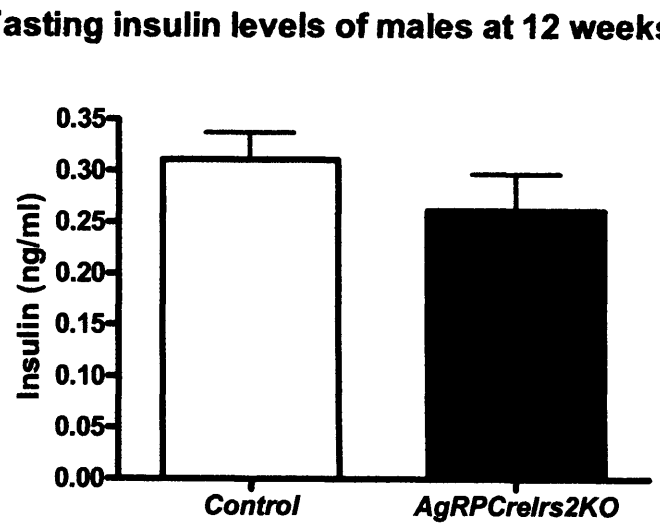

Figure 5.10: Fasting plasma insulin levels were measured on male *AgRPCreIrs2KO* and control mice following a 16-h overnight fast at 12 weeks of age. Data represent the mean ± SEM for 6-8 animals of each genotype.

5.5 Summary of hypothalamic function and glucose homeostasis of *AgRPCreIrs2KO* animals

AgRPCreIrs2KO animals exhibited normal body weight and body length compared to controls. Consistent with the lack of inceased adiposity, (as asessed by DEXA scanning) *AgRPCreIrs2KO* animals had normal fasting plasma leptin levels compared to controls. In addition, the daily food intake and fast-refeed response of *AgRPCreIrs2KO* animals was comparable to controls.

With regards to glucose homeostasis, *AgRPCreIrs2KO* animals exhibited normal fasting blood glucose levels, glucose tolerance and fasting insulin levels compared to control animals.

Chapter 6

Phenotypic characterisation of *AgRPCrep110βKO* animals

6 Characterisation of *AgRPCrep110βKO* mice

The dominant view in the field is that NPY/AgRP are primary first-order neurons that mediate the anorexigenic effects of insulin in the regulation of energy homeostasis. The ICV administration of insulin directly into the brain has been shown to inhibit expression of NPY and AgRP neuropeptides (Schwartz et al., 1992; Sipols et al., 1995). Leptin inhibits the release of AgRP (Hoggard et al., 2004), the expression of which is up-regulated in leptin reduction due to fasting or mutation (Hahn et al., 1998; Wilson et al., 1999). The inhibition of the hypothalamic expression of AgRP by leptin has been shown to be via a mechanism that requires intact PI3K signalling (Morrsion et al, 2005). Indeed, several studies have implicated PI3K as a point of convergence between the insulin and leptin signalling cascades, mediating the anorexigenic effects of both hormones in the regulation of energy and glucose homeostasis (Morrison et al., 2005; Morton et al., 2005; Niswender et al., 2003; Niswender et al., 2001). However, a recent study has shown that leptin and insulin have opposite effects on AgRP neurons, with membrane accumulation of PI3K inhibited by leptin but stimulated by insulin (Xu et al., 2005b).

In order to fully address the role of PI3K mediated signalling pathways in AgRP neurons, a number of studies were carried out on *AgRPCrep110βKO* mice (animals which lack functional expression of the catayltic p110β subunit in AgRP neruons), designed to assess the hypothalamic function and various parameters of glucose homeostasis in these animals.

6.1 Proof of *p110β* deletion

Prior to commencement of the phenotypic characterisation of *AgRPCrep110βKO* animals, studies aimed at confirming the lack of functional p110β expression in hypothalami of *AgRPCrep110βKO* animals were carried out. However, to date, all studies aimed at proving this have been unsuccessful. These studies have included PCR-based strategies designed to detect recombination of the *p110βlox* alleles, and also immunocytochemical (ICC) studies aimed at proving *loxP* recombination specifically in AgRP neurons. Possible explanations for this potentially stem from the fact that only a

very small percentage of hypothalamic neurons express AgRP. This neuropeptide is expressed exclusively within the ARC, and thus the use of PCR-based strategies perfomed on whole hypothalamic lysates may not be sensitive enough. With regards to ICC studies, although viable *AgRPCrep110βKOYFP* (animals which express enhanced yellow fluorescent protein in AgRP neurons lacking *p110β*) were generated, there are no reliable antibodies against the C-terminus of *p110β* currently on the market. It can be argued that given the important role for PI3K in the regulation of growth and proliferation, inactivation of the p110β subunit in AgRP neurons results in cell death. This could also explain the fact that recombination of the floxed alleles could not be detected in hypothalamic lysates from *AgRPCrep110βKO* animals. However, hypothalamic slices from *AgRPCrep110βKOYFP* animals clearly show the presence of flurescence in the ARC indicating that AgRP neurons lacking *p110β* are viable (Figure 6.1).

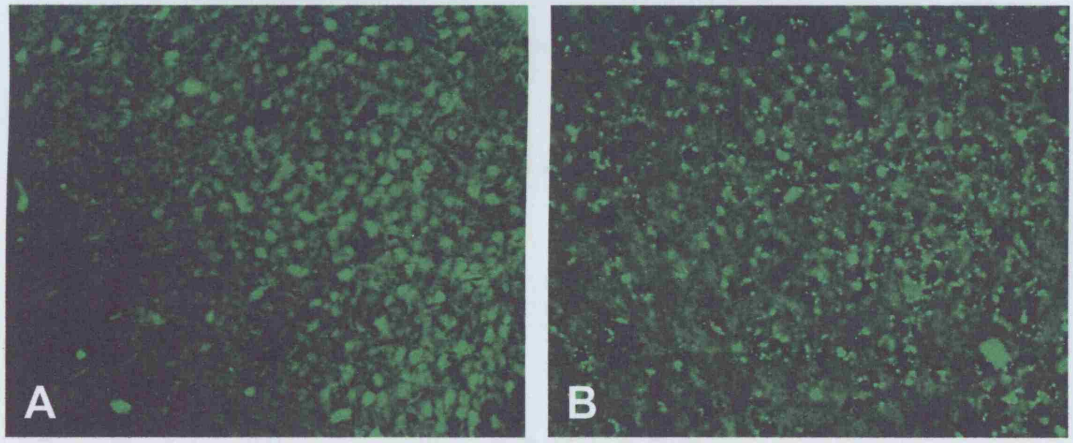

Figure 6.1: Proof of AgRP neuron viability in *AgRPCrep110βKO* animals. Hypothalamic sections from: A) *AgRPCreYFP* control animals and B) *AgRPCrep110βKOYFP* animals. No obvious alterations in AgRP neuron dimensions and number could be detected in *AgRPCrep110βKOYFP* animals compared to controls.

6.2 Hypothalamic function

In order to fully address the role of p110β mediated signalling pathways in AgRP neurons, studies were carried out on *AgRPCrep110βKO* mice designed to assess the hypothalamic function of these animals.

6.2.1 Analysis of body weight

From the ages of 10 and 17 weeks, male and female *AgRPCrep110βKO* animals respectively weighed significantly less than controls (Figure 6.2).

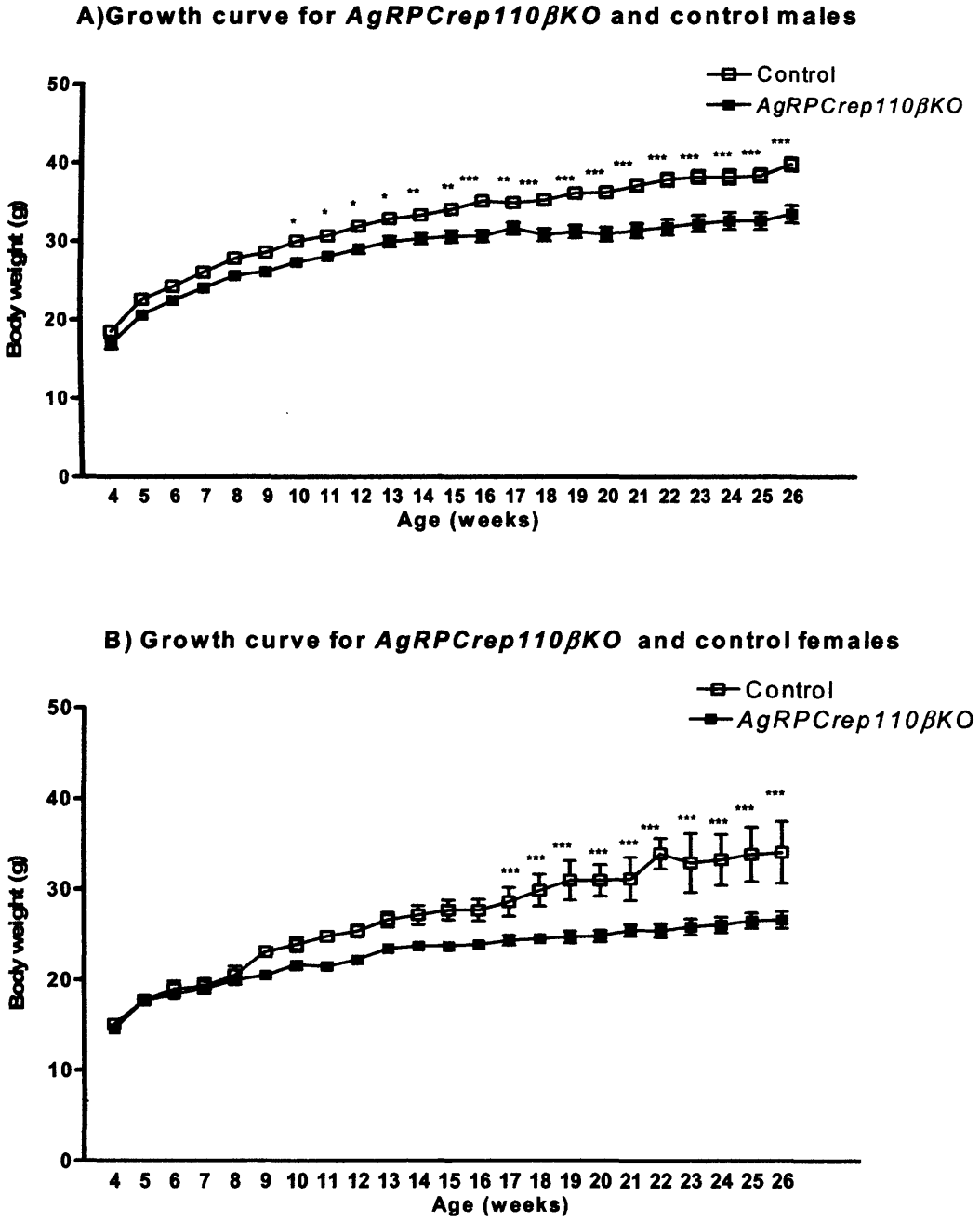

Figure 6.2: Growth curve for male *AgRPCrep110βKO* and control animals (A). Data represent the mean ± SEM for 26-52 animals of each genotype. Growth curve for female *AgRPCrep110βKO* and control animals (B). Data represent the mean ± SEM for 6-26 animals of each genotype. * $P < 0.05$, ** $P < 0.01$, *** $P < 0.001$.

6.2.2 Analysis of body length

Measurement of body length at 10 months of age showed male *AgRPCrep110βKO* animals were of normal body length, compared to control littermates (Figure 6.3).

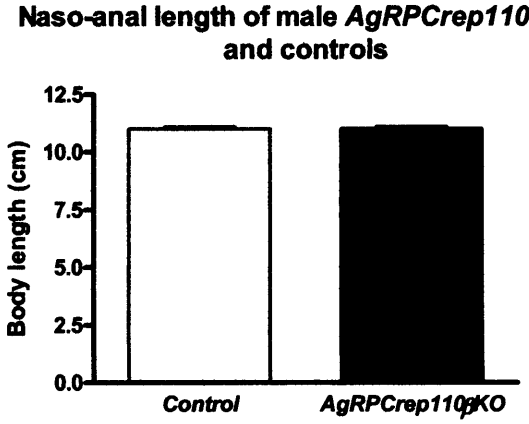

Figure 6.3: Naso-anal length (body length) was measured in male *AgRPCrep110βKO* and control mice at 10 months of age. Data represent the mean ± SEM for 8 animals of each genotype.

6.2.3 Plasma leptin levels

Measurement of the fasting plasma leptin levels of 10-month-old mice showed that *AgRPCrep110βKO* animals had an almost 4-fold reduction in leptin levels compared to controls (Figure 6.4).

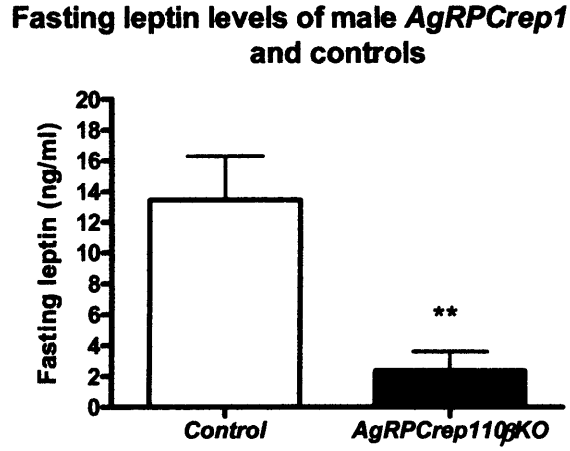

Figure 6.4: Fasting plasma leptin levels were measured on male *AgRPCrep110βKO* and control mice at 10 months of age following a 16-h overnight fast. Data represent the mean ± SEM for 6-8 animals of each genotype. ** $P < 0.01$.

6.2.4 Analysis of feeding behaviour

The reduced body weight of both male and female *AgRPCrep110βKO* animals suggested that this could be a result of decreased energy intake (i.e. food intake), increased energy expenditure or indeed a combination of these two defects. In order to ascertain the contribution of feeding to the lean phenotype, the daily food intake and the feeding response to fasting of male *AgRPCrep110βKO* and controls were analysed.

6.2.4.1 Analysis of food intake

At 4 months of age, *AgRPCrep110βKO* mice exhibited significantly reduced daily food intake compared to control animals (Figure 6.5).

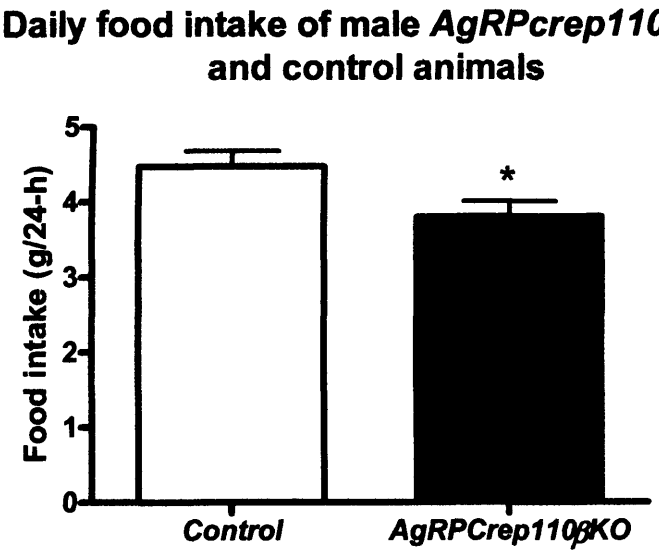

Figure 6.5: The daily (24-h) food intake of singly housed male *AgRPCrep110βKO* and controls at 4 months of age. Data represent the mean ± SEM for 13-15 animals of each genotype. * $P < 0.05$.

6.2.4.2 Response to fasting

At 6 months of age, *AgRPCrep110βKO* animals displayed normal food intake at 1, 2, 4 and 8-h post re-feeding compared to controls. However, consistent with the hypophagia displayed by *AgRPCrep110βKO* animals, *AgRPCrep110βKO* animals had significantly reduced cumulative food intake compared to controls at 24-h post re-feeding (Figure 6.6).

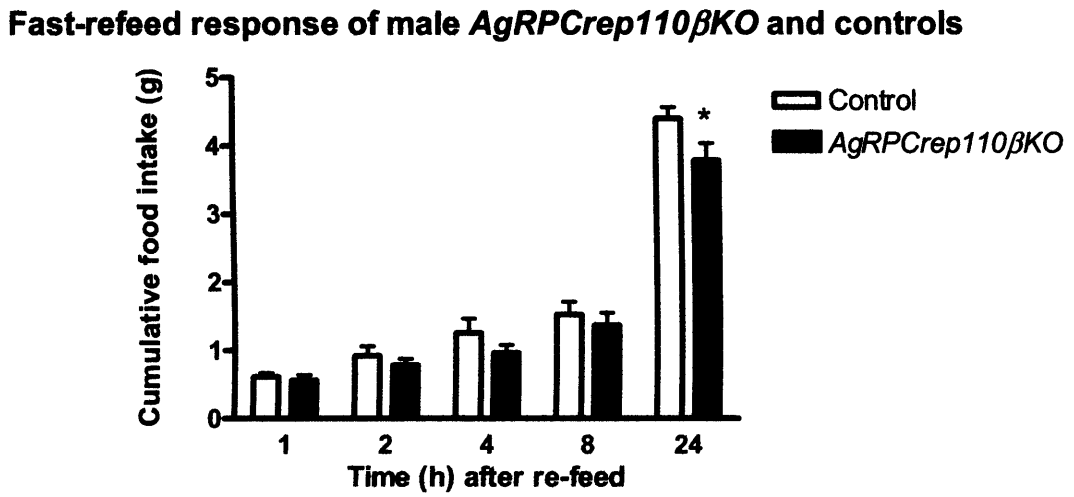

Figure 6.6: Re-feeding response following a 16-h overnight fast in 6 month old males. Data represent the mean ± SEM for 13-15 animals of each genotype. * $P < 0.05$.

6.2.5 Analysis of metabolic rate

In order to determine whether the lean phenotype of *AgRPCrep110βKO* animals was due solely to the hypophagia of these animals or also partly due to impairments in energy expenditure, the metabolic rate of 8-month-old male *AgRPCrep110βKO* mice and relevant controls was assessed. No significant difference in metabolic rate was seen between *AgRPCrep110βKO* mice and controls at thermoneutral (30±0.1°C) temperature (Figure 6.7). These results indicate that the reduced food intake of *AgRPCrep110βKO* animals is the major contributory factor to the lean phenotype of these animals.

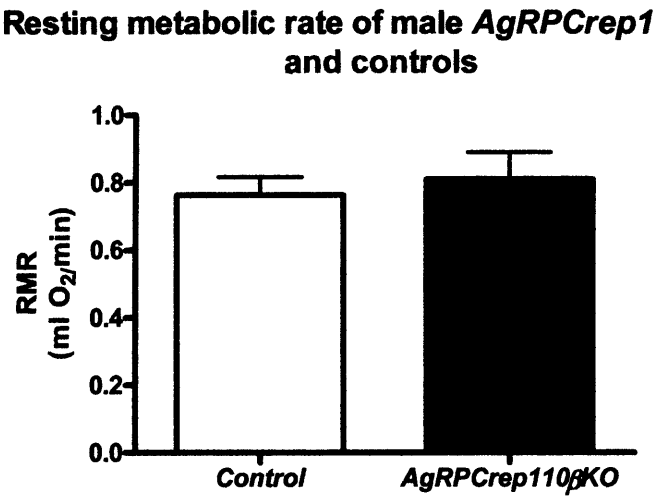

Figure 6.7: Analysis of metabolic rate in 10-month-old male *AgRPCrep110βKO* and control animals (thermoneutral). Data represent the mean ± SEM for 4-6 animals of each genotype.

6.2.6 Response to peripherally administered leptin

PI3K has previously been implicated as a point of convergence for insulin and leptin signalling. To assess the leptin sensitivity of *AgRPCrep110βKO* and control animals, leptin was administered peripherally to 10-month-old male mice for 3 consecutive days. Both cumulative food intake and body weight were measured over this period.

Following leptin treatment, control animals displayed a 3.3 % loss in body weight, compared with a 4.3 % loss in *AgRPCrep110βKO* mice (Figure 6.8a). In addition, leptin treatment (5mg/kg) inhibited food intake by 14 % in control mice and by 16 % in *AgRPCrep110βKO* mice, as compared to the food intake of the same animals following vehicle treatment (Figure 6.8b). These findings indicate that *AgRPCrep110βKO* animals are leptin sensitive. Indeed, it appears that *AgRPCrep110βKO* animals are more sensitive to the anorexigenic effects of leptin on body weight.

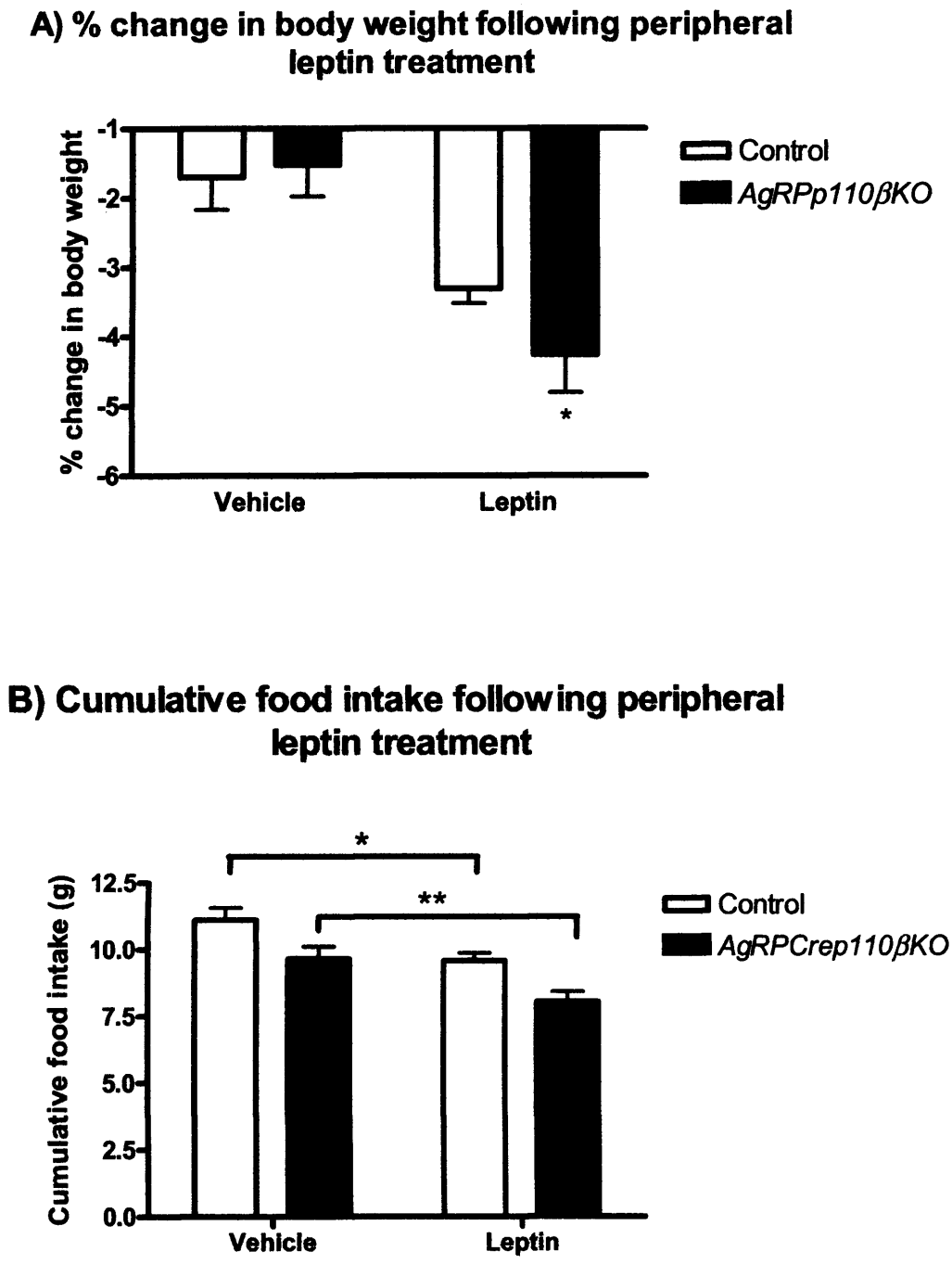

Figure 6.8: The response to 3 consecutive days of i.p.leptin administration upon A) body weight and B) food intake was determined in acclimatised male *AgRPCrep110βKO* and control mice at 10 months of age. Animals were injected once daily prior to the onset of the dark-phase with either leptin (5 mg/kg) or vehicle for three days in a cross-over design study. Data represent the mean ± SEM for 6-12 animals of each genotype. * $P < 0.05$, ** $P < 0.01$.

6.2.7 Response to peripherally administered MTII

To test whether the reduced lean phenotype and hypophagia of *AgRPCrep110βKO* animals was due to impairments in melancortin signalling, animals were subjected to i.p. treatment with MTII, a melanocortin receptor agonist.

Both control and *AgRPCrep110βKO* animals, which had received MTII treatment, ate significantly less than the equivalent vehicle treated group at 1, 2 and 4-h post re-feeding (Figure 6.9). No significant differences in food intake could be detected between MTII treated control and *AgRPCrep110βKO* animals at any time points. These studies thus demonstrate that *AgRPCrep110βKO* animals are sensitive to the anorexigenic effects of melanocortins.

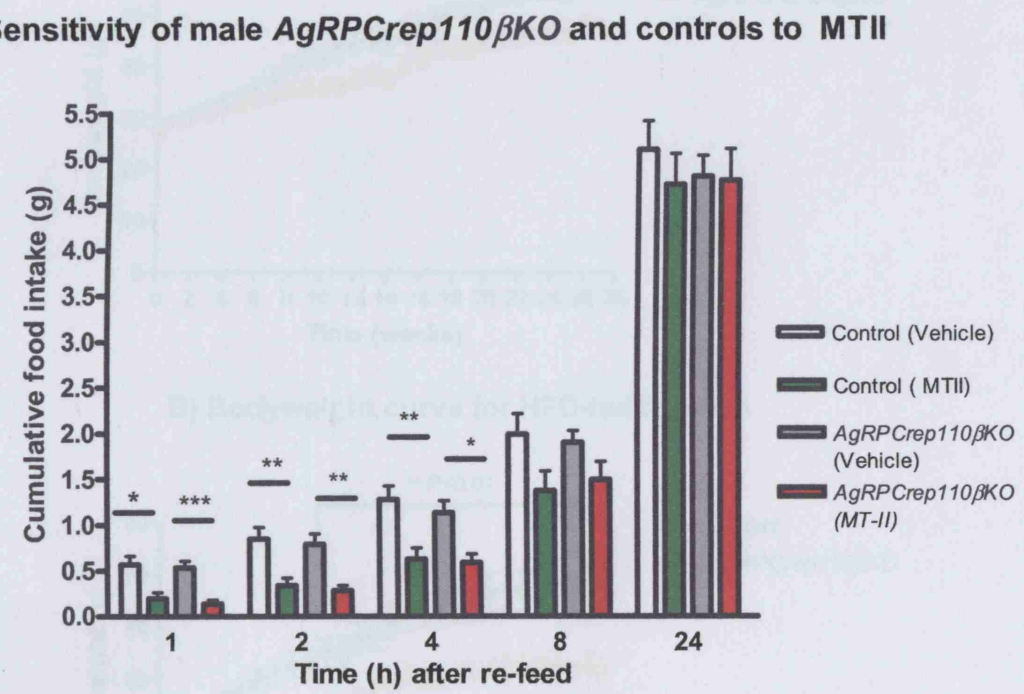

Figure 6.9: The fast-refeed response of animals following an i.p. injection of vehicle or MTII. Following a 16-h overnight fast, mice were injected with either vehicle or MTII, and approximately 50g of food was weighed and given to each animal. The food was then weighed after 1-h, 2-h, 4-h, 8-h and 24-h. Data represent the mean ± SEM for 13-15 animals of each genotype. * $P < 0.05$, ** $P < 0.01$, *** $P < 0.001$.

6.2.8 HFD trial

The sensitivity of male and female *AgRPCrep110βKO* and controls to HFD was assessed from the age of 6 weeks onwards, for the duration of 28 weeks.

6.2.8.1 Body weights of animals on HFD

Both male and female *AgRPCrep110βKO* animals gained significantly less weight than control animals on HFD at the end of the 28-week trial (Figure 6.10). Thus *AgRPCrep110βKO* animals are resistant to diet induced obesity (DIO).

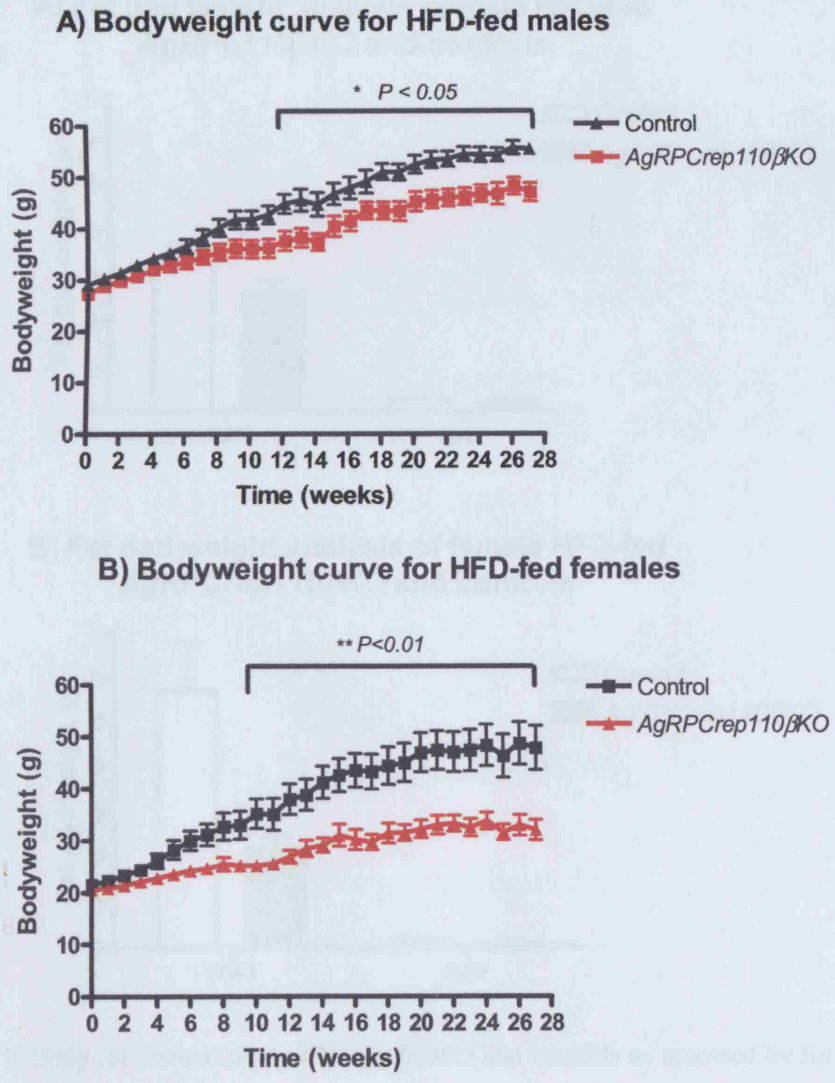

Figure 6.10: Body weight curve of *AgRPCrep110βKO* animals on HFD: A) male control and *AgRPCrep110βKO* mice, B) female control and *AgRPCrep110βKO* mice. Data represent the mean ± SEM for 6-9 animals of each genotype. * $P < 0.05$, ** $P < 0.01$.

6.2.8.2 Analysis of body fat content

The fat content of 10-month-old male and female *AgRPCrep110βKO* and controls on HFD was assessed by measurement of fat pads, namely WAT (gonadal and mesenteric) and BAT (two depots between the scapulae) tissue pads. Consistent with their resistance to DIO, both male and female *AgRPCrep110βKO* animals had significantly reduced WAT mass compared to controls although no significant diference in BAT levels were detected significant (Figure 6.11).

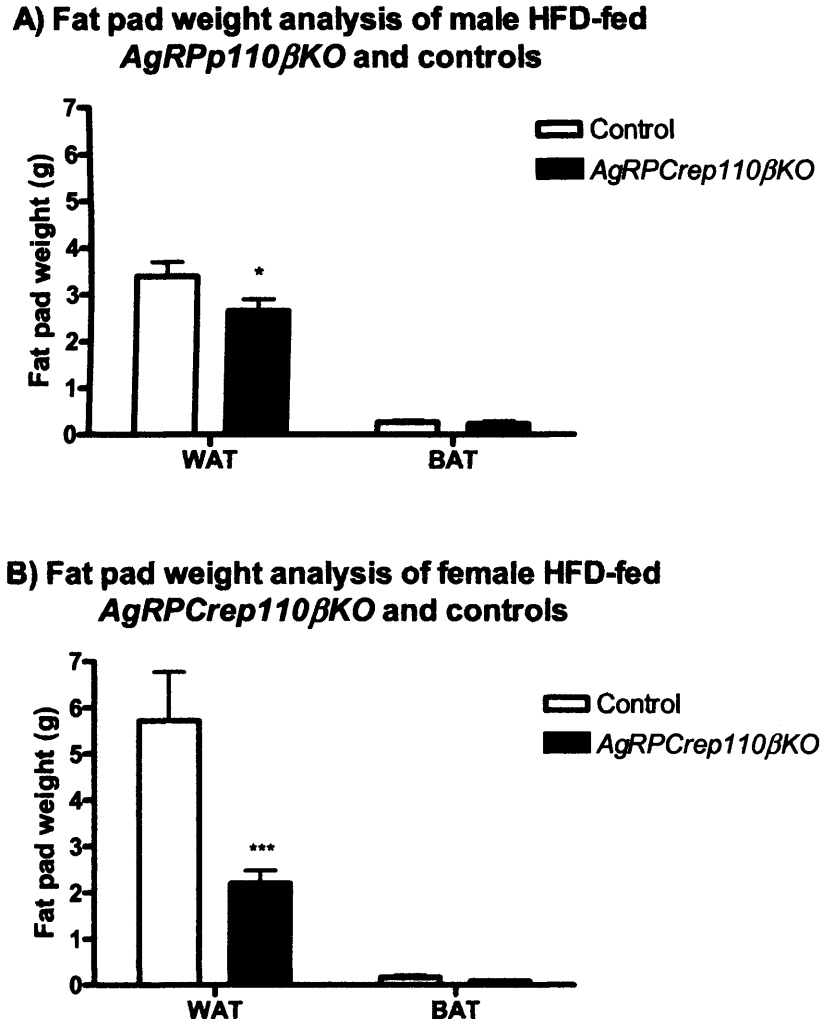

Figure 6.11: Body fat content of *AgRPCrep110βKO* and controls as assessed by fat pad weight analysis on HFD. Fat pad weights of A) males and B) of females. Data represent the mean ± SEM for 6-9 animals of each genotype. * $P < 0.05$, ** $P < 0.01$, *** $P < 0.001$.

6.2.8.3 Analysis of feeding behaviour

In order to understand the mechanims underlying the resistance of male and female *AgRPCrep110βKO* animals to DIO, the daily food intake of these animals on HFD was analysed. Similarly to *AgRPCrep110βKO* mice on a standard chow diet, HFD-fed *AgRPCrep110βKO* animals ate signifcantly less than controls (Figure 6.12).

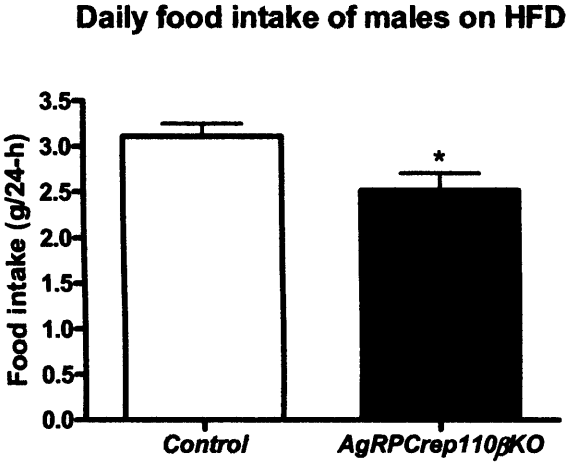

Figure 6.12: The daily (24-h) food intake of singly housed male *AgRPCrep110βKO* and controls on HFD at 8 months of age. Data represent the mean ± SEM for 13-15 animals of each genotype. * $P < 0.05$.

6.2.8.4 Analysis of metabolic rate

The metabolic rate of 8-month-old HFD-fed male *AgRPCrep110βKO* mice and controls as assessed to investigate if the resistance to DIO of these animals was due solely to hypophagia. No significant difference in metabolic rate was seen between *AgRPCrep110βKO* mice and controls at thermoneutral (30±0.1°C) temperature. This indicates that the reduced food intake of *AgRPCrep110βKO* animals is the major contributor to the resistance to DIO of these animals (Figure 6.13).

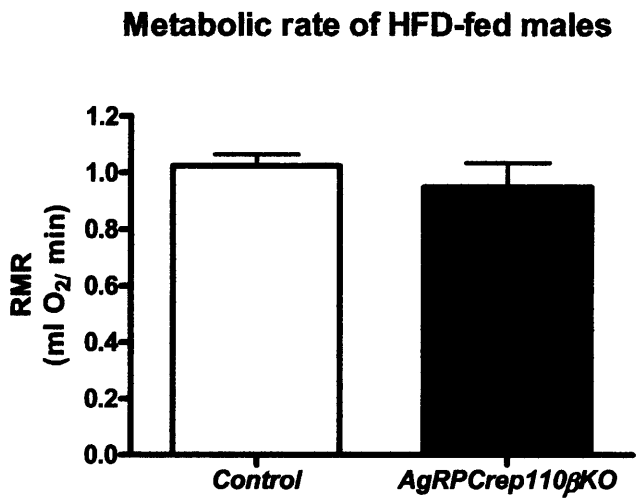

Figure 6.13: Analysis of metabolic rate in 8-month-old HFD-fed male *AgRPCrep110βKO* and control animals (thermoneutral). Data represent the mean ± SEM for 8 animals of each genotype.

6.3 Glucose Homeostasis

In order to investigate the effect on glucose homeostasis of the deletion of *p110β* in AgRP neurons, various metabolic studies were carried out on *AgRPCrep110βKO* mice.

6.3.1 Fasting blood glucose (FBG) levels

At 5 weeks and 10 months of age, both male and female *AgRPCrep110βKO* animals had indistinguishable FBG levels from controls (Figure 6.14A-D). In addition, at 10 months of age, no difference in fasting blood glucose levels could be detected between control and *AgRPCrep110β*KO animals of both sexes subjected to HFD for a duration of 28 weeks (Figure 6.14E and 6.14F).

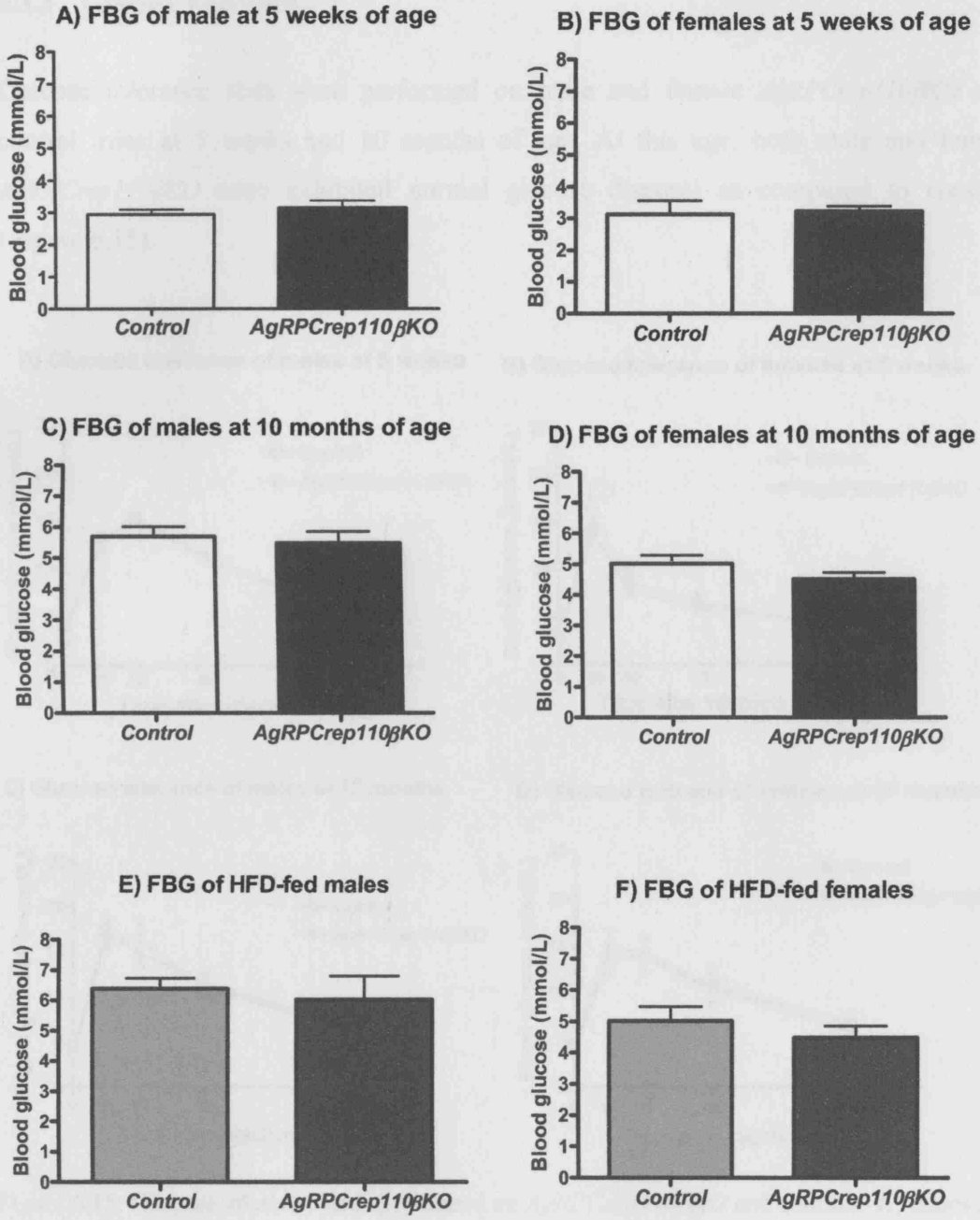

Figure 6.14: Fasting blood glucose levels of *AgRPCrep110βKO* and controls. A) 5 week old males, B) 5 week old females, C) 10 month old males, D) 10 month old females, E) males following 28 weeks on HFD and E) females following 28 weeks on HFD. Data represent the mean ± SEM for 6-8 mice of each genotype

6.3.2 Glucose tolerance

Glucose tolerance tests were performed on male and female *AgRPCrep110βKO* and control mice at 5 weeks and 10 months of age. At this age, both male and female *AgRPCrep110βKO* mice exhibited normal glucose disposal as compared to controls (Figure 6.15).

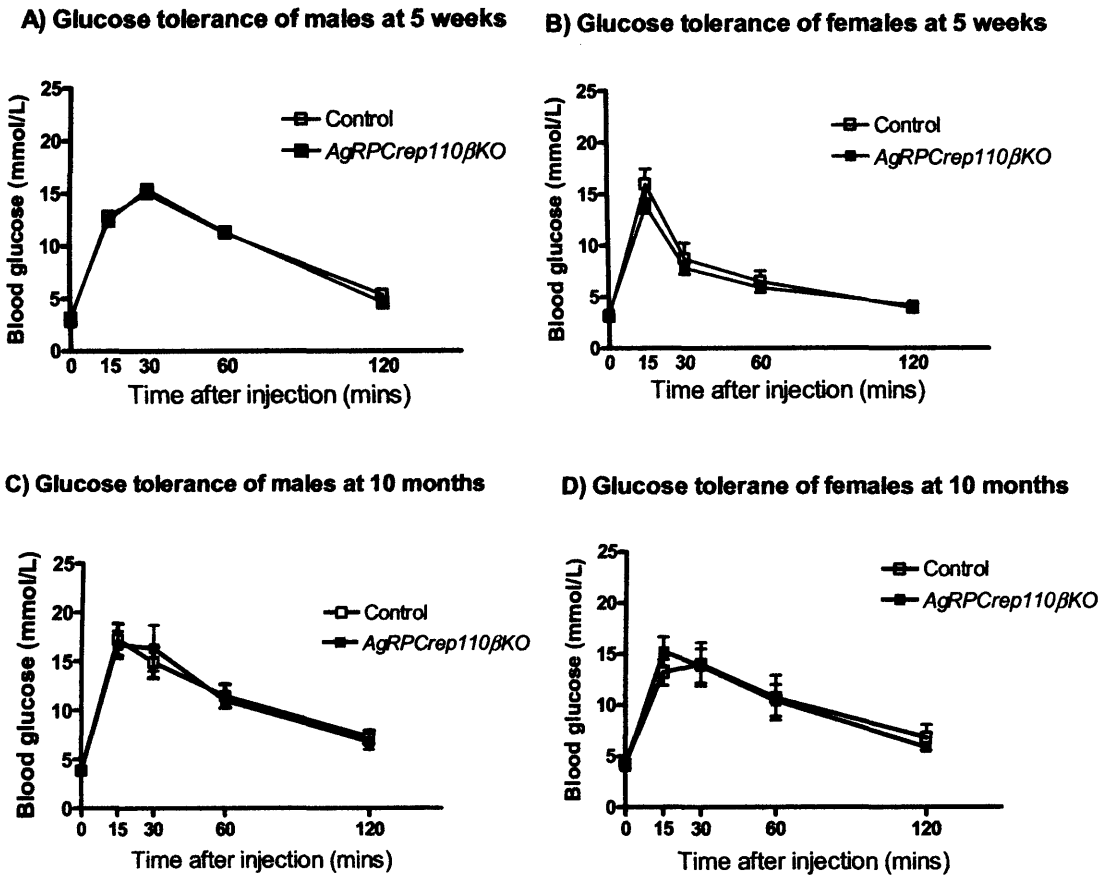

Figure 6.15: Glucose tolerance tests performed on *AgRPCrep110βKO* and controls. A) males at 5 weeks of age, B) females at 5 weeks of age, C) males at 10 months of age, D) females at 10 months of age. Data represent the mean ± SEM for 6-8 animals of each genotype.

Ten-month-old male and female *AgRPCrep110βKO* and control animals that had been subjected to HFD feeding for a duration of 28 weeks, were also subjected to glucose tolerance testing. Male *AgRPCrep110βKO* had improved glucose disposal compared to controls, although this was not statistically significant. On the other hand, female *AgRPCrep110βKO* had signifcantly improved glucose tolerance compared to control animals on HFD (Figure 6.16).

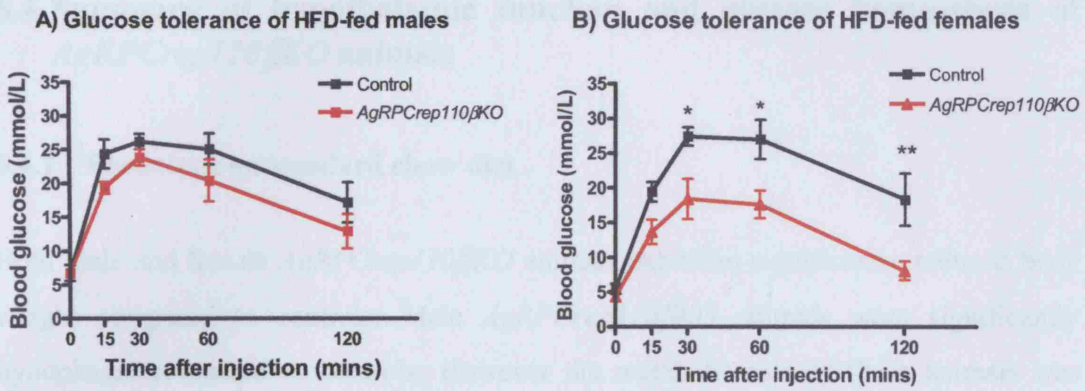

Figure 6.16: Glucose tolerance tests performed on: A) male *AgRPCrep110βKO* and controls and B) female *AgRPCrep110βKO* and control, following 28 weeks of HFD feeding. Data represent the mean ± SEM for 6-8 animals of each genotype. * $P < 0.05$, ** $P < 0.01$.

6.3.3 Fasting plasma insulin levels

At 10 months of age male *AgRPCrep110βKO* mice had signficantly reduced fasting insulin levels as compared to control animals (Figure 6.17).

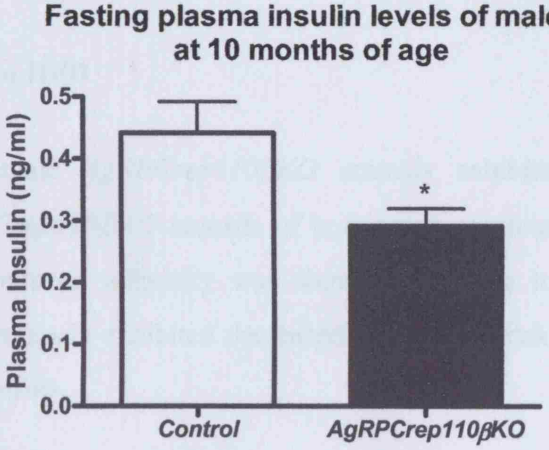

Figure 6.17: Fasting plasma insulin levels of 10 month old male *AgRPCrep110βKO* and control mice following a 16-h overnight fast at 10 months of age. Data represent the mean ± SEM for 6-8 animals of each genotype. . * $P < 0.05$.

6.4 Summary of hypothalamic function and glucose homeostasis of *AgRPCrep110βKO* animals

6.4.1 Phenotype on standard chow diet

Both male and female *AgRPCrep110βKO* animals exhibited significantly reduced body weight compared to controls. Male *AgRPCrep110βKO* animals were significantly hypophagic compared to controls. However the metabolic rate of these animals was normal. At 10 months of age, male *AgRPCrep110βKO* animals were significantly hypoleptinaemic and demonstrated increased sensitivity to the anorexigenic effects of peripheral leptin treatment, compared to controls. In addition, no abnormalities in naso-anal body length could be detected in *AgRPCrep110βKO* animals indicating no impairments in melanocortin system. Consistently, *AgRPCrep110βKO* animals exhibited normal sensitivity to the anorexigenic effects of peripheral MTII treatment.

With regards to glucose homeostasis, both male and female *AgRPCrep110βKO* animals exhibited normal FBG levels and glucose tolerance, as compared to controls. Consistent with their reduced body weight, 10-month-old male *AgRPCrep110βKO* animals were significantly hypoinsulinaemic compared to controls.

6.4.2 Phenotype on HFD

Both male and female *AgRPCrep110βKO* animals exhibited resistance to DIO. Consistently, *AgRPCrep110βKO* animals of both sexes exhibited significantly reduced WAT mass. This reduced adiposity was shown to be due to reduced food intake; *AgRPCrep110βKO* animals exhibited decreased daily food intake but normal metabolic rate compared to controls.

With regards to glucose homeostasis, both male and female *AgRPCrep110βKO* animals exhibited normal FBG levels. Although male *AgRPCrep110βKO* exhibited normal glucose tolerance, female *AgRPCrep110βKO* animals demonstrated significantly improved glucose tolerance compared to controls.

Chapter 7

Phenotypic characterisation of *POMCCrep110βKO* animals

7 Characterisation of *POMCCrep110βKO* mice

Within the ARC, POMC neurons have been shown to express both insulin and leptin receptors (Benoit et al., 2002; Cheung et al., 1997). Administration of both these hormones directly into the third ventricle of mice has been shown to result in increased hypothalamic expression of *Pomc* mRNA (Benoit et al., 2002; Brown et al., 2006). In addition, both insulin and leptin have been shown to activate PI3K expression in POMC neurons (Xu et al., 2005b), implicating this enzyme as a potential point of convergence between the two signalling cascades in the hypothalamic regulation of food intake and body weight. Treatment with PI3K inhibitors attenuates the anorexigenic effects of insulin and leptin (Niswender et al., 2003; Niswender et al., 2001). A role for hypothalamic PI3K-mediated pathways in the regulation of peripheral glucose homeostasis has also been suggested by various studies (Morrison et al., 2005; Morton et al., 2005).

In order to fully address the role of PI3K mediated signalling pathways in POMC neurons, a number of studies were carried out on *POMCCrep110βKO* mice designed to assess the hypothalamic function and various parameters of glucose homeostasis in these animals.

7.1 Proof of *p110β* deletion

Prior to commencement of the phenotypic characterisation of *POMCCrep110βKO* animals, studies aimed at confirming the lack of functional p110β expression in the hypothalami of *POMCCrep110βKO* animals were carried out. A nested-PCR strategy, performed on cDNA transcribed from hypothalamic lysates of *POMCCrep110βKO* animals, confirmed the recombination of the *p110βflox* alleles in the hypothalamus of these animals. This work was performed by Dr. Julie Guillermet at the Ludwig Institute, UCL (Figure 7.1A).

However, ICC studies aimed at proving recombination of the *p110βflox* alleles specifically within POMC neurons have been unsuccessful. Although viable

POMCCrep110βKOGFP (animals which express green fluorescent protein in POMC neurons lacking *p110β*) were generated, no reliable antibodies against the C-terminus of *p110β* are currently available. However, similarily to the situation in *AgRPCrep110βKO* animals, hypothalamic slices from *POMCCrep110βKOGFP* animals clearly show the presence of fluorescent neurons in the ARC, indicating that POMC neurons lacking *p110β* are viable.

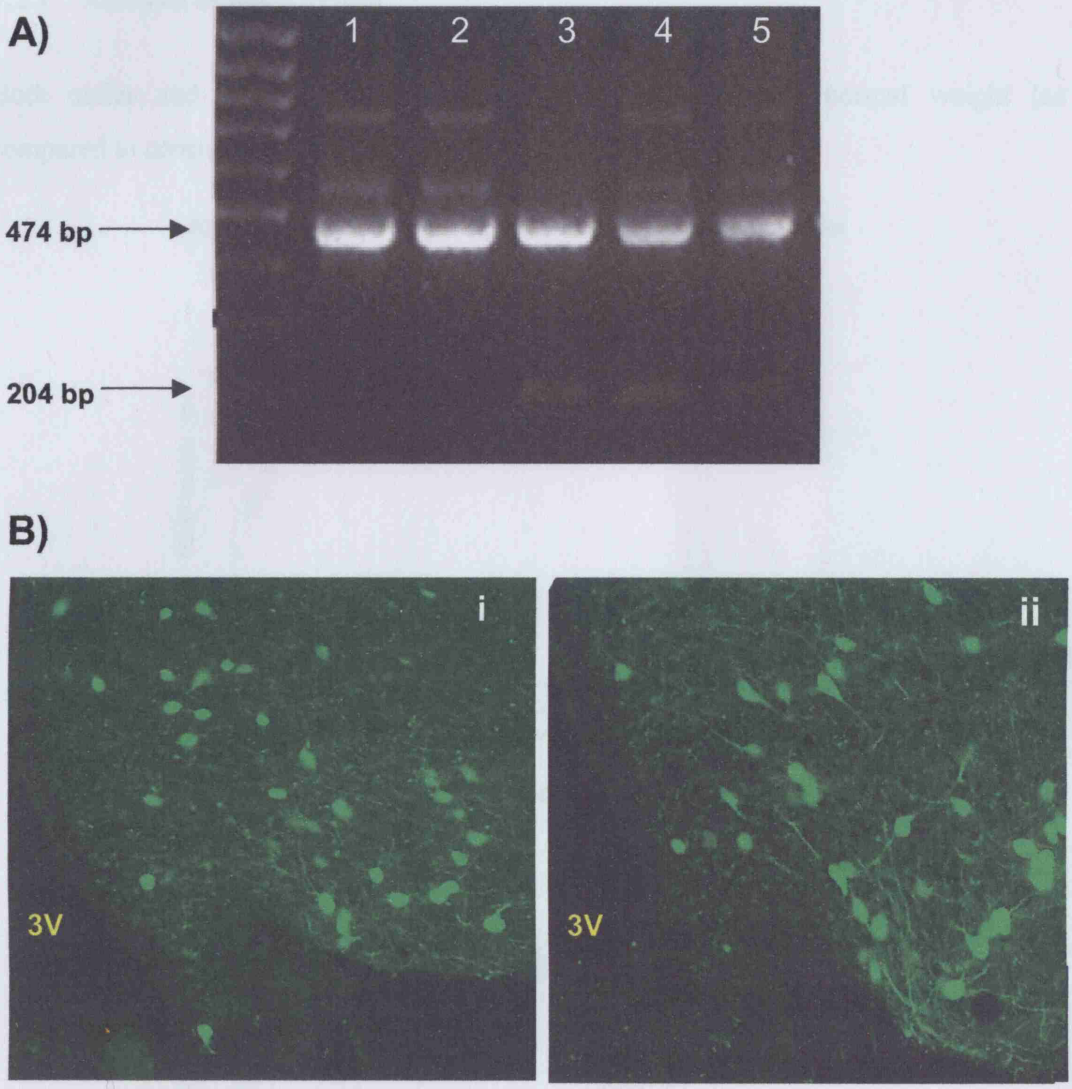

Figure 7.1: A) Proof of recombination of floxed alleles by a nested-PCR strategy. Samples 1 and 2 are hypothalamic cDNA samples from control animals. Samples 3, 4 and 5 are hypothalamic cDNA samples from *POMCCrep110βKO* animals. A 474 bp band indicates presence of the *p110βflox* allele. A 204 bp band indicates recombination of the floxed alleles. B). Proof of POMC neuron viability in *POMCCrep110βKO* animals. Hypothalamic sections from: i) *POMCCreYFP* control animals and ii) *POMCCrep110βKOYFP* animals. 3V, third ventricle.

7.2 Hypothalamic function

In order to fully address the role of p110β mediated signalling pathways in POMC neurons, a number of studies were carried out on *POMCCrep110βKO* mice designed to assess the hypothalamic function of these animals.

7.2.1 Analysis of body weight

Both males and female *POMCCrep110βKO* animals were of normal weight (as compared to control littermates) at all ages studied (Figure 7.2).

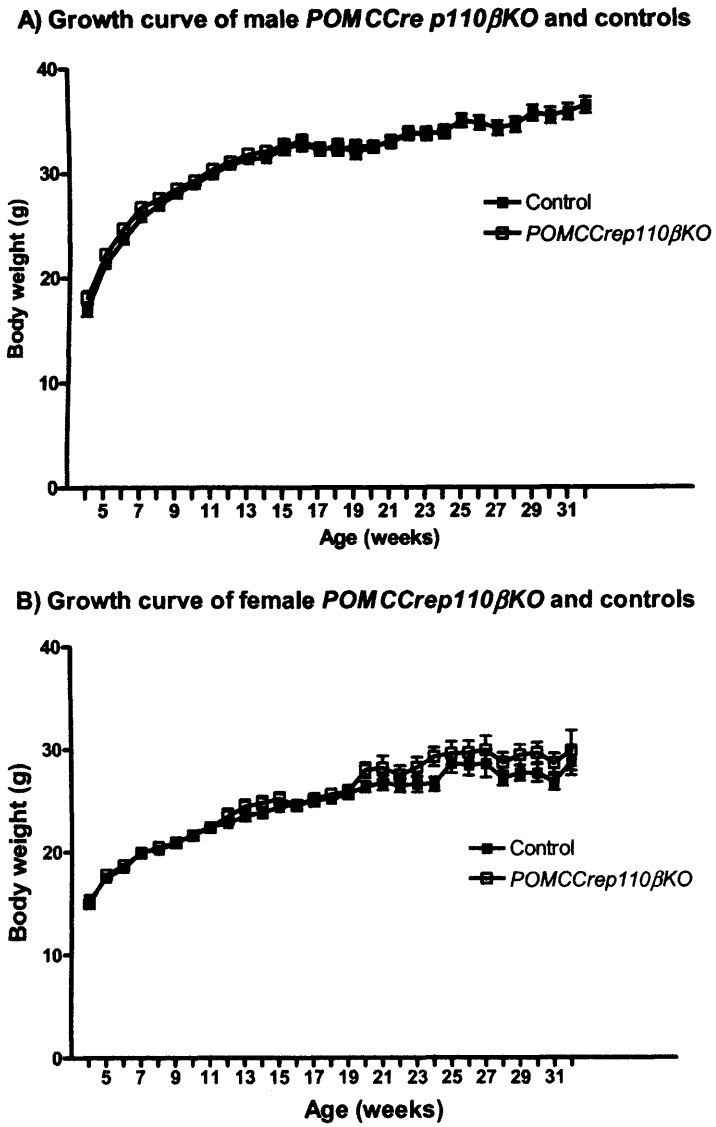

Figure 7.2: Growth curve for A) male *POMCCrep110βKO* and control animals and B) female *POMCCrep110βKO* and control animals. Data represent the mean ± SEM for 11-39 animals of each genotype.

7.2.2 Analysis of body length

Measurement of naso-anal body length at 10 months of age, showed male *POMCCrep110βKO* animals to be significantly longer than control littermates (Figure 7.3).

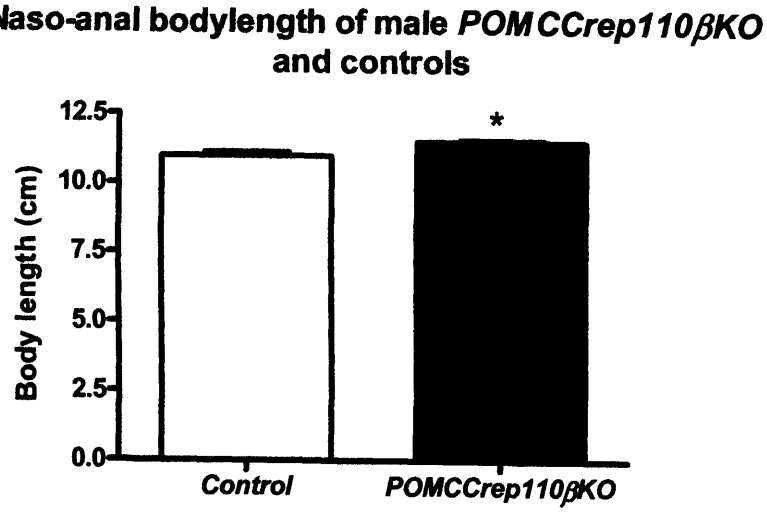

Figure 7.3: Naso-anal length (body length) was measured in male *POMCCrep110βKO* and controls at 10 months of age. Data represent the mean ± SEM for 6 animals of each genotype. * $P < 0.05$.

7.2.3 Analysis of body fat content by fat pad weights

The body fat content of 10-month-old male *POMCCrep110βKO* and controls was assessed by measurement of fat pads, namely WAT (gonadal and mesenteric) and BAT pads (two depots between the scapulae).

Interestingly, despite the normal body weight of *POMCCrep110βKO* animals compared to controls, *POMCCrep110βKO* animals had a significant increase in WAT mass (Figure 7.4).

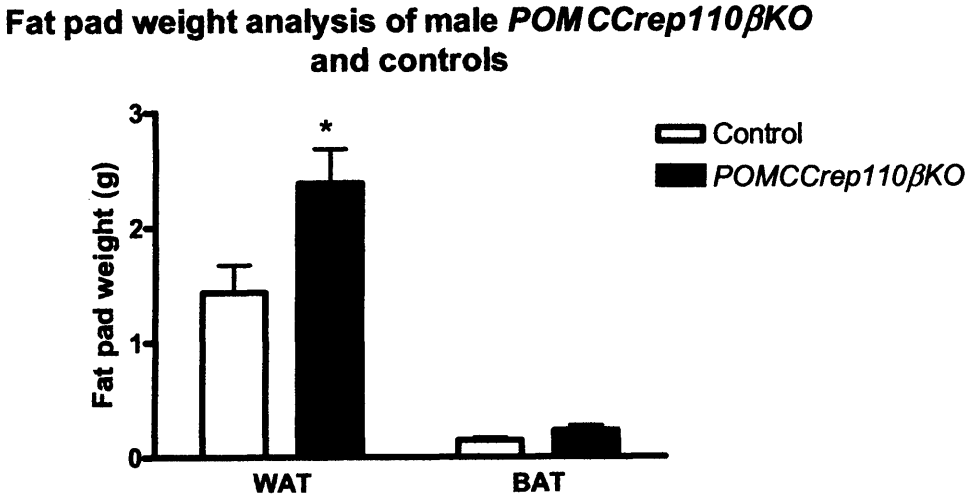

Figure 7.4: Fat content of male *POMCCrep110βKO* and controls as assessed by fat pad. Data represent the mean ± SEM for 6-7 animals of each genotype. * $P < 0.05$.

7.2.4 Plasma leptin levels

Measurement of the fasting leptin levels of 10-month-old mice, demonstrated that *POMCCrep110βKO* animals had indistinguishable leptin levels from controls (Figure 7.5).

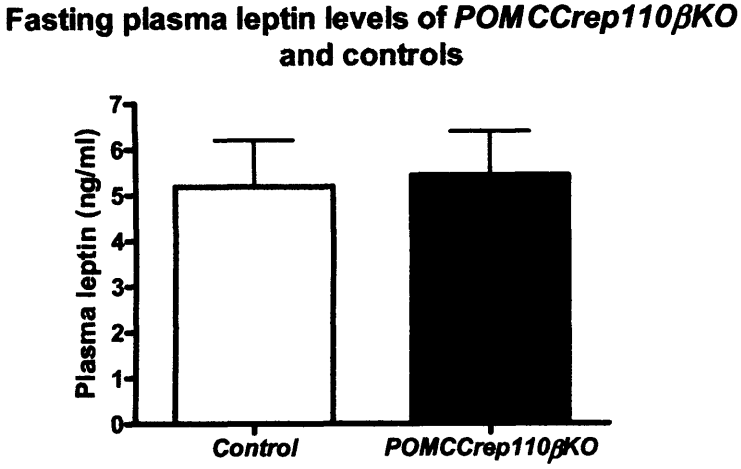

Figure 7.5: Fasting plasma leptin levels were measured on male *POMCCrep110BKO* and control mice at 10 months of age following a 16-h overnight fast. Data represent the mean ± SEM for 6-8 animals of each genotype.

7.2.5 Analysis of feeding behaviour

Despite the lack of differences found in the body weight of *POMCCrep110βKO* animals, the increased adiposity suggested that these animals might have impaired energy homeostasis regulation. In addition, the increased body length indicated potential impairments in melanocortin signalling. Thus, the feeding behaviour of these animals was investigated by analysis of the daily food intake and response to fasting of *POMCCrep110βKO* and control animals.

7.2.5.1 Analysis of food intake

At 4 months of age, male *POMCCrep110βKO* mice were significantly hyperphagic compared to control animals (Figure 7.6).

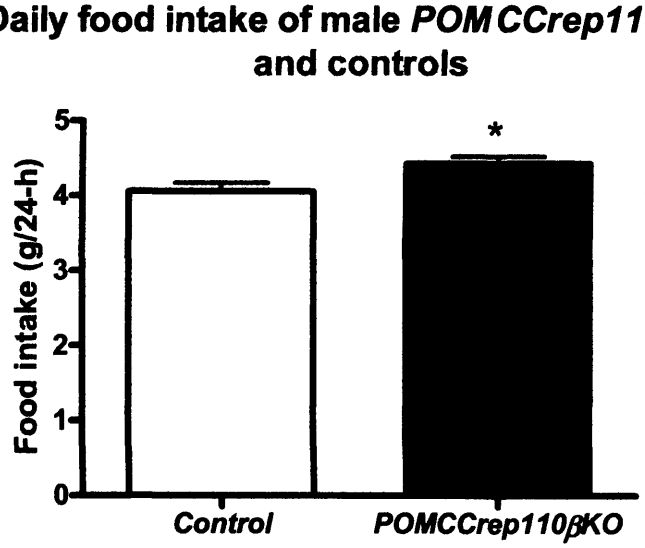

Figure 7.6: Daily (24-h) food intake was measured in male *POMCCrep110βKO* and control animals at 4 months of age. Data represent the mean ± SEM for 14-16 animals of each genotype. * $P < 0.05$.

7.2.5.2 Response to fasting

At 6 months of age, male *POMCCrep110βKO* animals displayed normal food intake at 1, 2, 4 and 8-h post re-feeding compared to controls. However, consistent with the hyperphagia of these animals, *POMCCrep110βKO* animals had significantly increased cumulative food intake compared to controls at 24-h post re-feeding (Figure 7.7).

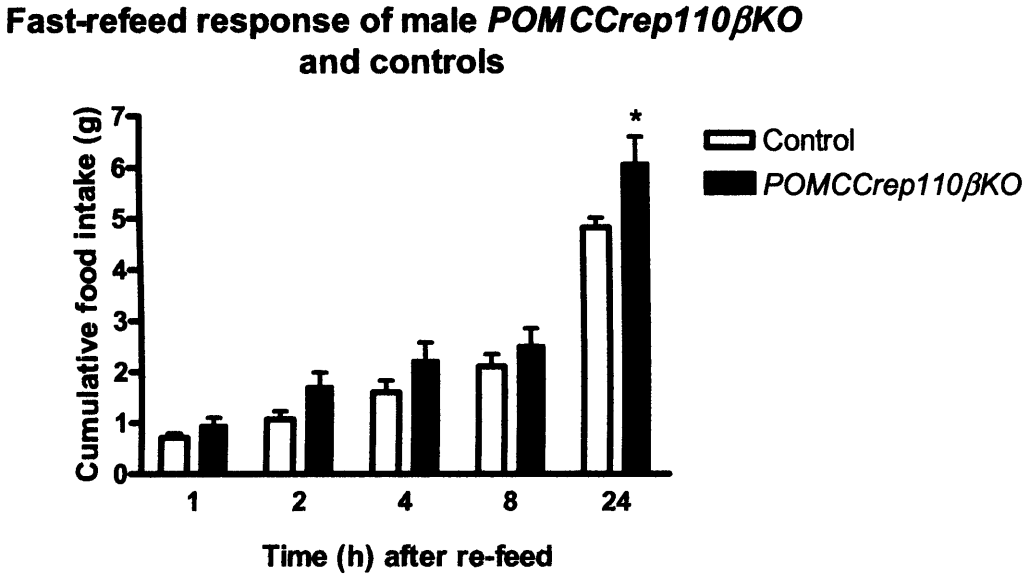

Figure 7.7: Re-feeding response following a 16-h overnight fast in 6 month old males. Data represent the mean ± SEM for 14-16 animals of each genotype. * $P < 0.05$.

7.2.6 Analysis of metabolic rate

In order to determine whether the increased adiposity of *POMCCrep110βKO* animals was due solely to the hyperphagia of these animals or also partly due to impairments in energy expenditure, the metabolic rate of 10-month-old male *POMCCrep110βKO* mice and relevant controls was assessed. *POMCCrep110βKO* displayed a non-significant trend for lower metabolic rate at thermoneutral (30±0.1°C) temperature, compared to controls (Figure 7.8).

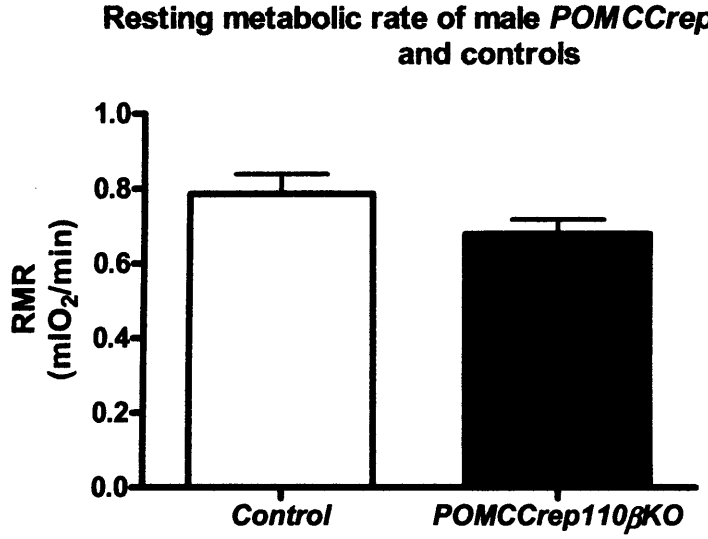

Figure 7.8: Summary of analysis of RMR in 10 month old male *POMCCre p110βKO* and control animals (thermoneutral). Data represent the mean ± SEM for 7 animals of each genotype.

7.2.7 Response to peripherally administered leptin

The hyperphagia and increased adiposity of *POMCCrep110βKO* animals at 10 months of age suggests a possible underlying resistance to leptin. PI3K has previously been implicated as a point of convergence for insulin and leptin signalling. To assess the leptin sensitivity of these animals, leptin was administered peripherally to 10-month-old male *POMCCrep110βKO* and control mice for 3 consecutive days.

Following leptin treatment, control animals displayed a 3.45 % loss in body weight, compared with a 4.12 % loss in *POMCCrep110βKO* mice. In addition, leptin treatment (5mg/kg) inhibited food intake by 15% in controls and by 27% in *POMCCrep110βKO* mice, as compared to the food intake of the same animals following vehicle treatment (Figure 7.9). Taken together, these reults demonstrate that *POMCCrep110βKO* animals are still sensitive to the anorexigenic effects of peripherally administered leptin.

A) % change in body weight following peripheral leptin treatment

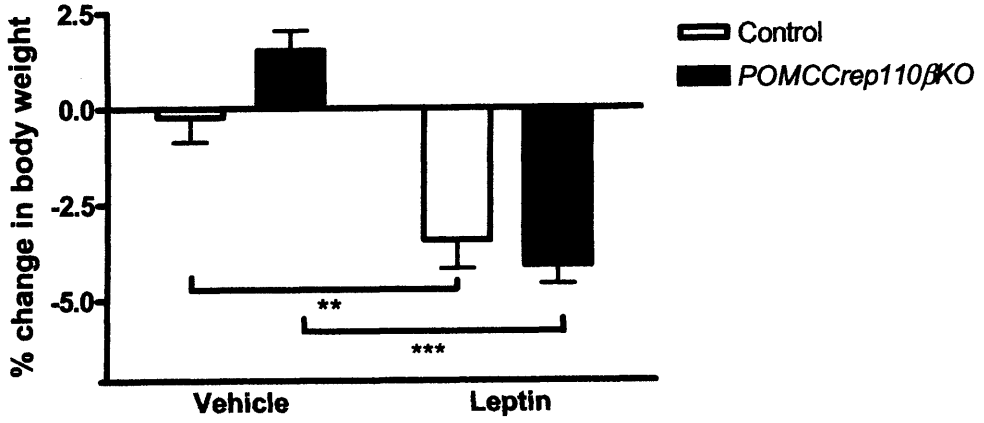

B) Cumulative food intake following peripheral leptin treatment

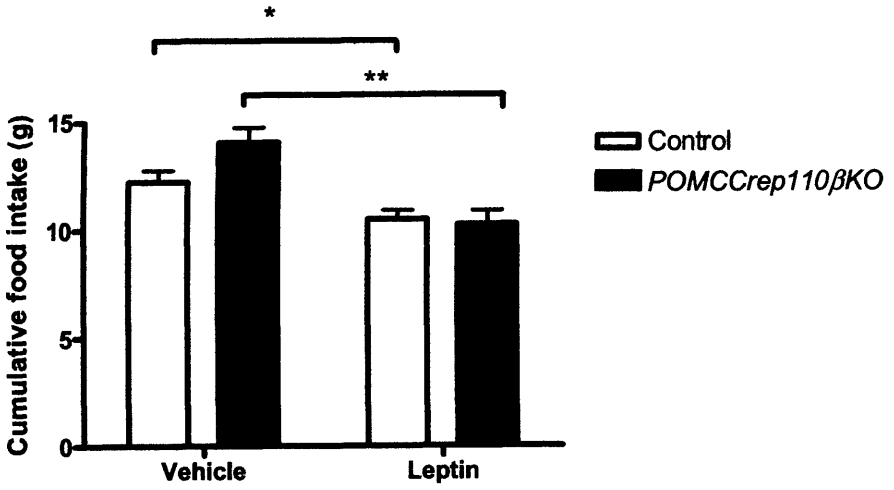

Figure 7.9: The response to 3 consecutive days of i.p. leptin administration upon A) body weight and B) food intake was determined in acclimatised male *POMCCrep110βKO* and control mice at 10 months of age. Data represent the mean ± SEM for 7-10 animals of each genotype. * $P < 0.05$, ** $P < 0.01$, *** $P < 0.001$.

7.2.8 Response to peripherally administered MTII

The increased body length and impaired feeding regulation of *POMCCrep110βKO* animals suggested that these animals have disrupted melanocortin signalling. Thus, to assess the melanocortin sensitivity of these animals, both *POMCCrep110βKO* and control animals were peripherally treated with MTII.

As expected, control animals ate significantly less during the first 8 hours post-refeed when treated with MTII compared to vehicle. *POMCCrep110βKO* were also sensitive to the food-inhibiting effects of MTII during the first 8 hours post-refeed (Figure 7.10). This demonstrates that *POMCCrep110βKO* animals remain sensitive to the anorexigenic effects of melanocortins, and that melanocortin pathways remain functional regardless of *p110β* deletion in POMC neurons.

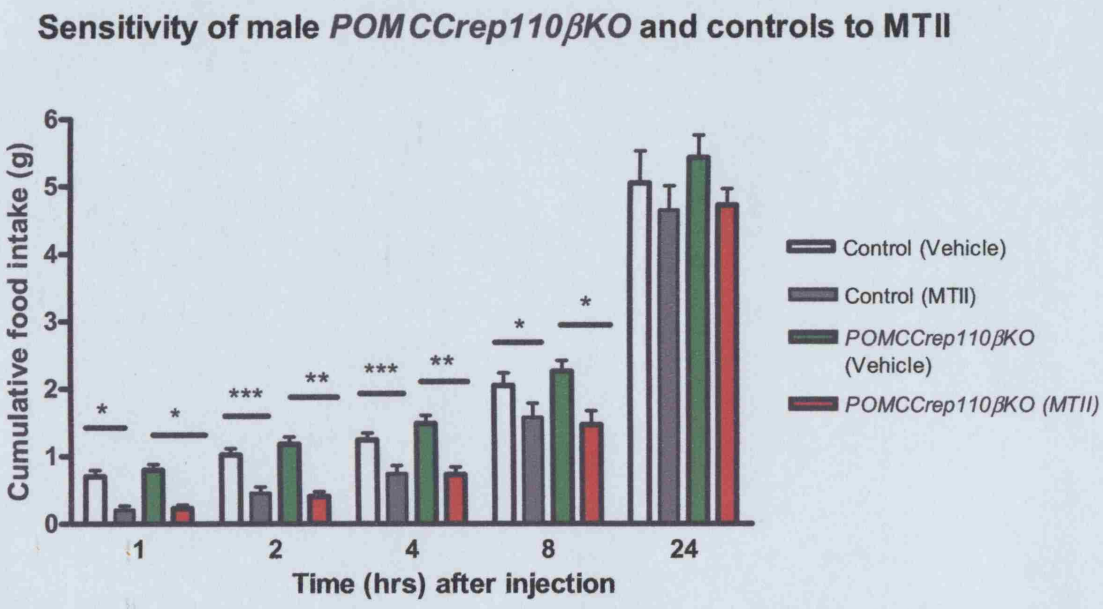

Figure 7.10: The fast-refeed response of animals following an i.p. injection of vehicle or MTII. Following a 16-h overnight fast, mice were injected with either vehicle or MTII, and approximately 50g of food was weighed and given to each animal. The food was then weighed after 1-h, 2-h, 4-h, 8-h and 24-h. Data represent the mean ± SEM for 14-16 animals of each genotype. * $P < 0.05$, ** $P < 0.01$, *** $P < 0.001$.

7.3 Glucose Homeostasis

In order to investigate the effect on glucose homeostasis of the deletion of *p110β* in POMC neurons, various metabolic studies were carried out on *POMCCrep110βKO* and control mice.

7.3.1 Fasting blood glucose (FBG) levels

At both 5 weeks and 10 months of age, male *POMCCrep110βKO* mice had indistinguishable FBG levels from control animals (Figure 7.11).

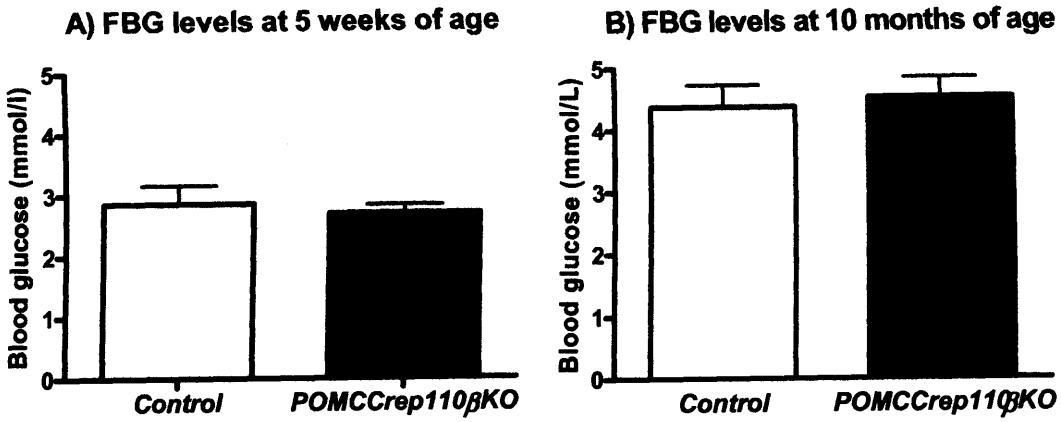

Figure 7.11: FBG levels (mmol/L) following a 16-h fast in male *POMCCrep110βKO* and controls at A) 5 weeks of age and B) at 10 months of age. Data represent the mean ± SEM for 7-9 mice of each genotype.

7.3.2 Glucose tolerance

Glucose tolerance tests were performed on male *POMCCrep110βKO* and control mice at 5 weeks and 10 months of age. At both ages, *POMCCrep110βKO* animals exhibited normal glucose disposal as compared to controls (Figure 7.12).

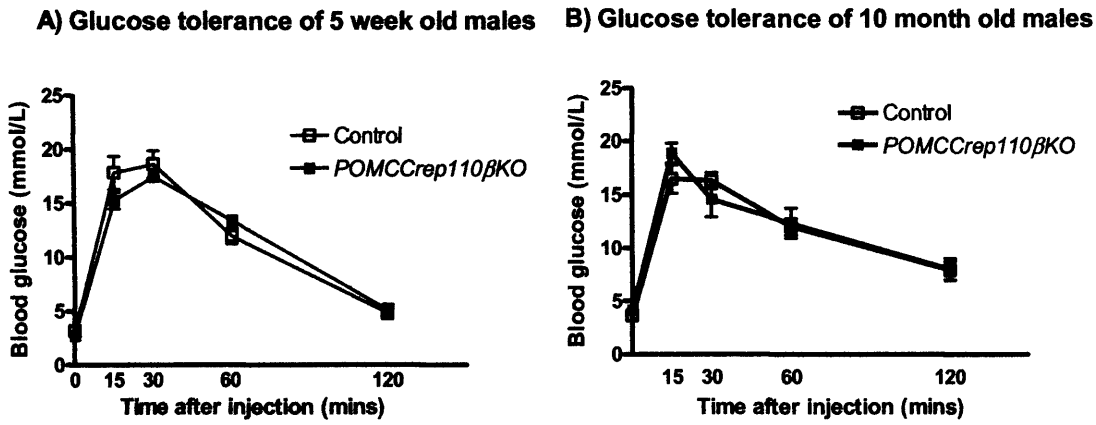

Figure 7.12: Glucose tolerance tests performed on male *POMCCrep110βKO* and controls at: A) 5 weeks of age and B) 10 months of age. Data represent the mean ± SEM for 7-9 mice of each genotype.

7.3.3 Fasting plasma insulin levels

At 10 months of age male *POMCCrep110βKO* mice had normal fasting insulin levels, as compared to control animals (Figure 7.13).

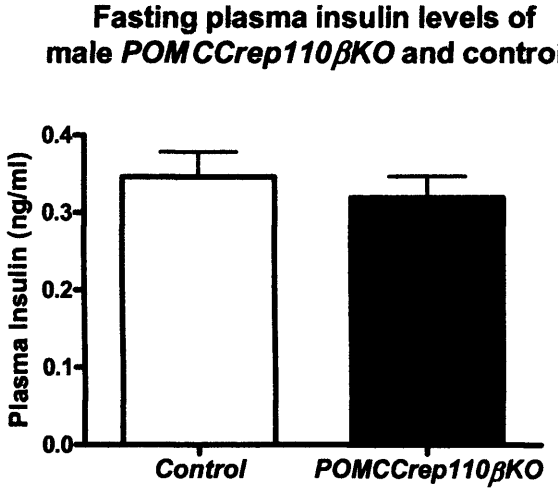

Figure 7.13: Fasting plasma insulin levels of 10-month-old male *POMCCrep110βKO* and control mice following a 16-h overnight fast. Data represent the mean ± SEM for 7-10 mice of each genotype.

7.4 Summary of hypothalamic function and glucose homeostasis of *POMCCrep110βKO* animals

Both male and female *POMCCrep110βKO* animals exhibited normal body weight compared to controls. Male *POMCCrep110βKO* animals were however shown to have significant increases in fat mass compared to controls, although fasting plasma leptin levels were normal. Consistently, *POMCCrep110βKO* animals were still sensitive to the anorexigenic effects of peripheral leptin treatment. Analysis of the feeding behaviour of male *POMCCrep110βKO* animals revealed that they were significantly hyperphagic and exhibited increased cumulative 24-h food intake following an overnight fast, compared to controls. The metabolic rate of male *POMCCrep110βKO* animals was indistinguishable from that of controls. Measurement of the body length of *POMCCrep110βKO* animals revealed that they were significantly longer than controls indicating impairments in melanocortin signalling. However, *POMCCrep110βKO* animals exhibited normal sensitivity to the anorexigenic effects of peripheral MTII treatment.

With regards to glucose homeostasis, *POMCCrep110βKO* animals exhibited normal FBG levels, glucose tolerance and fasting insulin levels compared to control animals.

Chapter 8
Discussion

8 Discussion

Obesity is defined medically as a state of increased body weight, more specifically adipose tissue, of sufficient magnitude to produce adverse health consequences (Kopelman, 2000). Obesity is especially linked with the development of insulin resistance and T2DM, although the mechanisms that underlie the association of these metabolic disorders are still unknown. Despite this, recent evidence has suggested a key role for the brain in the control of both body weight and glucose metabolism.

It is now a widely accepted view that the brain processes information from adiposity signals, and integrates this input with signals from nutrients and other molecules. In response, energy intake and energy expenditure are adjusted accordingly in ways that promote homeostasis of energy stores and fuel metabolism. Currently, only insulin and leptin meet all the criteria required of a putative adiposity signal. At the commencment of this work, these hormones were predicted to regulate energy homeostasis via their actions in the hypothalamus. This model is outlined below.

Insulin and leptin are proposed to enter the ARC region of the hypothalamus, where they bind to their corresponding receptors present on the first-order NPY/AgRP and POMC/CART neurons. NPY/AgRP neurons are proposed to be inhibited by leptin and insulin whereas POMC/CART neurons are stimulated by these hormones (Schwartz et al., 2000). These neurons then integrate information concerning the energy balance of the individual and relay this to second-order neurons located in other hypothalamic regions. This therefore results in the transduction of the insulin/leptin adiposity signal into a response, affecting the overall energy homeostasis status of the individual.

Prior to the commencement of this work, several lines of evidence had suggested a key role for CNS insulin action in the regulation of energy homeostasis. Administration of insulin directly to the brain has been shown to result in an anorexigenic effect, resulting in a reductions in body weight (Woods et al., 1979). In contrast, the selective decrease of hypothalamic insulin receptors by the administration of anti-sense oligodeoxynucleotide directed against the IR (Obici et al., 2002b) results in rapid-onset hyperphagia and

increased fat mass. The use of transgenic animal models has also implicated a role for intact CNS insulin signalling in the central regulation of energy homeostasis and peripheral glucose metabolism. *NIRKO* mice (with neuron specific deletion of the insulin receptor) are obese, hyperphagic and display mildly impaired glucose homeostasis (Bruning et al., 2000). Females with global deletion of *Irs2* (a major downstream effector of insulin receptor) also display a phenotype of hypothalamic dysfunction with the development of hyperphagia, obesity and infertility (Burks et al., 2000c). Male *Irs2* null animals develop insulin resistance, β-cell failure and a subsequent diabetic phenotype (Withers et al., 1998). Taken together, these studies implicate CNS insulin receptor signalling in the regulation of both energy homeostasis and peripheral glucose metabolism, and indicate that IRs in discrete areas of the hypothalamus have a physiological role in these actions.

Various studies have implicated a role for PI3K pathway in the regulation of hypothalamic energy homeostasis (Morrison et al., 2005; Niswender et al., 2003; Niswender et al., 2001; Spanswick et al., 2000). Classically viewed as a downstream effector of the insulin signalling pathway, increasing evidence suggests a role for this lipid kinase in mediating the anorexigenic effects of both insulin and leptin in the hypothalamic regulation of energy homeostasis. In addition, insulin and leptin have been shown to activate PI3K specifically in distinct hypothalamic neurons implicated in energy homeostasis regulation, namely POMC and AgRP neurons, suggesting a potential mechanism for the integration of these signals in discrete neuronal populations (Xu et al., 2005b).

The most intensively studied of the PI3Ks are those that belong to the class IA. The main role of this subgroup seems to be the direction of energy into cell growth and proliferation. PI3K is a heterodimer that consists of a p85 regulatory subunit and a p110 catalytic subunit. Three catalytic subunit isoforms exist (p110α, p110β and p110δ), with p110α and p110β broadly expressed (Engelman et al., 2006). The relative contributions of these isoforms to normal mammalian physiology remain unknown.

However, recent evidence indicates a critical role for p110α in growth factor and metabolic signalling (Foukas et al., 2006). Mice that were heterozygous for a knock-in mutation, that abrogated p110α kinase activity (but without altering the stoichiometry of other subunits), displayed severely blunted signalling via IRS proteins. These animals were hyperinsulinaemic, glucose intolerant, hyperphagic, and also displayed increased adiposity and reduced somatic growth. The authors also demonstrated a minimal contribution from p110β towards IRS associated lipid kinase activity.

Prior to the commencement of these studies, the exact identities of the neuronal populations mediating the effects of insulin on food intake and body weight regulation were still unknown (although POMC/CART and NPY/AgRP neurons were implicated). In addition, although the severe impaired glucose homeostasis of *Irs2* null animals was presumed to be a result of *Irs2* deletion in the β-cell, the relevant contribution of the CNS deletion of *Irs2* was unknown. Similarly, the extent (if any) of the CNS deletion of *Irs2* to the infertile phenotype of *Irs2* null females was also unclear. Finally, the resistance of *Irs2* null animals to the anorexigenic effects of leptin had also implicated IRS2 as a point of convergence between the insulin and leptin signalling pathways in the CNS.

The aim of the work described in this thesis, was to investigate the role of IRS2 mediated signalling pathways in the hypothalamic regulation of energy homeostasis, glucose homeostasis and reproductive function. The generation and phenotypic characterisation of transgenic mice with *Irs2* deletion in all neurons (*NesCreIrs2KO*), mice with *Irs2* deletion in POMC neurons (*POMCCreIrs2KO*) and mice with *Irs2* deletion in AgRP neurons (*AgRPCreIrs2KO*) allowed these points to be addressed in a tissue-specific and cell-specific manner.

8.1 Implications of the phenotypic characterisation of *NesCreIrs2KO* animals

8.1.1 Key role for CNS IRS2 pathways in the regulation of energy homeostasis

From approximately 8 weeks of age onwards, *NesCreIrs2KO* mice develop increased body weight and increased fat tissue mass. Consistently, these animals are hyperleptinaemic yet remain sensitive to the anorexigenic effects of peripheral leptin treatment. In addition, *NesCreIrs2KO* animals are significantly hyperphagic, indicating that the obesity of these animals is due to their increased caloric intake (no defects in resting metabolic rate were detected). Interestingly, *NesCreIrs2KO* animals are also significantly longer than controls, implicating disruption in CNS melanocortin signalling pathways. Consistently, *NesCreIrs2KO* animals demonstrated a significant reduction in *Pomc* mRNA levels compared to controls, although no changes in *Npy* or *Agrp* expression levels were detected.

The significant hypothalamic dysfunction of *NesCreIrs2KO* animals strongly supports growing evidence implicating a role for insulin signalling in the regulation of food intake and body weight. These studies also highlight the non-overlapping roles of the insulin receptor substrate proteins (IRS). No changes in hypothalamic *Irs1* mRNA expression in *NesCreIrs2KO* animals were detected, demonstrating that IRS1 is unable to compensate for IRS2 deficiency in the whole brain. Thus, IRS2 appears to be the major isoform involved in mediating the anorexigenic effects of insulin signalling in the brain.

8.1.2 CNS IRS2 pathways are not mandatory for leptin action

IRS2 has been implicated as a convergence point for both insulin and leptin action. *Irs2* null mice have defective leptin-stimulated hypothalamic STAT3 phosphorylation, suggesting potential convergence between leptin and insulin signalling in the hypothalamus (Burks et al., 2000b). However, the finding that *NesCreIrs2KO* animals remain sensitive to peripherally administered leptin suggests that the elevated leptin levels displayed by these animals results from their greater adiposity rather than primary

central leptin resistance. This is consistent with the observation that central leptin administration to *Irs2* null mice causes reduction in fat mass (Suzuki et al., 2004).. This is also consistent with the phenotype of *RipCreIrs2KO* animals, which lack *Irs2* in an uncharacterised population of ARC neurons (Choudhury et al., 2005). Although hyperleptinameic at 12 weeks of age, measurement of fasting leptin levels of these animals at 4 weeks of age (before the onset of obesity) indicates that the hyperleptinaemia is not due to intrinsic leptin resistance. In support of this, *RipCreIrs2KO* animals remained sensitive to the anorexigenic effects of peripheral leptin treatment (Choudhury et al., 2005). Taken together, these studies indicate that CNS IRS2 pathways are not mandatory for leptin action.

8.1.3 Possible role for CNS IRS2 pathways in the regulation of peripheral glucose homeostasis

A role for IRS2 mediated insulin signalling in the regulation of peripheral glucose homeostasis is also suggested by studies on *NesCreIrs2KO* animals. *NesCreIrs2KO* mice display hyperglycaemia, hyperinsulinaemia and impaired glucose tolerance. These findings are consistent with those of previous studies, which have also indicated a role for CNS insulin signalling in the regulation of peripheral glucose metabolism (Bruning et al., 2000; Obici et al., 2002a).

However, these results should be interpreted with caution as the relationship between obesity and impaired glucose homeostasis is complex. It thus remains unclear whether the impaired glucose tolerance of *NesCreIrs2KO* animals is a primary cause due to neuronal IRS2 deletion, or a secondary effect of the increased adiposity of these animals. The use of euglycaemic clamp studies would be required to assess the true contribution of CNS IRS2 pathways to the regulation of peripheral glucose homeostasis. However, hyperinsulinaemic-hypoglycaemic clamp studies performed on *NIRKO* animals do suggest that intact insulin signalling in the CNS is critical for the normal sympathoadrenal response to hypoglycaemia (Fisher et al., 2005). Thus, it is likely that altered neural insulin signalling could contribute to defective glucose counter-regulation in diabetes, and this is potentially true in the case of *NesCreIrs2KO* animals.

The use of *NesCreIrs2KO* mice has thus allowed disentanglement of the phenotypes displayed by the global *Irs2* null mouse with regards to glucose homeostasis (Burks et al., 2000a; Withers et al., 1998). Although *NesCreIrs2KO* animals display hyperglycaemia and impaired glucose tolerance, these phenotypes are relatively mild compared to the overt diabetes displayed by *Irs2* null animals (Burks et al., 2000a; Withers et al., 1998). The preservation of β-cell mass in *NesCreIrs2KO* mice also dissociates hypothalamic dysfunction from reduced β-cell mass, and indicates that the deletion of *Irs2* in the pancreatic β-cell is a major contributory factor to the impaired glucose homeostasis of *Irs2* null animals.

8.1.4 CNS IRS2 pathways are not required for normal reproductive function

Minimal reproductive abnormalities were detected in female *NesCreIrs2KO* animals. Female *NesCreIrs2KO* mice display an extended oestrous cycle, due to a mildly prolonged dioestrous phase. However, *NesCreIrs2KO* animals respond normally to superovulation, and display normal ovarian morphology. The dioestrous levels of oestradiol, progesterone, luteinising hormone, and follicle-stimulating hormone are also normal in *NesCreIrs2KO* animals. However, the level of prolactin in *NesCreIrs2KO* animals is significantly reduced compared to controls. Finally, the analysis of breeding performance of *NesCreIrs2KO* animals by timed mating studies revealed no abnormalities.

The use of *NesCreIrs2KO* mice has thus allowed disentanglement of the phenotypes displayed by female *Irs2* null mice with regards to reproductive function (Burks et al., 2000a; Withers et al., 1998). The use of *NesCreIrs2KO* indicates that the deletion of *Irs2* in the ovary and pituitary is the major contributory factor to the infertility of *Irs2* null females.

8.1.5 Evidence for a more important role for IRS2 mediated signalling pathways than IR pathways in the CNS regulation of energy and glucose homeostasis

Similarly to *NIRKO* animals, impaired energy homeostasis is a phenotype of *NesCreIrs2KO* mice, although the severity of this dysfunction is actually greater in these *NesCreIrs2KO* animals. The body weights of male *NIRKO* mice were indistinguishable from those of control littermates during the first 6 months of life, and no differences in the food intake of male *NIRKO* animals were detectable. However, female *NIRKO* animals displayed increased body weight and hyperphagia from approximately 16 weeks of age (Bruning et al., 2000). In contrast, *NesCreIrs2KO* animals demonstrate no sexual dimorphism, with both male and females exhibiting increased body weight and hyperphagia from approximately 8 weeks of ages onwards.

Similarly to *NIRKO* animals, *NesCreIrs2KO* animals exhibit impaired glucose homeostasis. However, again, the phenotype of *NesCreIrs2KO* animals appears to be more severe. Between the ages of 4 and 6 months of age, *NIRKO* mice showed normal FBG levels, but were significantly hyperinsulinaemic. However, even as young as 12 weeks of age, male and female *NesCreIrs2KO* demonstrate fasting hyperglycaemia, impaired glucose tolerance and hyperinsulinaemia. With regards to reproductive function, both female and male *NIRKO* animals demonstrated impaired fertility (Bruning et al., 2000). However, as previously mentioned, no defects in the reproductive function of *NesCreIrs2KO* females were found.

Taken together, these results indicate a more important role for IR-mediated pathways than IRS2-mediated pathways in the CNS regulation of reproductive function. However, these studies highlight a more important role for IRS2-mediated signalling pathways compared to insulin receptor pathways with regards to the CNS regulation of energy and glucose homeostasis. There are a number of potential explanations for this.

Firstly, the IGF-1 receptor can also bind insulin, although this is at approximately 70 % less affinity than IGF-1 (Smith et al., 1988). Thus, deletion of the IR in the brain of *NIRKO* mice is unlikely to be ablating insulin signalling completely, with signalling via the IGF-1 receptor potentially able to mildly compensate.

Secondly, in addition to its role in the insulin signalling cascade, IRS2 is also a downstream component of other signalling pathways such as those of BDNF, IGF-1, growth hormone and interleukin-2, -4, and –7 (Yamada et al., 1997). A role for the neurotrophin BDNF in particular, has been implicated in the hypothalamic regulation of energy homeostasis by a number of studies (Fox and Byerly, 2004; Kernie et al., 2000; Lyons et al., 1999; Xu et al., 2003). Thus, the more severe phenotype of *NesCreIrs2KO* animals compared to *NIRKO* animals can be potentially explained by the fact that deletion of *Irs2* in the CNS affects more than just the insulin signalling cascade. In contrast, deletion of IR signalling pathways in the CNS would directly affect only insulin signalling in this tissue.

With regards to the subfertility of both male and female *NIRKO* animals, the findings that female *NesCreIrs2KO* exhibit normal reproductive function suggests the importance of alternative downstream components of the IR signalling cascade. Indeed, it is possible that in the CNS of *NesCreIrs2KO* animals, IRS1 has the ability to compensate with regards to signalling pathways involved in the regulation of reproductive function.

Although the phenotype of the *NesCreIrs2KO* animal suggests a more important role for CNS IRS2 pathways than CNS IR pathways in terms of energy and glucose homeostasis, these implications should be interpreted with some caution. The genetic background of transgenic mouse lines, as well as the methods used in the creation of various mutants, has been shown to contribute considerably to the phenotypic outcome (Barthold, 2004).

8.2 Implications of the phenotypic characterisation of *POMCCreIrs2KO* and *AgRPCreIrs2KO* animals

No defects in hypothalamic function could be detected in *POMCCreIrs2KO* or *AgRPCreIrs2KO* animals. These animals exhibit no defects in body weight, body composition, body length, food intake and leptin levels compared to controls. Similarly, no defects in glucose homeostasis could be detected in *POMCCreIrs2KO* or *AgRPCreIrs2KO* animals. These animals exhibit no defects in FBG levels, glucose tolerance or insulin levels compared to control littermates.

Although the lack of phenotypic abnormality in either mouse line was unexpected, when interpreted in context with the robust phenotype of *NesCreIrs2KO* animals, these studies have considerable implications.

8.2.1 Non-essential role for IRS2 signalling in hypothalamic POMC and AgRP neurons

Hypothalamic POMC and AgRP neurons have long been implicated as having key roles in the regulation of energy homeostasis (Cowley et al., 2001). These neurons contain leptin and insulin receptors on their membrane and it is via these receptors, that insulin and leptin are proposed to exert their anorexigenic effects. However, *POMCCreIrs2KO* and *AgRPCreIrs2KO* mice did not exhibit impairments in either energy homeostasis or glucose metabolism. This indicates that POMC and AgRP neurons are not important for the effect of IRS2 mediated insulin signalling on energy homeostasis. Consistent with these findings, mice with deletion of the IR in POMC neurons *(POMCCreIRKO)* and with deletion of the IR in AgRP neurons (*AgRPCreIRKO*) also display no phenotypic abnormalities (J.C. Bruning, personal communication). These unpublished studies also question the potential contribution of insulin signalling in these neuronal populations.

Interestingly, deletion of the *LepR* in POMC neurons resulted in mice that were mildly obese, hyperleptinaemic and had altered expression of hypothalamic neuropeptides (Balthasar et al., 2004). Consistently, female *POMCCreSTAT3KO* mice (with *Stat3* deletion specifically within POMC neurons), exhibit a 2-fold increase in fat pad mass but only a slight increase in total body weight (Xu et al., 2007). Thus, it would appear that POMC neurons are important for mediating the anorexigenic effects of leptin but not insulin.

These findings correspond with our observations of the electrophysiological properties of POMC neurons, performed in animals with florescent POMC neurons (generated from crossing POMCCre and GFP animals). Leptin has been demonstrated to depolarise POMC neurons (Cowley et al., 2001). In contrast, although previously postulated to function in a similar way to leptin, insulin results in the hyperpolarisation and reduced action potential frequency in POMC neurons (Choudhury et al., 2005). These opposite

effects on POMC cell excitability perhaps explain the lack of phenotype in *POMCCreIrs2KO* mice. We are currently in the process of investigating the electrophysiological properties of AgRP neurons in collaboration with the laboratory of Professor Ashord, Dundee University.

It should be noted that the lack of phenotypic abnormalities in both *POMCCreIrs2KO* and *AgRPCreIrs2KO* can potentially be attributed to the fact that genetic manipulations within these neuronal populations are simply intervening in one limb of a multi-neuronal highly integrated circuit. Thus, physiological compensation or over-compensation of other limbs in these systems may occur (Morton et al., 2006). It is important to take into account the fact that POMC and AgRP neurons, besides being targets for insulin action, are also targets for other multiple signals regarding energy homeostasis. Thus, although deletion of *Irs2* in these populations may create a relative state of 'insulin resistance' in these neurons, due to the presence of other intact signalling pathways (e.g. leptin) still in place in these neurons, normal regulation of energy homeostasis may still proceed.

8.2.2 Potential role for other IRS proteins in the regulation of energy homeostasis in POMC and AgRP populations

A role for IRS1 mediated insulin signalling in the anorexigenic effects of insulin in POMC and AgRP neurons cannot be excluded. However, findings that no changes in hypothalamic *Irs1* mRNA expression in *NesCreIrs2KO* animals are observed, suggests that IRS2 is the major isoform involved in mediating the anorexigenic effects of insulin signalling in the brain. It is still possible however, that compensation by IRS1 may still be ocurring without detectable changes in gene expression levels.

Recent data also suggests a role for IRS4 in the regulation of central and peripheral energy homeostasis, when the IRS2 branch of the insulin signalling cascade is ablated (Dong et al, Abstract ADA 2006). Thus, a potential role for IRS4 in mediating the effects of insulin in POMC and AgRP neurons cannot be dismissed.

8.2.3 Role for IRS2 signalling in neurons distinct from POMC and AgRP populations

These present studies also implicate IRS2 signalling in neurons distinct from POMC and AgRP populations in the regulation of energy homeostasis. This is because in contrast to the lack of phenotypic abnormalities observed in *POMCCreIrs2KO* and *AgRPCreIrs2KO* animals, the deletion of *Irs2* in all neurons (*NesCreIrs2KO* mice) results in marked hypothalamic dysfunction and impaired glucose homeostasis.

Indeed, a recent study has identified a previously uncharacterised ARC population of neurons involved in IRS2 mediated insulin regulation of energy homeostasis (Choudhury et al., 2005). *RipCreIrs2KO* animals lack *Irs2* in the β-cell and also an uncharacterised population of ARC neurons. These animals exhibit many of the characteristics of *NesCreIrs2KO* animals; they are obese, hyperphagic and leptin sensitive despite hyperleptinaemia. Similarly to *NesCreIrs2KO* animals, the increased body length displayed by *RipCreIrs2KO* mice suggests altered melanocortin action. In addition, *RipCreIrs2KO* display impaired glucose tolerance and reduced β-cell mass mice due to *Irs2* deletion in the β-cell. These Rip neurons (which express the Rat insulin II promoter) have been shown to be neither POMC nor AgRP neurons (Choudhury et al., 2005) but may exist as a third population of first-order arcuate neurons in the regulation of energy balance.

In addition, the potential role of "non-ARC" neuronal populations in mediating the effects of adiposity signals, and other signals involved in the regulation of energy homeostasis, has been largely ignored. Recent work has shown that POMC neurons receive strong excitatory input from the VMH, highlighting an important role for VMH populations in energy balance (Sternson et al., 2005). Leptin has also been shown to depolarise and increase the firing rate of steroidogenic factor-1 (SF-1) positive neurons in this nucleus (Dhillon et al., 2006). *Sf-1CreLepRKO* mice, which lack the *LepR* in SF-1 neurons, develop obesity and hyperphagia. When placed on a HFD, these animals are particularly sensitive to DIO, displaying hyperphagia and marked impairments in the activation of diet-induced thermogenesis. Taken together, these results demonstrate that leptin action on neurons of the VMH plays an important role in controlling body weight and food intake.

Interestingly, the degree of obesity observed in *Sf-1CreLepRKO* mice is similar to that seen in *POMCCreLepRKO* mice, suggesting that these two groups of neurons play a quantitatively similar role in regulating body weight. Further, mice lacking LepRs in both SF-1 and POMC neurons have a body weight phenotype that is approximately the sum of that observed with loss of LepRs in either neuronal group alone, but less obese than *db/db* mice. This indicates that sites, other than these, are also important for leptin action in body weight regulation. Thus, SF1 neurons may also potentially mediate the anorexigenic effects of insulin, and studies involving the deletion of components of this pathway will be key in determining their contribution.

Consistently, a recent study has demonstrated hypothalamic *Irs2* expression exists mainly in the ARC, VMH and PVN, indicating a potential role for this isoform in ARC and 'non-ARC' neuronal populations (Pardini et al., 2006). The same study also implicates extra-hypothalamic regions as possible sites for insulin action in the regulation of energy homeostasis. In the hindbrain, *Irs2* expression is detectable in the area postrema (AP), medial nucleus of the solitary tract (NTS), motor nucleus of the vagus nerve (DMV) and the hypoglossal nucleus (HN). Interestingly, expression is also found in the ventral tegmental area (VTA), an important area for reward perception, and is detectable in dopamine neurons in this brain area. The IRS2-AKT pathway in dopamine neurons of the VTA has been shown to be key to the regulation of behavioural and cellular responses to opiates (Russo et al., 2007) .

8.3 Implications of phenotypic characterisation of *AgRPCrep110βKO* and *POMCCrep110βKO* animals

Despite the recent findings for a potentially dominant role for p110α in mediating the actions of PI3K on metabolism (Foukas et al., 2006), the relative contributions of other catalytic isoforms in the hypothalamic regulation of energy homeostasis remain unaddressed. As discussed previously, convergence between insulin and leptin signalling in the CNS, and more specifically in the hypothalamus, has been implicated in the regulation of food intake and body weight at the level of PI3K.

To fully address the role of PI3K in the hypothalamic regulation of energy balance and peripheral glucose homeostasis, mice with *p110β* deletion in AgRP neurons (*AgRPCrep110βKO)* and mice with *p110β* deletion in POMC neurons (*POMCCrep110βKO)* were generated. It should be noted that at the time of submission of this thesis, studies were at an early stage. Due to this, insights into the role of p110β pathways in the regulation of energy balance are incomplete. However, as a result of the interesting preliminary findings of these investigations, they have been included in this work.

8.3.1 Key role for hypothalamic p110β pathways in the regulation of energy homeostasis

AgRPCrep110βKO and *POMCCrep110βKO* animals exhibit opposing phenotypes of hypothalamic dysfunction, consistent with the neuropeptide phenotype of the neuronal populations involved.

Examination of the hypothalamic function of *AgRPCrep110βKO* animals, revealed that these animals have significantly reduced body weight and adiposity compared to controls. Consistently, *AgRPCrep110βKO* animals are also significantly hypoleptinaemic and hypophagic compared to controls. Interestingly, both male and female *AgRPCrep110βKO* animals exhibit resistance to diet induced obesity (DIO), with the reduced daily food intake of these animals on this diet found to be the main contributory factor. Conversely, examination of the hypothalamic function of *POMCCrep110βKO* animals revealed that these animals exhibit increased adiposity and are hyperphagic compared to controls. However, both *AgRPCrep110βKO* and *POMCCrep110βKO* animals remain sensitive to the anorexigenic effects of peripherally administered leptin and MTII. Interestingly, *AgRPCrep110βKO* animals are more sensitive than controls to the anorexigenic effects of leptin on body weight.

With regards to glucose homeostasis, no abnormalities in FBG levels or glucose tolerance could be detected in *AgRPCrep110βKO* and *POMCCrep110βKO* animals. However, at 10 months of age, male *AgRPCrep110βKO* animals are significantly hypoinsulinaemic compared to controls, consistent with their reduced body weight. At

the same age, *POMCCrep110βKO* animals have indistinguishable basal insulin levels compared to controls.

Our findings are consistent with those of Xu and colleagues, who showed that in the case of POMC neurons, both insulin and leptin resulted in activation of PI3K in this neuronal population (Xu et al., 2005b). With regards to the phenotype of *POMCCrep110βKO* animals, one can postulate that removal of the p110β isoform in POMC neurons results in reduced PI3K signalling. This could thus be mimicking a state of low insulin and leptin levels in this population, resulting in increased activation of downstream anabolic pathways. With regards to AgRP neurons, Xu and colleagues found that insulin and leptin had opposite effects, with PI3K activity inhibited by leptin but stimulated by insulin (Xu et al., 2005b). Our phenotypic characterisation of the *AgRPCrep110βKO* animal also supports this finding. Again, one can postulate that removal of the p110β isoform in AgRP neurons results in reduced PI3K signalling, thus mimicking a state of high leptin levels in this population, resulting in increased activation of downstream catabolic effector pathways.

Taken together, these preliminary studies implicate an important role for the p110β isoform of PI3K in the regulation of hypothalamic energy homeostasis, and specifically within AgRP and POMC neuronal populations of the ARC.

8.3.2 Potential role for p110β as a mediator of other non-insulin signalling pathways involved in the regulation of energy homeostasis in AgRP and POMC neurons

Phosphorylation of the tyrosine residues of IRS proteins results in the recruitment of p85, which in turn results in recruitment of the p110 catalytic subunit. In contrast to the lack of phenotype observed in *AgRPCreIrs2KO* and *POMCCreIrs2KO* animals, both *AgRPCrep110βKO* and *POMCCrep110βKO* animals exhibit significant defects in hypothalamic function. This suggests the existence of alternative pathways (i.e. non-insulin/IRS), which signal via p110β to influence the regulation of energy balance in AgRP and POMC neurons. In addition to its role in insulin signalling, PI3K plays a pivotal role as a signalling mediator in a wide variety of cellular responses to other

hormones, neurotransmitters, growth factors and cytokines (Vanhaesebroeck and Waterfield, 1999). Stimulation of almost every receptor that induces Tyr kinase activity also leads to class IA PI3K activation (Vanhaesebroeck and Waterfield, 1999).

8.3.3 Non-essential role for p110β-mediated signalling in hypothalamic leptin action in AgRP and POMC neurons

A number of studies support a role for hypothalamic PI3K action in mediating the effects of leptin on energy homeostasis. For example, the use of PI3K inhibitors has recently demonstrated that the inhibition of hypothalamic expression of NPY and AgRP by leptin involves a mechanism requiring intact PI3K signalling (Morrison et al., 2005). However, both *AgRPCrep110βKO* and *POMCCrep110βKO* animals remain leptin sensitive, indicating that the anorexigenic effects of leptin action in the hypothalamus are mediated by other PI3K isoforms in these neuronal populations. An alternative explanation is that the deletion of *p110β* at the embryonic stage in AgRP and POMC neurons, may be resulting in the activation of alternative compensatory mechanisms in these cells, aimed at maintaining the functional reponse to leptin.

The administration of ICV leptin to *AgRPCrep110βKO* and *POMCCrep110βKO* animals, and subsequent assessment of food intake and body weight changes should allow leptin action in these neuronal populations (lacking p110β) to be accurately assessed.

8.3.4 Non-essential role for p110β-mediated insulin signalling in AgRP and POMC neurons in peripheral glucose homeostasis

Despite recent studies supporting a role for PI3K function in mediating the actions of hypothalamic signalling on peripheral glucose homeostasis (Gelling et al., 2006; Morton et al., 2005), both *AgRPCrep110βKO* and *POMCCrep110βKO* animals exhibit no impairments in glucose homeostasis. This suggests a non-essential role for p110β-mediated insulin signalling in these neuronal populations with regards peripheral glucose homeostasis. Although *AgRPCrep110βKO* animals are hypoinsulinaemic compared to controls, this is consistent with their reduced body weight.

8.4 Conclusions

These studies have demonstrated that CNS IRS2 pathways acting in neuronal populations distinct from POMC and AgRP neurons regulate energy homeostasis and growth. A role for CNS IRS2 mediated insulin signalling in the control of peripheral glucose metabolism is also implicated. Furthermore these studies have shown that CNS IRS2 pathways are not required for leptin action or reproductive function.

Although these studies demonstrate an important role for IRS2 in the CNS regulation of food intake and body weight in mice, the relevance of this to human obesity remains unclear. It is currently not known whether low IRS2 levels in the human brain are involved in the pathogenesis of obesity and diabetes. However, there has been an encouraging proof of concept study with respect to the role of IRS2 in the pancreatic β-cell. It has now been shown that in patients with T2DM, there is a marked reduction in IRS2 expression in pancreatic islets (Gunton et al., 2005). This suggests that reduced IRS2 signalling in islets is involved in the pathogenesis of β-cell disease. Taken into context with the findings presented in this thesis, reduced IRS2 signalling in the CNS may also be a potential mechanism in the development of human obesity.

The investigations presented in this work also highlight a key role for hypothalamic p110β-mediated signalling pathways in the regulation of energy homeostasis. Although at a preliminary stage, these studies clearly demonstrate that p110β is an important mediator of signals that regulate energy balance in AgRP and POMC neuronal populations.

At the time of commencement of this work, the dominant view in the field was that the CNS mechanisms regulating energy homeostasis involved a key role for hypothalamic insulin action in distinct cell types. The studies discussed in this thesis have shown this not to be the case, and it is now evident that numerous signals acting in multiple brain regions are integrated to ensure the homeostatic preservation of energy stores. Overall these studies have provided new insights into the role of insulin signalling mechanisms in the hypothalamic regulation of energy homeostasis.

Future work

Studies involving *NesCreIrs2KO* animals

Although the impaired glucose homeostasis of *NesCreIrs2KO* animals suggests an important role for IRS2-mediated insulin signalling pathways in the regulation of peripheral glucose homeostasis, the relationship between obesity and impaired glucose homeostasis is complex. Thus, the use of hyperinsulinaemic-hypoglycaemic clamp studies will be required to assess the true contribution of CNS IRS2 pathways to the regulation of peripheral glucose homeostasis.

Studies involving *POMCCrep110βKO* and *AgRPCrep110βKO* animals

As mentioned above, these investigations are at an early stage and a number of additional studies are required to fully complete the phenotypic characterisation of *POMCCrep110βKO* and *AgRPCrep110βKO* animals. These are outlined below:

1. In order to prove deletion of this isoform specifically within POMC and AgRP neurons (of *POMCCrep110βKO* and *AgRPCrep110βKO* animals respectively), *in situ* hybridisation techniques will be established aimed at doing so.

2. The detailed analysis of the body composition of *POMCCrep110βKO* and *AgRPCrep110βKO* animals will be perfomed with the aid of MRI scanning. This work will be carried out in collaboration with Professor Jimmy Bell, Imperial College London.

3. The expression levels of various hypothalamic neuropeptides involved in the regulation of energy homeostasis will be determined. Leptin has recently shown to inhibit the hypothalamic expression of NPY and AgRP in a mechanism that requires intact PI3K signalling (Morrison et al., 2005). Thus, ablation of intact p110β signalling in these distinct neuronal populations may result in downstream changes in various neuropeptide systems.

4. A role for PI3K mediated mechanisms in the neuronal firing of hypothalamic neurons has been implicated in various studies. Thus, to address the role of the inhibition of functional p110β to the elctrophysiological characteristics of the POMC and AgRP neurons (within *POMCCrep110βKO* and *AgRPCrep110βKO* animals respectively) mice expressing fluorescent markers in these neuronal populations lacking *p110β* will be generated and studied. This work will be carried out in collaboration with the laboratory of Professor. Ashford, University of Dundee.

5. Similarly to studies involving *AgRPCrep110βKO* animals, male and female *POMCCrep110βKO* animals will be challenged with HFD from the age of 6 week onwards for a total duration of 26 weeks to assess their sensitivity to DIO.

6. The food intake of *POMCCrep110βKO* and *AgRPCrep110βKO* animals at younger ages will also be assessed. The food intake studies described in this thesis were carried out on male mice at approximately 4 months of age. In the case of *AgRPCrep110βKO* animals, which exhibit reduced body weight from the age of 10 weeks of age onwards, it is unclear if the hyophagia of these animals is the causative factor for their reduced body weight or a consequence of it.

References

Accili, D., and Arden, K. C. (2004). FoxOs at the crossroads of cellular metabolism, differentiation, and transformation. Cell *117*, 421-426.

Adashi, E. Y., Resnick, C. E., Payne, D. W., Rosenfeld, R. G., Matsumoto, T., Hunter, M. K., Gargosky, S. E., Zhou, J., and Bondy, C. A. (1997). The mouse intraovarian insulin-like growth factor I system: departures from the rat paradigm. Endocrinology *138*, 3881-3890.

Adrian, T. E., Savage, A. P., Sagor, G. R., Allen, J. M., Bacarese-Hamilton, A. J., Tatemoto, K., Polak, J. M., and Bloom, S. R. (1985). Effect of peptide YY on gastric, pancreatic, and biliary function in humans. Gastroenterology *89*, 494-499.

Ahren, B., Larsson, H., Wilhelmsson, C., Nasman, B., and Olsson, T. (1997). Regulation of circulating leptin in humans. Endocrine *7*, 1-8.

Air, E. L., Strowski, M. Z., Benoit, S. C., Conarello, S. L., Salituro, G. M., Guan, X. M., Liu, K., Woods, S. C., and Zhang, B. B. (2002). Small molecule insulin mimetics reduce food intake and body weight and prevent development of obesity. Nat Med *8*, 179-183.

Akabayashi, A., Wahlestedt, C., Alexander, J. T., and Leibowitz, S. F. (1994). Specific inhibition of endogenous neuropeptide Y synthesis in arcuate nucleus by antisense oligonucleotides suppresses feeding behavior and insulin secretion. Brain Res Mol Brain Res *21*, 55-61.

Araki, E., Lipes, M. A., Patti, M. E., Bruning, J. C., Haag, B., 3rd, Johnson, R. S., and Kahn, C. R. (1994). Alternative pathway of insulin signalling in mice with targeted disruption of the IRS-1 gene. Nature *372*, 186-190.

Araki, E., Shimada, F., Uzawa, H., Mori, M., and Ebina, Y. (1987). Characterization of the promoter region of the human insulin receptor gene. Evidence for promoter activity. J Biol Chem *262*, 16186-16191.

Arase, K., York, D. A., Shimizu, H., Shargill, N., and Bray, G. A. (1988). Effects of corticotropin-releasing factor on food intake and brown adipose tissue thermogenesis in rats. Am J Physiol *255*, E255-259.

Asakawa, A., Inui, A., Yuzuriha, H., Ueno, N., Katsuura, G., Fujimiya, M., Fujino, M. A., Niijima, A., Meguid, M. M., and Kasuga, M. (2003). Characterization of the effects of pancreatic polypeptide in the regulation of energy balance. Gastroenterology *124*, 1325-1336.

Audinot, V., Lahaye, C., Suply, T., Rovere-Jovene, C., Rodriguez, M., Nicolas, J. P., Beauverger, P., Cardinaud, B., Galizzi, J. P., Fauchere, J. L., *et al.* (2002). SVK14 cells express an MCH binding site different from the MCH1 or MCH2 receptor. Biochem Biophys Res Commun *295*, 841-848.

Bae, S. S., Cho, H., Mu, J., and Birnbaum, M. J. (2003). Isoform-specific regulation of insulin-dependent glucose uptake by Akt/protein kinase B. J Biol Chem *278*, 49530-49536.

Bagdade, J. D., Bierman, E. L., and Porte, D., Jr. (1967). The significance of basal insulin levels in the evaluation of the insulin response to glucose in diabetic and nondiabetic subjects. J Clin Invest *46*, 1549-1557.

Baggio, L. L., Huang, Q., Brown, T. J., and Drucker, D. J. (2004). Oxyntomodulin and glucagon-like peptide-1 differentially regulate murine food intake and energy expenditure. Gastroenterology *127*, 546-558.

Bagnol, D., Lu, X. Y., Kaelin, C. B., Day, H. E., Ollmann, M., Gantz, I., Akil, H., Barsh, G. S., and Watson, S. J. (1999). Anatomy of an endogenous antagonist: relationship between Agouti-related protein and proopiomelanocortin in brain. J Neurosci *19*, RC26.

Bai, F. L., Yamano, M., Shiotani, Y., Emson, P. C., Smith, A. D., Powell, J. F., and Tohyama, M. (1985). An arcuato-paraventricular and -dorsomedial hypothalamic neuropeptide Y-containing system which lacks noradrenaline in the rat. Brain Res *331*, 172-175.

Balthasar, N., Coppari, R., McMinn, J., Liu, S. M., Lee, C. E., Tang, V., Kenny, C. D., McGovern, R. A., Chua, S. C., Jr., Elmquist, J. K., and Lowell, B. B. (2004). Leptin receptor signaling in POMC neurons is required for normal body weight homeostasis. Neuron *42*, 983-991.

Balthasar, N., Dalgaard, L. T., Lee, C. E., Yu, J., Funahashi, H., Williams, T., Ferreira, M., Tang, V., McGovern, R. A., Kenny, C. D., *et al.* (2005). Divergence of melanocortin pathways in the control of food intake and energy expenditure. Cell *123*, 493-505.

Banks, A. S., Davis, S. M., Bates, S. H., and Myers, M. G., Jr. (2000). Activation of downstream signals by the long form of the leptin receptor. J Biol Chem *275*, 14563-14572.

Banks, W. A., Kastin, A. J., Huang, W., Jaspan, J. B., and Maness, L. M. (1996). Leptin enters the brain by a saturable system independent of insulin. Peptides *17*, 305-311.

Bannon, A. W., Seda, J., Carmouche, M., Francis, J. M., Jarosinski, M. A., and Douglass, J. (2001). Multiple behavioral effects of cocaine- and amphetamine-regulated transcript (CART) peptides in mice: CART 42-89 and CART 49-89 differ in potency and activity. J Pharmacol Exp Ther *299*, 1021-1026.

Bannon, A. W., Seda, J., Carmouche, M., Francis, J. M., Norman, M. H., Karbon, B., and McCaleb, M. L. (2000). Behavioral characterization of neuropeptide Y knockout mice. Brain Res *868*, 79-87.

Barsh, G. S., Ollmann, M. M., Wilson, B. D., Miller, K. A., and Gunn, T. M. (1999). Molecular pharmacology of Agouti protein in vitro and in vivo. Ann N Y Acad Sci *885*, 143-152.

Barsh, G. S., and Schwartz, M. W. (2002). Genetic approaches to studying energy balance: perception and integration. Nat Rev Genet *3*, 589-600.

Barthold, S. W. (2004). Genetically altered mice: phenotypes, no phenotypes, and Faux phenotypes. Genetica *122*, 75-88.

Baskin, D. G., Hahn, T. M., and Schwartz, M. W. (1999). Leptin sensitive neurons in the hypothalamus. Horm Metab Res *31*, 345-350.

Bates, S. H., Dundon, T. A., Seifert, M., Carlson, M., Maratos-Flier, E., and Myers, M. G., Jr. (2004). LRb-STAT3 signaling is required for the neuroendocrine regulation of energy expenditure by leptin. Diabetes *53*, 3067-3073.

Bates, S. H., Stearns, W. H., Dundon, T. A., Schubert, M., Tso, A. W., Wang, Y., Banks, A. S., Lavery, H. J., Haq, A. K., Maratos-Flier, E., *et al.* (2003). STAT3 signalling is required for leptin regulation of energy balance but not reproduction. Nature *421*, 856-859.

Batterham, R. L., Cowley, M. A., Small, C. J., Herzog, H., Cohen, M. A., Dakin, C. L., Wren, A. M., Brynes, A. E., Low, M. J., Ghatei, M. A., *et al.* (2002). Gut hormone PYY(3-36) physiologically inhibits food intake. Nature *418*, 650-654.

Baukrowitz, T., Schulte, U., Oliver, D., Herlitze, S., Krauter, T., Tucker, S. J., Ruppersberg, J. P., and Fakler, B. (1998). PIP2 and PIP as determinants for ATP inhibition of KATP channels. Science *282*, 1141-1144.

Belke, D. D., Betuing, S., Tuttle, M. J., Graveleau, C., Young, M. E., Pham, M., Zhang, D., Cooksey, R. C., McClain, D. A., Litwin, S. E., *et al.* (2002). Insulin signaling coordinately regulates cardiac size, metabolism, and contractile protein isoform expression. J Clin Invest *109*, 629-639.

Benoit, S. C., Air, E. L., Coolen, L. M., Strauss, R., Jackman, A., Clegg, D. J., Seeley, R. J., and Woods, S. C. (2002). The catabolic action of insulin in the brain is mediated by melanocortins. J Neurosci *22*, 9048-9052.

Berg, A. H., Combs, T. P., Du, X., Brownlee, M., and Scherer, P. E. (2001). The adipocyte-secreted protein Acrp30 enhances hepatic insulin action. Nat Med *7*, 947-953.

Bernard, C. (1855). Leçons de physiologie expérimentale appliquée à la médecine. Paris, Baillière, 1., Vol Vol. 1).

Bewick, G. A., Gardiner, J. V., Dhillo, W. S., Kent, A. S., White, N. E., Webster, Z., Ghatei, M. A., and Bloom, S. R. (2005). Post-embryonic ablation of AgRP neurons in mice leads to a lean, hypophagic phenotype. Faseb J *19*, 1680-1682.

Bi, L., Okabe, I., Bernard, D. J., and Nussbaum, R. L. (2002). Early embryonic lethality in mice deficient in the p110beta catalytic subunit of PI 3-kinase. Mamm Genome *13*, 169-172.

Bi, L., Okabe, I., Bernard, D. J., Wynshaw-Boris, A., and Nussbaum, R. L. (1999). Proliferative defect and embryonic lethality in mice homozygous for a deletion in the p110alpha subunit of phosphoinositide 3-kinase. J Biol Chem *274*, 10963-10968.

Billington, C. J., Briggs, J. E., Grace, M., and Levine, A. S. (1991). Effects of intracerebroventricular injection of neuropeptide Y on energy metabolism. Am J Physiol *260*, R321-327.

Bjornholm, M., He, A. R., Attersand, A., Lake, S., Liu, S. C., Lienhard, G. E., Taylor, S., Arner, P., and Zierath, J. R. (2002). Absence of functional insulin receptor substrate-3 (IRS-3) gene in humans. Diabetologia *45*, 1697-1702.

Bluher, M., Kahn, B. B., and Kahn, C. R. (2003). Extended longevity in mice lacking the insulin receptor in adipose tissue. Science *299*, 572-574.

Bluher, M., Michael, M. D., Peroni, O. D., Ueki, K., Carter, N., Kahn, B. B., and Kahn, C. R. (2002). Adipose tissue selective insulin receptor knockout protects against obesity and obesity-related glucose intolerance. Dev Cell *3*, 25-38.

Blundell, J. E. (1984). Serotonin and appetite. Neuropharmacology *23*, 1537-1551.

Borg, W. P., During, M. J., Sherwin, R. S., Borg, M. A., Brines, M. L., and Shulman, G. I. (1994). Ventromedial hypothalamic lesions in rats suppress counterregulatory responses to hypoglycemia. J Clin Invest *93*, 1677-1682.

Brachmann, S. M., Ueki, K., Engelman, J. A., Kahn, R. C., and Cantley, L. C. (2005). Phosphoinositide 3-kinase catalytic subunit deletion and regulatory subunit deletion have opposite effects on insulin sensitivity in mice. Mol Cell Biol *25*, 1596-1607.

Bray, G. A. (1997). Amino acids, protein, and body weight. Obes Res *5*, 373-376.

Broadwell, R. D., and Brightman, M. W. (1976). Entry of peroxidase into neurons of the central and peripheral nervous systems from extracerebral and cerebral blood. J Comp Neurol *166*, 257-283.

Broberger, C., De Lecea, L., Sutcliffe, J. G., and Hokfelt, T. (1998a). Hypocretin/orexin- and melanin-concentrating hormone-expressing cells form distinct populations in the rodent lateral hypothalamus: relationship to the neuropeptide Y and agouti gene-related protein systems. J Comp Neurol *402*, 460-474.

Broberger, C., Johansen, J., Johansson, C., Schalling, M., and Hokfelt, T. (1998b). The neuropeptide Y/agouti gene-related protein (AGRP) brain circuitry in normal, anorectic, and monosodium glutamate-treated mice. Proc Natl Acad Sci U S A *95*, 15043-15048.

Brown, L. M., Clegg, D. J., Benoit, S. C., and Woods, S. C. (2006). Intraventricular insulin and leptin reduce food intake and body weight in C57BL/6J mice. Physiol Behav *89*, 687-691.

Bruning, J. C., Gautam, D., Burks, D. J., Gillette, J., Schubert, M., Orban, P. C., Klein, R., Krone, W., Muller-Wieland, D., and Kahn, C. R. (2000). Role of brain insulin receptor in control of body weight and reproduction. Science *289*, 2122-2125.

Bruning, J. C., Michael, M. D., Winnay, J. N., Hayashi, T., Horsch, D., Accili, D., Goodyear, L. J., and Kahn, C. R. (1998). A muscle-specific insulin receptor knockout exhibits features of the metabolic syndrome of NIDDM without altering glucose tolerance. Mol Cell *2*, 559-569.

Bultman, S. J., Michaud, E. J., and Woychik, R. P. (1992). Molecular characterization of the mouse agouti locus. Cell *71*, 1195-1204.

Burcelin, R., Thorens, B., Glauser, M., Gaillard, R. C., and Pralong, F. P. (2003). Gonadotropin-releasing hormone secretion from hypothalamic neurons: stimulation by insulin and potentiation by leptin. Endocrinology *144*, 4484-4491.

Burks, D. J., de Mora, J. F., Schubert, M., Withers, D. J., Myers, M. G., Towery, H. H., Altamuro, S. L., Flint, C. L., and White, M. F. (2000a). IRS-2 pathways integrate female reproduction and energy homeostasis. Nature *407*, 377-382.

Burks, D. J., de Mora, J. F., Schubert, M., Withers, D. J., Myers, M. G., Towery, H. H., Altamuro, S. L., Flint, C. L., and White, M. F. (2000b). IRS-2 pathways integrate female reproduction and energy homeostasis. In Nature, pp. 377-382.

Burks, D. J., Font de Mora, J., Schubert, M., Withers, D. J., Myers, M. G., Towery, H. H., Altamuro, S. L., Flint, C. L., and White, M. F. (2000c). IRS-2 pathways integrate female reproduction and energy homeostasis. Nature *407*, 377-382.

Butler, A. A., Kesterson, R. A., Khong, K., Cullen, M. J., Pelleymounter, M. A., Dekoning, J., Baetscher, M., and Cone, R. D. (2000). A unique metabolic syndrome causes obesity in the melanocortin-3 receptor-deficient mouse. Endocrinology *141*, 3518-3521.

Butler, A. A., Marks, D. L., Fan, W., Kuhn, C. M., Bartolome, M., and Cone, R. D. (2001). Melanocortin-4 receptor is required for acute homeostatic responses to increased dietary fat. Nat Neurosci *4*, 605-611.

Campfield, L. A., Smith, F. J., Guisez, Y., Devos, R., and Burn, P. (1995). Recombinant mouse OB protein: evidence for a peripheral signal linking adiposity and central neural networks. Science *269*, 546-549.

Cantrell, D. A. (2001). Phosphoinositide 3-kinase signalling pathways. J Cell Sci *114*, 1439-1445.

Carroll, L., Voisey, J., and van Daal, A. (2005). Gene polymorphisms and their effects in the melanocortin system. Peptides *26*, 1871-1885.

Carvalheira, J. B., Torsoni, M. A., Ueno, M., Amaral, M. E., Araujo, E. P., Velloso, L. A., Gontijo, J. A., and Saad, M. J. (2005). Cross-talk between the insulin and leptin signaling systems in rat hypothalamus. Obes Res *13*, 48-57.

Challis, B. G., Coll, A. P., Yeo, G. S., Pinnock, S. B., Dickson, S. L., Thresher, R. R., Dixon, J., Zahn, D., Rochford, J. J., White, A., *et al.* (2004). Mice lacking pro-opiomelanocortin are sensitive to high-fat feeding but respond normally to the acute anorectic effects of peptide-YY(3-36). Proc Natl Acad Sci U S A *101*, 4695-4700.

Challis, B. G., Pinnock, S. B., Coll, A. P., Carter, R. N., Dickson, S. L., and O'Rahilly, S. (2003). Acute effects of PYY3-36 on food intake and hypothalamic neuropeptide expression in the mouse. Biochem Biophys Res Commun *311*, 915-919.

Chen, A. S., Metzger, J. M., Trumbauer, M. E., Guan, X. M., Yu, H., Frazier, E. G., Marsh, D. J., Forrest, M. J., Gopal-Truter, S., Fisher, J., *et al.* (2000). Role of the melanocortin-4 receptor in metabolic rate and food intake in mice. Transgenic Res *9*, 145-154.

Chen, W. S., Xu, P. Z., Gottlob, K., Chen, M. L., Sokol, K., Shiyanova, T., Roninson, I., Weng, W., Suzuki, R., Tobe, K., *et al.* (2001). Growth retardation and increased apoptosis in mice with homozygous disruption of the Akt1 gene. Genes Dev *15*, 2203-2208.

Cheung, C. C., Clifton, D. K., and Steiner, R. A. (1997). Proopiomelanocortin neurons are direct targets for leptin in the hypothalamus. Endocrinology *138*, 4489-4492.

Cho, H., Mu, J., Kim, J. K., Thorvaldsen, J. L., Chu, Q., Crenshaw, E. B., 3rd, Kaestner, K. H., Bartolomei, M. S., Shulman, G. I., and Birnbaum, M. J. (2001). Insulin resistance and a diabetes mellitus-like syndrome in mice lacking the protein kinase Akt2 (PKB beta). Science *292*, 1728-1731.

Choudhury, A. I., Heffron, H., Smith, M. A., Al-Qassab, H., Xu, A. W., Selman, C., Simmgen, M., Clements, M., Claret, M., Maccoll, G., *et al.* (2005). The role of insulin receptor substrate 2 in hypothalamic and beta cell function. J Clin Invest *115*, 940-950.

Clark, J. T., Kalra, P. S., Crowley, W. R., and Kalra, S. P. (1984). Neuropeptide Y and human pancreatic polypeptide stimulate feeding behavior in rats. Endocrinology *115*, 427-429.

Cohen, B., Novick, D., and Rubinstein, M. (1996). Modulation of insulin activities by leptin. Science *274*, 1185-1188.

Cohen, M. A., Ellis, S. M., Le Roux, C. W., Batterham, R. L., Park, A., Patterson, M., Frost, G. S., Ghatei, M. A., and Bloom, S. R. (2003). Oxyntomodulin suppresses appetite and reduces food intake in humans. J Clin Endocrinol Metab *88*, 4696-4701.

Cohen, P., Zhao, C., Cai, X., Montez, J. M., Rohani, S. C., Feinstein, P., Mombaerts, P., and Friedman, J. M. (2001). Selective deletion of leptin receptor in neurons leads to obesity. J Clin Invest *108*, 1113-1121.

Coleman, D. L. (1973). Effects of parabiosis of obese with diabetes and normal mice. Diabetologia *9*, 294-298.

Coleman, D. L., and Hummel, K. P. (1969). Effects of parabiosis of normal with genetically diabetic mice. Am J Physiol *217*, 1298-1304.

Cone, R. D. (2005). Anatomy and regulation of the central melanocortin system. Nat Neurosci *8*, 571-578.

Cone, R. D., Cowley, M. A., Butler, A. A., Fan, W., Marks, D. L., and Low, M. J. (2001). The arcuate nucleus as a conduit for diverse signals relevant to energy homeostasis. Int J Obes Relat Metab Disord *25 Suppl 5*, S63-67.

Cooper, S. J., Jackson, A., and Kirkham, T. C. (1985). Endorphins and food intake: kappa opioid receptor agonists and hyperphagia. Pharmacol Biochem Behav *23*, 889-901.

Cota, D., Proulx, K., Smith, K. A., Kozma, S. C., Thomas, G., Woods, S. C., and Seeley, R. J. (2006). Hypothalamic mTOR signaling regulates food intake. Science *312*, 927-930.

Cowley, M. A., Smart, J. L., Rubinstein, M., Cerdan, M. G., Diano, S., Horvath, T. L., Cone, R. D., and Low, M. J. (2001). Leptin activates anorexigenic POMC neurons through a neural network in the arcuate nucleus. Nature *411*, 480-484.

Cummings, D. E., and Schwartz, M. W. (2003). Genetics and pathophysiology of human obesity. Annu Rev Med *54*, 453-471.

Dakin, C. L., Gunn, I., Small, C. J., Edwards, C. M., Hay, D. L., Smith, D. M., Ghatei, M. A., and Bloom, S. R. (2001). Oxyntomodulin inhibits food intake in the rat. Endocrinology *142*, 4244-4250.

Dakin, C. L., Small, C. J., Batterham, R. L., Neary, N. M., Cohen, M. A., Patterson, M., Ghatei, M. A., and Bloom, S. R. (2004). Peripheral oxyntomodulin reduces food intake and body weight gain in rats. Endocrinology *145*, 2687-2695.

Dakin, C. L., Small, C. J., Park, A. J., Seth, A., Ghatei, M. A., and Bloom, S. R. (2002). Repeated ICV administration of oxyntomodulin causes a greater reduction in body weight gain than in pair-fed rats. Am J Physiol Endocrinol Metab *283*, E1173-1177.

Damsgaard, E. M., Froland, A., and Mogensen, C. E. (1997). Over-mortality as related to age and gender in patients with established non-insulin-dependent diabetes mellitus. J Diabetes Complications *11*, 77-82.

de Lecea, L., Kilduff, T. S., Peyron, C., Gao, X., Foye, P. E., Danielson, P. E., Fukuhara, C., Battenberg, E. L., Gautvik, V. T., Bartlett, F. S., 2nd, *et al.* (1998). The hypocretins: hypothalamus-specific peptides with neuroexcitatory activity. Proc Natl Acad Sci U S A *95*, 322-327.

de Luca, C., Kowalski, T. J., Zhang, Y., Elmquist, J. K., Lee, C., Kilimann, M. W., Ludwig, T., Liu, S. M., and Chua, S. C., Jr. (2005). Complete rescue of obesity, diabetes, and infertility in db/db mice by neuron-specific LEPR-B transgenes. J Clin Invest *115*, 3484-3493.

DeFronzo, R. A. (2004). Pathogenesis of type 2 diabetes mellitus. Med Clin North Am *88*, 787-835, ix.

Dhillon, H., Zigman, J. M., Ye, C., Lee, C. E., McGovern, R. A., Tang, V., Kenny, C. D., Christiansen, L. M., White, R. D., Edelstein, E. A., *et al.* (2006). Leptin directly activates SF1 neurons in the VMH, and this action by leptin is required for normal body-weight homeostasis. Neuron *49*, 191-203.

Di Marzo, V., and Matias, I. (2005). Endocannabinoid control of food intake and energy balance. Nat Neurosci *8*, 585-589.

Douglass, J., McKinzie, A. A., and Couceyro, P. (1995). PCR differential display identifies a rat brain mRNA that is transcriptionally regulated by cocaine and amphetamine. J Neurosci *15*, 2471-2481.

Drenick, E. J., and Johnson, D. (1978). Weight reduction by fasting and semistarvation in morbid obesity: long-term follow-up. Int J Obes *2*, 123-132.

Dunbar, J. C., and Lu, H. (2000). Proopiomelanocortin (POMC) products in the central regulation of sympathetic and cardiovascular dynamics: studies on melanocortin and opioid interactions. Peptides *21*, 211-217.

Edholm, O. G. (1977). Energy balance in man studies carried out by the Division of Human Physiology, National Institute for Medical Research. J Hum Nutr *31*, 413-431.

Edwards, C. M., Stanley, S. A., Davis, R., Brynes, A. E., Frost, G. S., Seal, L. J., Ghatei, M. A., and Bloom, S. R. (2001). Exendin-4 reduces fasting and postprandial glucose and decreases energy intake in healthy volunteers. Am J Physiol Endocrinol Metab *281*, E155-161.

Egawa, M., Yoshimatsu, H., and Bray, G. A. (1991). Neuropeptide Y suppresses sympathetic activity to interscapular brown adipose tissue in rats. Am J Physiol *260*, R328-334.

Elias, C. F., Aschkenasi, C., Lee, C., Kelly, J., Ahima, R. S., Bjorbaek, C., Flier, J. S., Saper, C. B., and Elmquist, J. K. (1999). Leptin differentially regulates NPY and POMC neurons projecting to the lateral hypothalamic area. Neuron *23*, 775-786.

Elias, C. F., Saper, C. B., Maratos-Flier, E., Tritos, N. A., Lee, C., Kelly, J., Tatro, J. B., Hoffman, G. E., Ollmann, M. M., Barsh, G. S., *et al.* (1998). Chemically defined projections linking the mediobasal hypothalamus and the lateral hypothalamic area. J Comp Neurol *402*, 442-459.

Elmquist, J. K., Bjorbaek, C., Ahima, R. S., Flier, J. S., and Saper, C. B. (1998a). Distributions of leptin receptor mRNA isoforms in the rat brain. J Comp Neurol *395*, 535-547.

Elmquist, J. K., Elias, C. F., and Saper, C. B. (1999). From lesions to leptin: hypothalamic control of food intake and body weight. Neuron *22*, 221-232.

Elmquist, J. K., Maratos-Flier, E., Saper, C. B., and Flier, J. S. (1998b). Unraveling the central nervous system pathways underlying responses to leptin. Nat Neurosci *1*, 445-450.

Engelman, J. A., Luo, J., and Cantley, L. C. (2006). The evolution of phosphatidylinositol 3-kinases as regulators of growth and metabolism. Nat Rev Genet *7*, 606-619.

Erickson, J. C., Hollopeter, G., and Palmiter, R. D. (1996). Attenuation of the obesity syndrome of ob/ob mice by the loss of neuropeptide Y. Science *274*, 1704-1707.

Fan, W., Boston, B. A., Kesterson, R. A., Hruby, V. J., and Cone, R. D. (1997). Role of melanocortinergic neurons in feeding and the agouti obesity syndrome. Nature *385*, 165-168.

Fantin, V. R., Wang, Q., Lienhard, G. E., and Keller, S. R. (2000). Mice lacking insulin receptor substrate 4 exhibit mild defects in growth, reproduction, and glucose homeostasis. Am J Physiol Endocrinol Metab *278*, E127-133.

Farooqi, I. S., Keogh, J. M., Yeo, G. S., Lank, E. J., Cheetham, T., and O'Rahilly, S. (2003). Clinical spectrum of obesity and mutations in the melanocortin 4 receptor gene. N Engl J Med *348*, 1085-1095.

Faust, I. M., Johnson, P. R., and Hirsch, J. (1977a). Adipose tissue regeneration following lipectomy. Science *197*, 391-393.

Faust, I. M., Johnson, P. R., and Hirsch, J. (1977b). Surgical removal of adipose tissue alters feeding behavior and the development of obesity in rats. Science *197*, 393-396.

Fekete, C., Mihaly, E., Luo, L. G., Kelly, J., Clausen, J. T., Mao, Q., Rand, W. M., Moss, L. G., Kuhar, M., Emerson, C. H., *et al.* (2000). Association of cocaine- and amphetamine-regulated transcript-immunoreactive elements with thyrotropin-releasing hormone-synthesizing neurons in the hypothalamic paraventricular nucleus and its role in the regulation of the hypothalamic-pituitary-thyroid axis during fasting. J Neurosci *20*, 9224-9234.

Fekete, C., Sarkar, S., Rand, W. M., Harney, J. W., Emerson, C. H., Bianco, A. C., Beck-Sickinger, A., and Lechan, R. M. (2002). Neuropeptide Y1 and Y5 receptors mediate the effects of neuropeptide Y on the hypothalamic-pituitary-thyroid axis. Endocrinology *143*, 4513-4519.

Fetissov, S. O., Meguid, M. M., Shafiroff, M., Miyata, G., and Torelli, G. F. (2000). Dopamine in the VMN of the hypothalamus is important for diurnal distribution of eating in obese male Zucker rats. Nutrition *16*, 65-66.

Fisher, S. J., Bruning, J. C., Lannon, S., and Kahn, C. R. (2005). Insulin signaling in the central nervous system is critical for the normal sympathoadrenal response to hypoglycemia. Diabetes *54*, 1447-1451.

Fisler, J. S., Egawa, M., and Bray, G. A. (1995). Peripheral 3-hydroxybutyrate and food intake in a model of dietary-fat induced obesity: effect of vagotomy. Physiol Behav *58*, 1-7.

Flegal, K. M., Carroll, M. D., Kuczmarski, R. J., and Johnson, C. L. (1998). Overweight and obesity in the United States: prevalence and trends, 1960-1994. Int J Obes Relat Metab Disord *22*, 39-47.

Flood, J. F., and Morley, J. E. (1989). Dissociation of the effects of neuropeptide Y on feeding and memory: evidence for pre- and postsynaptic mediation. Peptides *10*, 963-966.

Forbes, S., Bui, S., Robinson, B. R., Hochgeschwender, U., and Brennan, M. B. (2001). Integrated control of appetite and fat metabolism by the leptin-proopiomelanocortin pathway. Proc Natl Acad Sci U S A *98*, 4233-4237.

Foukas, L. C., Claret, M., Pearce, W., Okkenhaug, K., Meek, S., Peskett, E., Sancho, S., Smith, A. J., Withers, D. J., and Vanhaesebroeck, B. (2006). Critical role for the p110alpha phosphoinositide-3-OH kinase in growth and metabolic regulation. Nature *441*, 366-370.

Fox, E. A., and Byerly, M. S. (2004). A mechanism underlying mature-onset obesity: evidence from the hyperphagic phenotype of brain-derived neurotrophic factor mutants. Am J Physiol Regul Integr Comp Physiol *286*, R994-1004.

Franks, S., Gharani, N., and McCarthy, M. (1999). Genetic abnormalities in polycystic ovary syndrome. Ann Endocrinol (Paris) *60*, 131-133.

Fruebis, J., Tsao, T. S., Javorschi, S., Ebbets-Reed, D., Erickson, M. R., Yen, F. T., Bihain, B. E., and Lodish, H. F. (2001). Proteolytic cleavage product of 30-kDa adipocyte complement-related protein increases fatty acid oxidation in muscle and causes weight loss in mice. Proc Natl Acad Sci U S A *98*, 2005-2010.

Fruman, D. A., Mauvais-Jarvis, F., Pollard, D. A., Yballe, C. M., Brazil, D., Bronson, R. T., Kahn, C. R., and Cantley, L. C. (2000). Hypoglycaemia, liver necrosis and perinatal death in mice lacking all isoforms of phosphoinositide 3-kinase p85 alpha. Nat Genet *26*, 379-382.

Funahashi, H., Yada, T., Muroya, S., Takigawa, M., Ryushi, T., Horie, S., Nakai, Y., and Shioda, S. (1999). The effect of leptin on feeding-regulating neurons in the rat hypothalamus. Neurosci Lett *264*, 117-120.

Furuyama, T., Kitayama, K., Yamashita, H., and Mori, N. (2003). Forkhead transcription factor FOXO1 (FKHR)-dependent induction of PDK4 gene expression in skeletal muscle during energy deprivation. Biochem J *375*, 365-371.

Gabbay, R. A., Sutherland, C., Gnudi, L., Kahn, B. B., O'Brien, R. M., Granner, D. K., and Flier, J. S. (1996). Insulin regulation of phosphoenolpyruvate carboxykinase gene expression does not require activation of the Ras/mitogen-activated protein kinase signaling pathway. J Biol Chem *271*, 1890-1897.

Gao, Q., Wolfgang, M. J., Neschen, S., Morino, K., Horvath, T. L., Shulman, G. I., and Fu, X. Y. (2004). Disruption of neural signal transducer and activator of transcription 3 causes obesity, diabetes, infertility, and thermal dysregulation. Proc Natl Acad Sci U S A *101*, 4661-4666.

Garami, A., Zwartkruis, F. J., Nobukuni, T., Joaquin, M., Roccio, M., Stocker, H., Kozma, S. C., Hafen, E., Bos, J. L., and Thomas, G. (2003). Insulin activation of Rheb, a mediator of mTOR/S6K/4E-BP signaling, is inhibited by TSC1 and 2. Mol Cell *11*, 1457-1466.

Gelling, R. W., Morton, G. J., Morrison, C. D., Niswender, K. D., Myers, M. G., Jr., Rhodes, C. J., and Schwartz, M. W. (2006). Insulin action in the brain contributes to glucose lowering during insulin treatment of diabetes. Cell Metab *3*, 67-73.

Gibbs, J., Fauser, D. J., Rowe, E. A., Rolls, B. J., Rolls, E. T., and Maddison, S. P. (1979). Bombesin suppresses feeding in rats. Nature *282*, 208-210.

Gibbs, J., Young, R. C., and Smith, G. P. (1973). Cholecystokinin decreases food intake in rats. J Comp Physiol Psychol *84*, 488-495.

Gropp, E., Shanabrough, M., Borok, E., Xu, A. W., Janoschek, R., Buch, T., Plum, L., Balthasar, N., Hampel, B., Waisman, A., *et al.* (2005). Agouti-related peptide-expressing neurons are mandatory for feeding. Nat Neurosci *8*, 1289-1291.

Grundemar, L., Wahlestedt, C., and Reis, D. J. (1991). Long-lasting inhibition of the cardiovascular responses to glutamate and the baroreceptor reflex elicited by neuropeptide Y injected into the nucleus tractus solitarius of the rat. Neurosci Lett *122*, 135-139.

Gu, K., Cowie, C. C., and Harris, M. I. (1998). Mortality in adults with and without diabetes in a national cohort of the U.S. population, 1971-1993. Diabetes Care *21*, 1138-1145.

Gundlach, A. L. (2002). Galanin/GALP and galanin receptors: role in central control of feeding, body weight/obesity and reproduction? Eur J Pharmacol *440*, 255-268.

Gunton, J. E., Kulkarni, R. N., Yim, S., Okada, T., Hawthorne, W. J., Tseng, Y. H., Roberson, R. S., Ricordi, C., O'Connell, P. J., Gonzalez, F. J., and Kahn, C. R. (2005). Loss of ARNT/HIF1beta mediates altered gene expression and pancreatic-islet dysfunction in human type 2 diabetes. Cell *122*, 337-349.

Hachiya, H. L., Halban, P. A., and King, G. L. (1988). Intracellular pathways of insulin transport across vascular endothelial cells. Am J Physiol *255*, C459-464.

Hahn, T. M., Breininger, J. F., Baskin, D. G., and Schwartz, M. W. (1998). Coexpression of Agrp and NPY in fasting-activated hypothalamic neurons. Nat Neurosci *1*, 271-272.

Halaas, J. L., Gajiwala, K. S., Maffei, M., Cohen, S. L., Chait, B. T., Rabinowitz, D., Lallone, R. L., Burley, S. K., and Friedman, J. M. (1995). Weight-reducing effects of the plasma protein encoded by the obese gene. Science *269*, 543-546.

Harrold, J. A., Widdowson, P. S., and Williams, G. (1999). Altered energy balance causes selective changes in melanocortin-4(MC4-R), but not melanocortin-3 (MC3-R), receptors in specific hypothalamic regions: further evidence that activation of MC4-R is a physiological inhibitor of feeding. Diabetes *48*, 267-271.

Harvey, J., McKay, N. G., Walker, K. S., Van der Kaay, J., Downes, C. P., and Ashford, M. L. (2000). Essential role of phosphoinositide 3-kinase in leptin-induced K(ATP) channel activation in the rat CRI-G1 insulinoma cell line. J Biol Chem *275*, 4660-4669.

Havel, P. J. (2001). Peripheral signals conveying metabolic information to the brain: short-term and long-term regulation of food intake and energy homeostasis. Exp Biol Med (Maywood) *226*, 963-977.

Hetherington, A. W. a. R., S. W. (1940). Hypothalamic lesions and adiposity in the rat. The Anatomical Record *78*, 149-172.

Hillebrand, J. J., de Wied, D., and Adan, R. A. (2002). Neuropeptides, food intake and body weight regulation: a hypothalamic focus. Peptides *23*, 2283-2306.

Hoentjen, F., Hopman, W. P., and Jansen, J. B. (2001). Effect of circulating peptide YY on gallbladder emptying in humans. Scand J Gastroenterol *36*, 1086-1091.

Hoggard, N., Hunter, L., Duncan, J. S., and Rayner, D. V. (2004). Regulation of adipose tissue leptin secretion by alpha-melanocyte-stimulating hormone and agouti-related protein: further evidence of an interaction between leptin and the melanocortin signalling system. J Mol Endocrinol *32*, 145-153.

Horvath, T. L., Peyron, C., Diano, S., Ivanov, A., Aston-Jones, G., Kilduff, T. S., and van Den Pol, A. N. (1999). Hypocretin (orexin) activation and synaptic innervation of the locus coeruleus noradrenergic system. J Comp Neurol *415*, 145-159.

Huszar, D., Lynch, C. A., Fairchild-Huntress, V., Dunmore, J. H., Fang, Q., Berkemeier, L. R., Gu, W., Kesterson, R. A., Boston, B. A., Cone, R. D., *et al.* (1997). Targeted disruption of the melanocortin-4 receptor results in obesity in mice. Cell *88*, 131-141.

Jackson, Z. E., Stringer, B. M., and Foster, G. A. (1997). Identification of 5-HT receptor sub-types in a homogeneous population of presumptive serotoninergic neurones. Neuropharmacology *36*, 543-548.

Jacobowitz, D. M., and O'Donohue, T. L. (1978). alpha-Melanocyte stimulating hormone: immunohistochemical identification and mapping in neurons of rat brain. Proc Natl Acad Sci U S A *75*, 6300-6304.

Joseph, S. A., and Michael, G. J. (1988). Efferent ACTH-IR opiocortin projections from nucleus tractus solitarius: a hypothalamic deafferentation study. Peptides *9*, 193-201.

Joseph, S. A., Pilcher, W. H., and Bennett-Clarke, C. (1983). Immunocytochemical localization of ACTH perikarya in nucleus tractus solitarius: evidence for a second opiocortin neuronal system. Neurosci Lett *38*, 221-225.

Kaelin, C. B., Xu, A. W., Lu, X. Y., and Barsh, G. S. (2004). Transcriptional regulation of agouti-related protein (Agrp) in transgenic mice. Endocrinology *145*, 5798-5806.

Kahn, B. B., and Flier, J. S. (2000). Obesity and insulin resistance. J Clin Invest *106*, 473-481.

Kahn, C. R., Vicent, D., and Doria, A. (1996). Genetics of non-insulin-dependent (type-II) diabetes mellitus. Annu Rev Med *47*, 509-531.

Kaiyala, K. J., Woods, S. C., and Schwartz, M. W. (1995). New model for the regulation of energy balance and adiposity by the central nervous system. Am J Clin Nutr *62*, 1123S-1134S.

Kalra, S. P., Dube, M. G., Pu, S., Xu, B., Horvath, T. L., and Kalra, P. S. (1999). Interacting appetite-regulating pathways in the hypothalamic regulation of body weight. Endocr Rev *20*, 68-100.

Katso, R., Okkenhaug, K., Ahmadi, K., White, S., Timms, J., and Waterfield, M. D. (2001). Cellular function of phosphoinositide 3-kinases: implications for development, homeostasis, and cancer. Annu Rev Cell Dev Biol *17*, 615-675.

Keesey, R. E., and Powley, T. L. (1986). The regulation of body weight. Annu Rev Psychol *37*, 109-133.

Kellerer, M., Koch, M., Metzinger, E., Mushack, J., Capp, E., and Haring, H. U. (1997). Leptin activates PI-3 kinase in C2C12 myotubes via janus kinase-2 (JAK-2) and insulin receptor substrate-2 (IRS-2) dependent pathways. Diabetologia *40*, 1358-1362.

Kennedy, G. C. (1953). The role of depot fat in the hypothalamic control of food intake in the rat. Proc R Soc Lond B Biol Sci *140*, 578-596.

Kernie, S. G., Liebl, D. J., and Parada, L. F. (2000). BDNF regulates eating behavior and locomotor activity in mice. Embo J *19*, 1290-1300.

Kerouz, N. J., Horsch, D., Pons, S., and Kahn, C. R. (1997). Differential regulation of insulin receptor substrates-1 and -2 (IRS-1 and IRS-2) and phosphatidylinositol 3-kinase isoforms in liver and muscle of the obese diabetic (ob/ob) mouse. J Clin Invest *100*, 3164-3172.

Kido, Y., Nakae, J., and Accili, D. (2001). Clinical review 125: The insulin receptor and its cellular targets. J Clin Endocrinol Metab *86*, 972-979.

Kim, M. S., Pak, Y. K., Jang, P. G., Namkoong, C., Choi, Y. S., Won, J. C., Kim, K. S., Kim, S. W., Kim, H. S., Park, J. Y., *et al.* (2006). Role of hypothalamic Foxo1 in the regulation of food intake and energy homeostasis. Nat Neurosci *9*, 901-906.

Kim, Y. B., Uotani, S., Pierroz, D. D., Flier, J. S., and Kahn, B. B. (2000). In vivo administration of leptin activates signal transduction directly in insulin-sensitive tissues: overlapping but distinct pathways from insulin. Endocrinology *141*, 2328-2339.

Kissileff, H. R., Pi-Sunyer, F. X., Thornton, J., and Smith, G. P. (1981). C-terminal octapeptide of cholecystokinin decreases food intake in man. Am J Clin Nutr *34*, 154-160.

Kitamura, T., Feng, Y., Kitamura, Y. I., Chua, S. C., Jr., Xu, A. W., Barsh, G. S., Rossetti, L., and Accili, D. (2006). Forkhead protein FoxO1 mediates Agrp-dependent effects of leptin on food intake. Nat Med *12*, 534-540.

Kitamura, T., Nakae, J., Kitamura, Y., Kido, Y., Biggs, W. H., 3rd, Wright, C. V., White, M. F., Arden, K. C., and Accili, D. (2002). The forkhead transcription factor Foxo1 links insulin signaling to Pdx1 regulation of pancreatic beta cell growth. J Clin Invest *110*, 1839-1847.

Kong, W. M., Stanley, S., Gardiner, J., Abbott, C., Murphy, K., Seth, A., Connoley, I., Ghatei, M., Stephens, D., and Bloom, S. (2003). A role for arcuate cocaine and amphetamine-regulated transcript in hyperphagia, thermogenesis, and cold adaptation. Faseb J *17*, 1688-1690.

Kopelman, P. G. (2000). Obesity as a medical problem. Nature *404*, 635-643.

Kotz, C. M., Billington, C. J., and Levine, A. S. (1997). Opioids in the nucleus of the solitary tract are involved in feeding in the rat. Am J Physiol *272*, R1028-1032.

Kovacs, P., Matyas, S., Boda, K., and Kaali, S. G. (2003). The effect of endometrial thickness on IVF/ICSI outcome. Hum Reprod *18*, 2337-2341.

Kristensen, P., Judge, M. E., Thim, L., Ribel, U., Christjansen, K. N., Wulff, B. S., Clausen, J. T., Jensen, P. B., Madsen, O. D., Vrang, N., *et al.* (1998). Hypothalamic CART is a new anorectic peptide regulated by leptin. Nature *393*, 72-76.

Krude, H., Biebermann, H., and Gruters, A. (2003). Mutations in the human proopiomelanocortin gene. Ann N Y Acad Sci *994*, 233-239.

Krysiak, R., Obuchowicz, E., and Herman, Z. S. (1999). Interactions between the neuropeptide Y system and the hypothalamic-pituitary-adrenal axis. Eur J Endocrinol *140*, 130-136.

Kulkarni, R. N., Bruning, J. C., Winnay, J. N., Postic, C., Magnuson, M. A., and Kahn, C. R. (1999). Tissue-specific knockout of the insulin receptor in pancreatic beta cells creates an insulin secretory defect similar to that in type 2 diabetes. Cell *96*, 329-339.

Lambert, P. D., Couceyro, P. R., McGirr, K. M., Dall Vechia, S. E., Smith, Y., and Kuhar, M. J. (1998). CART peptides in the central control of feeding and interactions with neuropeptide Y. Synapse *29*, 293-298.

Lambert, P. D., Wilding, J. P., al-Dokhayel, A. A., Gilbey, S. G., and Bloom, S. R. (1993). The effect of central blockade of kappa-opioid receptors on neuropeptide Y-induced feeding in the rat. Brain Res *629*, 146-148.

Larhammar, D. (1996). Structural diversity of receptors for neuropeptide Y, peptide YY and pancreatic polypeptide. Regul Pept *65*, 165-174.

Larsen, P. J., Tang-Christensen, M., Stidsen, C. E., Madsen, K., Smith, M. S., and Cameron, J. L. (1999). Activation of central neuropeptide Y Y1 receptors potently stimulates food intake in male rhesus monkeys. J Clin Endocrinol Metab *84*, 3781-3791.

Larsen, P. J., Vrang, N., Petersen, P. C., and Kristensen, P. (2000). Chronic intracerebroventricular administration of recombinant CART(42-89) peptide inhibits and causes weight loss in lean and obese Zucker (fa/fa) rats. Obes Res *8*, 590-596.

Lauro, D., Kido, Y., Castle, A. L., Zarnowski, M. J., Hayashi, H., Ebina, Y., and Accili, D. (1998). Impaired glucose tolerance in mice with a targeted impairment of insulin action in muscle and adipose tissue. Nat Genet *20*, 294-298.

Lechan, R. M., and Fekete, C. (2006). The TRH neuron: a hypothalamic integrator of energy metabolism. Prog Brain Res *153*, 209-235.

Leibowitz, S. F. (1988). Hypothalamic paraventricular nucleus: interaction between alpha 2-noradrenergic system and circulating hormones and nutrients in relation to energy balance. Neurosci Biobehav Rev *12*, 101-109.

Leibowitz, S. F., and Miller, N. E. (1969). Unexpected adrenergic effects of chlorpromazine: eating elicited by injection into rat hypothalamus. Science *165*, 609-611.

Leibowitz, S. F., Weiss, G. F., and Shor-Posner, G. (1988). Hypothalamic serotonin: pharmacological, biochemical, and behavioral analyses of its feeding-suppressive action. Clin Neuropharmacol *11 Suppl 1*, S51-71.

Lendahl, U., Zimmerman, L. B., and McKay, R. D. (1990). CNS stem cells express a new class of intermediate filament protein. Cell *60*, 585-595.

Levine, A. S., and Billington, C. J. (1989). Opioids. Are they regulators of feeding? Ann N Y Acad Sci *575*, 209-219; discussion 219-220.

Levine, A. S., and Billington, C. J. (1997). Why do we eat? A neural systems approach. Annu Rev Nutr *17*, 597-619.

Levine, A. S., and Morley, J. E. (1982). Peripherally administered somatostatin reduces feeding by a vagal mediated mechanism. Pharmacol Biochem Behav *16*, 897-902.

Lewandoski, M. (2001). Conditional control of gene expression in the mouse. Nat Rev Genet *2*, 743-755.

Li, G., Mobbs, C. V., and Scarpace, P. J. (2003). Central pro-opiomelanocortin gene delivery results in hypophagia, reduced visceral adiposity, and improved insulin sensitivity in genetically obese Zucker rats. Diabetes *52*, 1951-1957.

Louvi, A., Accili, D., and Efstratiadis, A. (1997). Growth-promoting interaction of IGF-II with the insulin receptor during mouse embryonic development. Dev Biol *189*, 33-48.

Lu, D., Willard, D., Patel, I. R., Kadwell, S., Overton, L., Kost, T., Luther, M., Chen, W., Woychik, R. P., Wilkison, W. O., and et al. (1994). Agouti protein is an antagonist of the melanocyte-stimulating-hormone receptor. Nature *371*, 799-802.

Luquet, S., Perez, F. A., Hnasko, T. S., and Palmiter, R. D. (2005). NPY/AgRP neurons are essential for feeding in adult mice but can be ablated in neonates. Science *310*, 683-685.

Lyons, W. E., Mamounas, L. A., Ricaurte, G. A., Coppola, V., Reid, S. W., Bora, S. H., Wihler, C., Koliatsos, V. E., and Tessarollo, L. (1999). Brain-derived neurotrophic factor-deficient mice develop aggressiveness and hyperphagia in conjunction with brain serotonergic abnormalities. Proc Natl Acad Sci U S A *96*, 15239-15244.

MacGregor, G. G., Dong, K., Vanoye, C. G., Tang, L., Giebisch, G., and Hebert, S. C. (2002). Nucleotides and phospholipids compete for binding to the C terminus of KATP channels. Proc Natl Acad Sci U S A *99*, 2726-2731.

MacNeil, D. J., Howard, A. D., Guan, X., Fong, T. M., Nargund, R. P., Bednarek, M. A., Goulet, M. T., Weinberg, D. H., Strack, A. M., Marsh, D. J., *et al.* (2002). The role of melanocortins in body weight regulation: opportunities for the treatment of obesity. Eur J Pharmacol *440*, 141-157.

Marks, D. L., and Cone, R. D. (2001). Central melanocortins and the regulation of weight during acute and chronic disease. Recent Prog Horm Res *56*, 359-375.

Marsh, D. J., Weingarth, D. T., Novi, D. E., Chen, H. Y., Trumbauer, M. E., Chen, A. S., Guan, X. M., Jiang, M. M., Feng, Y., Camacho, R. E., *et al.* (2002). Melanin-concentrating hormone 1 receptor-deficient mice are lean, hyperactive, and hyperphagic and have altered metabolism. Proc Natl Acad Sci U S A *99*, 3240-3245.

Matsumoto, M., Han, S., Kitamura, T., and Accili, D. (2006). Dual role of transcription factor FoxO1 in controlling hepatic insulin sensitivity and lipid metabolism. J Clin Invest *116*, 2464-2472.

McGowan, M. K., Andrews, K. M., and Grossman, S. P. (1992). Chronic intrahypothalamic infusions of insulin or insulin antibodies alter body weight and food intake in the rat. Physiol Behav *51*, 753-766.

McGowan, M. K., Andrews, K. M., Kelly, J., and Grossman, S. P. (1990). Effects of chronic intrahypothalamic infusion of insulin on food intake and diurnal meal patterning in the rat. Behav Neurosci *104*, 373-385.

McLean, J. A., and Speakman, J. R. (2000). Effects of body mass and reproduction on the basal metabolic rate of brown long-eared bats (Plecotus auritus). Physiol Biochem Zool *73*, 112-121.

McMinn, J. E., Baskin, D. G., and Schwartz, M. W. (2000). Neuroendocrine mechanisms regulating food intake and body weight. Obes Rev *1*, 37-46.

McMinn, J. E., Liu, S. M., Liu, H., Dragatsis, I., Dietrich, P., Ludwig, T., Boozer, C. N., and Chua, S. C., Jr. (2005). Neuronal deletion of Lepr elicits diabesity in mice without affecting cold tolerance or fertility. Am J Physiol Endocrinol Metab *289*, E403-411.

Meeran, K., O'Shea, D., Edwards, C. M., Turton, M. D., Heath, M. M., Gunn, I., Abusnana, S., Rossi, M., Small, C. J., Goldstone, A. P., *et al.* (1999). Repeated intracerebroventricular administration of glucagon-like peptide-1-(7-36) amide or exendin-(9-39) alters body weight in the rat. Endocrinology *140*, 244-250.

Meister, B., Ceccatelli, S., Hokfelt, T., Anden, N. E., Anden, M., and Theodorsson, E. (1989). Neurotransmitters, neuropeptides and binding sites in the rat mediobasal hypothalamus: effects of monosodium glutamate (MSG) lesions. Exp Brain Res *76*, 343-368.

Mercer, J. G., Lawrence, C. B., and Atkinson, T. (1996). Hypothalamic NPY and CRF gene expression in the food-deprived Syrian hamster. Physiol Behav *60*, 121-127.

Michael, M. D., Kulkarni, R. N., Postic, C., Previs, S. F., Shulman, G. I., Magnuson, M. A., and Kahn, C. R. (2000). Loss of insulin signaling in hepatocytes leads to severe insulin resistance and progressive hepatic dysfunction. Mol Cell *6*, 87-97.

Michaud, J. L., Boucher, F., Melnyk, A., Gauthier, F., Goshu, E., Levy, E., Mitchell, G. A., Himms-Hagen, J., and Fan, C. M. (2001). Sim1 haploinsufficiency causes hyperphagia, obesity and reduction of the paraventricular nucleus of the hypothalamus. Hum Mol Genet *10*, 1465-1473.

Miner, J. L., Della-Fera, M. A., Paterson, J. A., and Baile, C. A. (1989). Lateral cerebroventricular injection of neuropeptide Y stimulates feeding in sheep. Am J Physiol *257*, R383-387.

Mirshamsi, S., Laidlaw, H. A., Ning, K., Anderson, E., Burgess, L. A., Gray, A., Sutherland, C., and Ashford, M. L. (2004). Leptin and insulin stimulation of signalling

pathways in arcuate nucleus neurones: PI3K dependent actin reorganization and KATP channel activation. BMC Neurosci *5*, 54.

Morgan, H. D., Sutherland, H. G., Martin, D. I., and Whitelaw, E. (1999). Epigenetic inheritance at the agouti locus in the mouse. Nat Genet *23*, 314-318.

Morrison, C. D., Morton, G. J., Niswender, K. D., Gelling, R. W., and Schwartz, M. W. (2005). Leptin inhibits hypothalamic Npy and Agrp gene expression via a mechanism that requires phosphatidylinositol 3-OH-kinase signaling. Am J Physiol Endocrinol Metab *289*, E1051-1057.

Morton, G. J., Cummings, D. E., Baskin, D. G., Barsh, G. S., and Schwartz, M. W. (2006). Central nervous system control of food intake and body weight. Nature *443*, 289-295.

Morton, G. J., Gelling, R. W., Niswender, K. D., Morrison, C. D., Rhodes, C. J., and Schwartz, M. W. (2005). Leptin regulates insulin sensitivity via phosphatidylinositol-3-OH kinase signaling in mediobasal hypothalamic neurons. Cell Metab *2*, 411-420.

Mountjoy, K. G., Mortrud, M. T., Low, M. J., Simerly, R. B., and Cone, R. D. (1994). Localization of the melanocortin-4 receptor (MC4-R) in neuroendocrine and autonomic control circuits in the brain. Mol Endocrinol *8*, 1298-1308.

Nagase, H., Bray, G. A., and York, D. A. (1996). Effects of pyruvate and lactate on food intake in rat strains sensitive and resistant to dietary obesity. Physiol Behav *59*, 555-560.

Naimi, M., Gautier, N., Chaussade, C., Valverde, A. M., Accili, D., and Van Obberghen, E. (2007). Nuclear forkhead box o1 controls and integrates key signaling pathways in hepatocytes. Endocrinology *148*, 2424-2434.

Nakae, J., Kido, Y., and Accili, D. (2001). Distinct and overlapping functions of insulin and IGF-I receptors. Endocr Rev *22*, 818-835.

Nakae, J., Kitamura, T., Kitamura, Y., Biggs, W. H., 3rd, Arden, K. C., and Accili, D. (2003). The forkhead transcription factor Foxo1 regulates adipocyte differentiation. Dev Cell *4*, 119-129.

Nandi, A., Kitamura, Y., Kahn, C. R., and Accili, D. (2004). Mouse models of insulin resistance. Physiol Rev *84*, 623-647.

Nicolaidis, S., and Rowland, N. (1976). Metering of intravenous versus oral nutrients and regulation of energy balance. Am J Physiol *231*, 661-668.

Nilaver, G., Zimmerman, E. A., Defendini, R., Liotta, A. S., Krieger, D. T., and Brownstein, M. J. (1979). Adrenocorticotropin and beta-lipotropin in the hypothalamus. Localization in the same arcuate neurons by sequential immunocytochemical procedures. J Cell Biol *81*, 50-58.

Niswender, K. D., Morrison, C. D., Clegg, D. J., Olson, R., Baskin, D. G., Myers, M. G., Jr., Seeley, R. J., and Schwartz, M. W. (2003). Insulin activation of phosphatidylinositol 3-kinase in the hypothalamic arcuate nucleus: a key mediator of insulin-induced anorexia. Diabetes *52*, 227-231.

Niswender, K. D., Morton, G. J., Stearns, W. H., Rhodes, C. J., Myers, M. G., Jr., and Schwartz, M. W. (2001). Intracellular signalling. Key enzyme in leptin-induced anorexia. Nature *413*, 794-795.

Novak, A., Guo, C., Yang, W., Nagy, A., and Lobe, C. G. (2000). Z/EG, a double reporter mouse line that expresses enhanced green fluorescent protein upon Cre-mediated excision. Genesis *28*, 147-155.

Novin, D., Robinson, K., Culbreth, L. A., and Tordoff, M. G. (1985). Is there a role for the liver in the control of food intake? Am J Clin Nutr *42*, 1050-1062.

Obici, S., Feng, Z., Karkanias, G., Baskin, D. G., and Rossetti, L. (2002a). Decreasing hypothalamic insulin receptors causes hyperphagia and insulin resistance in rats. Nat Neurosci *5*, 566-572.

Obici, S., Feng, Z., Tan, J., Liu, L., Karkanias, G., and Rossetti, L. (2001). Central melanocortin receptors regulate insulin action. J Clin Invest *108*, 1079-1085.

Obici, S., Zhang, B. B., Karkanias, G., and Rossetti, L. (2002b). Hypothalamic insulin signaling is required for inhibition of glucose production. Nat Med *8*, 1376-1382.

Okumura, T., Yamada, H., Motomura, W., and Kohgo, Y. (2000). Cocaine-amphetamine-regulated transcript (CART) acts in the central nervous system to inhibit gastric acid secretion via brain corticotropin-releasing factor system. Endocrinology *141*, 2854-2860.

Ollmann, M. M., Lamoreux, M. L., Wilson, B. D., and Barsh, G. S. (1998). Interaction of Agouti protein with the melanocortin 1 receptor in vitro and in vivo. Genes Dev *12*, 316-330.

Ollmann, M. M., Wilson, B. D., Yang, Y. K., Kerns, J. A., Chen, Y., Gantz, I., and Barsh, G. S. (1997). Antagonism of central melanocortin receptors in vitro and in vivo by agouti-related protein. Science *278*, 135-138.

Oomura, Y., Ono, T., Ooyama, H., and Wayner, M. J. (1969). Glucose and osmosensitive neurones of the rat hypothalamus. Nature *222*, 282-284.

Pardini, A. W., Nguyen, H. T., Figlewicz, D. P., Baskin, D. G., Williams, D. L., Kim, F., and Schwartz, M. W. (2006). Distribution of insulin receptor substrate-2 in brain areas involved in energy homeostasis. Brain Res *1112*, 169-178.

Pelleymounter, M. A., Cullen, M. J., Baker, M. B., Hecht, R., Winters, D., Boone, T., and Collins, F. (1995). Effects of the obese gene product on body weight regulation in ob/ob mice. Science *269*, 540-543.

Pende, M., Kozma, S. C., Jaquet, M., Oorschot, V., Burcelin, R., Le Marchand-Brustel, Y., Klumperman, J., Thorens, B., and Thomas, G. (2000). Hypoinsulinaemia, glucose intolerance and diminished beta-cell size in S6K1-deficient mice. Nature *408*, 994-997.

Pierroz, D. D., Ziotopoulou, M., Ungsunan, L., Moschos, S., Flier, J. S., and Mantzoros, C. S. (2002). Effects of acute and chronic administration of the melanocortin agonist MTII in mice with diet-induced obesity. Diabetes *51*, 1337-1345.

Pilcher, W. H., Joseph, S. A., and McDonald, J. V. (1988). Immunocytochemical localization of pro-opiomelanocortin neurons in human brain areas subserving stimulation analgesia. J Neurosurg *68*, 621-629.

Pittner, R. A., Moore, C. X., Bhavsar, S. P., Gedulin, B. R., Smith, P. A., Jodka, C. M., Parkes, D. G., Paterniti, J. R., Srivastava, V. P., and Young, A. A. (2004). Effects of PYY[3-36] in rodent models of diabetes and obesity. Int J Obes Relat Metab Disord *28*, 963-971.

Plata-Salaman, C. R. (1995). Cytokines and feeding suppression: an integrative view from neurologic to molecular levels. Nutrition *11*, 674-677.

Plum, L., Belgardt, B. F., and Bruning, J. C. (2006). Central insulin action in energy and glucose homeostasis. J Clin Invest *116*, 1761-1766.

Pocai, A., Lam, T. K., Gutierrez-Juarez, R., Obici, S., Schwartz, G. J., Bryan, J., Aguilar-Bryan, L., and Rossetti, L. (2005). Hypothalamic K(ATP) channels control hepatic glucose production. Nature *434*, 1026-1031.

Polonsky, K. S., Given, B. D., Hirsch, L., Shapiro, E. T., Tillil, H., Beebe, C., Galloway, J. A., Frank, B. H., Karrison, T., and Van Cauter, E. (1988a). Quantitative study of insulin secretion and clearance in normal and obese subjects. J Clin Invest *81*, 435-441.

Polonsky, K. S., Given, B. D., and Van Cauter, E. (1988b). Twenty-four-hour profiles and pulsatile patterns of insulin secretion in normal and obese subjects. J Clin Invest *81*, 442-448.

Poretsky, L., Cataldo, N. A., Rosenwaks, Z., and Giudice, L. C. (1999). The insulin-related ovarian regulatory system in health and disease. Endocr Rev *20*, 535-582.

Puigserver, P., Rhee, J., Donovan, J., Walkey, C. J., Yoon, J. C., Oriente, F., Kitamura, Y., Altomonte, J., Dong, H., Accili, D., and Spiegelman, B. M. (2003). Insulin-regulated hepatic gluconeogenesis through FOXO1-PGC-1alpha interaction. Nature *423*, 550-555.

Qi, Y., Takahashi, N., Hileman, S. M., Patel, H. R., Berg, A. H., Pajvani, U. B., Scherer, P. E., and Ahima, R. S. (2004). Adiponectin acts in the brain to decrease body weight. Nat Med *10*, 524-529.

Qian, S., Chen, H., Weingarth, D., Trumbauer, M. E., Novi, D. E., Guan, X., Yu, H., Shen, Z., Feng, Y., Frazier, E., *et al.* (2002). Neither agouti-related protein nor neuropeptide Y is critically required for the regulation of energy homeostasis in mice. Mol Cell Biol *22*, 5027-5035.

Qu, D., Ludwig, D. S., Gammeltoft, S., Piper, M., Pelleymounter, M. A., Cullen, M. J., Mathes, W. F., Przypek, R., Kanarek, R., and Maratos-Flier, E. (1996). A role for melanin-concentrating hormone in the central regulation of feeding behaviour. Nature *380*, 243-247.

Roberts, T. M. (1992). Cell biology. A signal chain of events. Nature *360*, 534-535.

Roselli-Rehfuss, L., Mountjoy, K. G., Robbins, L. S., Mortrud, M. T., Low, M. J., Tatro, J. B., Entwistle, M. L., Simerly, R. B., and Cone, R. D. (1993). Identification of a

receptor for gamma melanotropin and other proopiomelanocortin peptides in the hypothalamus and limbic system. Proc Natl Acad Sci U S A *90*, 8856-8860.

Ross, R., Leger, L., Guardo, R., De Guise, J., and Pike, B. G. (1991). Adipose tissue volume measured by magnetic resonance imaging and computerized tomography in rats. J Appl Physiol *70*, 2164-2172.

Rossi, M., Kim, M. S., Morgan, D. G., Small, C. J., Edwards, C. M., Sunter, D., Abusnana, S., Goldstone, A. P., Russell, S. H., Stanley, S. A., *et al.* (1998). A C-terminal fragment of Agouti-related protein increases feeding and antagonizes the effect of alpha-melanocyte stimulating hormone in vivo. Endocrinology *139*, 4428-4431.

Rothwell, N. J. (1990). Central effects of CRF on metabolism and energy balance. Neurosci Biobehav Rev *14*, 263-271.

Russo, S. J., Bolanos, C. A., Theobald, D. E., DeCarolis, N. A., Renthal, W., Kumar, A., Winstanley, C. A., Renthal, N. E., Wiley, M. D., Self, D. W., *et al.* (2007). IRS2-Akt pathway in midbrain dopamine neurons regulates behavioral and cellular responses to opiates. Nat Neurosci *10*, 93-99.

Sabbatini, P., and McCormick, F. (1999). Phosphoinositide 3-OH kinase (PI3K) and PKB/Akt delay the onset of p53-mediated, transcriptionally dependent apoptosis. J Biol Chem *274*, 24263-24269.

Sakurai, T., Amemiya, A., Ishii, M., Matsuzaki, I., Chemelli, R. M., Tanaka, H., Williams, S. C., Richarson, J. A., Kozlowski, G. P., Wilson, S., *et al.* (1998). Orexins and orexin receptors: a family of hypothalamic neuropeptides and G protein-coupled receptors that regulate feeding behavior. Cell *92*, 1 page following 696.

Saltiel, A. R., and Kahn, C. R. (2001). Insulin signalling and the regulation of glucose and lipid metabolism. Nature *414*, 799-806.

Salvi, R., Castillo, E., Voirol, M. J., Glauser, M., Rey, J. P., Gaillard, R. C., Vollenweider, P., and Pralong, F. P. (2006). Gonadotropin-releasing hormone-expressing neurons immortalized conditionally are activated by insulin: implication of the mitogen-activated protein kinase pathway. Endocrinology *147*, 816-826.

Sasaki, A., Uehara, M., Horiuchi, N., Hasegawa, K., and Shimizu, T. (1997). A 15-year follow-up study of patients with non-insulin-dependent diabetes mellitus (NIDDM) in Osaka, Japan. Factors predictive of the prognosis of diabetic patients. Diabetes Res Clin Pract *36*, 41-47.

Sauer, B., and Henderson, N. (1988). Site-specific DNA recombination in mammalian cells by the Cre recombinase of bacteriophage P1. Proc Natl Acad Sci U S A *85*, 5166-5170.

Sawchenko, P. E. (1998). Toward a new neurobiology of energy balance, appetite, and obesity: the anatomists weigh in. J Comp Neurol *402*, 435-441.

Saxena, R., Voight, B. F., Lyssenko, V., Burtt, N. P., de Bakker, P. I., Chen, H., Roix, J. J., Kathiresan, S., Hirschhorn, J. N., Daly, M. J., *et al.* (2007). Genome-Wide Association Analysis Identifies Loci for Type 2 Diabetes and Triglyceride Levels. Science.

Scalera, G., and Tarozzi, G. (1998). Somatostatin administration modifies food intake, body weight, and gut motility in rat. Peptides *19*, 991-997.
Schwartz, M. W. (1997). Regulation of appetite and body weight. Hosp Pract (Minneap) *32*, 109-112, 117-109.

Schwartz, M. W. (2001). Progress in the search for neuronal mechanisms coupling type 2 diabetes to obesity. J Clin Invest *108*, 963-964.

Schwartz, M. W., Baskin, D. G., Bukowski, T. R., Kuijper, J. L., Foster, D., Lasser, G., Prunkard, D. E., Porte, D., Jr., Woods, S. C., Seeley, R. J., and Weigle, D. S. (1996a). Specificity of leptin action on elevated blood glucose levels and hypothalamic neuropeptide Y gene expression in ob/ob mice. Diabetes *45*, 531-535.

Schwartz, M. W., Peskind, E., Raskind, M., Boyko, E. J., and Porte, D., Jr. (1996b). Cerebrospinal fluid leptin levels: relationship to plasma levels and to adiposity in humans. Nat Med *2*, 589-593.

Schwartz, M. W., Seeley, R. J., Campfield, L. A., Burn, P., and Baskin, D. G. (1996c). Identification of targets of leptin action in rat hypothalamus. J Clin Invest *98*, 1101-1106.

Schwartz, M. W., Sipols, A. J., Marks, J. L., Sanacora, G., White, J. D., Scheurink, A., Kahn, S. E., Baskin, D. G., Woods, S. C., Figlewicz, D. P., and et al. (1992). Inhibition of hypothalamic neuropeptide Y gene expression by insulin. Endocrinology *130*, 3608-3616.

Schwartz, M. W., Woods, S. C., Porte, D., Jr., Seeley, R. J., and Baskin, D. G. (2000). Central nervous system control of food intake. Nature *404*, 661-671.

Scott, L. J., Mohlke, K. L., Bonnycastle, L. L., Willer, C. J., Li, Y., Duren, W. L., Erdos, M. R., Stringham, H. M., Chines, P. S., Jackson, A. U., *et al.* (2007). A Genome-Wide Association Study of Type 2 Diabetes in Finns Detects Multiple Susceptibility Variants. Science.

Seeley, R. J., van Dijk, G., Campfield, L. A., Smith, F. J., Burn, P., Nelligan, J. A., Bell, S. M., Baskin, D. G., Woods, S. C., and Schwartz, M. W. (1996). Intraventricular leptin reduces food intake and body weight of lean rats but not obese Zucker rats. Horm Metab Res *28*, 664-668.

Segal-Lieberman, G., Trombly, D. J., Juthani, V., Wang, X., and Maratos-Flier, E. (2003). NPY ablation in C57BL/6 mice leads to mild obesity and to an impaired refeeding response to fasting. Am J Physiol Endocrinol Metab *284*, E1131-1139.

Seidell, J. C., Verschuren, W. M., van Leer, E. M., and Kromhout, D. (1996). Overweight, underweight, and mortality. A prospective study of 48,287 men and women. Arch Intern Med *156*, 958-963.

Selman, C., Lumsden, S., Bunger, L., Hill, W. G., and Speakman, J. R. (2001). Resting metabolic rate and morphology in mice (Mus musculus) selected for high and low food intake. J Exp Biol *204*, 777-784.

Shepherd, P. R., Withers, D. J., and Siddle, K. (1998). Phosphoinositide 3-kinase: the key switch mechanism in insulin signalling. Biochem J *333 (Pt 3)*, 471-490.

Shutter, J. R., Graham, M., Kinsey, A. C., Scully, S., Luthy, R., and Stark, K. L. (1997). Hypothalamic expression of ART, a novel gene related to agouti, is up-regulated in obese and diabetic mutant mice. Genes Dev *11*, 593-602.

Shyng, S. L., and Nichols, C. G. (1998). Membrane phospholipid control of nucleotide sensitivity of KATP channels. Science *282*, 1138-1141.

Sipols, A. J., Baskin, D. G., and Schwartz, M. W. (1995). Effect of intracerebroventricular insulin infusion on diabetic hyperphagia and hypothalamic neuropeptide gene expression. Diabetes *44*, 147-151.

Sivitz, W. I., Walsh, S. A., Morgan, D. A., Thomas, M. J., and Haynes, W. G. (1997). Effects of leptin on insulin sensitivity in normal rats. Endocrinology *138*, 3395-3401.

Sladek, R., Rocheleau, G., Rung, J., Dina, C., Shen, L., Serre, D., Boutin, P., Vincent, D., Belisle, A., Hadjadj, S., *et al.* (2007). A genome-wide association study identifies novel risk loci for type 2 diabetes. Nature *445*, 881-885.

Smith, G. P., and Epstein, A. N. (1969). Increased feeding in response to decreased glucose utilization in the rat and monkey. Am J Physiol *217*, 1083-1087.

Smith, G. P., Jerome, C., and Gibbs, J. (1981). Abdominal vagotomy does not block the satiety effect of bombesin in the rat. Peptides *2*, 409-411.

Smith, P. J., Wise, L. S., Berkowitz, R., Wan, C., and Rubin, C. S. (1988). Insulin-like growth factor-I is an essential regulator of the differentiation of 3T3-L1 adipocytes. J Biol Chem *263*, 9402-9408.

Soriano, P. (1999). Generalized lacZ expression with the ROSA26 Cre reporter strain. Nat Genet *21*, 70-71.

Spanswick, D., Smith, M. A., Mirshamsi, S., Routh, V. H., and Ashford, M. L. (2000). Insulin activates ATP-sensitive K+ channels in hypothalamic neurons of lean, but not obese rats. Nat Neurosci *3*, 757-758.

Srinivas, S., Watanabe, T., Lin, C. S., William, C. M., Tanabe, Y., Jessell, T. M., and Costantini, F. (2001). Cre reporter strains produced by targeted insertion of EYFP and ECFP into the ROSA26 locus. BMC Dev Biol *1*, 4.

Stallone, D. D., Stunkard, A. J., Wadden, T. A., Foster, G. D., Boorstein, J., and Arger, P. (1991). Weight loss and body fat distribution: a feasibility study using computed tomography. Int J Obes *15*, 775-780.

Stanley, B. G., Kyrkouli, S. E., Lampert, S., and Leibowitz, S. F. (1986). Neuropeptide Y chronically injected into the hypothalamus: a powerful neurochemical inducer of hyperphagia and obesity. Peptides *7*, 1189-1192.

Stanley, S., Wynne, K., McGowan, B., and Bloom, S. (2005). Hormonal regulation of food intake. Physiol Rev *85*, 1131-1158.

Stanley, S. A., Small, C. J., Murphy, K. G., Rayes, E., Abbott, C. R., Seal, L. J., Morgan, D. G., Sunter, D., Dakin, C. L., Kim, M. S., *et al.* (2001). Actions of cocaine- and

amphetamine-regulated transcript (CART) peptide on regulation of appetite and hypothalamo-pituitary axes in vitro and in vivo in male rats. Brain Res *893*, 186-194.

Stark, W. M., Boocock, M. R., and Sherratt, D. J. (1992). Catalysis by site-specific recombinases. Trends Genet *8*, 432-439.

Stellar, E. (1954). The physiology of motivation. Psychol Rev *61*, 5-22.
Stern, M. P. (2000). Strategies and prospects for finding insulin resistance genes. J Clin Invest *106*, 323-327.

Sternberg, N., and Hamilton, D. (1981). Bacteriophage P1 site-specific recombination. I. Recombination between loxP sites. J Mol Biol *150*, 467-486.

Sternson, S. M., Shepherd, G. M., and Friedman, J. M. (2005). Topographic mapping of VMH --> arcuate nucleus microcircuits and their reorganization by fasting. Nat Neurosci *8*, 1356-1363.

Strachan, T. and Read, A.P. (1999) Human Molecular Genetics, 2nd edn.BIOS Scientific, Oxford

Strubbe, J. H., and Mein, C. G. (1977). Increased feeding in response to bilateral injection of insulin antibodies in the VMH. Physiol Behav *19*, 309-313.

Stumvoll, M., Goldstein, B. J., and van Haeften, T. W. (2005). Type 2 diabetes: principles of pathogenesis and therapy. Lancet *365*, 1333-1346.

Summers, S. A., Yin, V. P., Whiteman, E. L., Garza, L. A., Cho, H., Tuttle, R. L., and Birnbaum, M. J. (1999). Signaling pathways mediating insulin-stimulated glucose transport. Ann N Y Acad Sci *892*, 169-186.

Suzuki, R., Tobe, K., Aoyama, M., Inoue, A., Sakamoto, K., Yamauchi, T., Kamon, J., Kubota, N., Terauchi, Y., Yoshimatsu, H., *et al.* (2004). Both insulin signaling defects in the liver and obesity contribute to insulin resistance and cause diabetes in Irs2(-/-) mice. J Biol Chem *279*, 25039-25049.

Takeda, K., Noguchi, K., Shi, W., Tanaka, T., Matsumoto, M., Yoshida, N., Kishimoto, T., and Akira, S. (1997). Targeted disruption of the mouse Stat3 gene leads to early embryonic lethality. Proc Natl Acad Sci U S A *94*, 3801-3804.

Tang, H., Vasselli, J. R., Wu, E. X., Boozer, C. N., and Gallagher, D. (2002). High-resolution magnetic resonance imaging tracks changes in organ and tissue mass in obese and aging rats. Am J Physiol Regul Integr Comp Physiol *282*, R890-899.

Tang-Christensen, M., Vrang, N., and Larsen, P. J. (2001). Glucagon-like peptide containing pathways in the regulation of feeding behaviour. Int J Obes Relat Metab Disord *25 Suppl 5*, S42-47.

Taniguchi, C. M., Emanuelli, B., and Kahn, C. R. (2006). Critical nodes in signalling pathways: insights into insulin action. Nat Rev Mol Cell Biol *7*, 85-96.

Tartaglia, L. A., Dembski, M., Weng, X., Deng, N., Culpepper, J., Devos, R., Richards, G. J., Campfield, L. A., Clark, F. T., Deeds, J., *et al.* (1995). Identification and expression cloning of a leptin receptor, OB-R. Cell *83*, 1263-1271.

Tatemoto, K., Carlquist, M., and Mutt, V. (1982). Neuropeptide Y--a novel brain peptide with structural similarities to peptide YY and pancreatic polypeptide. Nature *296*, 659-660.

Thiele, T. E., Van Dijk, G., Campfield, L. A., Smith, F. J., Burn, P., Woods, S. C., Bernstein, I. L., and Seeley, R. J. (1997). Central infusion of GLP-1, but not leptin, produces conditioned taste aversions in rats. Am J Physiol *272*, R726-730.

Thim, L., Kristensen, P., Nielsen, P. F., Wulff, B. S., and Clausen, J. T. (1999). Tissue-specific processing of cocaine- and amphetamine-regulated transcript peptides in the rat. Proc Natl Acad Sci U S A *96*, 2722-2727.

Thompson, D. A., and Campbell, R. G. (1977). Hunger in humans induced by 2-deoxy-D-glucose: glucoprivic control of taste preference and food intake. Science *198*, 1065-1068.

Thorsell, A., and Heilig, M. (2002). Diverse functions of neuropeptide Y revealed using genetically modified animals. Neuropeptides *36*, 182-193.

Tomlinson, D. R. (1999). Mitogen-activated protein kinases as glucose transducers for diabetic complications. Diabetologia *42*, 1271-1281.

Tovar, S., Nogueiras, R., Tung, L. Y., Castaneda, T. R., Vazquez, M. J., Morris, A., Williams, L. M., Dickson, S. L., and Dieguez, C. (2005). Central administration of resistin promotes short-term satiety in rats. Eur J Endocrinol *153*, R1-5.

Tronche, F., Kellendonk, C., Kretz, O., Gass, P., Anlag, K., Orban, P. C., Bock, R., Klein, R., and Schutz, G. (1999). Disruption of the glucocorticoid receptor gene in the nervous system results in reduced anxiety. Nat Genet *23*, 99-103.

Tschop, M., Smiley, D. L., and Heiman, M. L. (2000). Ghrelin induces adiposity in rodents. Nature *407*, 908-913.

Tsukamura, H., Thompson, R. C., Tsukahara, S., Ohkura, S., Maekawa, F., Moriyama, R., Niwa, Y., Foster, D. L., and Maeda, K. (2000). Intracerebroventricular administration of melanin-concentrating hormone suppresses pulsatile luteinizing hormone release in the female rat. J Neuroendocrinol *12*, 529-534.

Turton, M. D., O'Shea, D., Gunn, I., Beak, S. A., Edwards, C. M., Meeran, K., Choi, S. J., Taylor, G. M., Heath, M. M., Lambert, P. D., *et al.* (1996). A role for glucagon-like peptide-1 in the central regulation of feeding. Nature *379*, 69-72.

Ueki, K., Yballe, C. M., Brachmann, S. M., Vicent, D., Watt, J. M., Kahn, C. R., and Cantley, L. C. (2002). Increased insulin sensitivity in mice lacking p85beta subunit of phosphoinositide 3-kinase. Proc Natl Acad Sci U S A *99*, 419-424.

Um, S. H., Frigerio, F., Watanabe, M., Picard, F., Joaquin, M., Sticker, M., Fumagalli, S., Allegrini, P. R., Kozma, S. C., Auwerx, J., and Thomas, G. (2004). Absence of S6K1

protects against age- and diet-induced obesity while enhancing insulin sensitivity. Nature *431*, 200-205.

van den Pol, A. N. (2003). Weighing the role of hypothalamic feeding neurotransmitters. Neuron *40*, 1059-1061.

Van Duyne, G. D. (2001). A structural view of cre-loxp site-specific recombination. Annu Rev Biophys Biomol Struct *30*, 87-104.

Van Obberghen, E., Baron, V., Delahaye, L., Emanuelli, B., Filippa, N., Giorgetti-Peraldi, S., Lebrun, P., Mothe-Satney, I., Peraldi, P., Rocchi, S., *et al.* (2001). Surfing the insulin signaling web. Eur J Clin Invest *31*, 966-977.

Vanhaesebroeck, B., and Alessi, D. R. (2000). The PI3K-PDK1 connection: more than just a road to PKB. Biochem J *346 Pt 3*, 561-576.

Vanhaesebroeck, B., Ali, K., Bilancio, A., Geering, B., and Foukas, L. C. (2005). Signalling by PI3K isoforms: insights from gene-targeted mice. Trends Biochem Sci *30*, 194-204.

Vanhaesebroeck, B., and Waterfield, M. D. (1999). Signaling by distinct classes of phosphoinositide 3-kinases. Exp Cell Res *253*, 239-254.

Verdich, C., Flint, A., Gutzwiller, J. P., Naslund, E., Beglinger, C., Hellstrom, P. M., Long, S. J., Morgan, L. M., Holst, J. J., and Astrup, A. (2001). A meta-analysis of the effect of glucagon-like peptide-1 (7-36) amide on ad libitum energy intake in humans. J Clin Endocrinol Metab *86*, 4382-4389.

Vicent, D., Ilany, J., Kondo, T., Naruse, K., Fisher, S. J., Kisanuki, Y. Y., Bursell, S., Yanagisawa, M., King, G. L., and Kahn, C. R. (2003). The role of endothelial insulin signaling in the regulation of vascular tone and insulin resistance. J Clin Invest *111*, 1373-1380.

Wang, C., Billington, C. J., Levine, A. S., and Kotz, C. M. (2000). Effect of CART in the hypothalamic paraventricular nucleus on feeding and uncoupling protein gene expression. Neuroreport *11*, 3251-3255.

Watson, S. J., Richard, C. W., 3rd, and Barchas, J. D. (1978). Adrenocorticotropin in rat brain: immunocytochemical localization in cells and axons. Science *200*, 1180-1182.

Weigle, D. S. (1994). Appetite and the regulation of body composition. Faseb J *8*, 302-310.

Weingarten, H. P., Chang, P. K., and McDonald, T. J. (1985). Comparison of the metabolic and behavioral disturbances following paraventricular- and ventromedial-hypothalamic lesions. Brain Res Bull *14*, 551-559.

Weir, J. B. (1949). New methods for calculating metabolic rate with special reference to protein metabolism. J Physiol *109*, 1-9.

White, M. F. (2002). IRS proteins and the common path to diabetes. Am J Physiol Endocrinol Metab *283*, E413-422.

Wielinga, P. Y., Alder, B., and Lutz, T. A. (2007). The acute effect of amylin and salmon calcitonin on energy expenditure. Physiol Behav.

Wilding, J. P., Gilbey, S. G., Bailey, C. J., Batt, R. A., Williams, G., Ghatei, M. A., and Bloom, S. R. (1993). Increased neuropeptide-Y messenger ribonucleic acid (mRNA) and decreased neurotensin mRNA in the hypothalamus of the obese (ob/ob) mouse. Endocrinology *132*, 1939-1944.

Williams, G., Bing, C., Cai, X. J., Harrold, J. A., King, P. J., and Liu, X. H. (2001). The hypothalamus and the control of energy homeostasis: different circuits, different purposes. Physiol Behav *74*, 683-701.

Willis, D., Mason, H., Gilling-Smith, C., and Franks, S. (1996). Modulation by insulin of follicle-stimulating hormone and luteinizing hormone actions in human granulosa cells of normal and polycystic ovaries. J Clin Endocrinol Metab *81*, 302-309.

Wilson, B. D., Bagnol, D., Kaelin, C. B., Ollmann, M. M., Gantz, I., Watson, S. J., and Barsh, G. S. (1999). Physiological and anatomical circuitry between Agouti-related protein and leptin signaling. Endocrinology *140*, 2387-2397.

Wilson, T. J., and Kola, I. (2001). The LoxP/CRE system and genome modification. Methods Mol Biol *158*, 83-94.

Wisse, B. E., Campfield, L. A., Marliss, E. B., Morais, J. A., Tenenbaum, R., and Gougeon, R. (1999). Effect of prolonged moderate and severe energy restriction and refeeding on plasma leptin concentrations in obese women. Am J Clin Nutr *70*, 321-330.

Withers, D. J. (2001). Insulin receptor substrate proteins and neuroendocrine function. Biochem Soc Trans *29*, 525-529.

Withers, D. J., Burks, D. J., Towery, H. H., Altamuro, S. L., Flint, C. L., and White, M. F. (1999). Irs-2 coordinates Igf-1 receptor-mediated beta-cell development and peripheral insulin signalling. Nat Genet *23*, 32-40.

Withers, D. J., Gutierrez, J. S., Towery, H., Burks, D. J., Ren, J. M., Previs, S., Zhang, Y., Bernal, D., Pons, S., Shulman, G. I., *et al.* (1998). Disruption of IRS-2 causes type 2 diabetes in mice. Nature *391*, 900-904.

Wolff, G. L., Roberts, D. W., and Mountjoy, K. G. (1999). Physiological consequences of ectopic agouti gene expression: the yellow obese mouse syndrome. Physiol Genomics *1*, 151-163.

Wolfrum, C., Asilmaz, E., Luca, E., Friedman, J. M., and Stoffel, M. (2004). Foxa2 regulates lipid metabolism and ketogenesis in the liver during fasting and in diabetes. Nature *432*, 1027-1032.

Woods, S. C., Chavez, M., Park, C. R., Riedy, C., Kaiyala, K., Richardson, R. D., Figlewicz, D. P., Schwartz, M. W., Porte, D., Jr., and Seeley, R. J. (1996). The evaluation of insulin as a metabolic signal influencing behavior via the brain. Neurosci Biobehav Rev *20*, 139-144.

Woods, S. C., Decke, E., and Vasselli, J. R. (1974). Metabolic hormones and regulation of body weight. Psychol Rev *81*, 26-43.

Woods, S. C., Lotter, E. C., McKay, L. D., and Porte, D., Jr. (1979). Chronic intracerebroventricular infusion of insulin reduces food intake and body weight of baboons. Nature *282*, 503-505.

Woods, S. C., and Seeley, R. J. (2000). Adiposity signals and the control of energy homeostasis. Nutrition *16*, 894-902.

Woods, S. C., Seeley, R. J., Baskin, D. G., and Schwartz, M. W. (2003). Insulin and the blood-brain barrier. Curr Pharm Des *9*, 795-800.

Woods, S. C., Seeley, R. J., Porte, D., Jr., and Schwartz, M. W. (1998). Signals that regulate food intake and energy homeostasis. Science *280*, 1378-1383.

Woods, S. C., Stein, L. J., McKay, L. D., and Porte, D., Jr. (1984). Suppression of food intake by intravenous nutrients and insulin in the baboon. Am J Physiol *247*, R393-401.

Wortley, K. E., Anderson, K. D., Yasenchak, J., Murphy, A., Valenzuela, D., Diano, S., Yancopoulos, G. D., Wiegand, S. J., and Sleeman, M. W. (2005). Agouti-related protein-deficient mice display an age-related lean phenotype. Cell Metab *2*, 421-427.

Wortley, K. E., Chang, G. Q., Davydova, Z., Fried, S. K., and Leibowitz, S. F. (2004). Cocaine- and amphetamine-regulated transcript in the arcuate nucleus stimulates lipid metabolism to control body fat accrual on a high-fat diet. Regul Pept *117*, 89-99.

Wren, A. M., Seal, L. J., Cohen, M. A., Brynes, A. E., Frost, G. S., Murphy, K. G., Dhillo, W. S., Ghatei, M. A., and Bloom, S. R. (2001a). Ghrelin enhances appetite and increases food intake in humans. J Clin Endocrinol Metab *86*, 5992.

Wren, A. M., Small, C. J., Abbott, C. R., Dhillo, W. S., Seal, L. J., Cohen, M. A., Batterham, R. L., Taheri, S., Stanley, S. A., Ghatei, M. A., and Bloom, S. R. (2001b). Ghrelin causes hyperphagia and obesity in rats. Diabetes *50*, 2540-2547.

Wynne, K., Stanley, S., McGowan, B., and Bloom, S. (2005). Appetite control. J Endocrinol *184*, 291-318.

Xu, A. W., Kaelin, C. B., Morton, G. J., Ogimoto, K., Stanhope, K., Graham, J., Baskin, D. G., Havel, P., Schwartz, M. W., and Barsh, G. S. (2005a). Effects of hypothalamic neurodegeneration on energy balance. PLoS Biol *3*, e415.

Xu, A. W., Kaelin, C. B., Takeda, K., Akira, S., Schwartz, M. W., and Barsh, G. S. (2005b). PI3K integrates the action of insulin and leptin on hypothalamic neurons. J Clin Invest *115*, 951-958.

Xu, A. W., Ste-Marie, L., Kaelin, C. B., and Barsh, G. S. (2007). Inactivation of signal transducer and activator of transcription 3 in proopiomelanocortin (Pomc) neurons causes decreased pomc expression, mild obesity, and defects in compensatory refeeding. Endocrinology *148*, 72-80.

Xu, B., Goulding, E. H., Zang, K., Cepoi, D., Cone, R. D., Jones, K. R., Tecott, L. H., and Reichardt, L. F. (2003). Brain-derived neurotrophic factor regulates energy balance downstream of melanocortin-4 receptor. Nat Neurosci *6*, 736-742.

Yamada, M., Ohnishi, H., Sano, S., Nakatani, A., Ikeuchi, T., and Hatanaka, H. (1997). Insulin receptor substrate (IRS)-1 and IRS-2 are tyrosine-phosphorylated and associated with phosphatidylinositol 3-kinase in response to brain-derived neurotrophic factor in cultured cerebral cortical neurons. J Biol Chem *272*, 30334-30339.

Yamamoto, H., Kishi, T., Lee, C. E., Choi, B. J., Fang, H., Hollenberg, A. N., Drucker, D. J., and Elmquist, J. K. (2003). Glucagon-like peptide-1-responsive catecholamine neurons in the area postrema link peripheral glucagon-like peptide-1 with central autonomic control sites. J Neurosci *23*, 2939-2946.

Yamauchi, T., Kamon, J., Waki, H., Terauchi, Y., Kubota, N., Hara, K., Mori, Y., Ide, T., Murakami, K., Tsuboyama-Kasaoka, N., *et al.* (2001). The fat-derived hormone adiponectin reverses insulin resistance associated with both lipoatrophy and obesity. Nat Med *7*, 941-946.

Yamauchi, T., Nio, Y., Maki, T., Kobayashi, M., Takazawa, T., Iwabu, M., Okada-Iwabu, M., Kawamoto, S., Kubota, N., Kubota, T., *et al.* (2007). Targeted disruption of AdipoR1 and AdipoR2 causes abrogation of adiponectin binding and metabolic actions. Nat Med *13*, 332-339.

Yang, Y. K., Ollmann, M. M., Wilson, B. D., Dickinson, C., Yamada, T., Barsh, G. S., and Gantz, I. (1997). Effects of recombinant agouti-signaling protein on melanocortin action. Mol Endocrinol *11*, 274-280.

Yaswen, L., Diehl, N., Brennan, M. B., and Hochgeschwender, U. (1999). Obesity in the mouse model of pro-opiomelanocortin deficiency responds to peripheral melanocortin. Nat Med *5*, 1066-1070.

Zander, M., Madsbad, S., Madsen, J. L., and Holst, J. J. (2002). Effect of 6-week course of glucagon-like peptide 1 on glycaemic control, insulin sensitivity, and beta-cell function in type 2 diabetes: a parallel-group study. Lancet *359*, 824-830.

Zeggini, E., Weedon, M. N., Lindgren, C. M., Frayling, T. M., Elliott, K. S., Lango, H., Timpson, N. J., Perry, J. R., Rayner, N. W., Freathy, R. M., *et al.* (2007). Replication of Genome-Wide Association Signals in U.K. Samples Reveals Risk Loci for Type 2 Diabetes. Science.

Zhang, Y., Proenca, R., Maffei, M., Barone, M., Leopold, L., and Friedman, J. M. (1994). Positional cloning of the mouse obese gene and its human homologue. Nature *372*, 425-432.

Zhao, A. Z., Shinohara, M. M., Huang, D., Shimizu, M., Eldar-Finkelman, H., Krebs, E. G., Beavo, J. A., and Bornfeldt, K. E. (2000). Leptin induces insulin-like signaling that antagonizes cAMP elevation by glucagon in hepatocytes. J Biol Chem *275*, 11348-11354.

Zimmet, P., Alberti, K. G., and Shaw, J. (2001). Global and societal implications of the diabetes epidemic. Nature *414*, 782-787.

Publications

The following publications have arisen as a result of this work:

1) Choudhury, A. I., H. Heffron, Smith, M.A, **Al-Qassab, H,** et al. (2005). "The role of insulin receptor substrate 2 in hypothalamic and beta cell function." J Clin Invest **115**(4): 940-50.

2) Neganova, I., **Al-Qassab, H.** et al. (2007). "Role of Central Nervous System and Ovarian Insulin Receptor Substrate 2 Signaling in Female Reproductive Function in the Mouse." Biol Reprod. **76**(6): 1045-53.